

University of Southampton Research Repository

Copyright © and Moral Rights for this thesis and, where applicable, any accompanying data are retained by the author and/or other copyright owners. A copy can be downloaded for personal non-commercial research or study, without prior permission or charge. This thesis and the accompanying data cannot be reproduced or quoted extensively from without first obtaining permission in writing from the copyright holder/s. The content of the thesis and accompanying research data (where applicable) must not be changed in any way or sold commercially in any format or medium without the formal permission of the copyright holder/s.

When referring to this thesis and any accompanying data, full bibliographic details must be given, e.g.

Thesis: Author (Year of Submission) "Full thesis title", University of Southampton, name of the University Faculty or School or Department, PhD Thesis, pagination.

Data: Author (Year) Title. URI [dataset]

UNIVERSITY OF SOUTHAMPTON

FACULTY OF NATURAL AND ENVIRONMENTAL SCIENCES

Ocean and Earth Science



The macroecology of globally-distributed deep-sea jellyfish

by

Graihagh Hardinge

Thesis for the degree of Doctor of Philosophy

September 2019

Supervisors:

Prof Cathy Lucas (University of Southampton)

Prof Beth Okamura (Natural History Museum London)

UNIVERSITY OF SOUTHAMPTON

ABSTRACT

FACULTY OF NATURAL AND ENVIRONMENTAL SCIENCES

Ocean and Earth Science

Thesis for the degree of Doctor of Philosophy

The macroecology of globally-distributed deep-sea jellyfish

By Graihagh Hardinge

Macroecology provides a framework for understanding how local- and regional-scale processes interact, allowing us to understand how the biological and ecological traits of individual species influence large-scale patterns in diversity. The majority of macroecological studies to date have been centred on the terrestrial environment where large databases on species ranges, body size and associated environmental variables are readily available. Due to the inaccessibility of the deep sea, coupled with its relatively recent exploration, deep sea macroecology is the least represented within marine macroecology as a whole. Jellyfish, a significant constituent of the zooplankton, form important and often conspicuous components of marine ecosystems. Jellyfish studies covering large spatial scales are mostly focused on the shallow-water, bloom-forming species that have more apparent anthropogenic interactions, such as *Aurelia aurita*. The structural simplicity of jellyfish permits the rapid adaptation to changing environments. Plasticity in traits such as feeding, physiology, reproductive output, somatic growth and size are common; and as such allow populations to persist. The coronate medusae *Periphylla periphylla* Péron and Lesueur, 1810 and *Atolla* spp. are the most recognised deep-sea jellyfish, and both have cosmopolitan distributions. Little remains known about these genera beyond the early descriptions of the species, particularly relating to their macroecology and the expression of plastic traits according to varying environments. This study presents a large volume of morphological data using museum collections genera in order to better describe morphological variation on a global scale and to examine what factors might drive such variation.

P. periphylla and *Atolla* spp. exhibit cosmopolitan distributions across the global dataset, found at depths ranging from 0 to 5486 m and 4900 m respectively. Across the global oceanic dataset and case study areas of the Iberian Basin and Porcupine Abyssal Plain, *P. periphylla* demonstrate no morphological plasticity across temporal or spatial scales, with variation in tentacle number observed within a number of *Atolla* species, *A. gigantea*, *A. parva*, *A. vanhoeffeni* and *A. russelli*. This may be indicative of the genetic distance between the two species within Coronatae. The first comprehensive comparison between fjord and oceanic *P. periphylla* populations is described. Contrasting patterns were observed between

fjord and oceanic environments, with larger males than females within the fjord population, and larger females than males within the oceanic population. Larger fjord specimens were observed across all sample seasons. The oceanic population provides evidence of the prioritisation of reproductive output within the more variable oceanic environments. Novel methods to further the understanding of volumes of statoliths within medusae statocysts were explored, with specimens of *P. periphylla* of varying sizes demonstrating a range of statolith numbers, sizes and crystalline morphologies. Statoliths form part of the sensory organs and represent the only hard structures within medusae. Both the number and size of statoliths is proposed to be indicative of the individual medusa age. This thesis shows that macroecological scales are important to consider when comparing globally-distributed species, and highlights the potential of using historical collections to identify ecological patterns. By combining the morphological data with molecular analyses, it would be possible to further the understanding of ecological divergence and speciation in deep sea coronates. Rearing specimens of a known age would also further the understanding of sclerochronological processes and help to determine age in medusae which are believed to be long-lived.

Table of Contents

Table of Contents	i
List of Tables	vii
List of Figures	xi
List of Accompanying Materials	xxiii
DECLARATION OF AUTHORSHIP	xxv
Acknowledgements	xxvii
Chapter 1:Introduction	1
1.1 Gelatinous zooplankton: An Introduction	1
1.1.1 Progression of jellyfish research	2
1.1.2 Biology and relationships of medusae	3
1.1.3 Macroecology of gelatinous zooplankton	8
1.2 The study organisms	9
1.2.1 Current classification of <i>Periphylla</i> and <i>Atolla</i>	13
1.3 Use of collections for ecological research	20
1.4 Aim and objectives of thesis	23
Chapter 2:Analysis of the global species distributions of the deep-sea coronate jellyfish, <i>Periphylla periphylla</i> and <i>Atolla</i> spp.	25
2.1 Abstract	25
2.2 Introduction	26
2.2.1 Aim and hypothesis	28
2.3 Methods	29
2.3.1 Samples and study area	29
2.3.2 Morphology	34
1.1.1 Data analysis	35
1.1.2 Environmental variables	36
2.3.3 Molecular analysis	37
2.3.4 Histology	Error! Bookmark not defined.
2.4 Results	37

2.4.1	General distribution and species identification	37
2.4.2	Morphological variation in <i>Atolla</i> and <i>Periphylla</i>	41
2.4.3	Development of new pedalia within <i>Atolla</i>	49
2.4.4	Latitudinal variation in morphology.....	51
2.4.5	Depths of deep-sea coronate species.....	52
2.4.6	Impact of environmental data on coronate species occurrence	55
2.5	Discussion	60
2.5.1	Distribution of <i>Atolla</i> spp. and <i>P. periphylla</i>	60
2.5.2	Morphological variation in <i>Atolla</i> spp. and <i>P. periphylla</i>	61
2.5.3	Implications for marine macroecology	64
2.5.4	Conclusions	65
Chapter 3: Investigating temporal morphological variation in deep-sea jellyfish within the Iberian Basin.		67
3.1	Abstract.....	67
3.2	Introduction.....	67
3.2.1	Temporal studies on gelatinous zooplankton	69
3.2.2	Aims and objectives	70
3.3	Materials and methods.....	71
3.3.1	Samples and study area	71
3.3.2	Morphometric measurements of <i>Periphylla</i> and <i>Atolla</i>	72
3.3.3	Environmental variables	72
3.3.4	Data analysis	74
3.3.5	Molecular methods	74
3.4	Results.....	75
3.4.1	Temporal distribution of coronate species	75
3.4.2	Morphological patterns over time	77
3.4.3	Chlorophyll- <i>a</i> fluctuations and influence on medusae.....	81
3.4.4	Influence of climatic indices data.....	87
3.5	Discussion	95
3.5.1	Effects of climate and phytoplankton variation on deep-sea jellyfish	97
3.5.2	Temporal variation in morphological traits within deep-sea coronates.....	98

3.5.3	Resilience of deep-sea jellyfish?	100
3.5.4	Conclusions	101

Chapter 4: Population structure and reproduction of *Periphylla* and *Atolla* within the Porcupine Abyssal Plain (NE Atlantic)

4.1	Abstract	103
4.2	Introduction	104
4.2.1	Reproduction in deep-sea jellyfish	104
4.2.2	Deep-sea research within the North Atlantic, including the Porcupine Abyssal Plain and Seabight.....	106
4.2.3	Aims and objectives	110
4.3	Methods	110
4.3.1	Samples and study area.....	110
4.3.2	Data collection	112
4.3.3	Histology.....	113
4.3.4	Accompanying data	116
4.3.5	Data analysis	116
4.4	Results	117
4.4.1	Body size with depth	127
4.4.2	Zooplankton biomass	130
4.4.3	Reproductive traits	134
4.5	Discussion.....	144
4.5.1	Coronate distributions and evidence for vertical migration.....	144
4.5.2	Body size variation in deep sea organisms	146
4.5.3	Zooplankton relationships – prey or parasitism?	147
4.5.4	Conclusions	149

Chapter 5:A comparison between fjord and oceanic populations of *Periphylla periphylla*.....

5.1	Abstract	151
5.2	Introduction	151
5.2.1	Aim and objective	153

5.3	Methods.....	154
5.3.1	Samples and study area	154
5.3.2	Data analysis	157
5.4	Results.....	158
5.4.1	Morphological comparisons between oceanic and fjord environments.....	158
5.5	Discussion	165
5.5.1	Sizes of individuals in oceanic and fjord populations	165
5.5.2	Other life history comparisons and differences between oceanic and fjord populations	166
5.5.3	Conclusions	167
Chapter 6:Sclerochronology of <i>Periphylla periphylla</i> statoliths		
		169
6.1	Abstract.....	169
6.2	Introduction.....	169
6.2.1	Aims and Objectives	171
6.3	Materials and methods.....	172
6.3.1	Study samples	172
6.3.2	Preparation of statoliths for scanning electron microscopy	172
6.3.3	Preparation of statoliths for micro-computed tomography	175
6.4	Results.....	177
6.4.1	Initial observations on <i>P. periphylla</i> statolith structures.....	177
6.4.2	<i>P. periphylla</i> statolith analysis	180
6.4.3	Statocyst computed tomography.....	183
6.5	Discussion	184
6.5.1	Statoliths of deep-sea medusae and elucidating age	184
6.5.2	Conclusions	186
Chapter 7:Conclusions		
		188
7.1	The macroecology of globally-distributed deep-sea jellyfish	188
7.2	Deep sea macroecology.....	190

7.3	Deep-sea jellyfish macroecology: evidence of plasticity to environmental variation?	191
7.4	Molecular analysis	192
7.5	Deep-sea jellyfish macroecology: evidence of plasticity over temporal scales?	Error! Bookmark not defined.
7.6	Exploiting museum collections for macroecological studies.....	194
7.7	Deep-sea jellyfish macroecology: evidence for determining age in medusae? ..	195
7.8	Future studies on jellyfish macroecology and deep-sea medusae.	196
Appendices		199
Appendix A.....		199
Appendix B–List	of	gear
types		215
Appendix C–	Lurefjorden	fieldwork
images		216
List of References		225

List of Tables

Table 1.1 Documented geographic occurrence, specific characters and key references for deep-sea coronates.	18
Table 2.1 Sample numbers of species collected across the various areas across the globe and split according to data source. SuperAtolla refers to a potential species nova, and Unknown refers to <i>Atolla</i> samples that were not identified to species level.	32
Table 2.2 Sample numbers of species collected between 1880 to 2000 from the respective data sources. SuperAtolla refers to a potential species nova, and Unknown refers to <i>Atolla</i> samples that were not identified to species level.	33
Table 2.3 GLM output of tentacle number variation according to spatial area (distance group) within the global study. <i>Atolla</i> species with tentacle ranges that incorporate 4 different number of tentacles are included.	49
Table 2.4 <i>Atolla</i> individuals within the NHM global study exhibiting developing pedalia, along with date and location sampled, weight (mm), total number of tentacles observed and description.	50
Table 2.5 Summary of key size and depth information for the various coronate species from the NHM and Smithsonian data. ND = no data available. Majority tentacle number is determined by the highest instance of that tentacle number. Diameter, weight and tentacle number information available from the NHM dataset only.	53
Table 2.6 Zooplankton diversity (Simpson's Index) across the key global sampling areas within the NHM dataset study area.	56
Table 2.7 General linear model (GLM) output for the influence of environmental factors (chlorophyll- <i>a</i> and zooplankton diversity) on deep-sea coronate distribution according to global distance group generated by the geographic distance matrix for the global study area.	59
Table 3.1 Number of deep-sea coronates sampled following removal of species with poor temporal representation within the Iberian Basin collections. Figures highlighted	

in red represented too small a sample size for subsequent analyses and were removed.....76

Table 3.2 General linear model (GLM) output predicting variation in tentacle number for *A. parva* within the Iberian Basin (1958-1984) (n = 226). Year, NAOI and average depth could not be estimated and were removed from the model. ***significant to > 99% confidence level.....93

Table 4.1 Protocol for staining with haemotoxylin and eosin.....114

Table 4.2 One-way ANOVA output for variation in species depth sampled between day and night hauls within the study area. Mean depth values (in metres) during the day and night are within brackets. Significant results to the 99% confidence level are noted with ***.126

Table 4.3 Generalised linear model (GLM) output for body size according to depth across day and night sample hauls within the PAP study area. Significant results to 99% confidence level notated with ***.129

Table 4.4 Multiple regression analysis predicting coronate body size according to different environmental variables sampled within the PAP study area. *P. periphylla* body size (coronal diameter) = $20.9 - 0.047 \text{ temperature} - 0.590 \text{ salinity} + 0.085 \text{ nitrate} + 0.94 \text{ oxygen} - 7.04 \text{ phosphate} - 0.0948 \text{ silicate}$. *A. wyvillei* body size (bell diameter) = $-26.59 + 0.2993 \text{ temperature} + 0.328 \text{ salinity} + 0.232 \text{ nitrate} + 2.187 - 0.69 \text{ phosphate} + 0.0030 \text{ silicate}$130

Table 4.5 Model output from forward stepwise regression for predicting coronate occurrence with zooplankton biomass (displacement volume). Zooplankton taxa represent the independent variables that were retained within the model. Regression equation: *A. wyvillei* presence = $1.68 + 0.0166 \text{ MED} + 0.0053 \text{ FIS} + 0.013 \text{ POL} - 0.0095 \text{ PTE} + 0.023 \text{ AMP}$. Regression equation: *P. periphylla* presence = $4.175 + 0.614 \text{ POL} + 0.0033 \text{ EUP} - 0.0519 \text{ DEC} - 0.01578 \text{ AMP}$. *** indicates significant results to the 99% confidence level.....134

Table 5.1 Numbers of *P. periphylla* measured following fieldwork in Lurefjorden, Norway and sampling of museum collections from the Iceland Basin. Supplementary information from the Jelly Farm Project 2010, 2011 and 2016 cruises listed.158

Table 6.1 Methods trialled to isolate statoliths from statocyst tissue (preserved in 100% ethanol) for SEM analysis.....	174
Table 6.2 General linear results describing changes in statolith composition as a function of changes in the coronal diameter of the <i>P. periphylla</i> medusae.	183
Table 7.1 Summary of molecular methods trialled within the study. Sample sources used include historical collections (formalin-fixed <i>Atolla</i> spp. and <i>P. periphylla</i>), fresh tissue (ethanol-fixed <i>P. periphylla</i>) and fresh tissue (frozen <i>Rhizostoma</i> , control).	194

Appendices Tables

Table 1 Station list of NHM samples used within this study
Table 2 List of samples from the Smithsonian used within this study
Table 3 List of species data sourced from the Global Biodiversity Information Facility (GBIF)
Table 4 List of gear types used to collect samples within the NHM collections
Table 5 List of <i>P. periphylla</i> specimens used within Chapter 6 for the extraction of statoliths.

List of Figures

- Figure 1.1** Phylogenetic relationships within the Scyphozoa based on 18S small subunit and 28S large subunit ribosomal RNA sequences, with deep-sea coronate species highlighted in yellow. Adapted from Bayha and Dawson (2010)..... 4
- Figure 1.2** Diagram of key external morphological landmarks within deep-sea coronates, here using *A. wyvillei* as an example. Illustration by author. 10
- Figure 1.3** Diagrammatical representations of *Atolla* and *Periphylla* body shapes as found within the literature. *Atolla* is mostly depicted in dorso-ventral orientation due to its disc-like structure, with *P. periphylla* depicted in lateral orientation due to conical shape. a: *A. wyvillei* lateral view with pigmentation (Russell, 1970); b: *Atolla* genus dorso-ventral view (Russell, 1976); c: *P. periphylla* lateral view (Sötje et al., 2007); d: *P. periphylla* lateral view with gonads visible (Tiemann and Jarms, 2010); e: *P. periphylla* lateral view with pigmentation visible (Russell, 1970); f: *P. periphylla* lateral view (Russell, 1970). 14
- Figure 1.4** Composite drawings of *Atolla* specimens and photographs depicting key morphological landmarks for species differentiation. Scales marked for each species respectively. See accompanying table (Table 1.1) for further detail. Landmark key: *A. wyvillei* – te = tentacle, cm = coronal muscle, so = stomach ostia, gs = gastric sinus, go = gonad, rs = radial septa, la = marginal lappet; *A. vanhoeffeni* – sp = black spots around stomach ostia; *A. chuni* – pw = pedalial warts, rw = radial warts. Figure continued on following page. Photographs were available only for *A. tenella* and Super*Atolla* due to the paucity of data with which to draw composite drawings of the species. This species and potential species nova remain poorly understood and not yet fully documented. Drawings and photographs author's own with the exception of: *A. vanhoeffeni* photograph (Russell, 1970); *A. chuni* photograph (Smithsonian, available at: <https://www.gbif.org/occurrence/1320668521>);..... 16
- Figure 2.1** Depiction of *P. periphylla* and *Atolla* sp. to demonstrate key features and the landmarks used for the morphological analysis of both coronates. Illustrations by the author, adapted from Russell (1970)..... 34

- Figure 2.2** Distribution of all samples collated within this study, including the primary dataset of the NHM (yellow circles), Smithsonian (green triangles) and GBIF (black triangles).38
- Figure 2.3** Distribution of deep sea coronates found within this study. a: *P. periphylla*; b: *Atolla* sp. Legend for *Atolla* show that in some instances there were two species possibilities for the sample. These were noted and removed from subsequent data analysis. All 7 described species of *Atolla* were found within the data, along with an additional potential species nova, referred to as ‘SuperAtolla’. Undeterminable species are noted with a red cross and discounted from subsequent analyses.39
- Figure 2.4** Morphological relationships for *P. periphylla* (a +b) and the species of *Atolla* (c – e) across the global dataset. e: *Atolla* mean bell diameter across the global dataset for the various species. Letters next to bars denote significantly different species sizes, Tukey’s test, $p < 0.05$). Standard error bars to 95% confidence level.42
- Figure 2.5** Cubic regression of *P. periphylla* length-weight relationship using preserved wet weight and coronal diameter, $p < 0.001$. Regression equation: The regression equation is: $\text{Weight} = -0.966 + 0.0795 \text{ CD} + 0.000158 \text{ CD}^2 + 0.000218 \text{ CD}^3$.43
- Figure 2.6** Cubic regression of *Atolla* length-weight relationship using preserved wet weight and coronal diameter. *A. chuni* was omitted from the dataset due to paucity of data. All regressions $p < 0.001$. Regression equations: *A. wyvillei*: $y = 8.043 - 0.718x + 0.018x^2 - 0.0002x^3$; *A. vanhoeffeni*: $y = 0.121 - 0.003x + 0.0003x^2 + 0.0001x^3$; *A. russelli*: $y = 3.531 - 0.528x + 0.019x^2 - 0.00074x^3$; *A. parva*: $y = 1.772 - 0.2668x + 0.0103x^2 + 0.0002x^3$; *A. gigantea*: $y = 16.54 - 1.073x + 0.021x^2 + 0.00025x^3$.44
- Figure 2.7** Size frequency histograms and distribution lines of fit for *Atolla* species across the global NHM dataset, excluding *A. chuni* due to lack of sufficient data. Mean, standard deviations (StDev) and number of individuals noted on each panel.46
- Figure 2.8** Size frequency histograms and distribution lines of fit for *P. periphylla* specimens within the NHM global dataset. Smaller specimens (<20 mm diameter) separated out in separate panel due to the large volume of smaller samples ($n = 1111$).47
- Figure 2.9** Percentage frequency variation in tentacle number observed across the global study area using NHM data for each deep-sea coronate species. Numbers above

bars are the number of tentacles. Light grey bars are 20 tentacles and under, dark grey bars are 21 – 24 tentacles, and blue bars are 25 tentacles and over. Striped bar is 12 tentacles (<i>P. periphylla</i> only).	48
Figure 2.10 Quadratic regression analysis for change in body size (coronal diameter, CD for <i>P. periphylla</i> n = 1321 and bell diameter, BD for <i>Atolla</i> species n =) according to latitude, $p > 0.05$ for all species.....	51
Figure 2.11 Depth distribution percentage frequency histograms of the deep-sea coronates within the global study using NHM and Smithsonian data. No data was available for <i>A. tenella</i>	54
Figure 2.12 Average depths of the deep-sea coronates within the global study, using data sourced from the NHM and Smithsonian. No data available for <i>A. tenella</i> . Significantly different groups indicated with letters above bars, Tukey test, $p < 0.05$	55
Figure 2.13 Chlorophyll- <i>a</i> percentage frequency concentrations according to geographical sample area within the global study area.....	57
Figure 2.14 Relationships between <i>P. periphylla</i> coronal diameter and chlorophyll- <i>a</i> concentration (mg m^{-3}) across seasons within the different sample areas across the global dataset. Winter and spring information was unavailable for the Southern Ocean, along with winter information for the Iberian region. Insufficient data was available for the Indian Ocean (n = 2 values in total) and as such was omitted.....	58
Figure 2.15 Photographs of developing pedalia and tentacles in a : <i>A. russelli</i> (bell diameter = 59.7 mm) and b : <i>A. wyvillei</i> (bell diameter 64.6 mm) from the museum collections used within this study.	62
Figure 3.1 Map of the Iberian Basin sample area, with sample station locations of deep-sea coronate medusae within the NHM Discovery Collections dataset colour coded according to year collected. Base map source: ESRI.....	72

Figure 3.2 Map of the deep-sea corionate species found within the Iberian Basin study area.

Clustered samples are depicted within the magnified circles. Base map source: ESRI. 75

Figure 3.3 Mean diameter (bell diameter for *Atolla*, coronal diameter for *Periphylla*) and standard error (95% confidence) variation across the time series within the Iberian Basin study area. *A. parva*, n = 325, *A. wyvillei*, n = 130, *P. periphylla*, n = 43. Asterisks (*) = samples removed due to small size.77

Figure 3.4 Relative body sizes of the species within the Iberian dataset. Sizes illustrative of the mean sizes found (*A. parva* mean = 13 mm; *A. wyvillei* mean = 35 mm; *P. periphylla* mean = 38mm diameter). Illustrations drawn by author.78

Figure 3.5 Variation in the corrected mean diameter of *A. parva*, *A. wyvillei* and *P. periphylla* within the Iberian Basin between 1978 and 1984. Significantly different groups indicated with letters above bars, one-way ANOVA, $p < 0.05$. Standard error bars to 95% confidence level.....79

Figure 3.6 Mean tentacle number variation in *A. parva* between 1958 to 1984. Hatched bars represent small sample sizes that were not used for subsequent statistical analysis. Standard error bars to 95% confidence limits.80

Figure 3.7 Relationship between depth and chlorophyll-*a* concentrations in the Iberian Basin overall (pooled years). Source of raw data: NOAA World Ocean Database.

81

Figure 3.8 Fluctuations in chlorophyll-*a* within the top 10 m of the Iberian Basin sample area over time (1957 – 1990).....81

Figure 3.9 Log body size and surface spring (Mar-May) chlorophyll-*a* for *A. parva*, *A. wyvillei* and *P. periphylla* within the Iberian Basin study area, with linear regression line (blue) to 95% confidence interval (red dashed lines). Regression equations *A. parva* $y = 0.6575 + 0.1954x$, $r^2 = 0.016$; *A. wyvillei* $y = 1.441 + 0.01145x$, $r^2 = 0.01$; *P. periphylla* $y = 1.470 + 0.4945x$, $r^2 = 0.08$85

Figure 3.10 Phytoplankton Colour Index (PCI) and associated number of tentacles observed within *A. parva* within the study area. No PCI data was available for 1984 hence

was omitted. Standard error bars to the 95% confidence limits. Source of raw PCI data: CPR.	86
Figure 3.11 Annual NAOI fluctuations, displaying the difference of normalised sea level pressures between Ponta Delgada, Azores (high) and Reykjavik, Iceland (low) across the study sample period (1958 to 1984). Raw data source: NCAR, UCAR.	87
Figure 3.12 Normalised winter NAOI (December-March) Index (bars) and scaled log-transformed body size for <i>A. parva</i> , <i>A. wyvillei</i> and <i>P. periphylla</i> (dots). For ease of visual interpretation, the body size was log-transformed and plotted on the secondary axis. Small sample sizes present during 1958, 1961 and 1974, with $n = 1$ for <i>A. parva</i> and <i>A. wyvillei</i> during 1958.	88
Figure 3.13 Variation in bell diameter according to NAO Index within the Iberian study area, with year groups pooled. Significantly different groups indicated with letters above bars, Tukey test, $p < 0.05$. Standard error bars to 95% confidence limits.	89
Figure 3.14 Winter NAO Index and associated tentacle number observed in <i>A. parva</i> within the study area, years pooled. Hatched bars represent low sample numbers. Standard error bars to the 95% confidence limit.	90
Figure 3.15 Average depths of <i>A. parva</i> ($n = 206$) and <i>A. wyvillei</i> ($n = 91$) against the winter (Dec-Mar) NAO Index. All depths taken during day cruises. Coloured sections represent the mesopelagic (light blue) and bathypelagic (dark blue) depth zones at which coronates were sampled. <i>A. wyvillei</i> were sampled across a broader set of NAO indices and depths than <i>A. parva</i> . Letters above bars indicate significantly different groups (Tukey's test, $p < 0.01$). Standard error bars to 95% confidence limit.	92
Figure 4.1 Map of the Porcupine Abyssal Plain and Seabight (PAP) study area and sample locations held within the <i>Discovery</i> collections from Cruise 92 (1978).	111
Figure 4.2 Drawings and photographs of museum specimens to illustrate measurement of body size on <i>P. periphylla</i> (lateral orientation) and <i>Atolla</i> spp. (here <i>A. wyvillei</i> subumbrella depicted in ventro-dorsal orientation). Gonads marked with red arrows. Drawings by the author, adapted from Russell (1970), photographs by author.	113

- Figure 4.3** Example of sectioned mature *A. wyvillei* gonad with numbered oocytes using the ImageJ Cell Counter Tool.115
- Figure 4.4** Deep-sea coronate species found within the PAP study area on map (samples overlapped when more than one species found within that location) and frequency chart with number of each species found: *P. periphylla* (orange triangles, $n = 77$), *A. parva* (yellow circles, $n = 740$), *A. wyvillei* (magenta circles, $n = 251$), *A. russelli* (green circles, $n = 111$), *A. vanhoeffeni* (blue circles, $n = 107$), *A. gigantea* (orange circles, $n = 14$).117
- Figure 4.5** Size frequency histograms with normal distribution lines for deep-sea coronates within the sample area. Mean, standard deviation (StDev) and number of specimens within each species sample noted on respective charts. Histograms plotting smaller individuals (< 15 mm) were also produced for *A. parva* and *A. vanhoeffeni* and for *A. wyvillei* smaller and larger than 40 mm diameter.119
- Figure 4.6** Depth distributions during the day and night for the coronate species within the PAP study area. Significantly different groups indicated with letters above bars, Tukey's test $p < 0.001$. Standard error bars to 95% confidence level. Samples that had depths reported in broad ranges of over 200 m were omitted from this study ($n = 203$), all of which were found from 0 to 1000 m deep.122
- Figure 4.7** Percentage frequency depth distributions according to day (light grey bars) and night (dark grey bars) of deep-sea coronate species within the study area. Depths grouped into 250 m bins, from 0 – 250 m to 4000 – 4250 m.123
- Figure 4.8** Depth distributions of coronate species within the PAP study area according to size (bell diameter in *Atolla* sp., coronal diameter in *P. periphylla*) from 0 to 4000 m during the day (left plots) and night (right plots). Continued on next page.127
- Figure 4.9** Percentage relative abundances of zooplankton taxa sampled during day (light grey bars) and night (dark grey bars) trawls at different depths during Discovery Cruise 92 within the PAP study area. Zooplankton samples were recorded as ml per 1000 m³ displacement volumes. Key to taxa: Medusae (MED), Siphonophorae (SIP), Fish (FIS), Chaetognatha (CHA), Polychaeta (POL), Amphipoda (AMP), Decapoda (DEC), Euphausia (EUP), Pteropoda (PTE) and Mysidae (MYS). Numbers

on charts are the individual taxa sample volumes (ml 1000m³⁻¹) for day and night trawls. 132

Figure 4.10 Relative abundances of all zooplankton taxa biomass sampled during day and night trawls. Taxa were recorded in ml per 1000 m³ displacement volumes. Relative abundances are according to depth, with individual taxa relative to the overall proportion sampled at that depth. 133

Figure 4.11 *P. periphylla* (a, c) and *A. wyvillei* (b,d) from the PAP study side split according to male, female and 'unknown' (see text) (a,b) and stage of maturity (c,d) according to size class. Coronal diameter used to determine size in *P. periphylla* and bell diameter in *A. wyvillei*. 136

Figure 4.12 *P. periphylla* gonads at various stages of development from the PAP study area. First appearing as straight white ridges above the coronal groove, they become hooked and folded with the growth of the gastric sinus to form a J-shape (images a – d). The folds increase in volume as the medusa develops, producing a U-shape in maturity (images e + f). In the female gonad (image e) the young eggs originate at the point of origin of the fold and then migrate outwards, with the largest eggs > 1 mm diameter (Russell, 1970). The male gonads have secondary diverticula giving a more folded appearance (image f). Image a coronal diameter = 6.4 mm; image b = 7.1 mm; image c = 13.7 mm; image d = 9.2 mm; image e = 60 mm; image f = 82.7 mm. Key to images: s (stomach); cg (coronal groove); dg (developing gonad); tmb (tentacular muscular bundle); mg (mature gonad). 137

Figure 4.13 *A. wyvillei* gonads at various stages of development from the PAP study area. Gonads develop as crescent-shaped thickenings that are clearly visible at an early age (images a (entire specimen) + b (gonad only)). The gonads develop over time to form thick protrusions on the medusa subumbrella, with a mesogloal pad between the gastric endoderm and the germinal epithelium (Russell, 1970). The mesogloal pad is thinner in male gonads than female, with oval sperm follicles in a single layer next to each other, making the gonads appear dense (images c + e). In female gonads the mesogloal pad is dense, with oocytes originating near the periphery and migrating into the centre at maturity. The overall shape of the gonad in females resembles a bean shape (images d + f). Image a bell diameter =

2.2 mm; image **b** = 4.2 mm; image **c** + **e** = 45 mm; image **d** + **f** = 50.1 mm. Scale bars all 1 mm.138

Figure 4.14 Subumbrella view of *A. wyvillei* (male) and *P. periphylla* (female) whole specimens with gonad locations (arrows). One gonad missing in *A. wyvillei*, one gonad damaged in *P. periphylla*. *A. wyvillei* specimen size bell diameter = 48.3 mm; *P. periphylla* specimen size coronal diameter = 32.3 mm. Scale bars all 1 cm.139

Figure 4.15 *P. periphylla* histology cross-sections of male (images a (whole gonad) + b (sub-section of a gonad)) and female (images c (whole gonad) + d (sub-section of a gonad)) gonads from specimens sampled from the PAP study area. Gonad folds are clearly visible in both male and female specimens, with the male sperm follicles more heavily stained than the female tissue overall. Key to images: f (sperm follicles); m (mesoglea); g (gastrodermis); bo (immature basophilic oocytes); ao (mature acidophilic oocytes); n (nucleus).140

Figure 4.16 *A. wyvillei* histology cross-sections of developing (images a – c), mature female (images d + f) and mature male (images e + g) gonads from specimens sampled within the PAP study area. Sperm follicle arrangement (f) is indicative of the lobed mesogloal pad. Key to images: bo (basophilic oocytes); io (immature oocytes); ao (mature acidophilic oocytes); g (gastrodermis); f (sperm follicles).141

Figure 4.17 Number of oocytes against medusa bell diameter (mm) for *A. wyvillei* within the PAP study site. Regression equation: $y = 58.52 - 0.158 x$142

Figure 4.18 Maximum feret diameter (μm) according to bell diameter for *A. wyvillei* individuals sampled within the PAP study site.143

Figure 5.1 Sample site for the collection of fresh *P. periphylla* samples, Lurefjorden, Norway (60°41.7'N, 05°08.5'E). Lurefjorden is outlined with yellow rectangle, and sample site is marked with blue dot (depth = 440 m).155

Figure 5.2 Sample stations (station numbers 7709, n = 28) within the Iceland Basin for the oceanic specimens used within this study held within the Discovery Collections at the Natural History Museum London. All samples collected during 1971. ...157

Figure 5.3 Examples of *P. periphylla* caught during the Lurefjorden field work, August 2015 aboard 'MS Solvik'. a + c + e: example of hauls following vertical tows; b: example

of the rapid extent of porphyrin pigmentation degradation following the exposure to light and handling (note red flecks against white tray); f: mature male specimen with gonads (white) clearly visible on the subumbrella.	159
Figure 5.4 Size frequency histograms for the oceanic and fjord populations within the Lurefjorden and Iceland Basin study sites.	160
Figure 5.5 Mean coronal diameters of <i>P. periphylla</i> medusae in fjord and ocean sample areas. Boxplots depicting interquartile range and outliers of the observed coronal diameters within each area.	161
Figure 5.6 Mean coronal diameters of ,ale, female and undetermined specimens from the oceanic (lighter bars) and fjord (darker bars) sample areas. Bars represent two standard errors.	162
Figure 5.7 Variation in <i>P. periphylla</i> body size according to sample season within the fjord and oceanic study areas. Bars represent two standard errors.	163
Figure 5.8 Relationship between <i>P. periphylla</i> medusa size and gonad length and tentacle length for fjord and oceanic samples within the study. a: Regression equations: Oceanic $y = -1.214 + 0.2946 x$, $r^2 = 91.7\%$, $F = 98.97$, $p < 0.001$, $n = 9$; Fjord regression equation: $y = 6.069 + 0.02117 x$, $r^2 = 8.5\%$, $F = 0.33$, $p > 0.05$, $n = 25$. b: Regression equations: Oceanic regression equation, $y = -4.052 + 2.036 x$, $r^2 = 83.7\%$, $F = 370.5$, $p < 0.01$, $n = 76$; Fjord $y = 8.87 + 1.86 x$, $r^2 = 57.5\%$, $F = 35.4$, $p < 0.01$, $n = 36$	164
Figure 6.1 Scanning electron and light micrographs depicting methods trialled to liberate statoliths. a + b: Scanning electron micrographs of critical point dried specimens, with statoliths seen spilling out of the thin dried rhopalial tissue. Scale bars = 100 μ m. c: Scanning electron micrograph of statocyst tissue dissolved in weak bleach and mounted on SEM stub, illustrating the degradation of the liths. Scale bar = 20 μ m. d: Light micrograph of rhopalial bulb from formalin-fixed tissue. Here the statocyst bulb and hood remain intact, but the statoliths are completely dissolved as a result of the lack of glycerophosphate buffer within the preservation fluid. Scale bar = 1 mm.	175

Figure 6.2 Samples prepared for micro-computed tomography for 3D visualisation of statoliths. a: Statocyst embedded in polymerised LR white in sealed gelatin capsule. b: Statocyst embedded in polymerised LR white in gelatin capsule and sealed with dental wax. c: Statocysts in low density tube containing glycerol. d: Samples loaded into X-ray chamber and held in place with Pasteur pipettes for scanning.	177
Figure 6.3 Scanning electron micrograph of a single <i>P. periphylla</i> bassanite crystal, depicting its trigonal structure. Scale bar = 10 µm.	178
Figure 6.4 Scanning electron micrograph of statoliths retained within a critically point dried statocyst bulb, illustrating the various crystal formations (1,2,3). Scale bar = 20 µm. (Note: slight distortion of image during scanning).	179
Figure 6.5 Computed tomography imagery of statoliths housed within intact statocyst bulb (rhopalial tissue was not stained and so is not detectable in the micro-CT chamber). The distribution of statoliths within the cyst is visible, with smaller crystals located at the origin of the rhopalial bulb (a), with larger crystals migrating towards the opposite edge of the statocyst (b).....	180
Figure 6.6 Labelled statoliths on SEM stub using ImageJ Particle Counter.....	181
Figure 6.7 Regression analysis of statolith composition from scanning electron data. a: max statolith length against coronal diameter; b: total statolith lengths against coronal diameter; c: statolith length against statolith width; d: number of statoliths against coronal diameter.....	182
Figure 6.8: Frequency histogram of statolith volumes within scanned statocyst bulb. Coronal diameter of medusa = 96 mm.....	183
Figure 6.9 Micro-CT slices of statocyst containing statolith crystals. a: raw micro-CT data; b: Labelled and quantified statoliths following Watershed analysis, with loss of trigonal definition due to crystal overlap.....	183
Figure 6.10 Frequency histogram of statolith volumes within scanned statocyst bulb. Coronal diameter of medusa = 96 mm.....	184
Figure 6.11 Light micrograph of liberated statolith crystals from the statocyst bulb, with the trigonal structure visible, along with the various morphological distinctions.....	186

Figure 7.1 Map illustrating the global extent of this study. Red dots represent sample locations of *Atolla* and *Periphylla* from the NHM Discovery collections where morphometric and histological data was gathered; yellow dots represent sample locations of *Atolla* and *Periphylla* from the Smithsonian Collections which were used to confirm cosmopolitan distributions of the species; green circles represent other isolated studies..... 189

List of Accompanying Materials

Appendix A. Station lists for all deep-sea carbonate samples used within this study.

Appendix B. List of gear types used to sample the Discovery collections used within this study.

Appendix C. Lurefjorden fieldwork images (Chapter 5).

Appendix D. List of samples used within the statolith study (Chapter 6).

DECLARATION OF AUTHORSHIP

I, Graihagh Hardinge

declare that this thesis and the work presented in it are my own and has been generated by me as the result of my own original research.

The macroecology of globally-distributed deep-sea jellyfish

I confirm that:

1. This work was done wholly or mainly while in candidature for a research degree at this University;
2. Where any part of this thesis has previously been submitted for a degree or any other qualification at this University or any other institution, this has been clearly stated;
3. Where I have consulted the published work of others, this is always clearly attributed;
4. Where I have quoted from the work of others, the source is always given. With the exception of such quotations, this thesis is entirely my own work;
5. I have acknowledged all main sources of help;
6. Where the thesis is based on work done by myself jointly with others, I have made clear exactly what was done by others and what I have contributed myself;
7. None of this work has been published before submission.

Signed: Graihagh Hardinge

Date: 23rd September 2019

Acknowledgements

I would like to thank my supervisors, Cathy Lucas and Beth Okamura, for their support throughout this process. Their knowledge and enthusiasm for the subject matter has been much appreciated. Thanks to Adam Reed for his advice on the histological work. Thanks to Andrew Sweetman for allowing me to join the JellyFarm Project cruise so that I could collect valuable samples, and to the University of Bergen for the Christoffer Schander Memorial Fund that allowed me to travel to Norway and complete my fieldwork. Finally, thanks to all of my family who have provided their endless support.

Chapter 1: Introduction

1.1 Gelatinous zooplankton: An Introduction

Jellyfish are conspicuous constituents of the zooplankton and are important components of marine ecosystems (Condon et al., 2012). The term generally applies to predatory medusa phases of the Scyphozoa, Cubozoa, Hydrozoa and Ctenophora, which are often grouped together due to their structural similarities and because their water content often exceeds 95% (Haddock, 2004; Brotz et al., 2012). Historically overlooked for their apparently insignificant roles in marine food webs, jellyfish are now recognised as significant ecological players. They are important predators, feeding on a large range of prey types (Madin, 1988; Lynam et al., 2006; Flynn and Gibbons, 2007). They serve as occasional or predominant food sources for 158 different marine species (Pauly et al., 2009). They contribute to nutrient cycling via excretion, mucous production and excretion of prey remains (Riemann et al., 2006). They contribute to potentially important carbon sinks through jellyfish falls and excretion. Finally they provide sources of food for humans and novel compounds (Doyle et al., 2014).

Jellyfish are present in all of the world's oceans, from the poles to the Equator. They are particularly abundant and diverse in the deep sea (Larson, 1986). Endemism in jellyfish is difficult to assess, as they are opportunistic colonisers with extensive larval dispersal (Graham and Bayha, 2007). Holopelagic taxa may be particularly widespread and potentially invasive as they lack a benthic polyp stage in their life cycle (Hanken, 2003). However, the presence of cryptic species contributes to the confusion of native versus non-indigenous jellyfish taxa within certain areas (Vinogradov et al., 1989) (e.g. *Blackfordia virginica*, Mayer, 1910 (Bayha and Graham, 2014)). The widespread to apparently cosmopolitan distributions exhibited by many jellyfish species make them highly suitable for macroecological investigations. Such studies could provide insights into how pelagic animals adapt to varying environmental conditions along with recognition of cryptic species and species complexes. The current dearth of macroecological studies of jellyfish, especially in the deep sea, may reflect difficulties in obtaining sufficient material across broad spatial scales as is required for such study.

1.1.1 Progression of jellyfish research

The public perception of jellyfish at present is largely negative, as a result of stings to humans and research focusing on the impacts of bloom populations (Duarte et al., 2014). This negative perception, however, was not always apparent. From the mid-1800s to early 1900s, there was a more positive attitude about jellyfish arising from research by scientists including Huxley, Haeckel, Vogt, Leuckart, Agassiz and Darwin who were keen to study these alien-like organisms in order to understand the origins of life and to answer basic evolutionary questions. This research subsequently resulted in a public awareness of and fascination for ctenophores and cnidarians (Haddock, 2004). It was during this 'golden age of gelata' (as termed by Haddock (2004)) that the highly accurate glass sculptures of gelatinous zooplankton were crafted by the Blaschkas (Brierley, 2009).

Subsequent lulls in jellyfish research coincided with faster ships that made collecting intact samples more difficult, along with general changes in scientific questions. Apart from pioneering works from Bieri (1966), Ceccaldi (1972), Hamner (1974; 1975) and Russell during the 1960s and 70s, gelatinous zooplankton research did not substantially increase until it was required in relation to social, medical and commercial issues (Purcell et al., 2007). These issues included stings to humans (Burnett, 2001; Brinkman et al., 2012), scientific uses of bioluminescent proteins (see Chalfie, 1995 for example) and the commercial impacts of bloom species (Uye, 2008; Bosch-Belmar et al., 2017). For example, research on species with particularly harmful stinging capacities, including the cubozoans *Chironex* (Brinkman et al., 2012) and *Carybdea* (Hartwick, 1991), and the siphonophore *Physalia physalis* Linnaeus, 1758, (the Portuguese man o' war) (Burnett, 2001) has enabled biomedical advances, including applications to human health and diagnostics (Bailey et al., 2003).

Jellyfish blooms are arguably the greatest stimulus for modern jellyfish research in order to understand changing ecologies that result in bloom formation (Richardson et al., 2009). Jellyfish blooms directly interfere with various human activities, affecting the tourism, fishing and energy sectors (Richardson et al., 2009; Brotz et al., 2012). Bloom impacts include stinging and disruption of bathers (Cegolon et al., 2013); beach closures, injuries and occasional fatalities, and the clogging of industrial coastal intakes (Dong et al., 2010). The latter can involve supplying power plant coolants, mining and military operations, shipping

and aquaria (Lucas et al., 2014). Blooms can also disturb fishing activities by damaging gear, capsizing boats, wasting time at sea and interfering with aquaculture as influxes of jellyfish overwhelm coastal cages (see Lo et al., 2008 for example). Jellyfish also have uncertain ecosystem impacts on fisheries resources (Purcell et al., 2007). These various influences of jellyfish blooms on many aspects of local infrastructure can have significant economic setbacks (Barbier, 2001).

It is now well-established that the development of cnidarian and ctenophore blooms is linked to human perturbations on the marine environment. These include overfishing (Pauly and Deng Palomares, 2001; Link and Ford, 2006; Uye, 2011); eutrophication (Arai, 2001; Purcell et al., 2001); hard substrate additions (Dong et al., 2010); transport of non-indigenous species (Graham and Bayha, 2007); aquaculture (Brotz et al., 2012) and climate change (Mills, 2001; Licandro et al., 2010; Purcell, 2012). Hamner and Dawson (2009) used taxonomic and molecular data to evaluate the phylogenetic distribution of bloom taxa. They found that most bloom species fall within the order Scyphozoa, feed exclusively on small prey, do not require a metagenic life cycle, and are usually members of a diverse group. They also found that mid-water, deep-sea and epibenthic medusae rarely bloom or swarm; neither do large carnivores that feed on large prey.

Condon et al. (2012, 2013) undertook a meta-analysis of global jellyfish data to assess whether or not jellyfish are increasing in abundance across the world's oceans. By using long-term empirical data, instead of anecdotal evidence, they found that jellyfish blooms are subject to episodic, global oscillations with a periodicity of approximately 20 years. An exception to their 'peak-and-trough' findings was a slight increase in abundances after 1970; a shift that cannot yet be explained without sustained monitoring over a longer timescale to infer the context of such a rise.

1.1.2 Biology and relationships of medusae

Jellyfish are the predatory medusa stage produced by certain cnidarians (Arai, 1997). Most are pelagic although there are some exceptions (e.g. staurozoans). Medusae are characteristic of the Medusozoa which includes the Hydrozoa, Scyphozoa, Cubozoa (A. Collins, 2002). Recent phylogenomic analyses place Staurozoa as sister to Scyphozoa and Cubozoa in the Acraspeda, which together with Hydrozoa comprise the Medusozoa (Kayal et al. 2018).

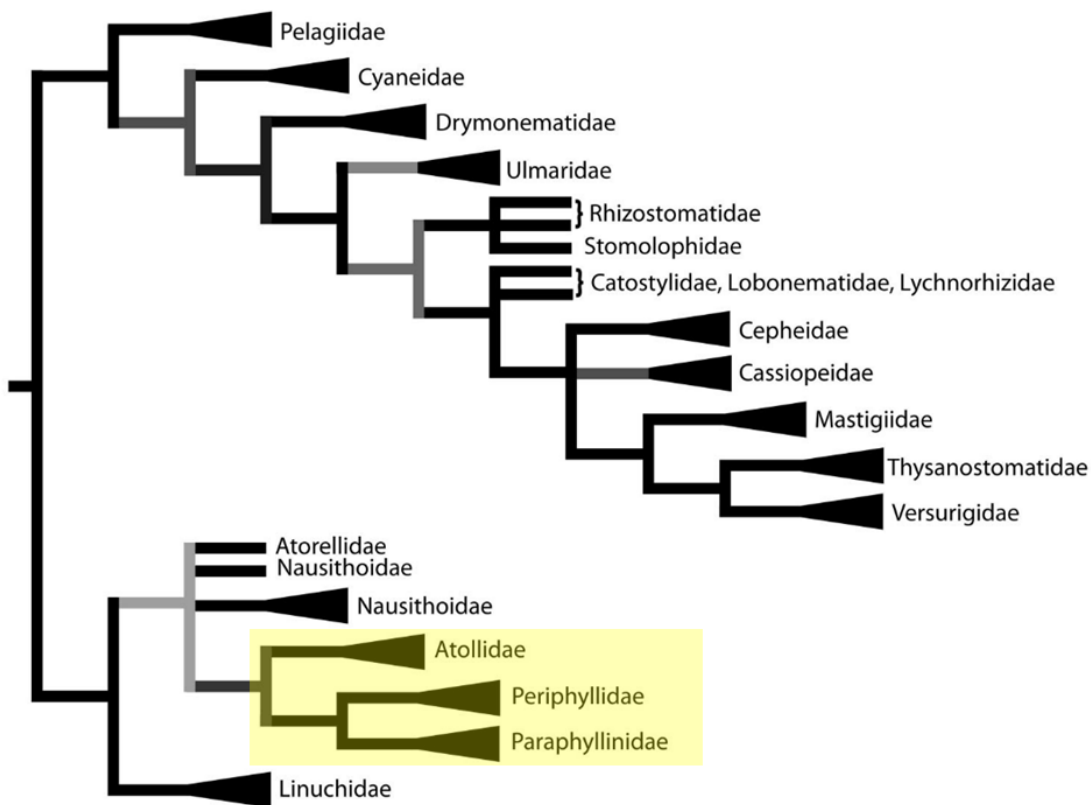


Figure 1.1 Phylogenetic relationships within the Scyphozoa based on 18S small subunit and 28S large subunit ribosomal RNA sequences, with deep-sea coronate species highlighted in yellow. Adapted from Bayha and Dawson (2010).

The Atollidae and Periphyllidae families are considered to be reciprocally monophyletic groups within the order Coronatae (Bayha et al., 2010), with Atollidae derived from an earlier lineage to Periphyllidae. Periphyllidae and Paraphyllinidae are sister groups derived from a common ancestor (Figure 1.1). Resolution within the Coronatae however is poor, particularly amongst the deep-sea medusae where the data are not as readily available as for the shallow species such as *Linuche* and *Nausithoe*. Successful sequencing of *Atolla* specimens has been particularly low (Lindsay, 2018), limiting the current phylogenetic understanding of the coronates.

Pelagic medusae swim using muscles and their highly elastic mesoglea to contract and expand their bell-shaped bodies pushing water behind them (Costello and Colin, 1995). Statocysts serve as sensors for detecting gravity or inertia and so are used for navigation and orientation (Spangenberg and Jernigan, 1994; Becker et al., 2005). The structure and function of statocysts is similar to otoliths in the ears of fish and mammals (Mendoza, 2006).

Chapter 1

As the medusa moves, dense statoliths contained within the statocysts brush against mechanoreceptor cells (also called ‘hair cells’) on the touch plates, sending signals to neurons (Sötje et al., 2011).

Jellyfish traits including rapid growth, high fecundity and early maturation have been interpreted to reflect adaptations to unpredictable and ephemeral environments (Deibel and Lowen, 2012). Indeed, their capacity to form mass aggregations, or ‘blooms’, demonstrates that jellyfish are opportunistic organisms that respond rapidly to variable food environments often in conditions that are too hostile for other organisms (Dong et al., 2010). In coastal areas with elevated nutrient levels and low oxygen concentrations, jellyfish populations can reach vast sizes (Malej et al., 2012). Their structural simplicity may permit these gelatinous fauna to quickly adapt to changing environments, often via phenotypic plasticity (Nawroth et al., 2010). Plasticity in traits such as feeding, physiology, reproductive output, somatic growth and size are common and allow populations to persist (Lucas and Dawson, 2014). Plasticity also enables many species to become invasive, capable of reaching great numbers and outcompeting native species (Bayha and Graham, 2014). The classic example of an invasive jellyfish species is the ctenophore, *Mnemiopsis leidyi* Agassiz, 1865, which was accidentally introduced to the Black Sea through ballast water (Zaitsev, 1992; Kideys, 1994; Shiganova, 1998) and decimated local fish stocks through efficient predation of zooplankton. Other examples include the scyphozoan jellyfish *Phyllorhiza punctata* Lendenfield, 1884 (Doty, 1961; Devaney and Eldredge, 1977), *Aurelia aurita* Linnaeus, 1758 (Dawson and Jacobs, 2001; Schroth et al., 2002), *Cassiopea* spp. Péron and Lesueur, 1810 (Holland et al., 2004), and the hydrozoan *Blackfordia virginica* (Mills and Sommer, 1995).

Jellyfish medusae have the capability to shrink during periods of adversity, to subsequently regrow, and to heal injuries and regenerate lost body parts (Goldstein and Riisgard, 2016). These processes are difficult to identify and monitor within wild populations, and so along with phenotypic plasticity contribute to taxonomic confusion. Shrinkage of jellyfish appears to relate to the fact that medusae contain approximately half the lipid content (% ash-free dry weight, AFDW) of other pelagic taxa (Clarke et al., 1992). When food is scarce, medusae lack the lipid resources to sustain their mass, so instead catabolise their own tissue to reduce in size (Hamner and Jenssen, 1974; Arai et al., 1989). Within the Scyphozoa, *Cassiopea* sp. can shrink by up to 99% (Mayer 1910, see Pitt et al. 2014), and *Aurelia aurita* by up to 75% (Hamner and Jenssen, 1974). However, the hydromedusan *Cladonema californicum* Hyman,

Chapter 1

1947 increases in diameter following periods of adversity, despite losing 69-77% of its dry mass (Costello, 1998). Shrinkage can cause a reduction in bell diameter which compromises the ability to swim. Unlike shrinkage, the regeneration of injuries and body parts can be recognised by scarring (Pitt et al., 2014). The same body part can be regrown multiple times (Zeleney, 1907).

Reproduction in many jellyfish (Rottini Sandrini and Avian, 1991a; Lucas and Reed, 2010) appears to occur year round as oocytes in all stages of maturation are observed throughout the year. Scyphomedusae eggs are usually retained in the gastrovascular cavity or are attached to the fringes of the oral tentacles, although the coronate *Linuche unguiculata* Schwartz, 1788 sheds its eggs directly into the surrounding water (Berrill, 1949). Direct development in deep sea jellyfish involves the production of few large oocytes which may be provisioned by yolk (Eckelbarger & Larson 1992) and wandering nurse cells (trophocytes) (Tiemann and Jarms 2010). The rate of egg production is linked to changes in environmental conditions, specifically depth inhabited. Larson (1986) speculated that mesopelagic coronates produce eggs very slowly (a few eggs per day). This contrasts greatly with the epipelagic *L. unguiculata*, which can produce over 100 eggs per day (Kremer et al., 1990). The large, slowly formed eggs of the deep-sea species develop holopelagically from egg to medusa. Deep-sea jellyfish are generally considered to have atypical scyphozoan life cycles because they involve reduced and/or parasitic polyp stages or direct holopelagic development with no polyp stage (Russell, 1953; Kramp, 1961; Osborn, 2000; Lucas and Reed, 2009).

Determining the age of jellyfish is of great interest as this would provide insights into population structure, demography and longevity. The traditional method for determining age in Scyphozoa is through the measurement of bell diameter, however this is not a robust method in view of their capacity for shrinking and regrowing. The lack of adequate ageing techniques has limited the scope for jellyfish population research, however there is growing interest in the use of statoliths for this purpose. Statoliths are the only hard structures within jellyfish and are unlikely to be subject to shrinkage and regrowth. Statoliths have thus been adopted as a more robust proxy for age than bell diameter. Cubozoan and scyphozoan statoliths are made of calcium sulphate hemihydrate ($\text{CaSO}_4 \cdot 0.5\text{H}_2\text{O}$), or 'bassanite', a dehydrated phase of gypsum. Bassanite is rare in biological systems (Tiemann et al. 2002, 2006) and cannot be crystallised from aqueous solution except at high temperatures or at

high salinity. As it is a dehydrated phase of gypsum, discovering this substance within an organism made up of mostly water was surprising. The crystals must be permanently protected against the aqueous environment in order to prevent hydration. The statoliths of hydrozoans are made of calcium magnesium phosphate ($\text{CaMg}[\text{PO}_4]_2$).

The accretion of hard structures in cubozoan statocysts provides an established means of determining the age of medusae within this class. The approach is essentially that of sclerochronology (also referred to as osseochronometry) which measures or estimates ages or time intervals from the growth patterns of mineralised biogenic deposits of animals or plants. Cubozoan statoliths change over time from isolated prismatic crystals to an ellipsoid concretion. As outlined by Ueno et al. (1995), cubozoan statoliths are similar to fish otoliths with calcium accreting to produce distinct layers. This and a number of studies have established that in cubozoans one concentric ring of bassanite corresponds to one day (Tiemann et al., 2006a; Kingsford and Mooney, 2014). The bassanite rings can then be counted using a light microscope and oil immersion. By calculating the age of individual box jellyfish medusae such as *Chironex fleckeri* Southcott, 1956, ecological insights can be gathered relating to temporal variation in medusae growth, development and population structure. In areas significantly affected by so-called 'sting seasons' such as the Australian tropics, these insights could have a significant impact on the way in which coastal areas are managed.

Scyphozoan statocysts contain multiple statoliths that increase in size and number as the medusa develops. Hopf and Kingsford (2013) investigated the link between an increase in statolith number and development of laboratory-reared individuals of *Cassiopea* sp. They deduced the number of statoliths by manually counting light micrographs of statoliths liberated from statocysts. Statolith number provided less accurate estimates of age than bell diameter under constant conditions. However, as bell diameter is subject to great change under varying conditions their study suggests further exploration of the use of statoliths as proxies for age is merited. Other proxies for determining age in jellyfish, such as the number of radial canal branching points (Iyake et al., 1997) and ATP-related compound concentrations (Ishii et al., 1995; Lucas, 2001) have been dismissed due to their low levels of accuracy.

1.1.3 Macroecology of gelatinous zooplankton

There are few long-term, large-scale data regarding the distribution and abundances of gelatinous zooplankton (see Brodeur et al., 2002; Condon et al., 2012; Lucas et al., 2014). Commercial fishing catch datasets provide an invaluable resource for assessing fish stocks. Unfortunately, jellyfish have historically been discarded from fishing catch records due to a lack of taxonomic knowledge and interest. This coupled with a general lack of interest in jellyfish has resulted in only a small number of macroecological studies centred on jellyfish. However, recent heightened public and scientific interest as a result of jellyfish bloom events has led to further investigation of jellyfish macroecology. The Global Jellyfish Project, a recent meta-analysis conducted by Condon et al. (2012, 2013), was the first macroecological study of this kind. The study used large-scale temporal and spatial information on jellyfish catches and sightings from a range of sources to infer whether or not bloom populations are increasing. A subsequent study by Lucas et al. (Lucas et al. 2014) compiled gelatinous zooplankton abundance data (for Cnidaria, Ctenophora and Thaliacea) from the Jellyfish Database Initiative (JeDI, accessible at <http://jedi.nceas.ucsb.edu>) spanning 1934 to 2011. This high resolution dataset (91,765 quantitative abundances within the upper 200 m covering 33% of the total ocean area) indicated increases in biomass at higher latitudes in the Northern and Southern Hemispheres. In more data-rich areas such as the North Atlantic, significant positive relationships were variously observed between biomass and apparent oxygen utilisation, sea surface temperature and areas of low productivity.

Citizen science-based marine studies are on the increase (Silvertown, 2009) and can be informative. For example, studies based on citizen science data on turtles (Witt et al., 2007), basking sharks (Leeney et al., 2008) and cetaceans (Pikesley et al., 2012) were able to identify significant spatial and temporal trends, and provide insights into larger-scale distributions.

Pikesley et al. (2014) demonstrated the efficacy of citizen science in a jellyfish-driven macroecological study. Using coastal sightings collated over a period of nine years by the Marine Conservation Society, Pikesley et al. (2014) provided a detailed account of the occurrences of six scyphozoan and two hydrozoan species in UK waters. The resolution of the data was high enough to demonstrate seasonality in sightings, however it was not sufficient to demonstrate correlations with e.g. large-scale climatic variability (here the North Atlantic Oscillation, NAO). This study established the potential of using citizen science to contribute to existing jellyfish databases to identify large-scale patterns. However, it is

also noted that citizen science should be used cautiously, particularly when no degree of effort is recorded. Furthermore, the observations of the taxa in citizen science studies are likely mostly to be restricted to the coasts. There is also likely to be a bias in the more conspicuous beach strandings than pelagic taxa (Pitt et al., 2014). Ultimately, such studies are restricted to conspicuous, shallow-water species that can be sighted by non-scientists around the coast. Observations of deep-sea species are essentially dependent on participation in research cruises and examination of museum collections to obtain data for meaningful macroecological study. At present such macroecological studies of deep sea gelatinous zooplankton are lacking.

1.2 The study organisms

Periphylla and *Atolla* are deep-sea scyphozoan medusae belonging to the order Coronatae. The coronate jellyfish are composed of five families, Linuchidae, Nausithoidae, Paraphyllinidae, Atollidae and Periphyllidae (Arai, 1997; Jarms et al., 2002). The latter three families are comprised of exclusively deep-sea species. Species of the Nausithoidae are found in both shallow and deep waters while those belonging to the Linuchidae occur in shallow waters (Jarms et al., 1999; Morandini and da Silveira, 2001). A sixth coronate family, Atorellidae, has been proposed (Hale, 1999; Eggers and Jarms, 2007; Bayha et al., 2010), but has not been formally accepted (Mills et al., 1987; Lucas and Reed, 2010). The genus *Atorella* has been placed within both the Atorellidae (Jarms et al., 2002) and the Nausithoidae (Mills et al., 1987). Phylogenetic relationships amongst the coronates are not well resolved and no strong evidence for or against reciprocal monophyly for Atorellidae can be determined (Bayha et al., 2010).

The coronate jellyfish are recognised by the coronal groove; a deep furrow dividing the exumbrella about midway into a central disc and a peripheral zone (Morandini and Jarms, 2005). The peripheral zone, a scalloped bell beneath the furrow, is comprised of peripheral thickenings of jelly, pedalia (Figure 1.2). A single tentacle and marginal sense organ is associated with each pedalion. The stomach is attached to the subumbrella over four triangular gastric septa fusion areas, with radial septa in the gastrovascular sinus and simple lips (Russell, 1970; Arai, 1997). The most extensive descriptions of the Coronatae to date are by Russell (1970) in his book entitled *The Medusae of the British Isles, Volume II*.

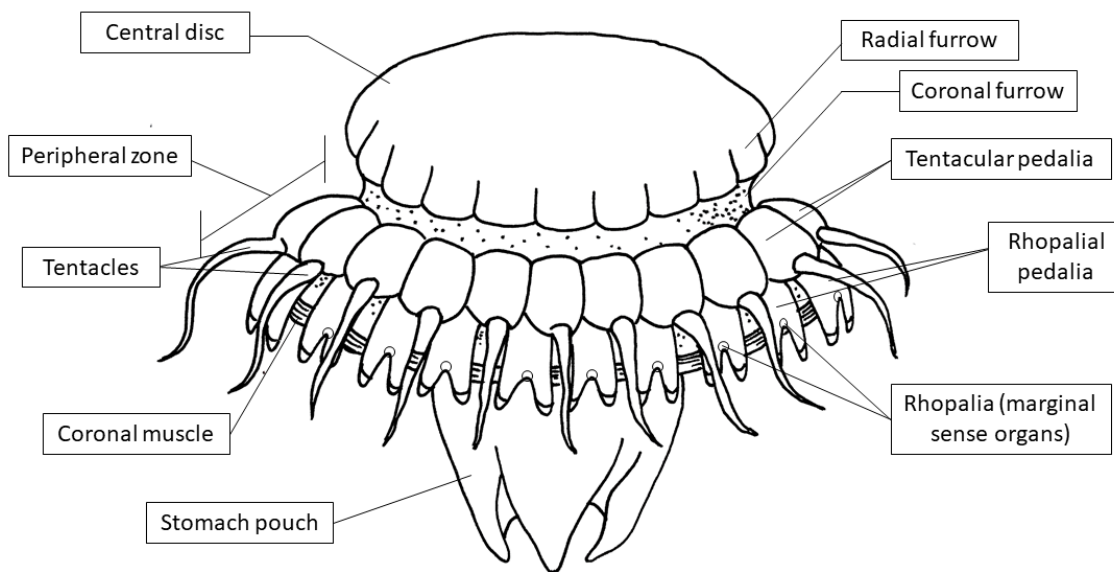


Figure 1.2 Diagram of key external morphological landmarks within deep-sea coronates, here using *A. wyvillei* as an example. Illustration by author.

P. periphylla has been the most frequently studied coronate due to the high concentrations of medusae in various Norwegian fjords (Fosså 1992; Sørnes et al., 2007). It comprises the only recognised species within the genus *Periphylla*. Much less is known about the biology and ecology of species of *Atolla* beyond Russell's early descriptions (1959, 1970). Species of both *Periphylla* and *Atolla* are viewed to have cosmopolitan distributions, to occur at mesopelagic and bathypelagic depths (200 – 4000 m), to participate in diel vertical migration for feeding and mating purposes (Kaartvedt et al., 2007; Youngbluth et al., 2008), and can be found at the surface during periods of darkness (Kaartvedt et al., 2007). Abundances of *P. periphylla* have been estimated to range from 1 ind 1000 m⁻³ to 2 ind 100 m⁻³ (Pages et al., 1996; Dalpadado et al., 1998; Youngbluth et al., 2008)

As deep-sea species that live outside the photic zone (apart from at night), *Periphylla* and *Atolla* are covered in a dark red pigment, protoporphyrin. This pigment camouflages their presence at depth, and also masks shorter light wavelengths of any ingested bioluminescent prey (Jarms et al., 2002). Porphyrin is photoreactive, and when exposed to light will transform into compounds highly toxic to the organism, causing tissue damage (Arai, 1997). *Periphylla* and *Atolla* are negatively phototactic, and only breach the epipelagic zone during periods of darkness, such as night or winter at higher latitudes (Youngbluth and Båmstedt, 2001).

Chapter 1

Deep sea coronate medusae are also bioluminescent. Laboratory tests demonstrate bioluminescence typically results in response to mechanical stimulation equivalent to contact with another organism (Herring and Widder, 2004). Bioluminescence can be in the form of a brief flash of blue light ($\lambda_{\text{max}} = 470 \text{ nm}$), propagated waves, or as a bioluminescent secretion, which acts to confuse predators (Haddock and Case, 1999). The production of light in coronates is assumed to be restricted to defense against visual predators (as opposed to luring prey), as light is only produced in response to external stimuli (Morin, 1983; Herring and Widder, 2004).

Studies on *P. periphylla* have revealed a number of behavioural traits relating to feeding, mating and responding to stimuli. Using ROV video footage and observing individuals *in situ*, Sötje et al. (2007) identified eight different tentacle postures, which reflected different situations. The dominant position observed during the day was motionless with tentacles posed straight upwards, extending to the oral-aboral body axis. After dusk, medusae were observed contracting their swimming bell continuously. If threatened, *P. periphylla* were seen to tuck all of their relatively few tentacles inside the stomach pouch, presumably to protect their tentacles from either light or physical damage (Youngbluth and Båmstedt, 2001).

P. periphylla are considered to be voracious predators, using different predation techniques depending on the size of the medusa (Sötje et al., 2007). Smaller medusae, which have a more oblate body shape and a less pronounced vertical migration, act as cruising predators, with their closely spaced tentacles poised downwards towards the stomach (Jarms et al., 2002). Larger medusae, which have the ability to travel greater vertical distances, alternate between ambush and 'ramming' predation strategies (Youngbluth and Båmstedt, 2001; Sötje et al., 2007). During 'ramming' periods, as described by Raskoff (2002), the tentacles are held stiffly upwards away from the stomach during slow swimming. This mode reduces the degree of turbulent disturbance that could alert potential prey (Sørnes et al., 2007; Klevjer et al., 2009).

The diet of *P. periphylla* medusae is dominated by faster, larger prey (Larson, 1979; Madin, 1988; Fosså, 1992; Youngbluth and Båmstedt, 2001; Klevjer et al., 2009), and is limited by tentacle density and spacing, and the properties of nematocysts (Madin, 1988). *P. periphylla* tentacles are strong and easily coil around prey items, which are then transferred into its

relatively large mouth (Sötje et al., 2007). Large and active prey types have been found within the stomach contents, including crustaceans, squid and fish (Larson, 1979). Fosså (1992) found two large copepod species (*Calanus finmarchius* Gunnerus, 1770 and *Euchaeta norvegica* Boeck, 1872) in the stomach pouch of medusae. Youngbluth and Båmstedt (2001) discovered large copepods, large ostracods (*Conchoecia*), chaetognaths and krill (*Maganyctiphanes norvegica* Sars, 1857) within the stomachs of *P. periphylla*.

There are no reliable assessments of *Atolla* spp. diets, as ROV observations and targeted sampling are lacking for this genus. *Atolla* spp. are found at greater depths than *P. periphylla* in the ocean and have not been found in easily accessible fjords. Gut contents from trawled and net-caught specimens are considered unreliable estimates of typical prey types and volumes, as studies on trawled medusae suggest an atypically high level of prey in the stomach pouch as a consequence of the availability of prey items in the net (Youngbluth and Båmstedt, 2001). Larson (1979) suggests that *Atolla* spp. and *P. periphylla* are likely to share the same feeding strategies as other coronates because the coronal groove acts as a hinge during swimming and feeding. However, Madin (1988) proposed that prey items captured by *Atolla* spp. would differ from those captured by *P. periphylla* due to the differences in tentacle number, strength, density and spacing.

The diel vertical migration of *Periphylla* and *Atolla* is believed to facilitate feeding and mating (Kaartvedt et al., 2007). The upper 200 m of the water column is the area of greatest productivity and feeding on food sources in this region can occur at night, thus avoiding phototoxic effects. Migrating upwards at night towards the surface also increases the chances of encountering a mate (Youngbluth and Båmstedt, 2001). Accordingly, larger, sexually mature medusae have more pronounced vertical migration patterns (Sørnes et al. 2007). Vertical migration may explain why all stages of development within the coronates are present throughout the year (Jarms et al., 1999). Tiemann et al. (2009) observed individuals of *P. periphylla* aggregating at night, often engaging in contact with another through tentacle entanglement. This mating strategy is similar to the “wedding dance” observed in a number of cubozoans (Lewis and Long, 2005). It is through this entanglement that the spermatozooids are presumably transferred into the stomach of the female for internal fertilisation, based on circumstantial evidence of other species of medusae (Werner, 1980; Yamaguchi and Hartwick, 1980; Hartwick, 1991; Williamson et al., 1996).

Molecular analyses on *Atolla* and *Periphylla* have been incorporated into studies that served to further understand basic metazoan lineages (Medina et al., 2001), evolution amongst gelatinous zooplankton (Bayha and Dawson, 2010) and identify cryptic species and further the understanding of phylogenetics and speciation amongst jellyfish (Ortman et al., 2010). Relatively recent exposure of cryptic jellyfish species using molecular methods has increased the predicted scyphozoan species richness figures up to tenfold (Holland et al., 2004; Hamner and Dawson, 2009).

1.2.1 Current classification of *Periphylla* and *Atolla*

Periphylla

Figure 1.3 provides a general view of features morphological features of *Periphylla* and *Atolla*. Both *Periphylla* and *Atolla* have been subject to taxonomic revisions. The early descriptions of *Periphylla* included several distinct morphological species, including *P. hyacinthina* Steenstrup 1837, *P. dodechabostrycha* Brandt 1838, *P. regina* Haeckel 1880 and *P. mirabilis* Haeckel 1880 (Broch, 1913). However, Mayer (1910) deduced that the size and shape of *Periphylla* medusae change with age. He thus equated growth stages to early-described species as follows: medusa up to 35 mm diameter represented '*P. dodechabostrycha*', medusa up to 80 mm diameter represented '*P. hyacinthina*', and medusa up to 200 mm diameter represented '*P. regina*' (Stiasny, 1934; Bigelow, 1938). As a consequence, there is now one recognised species - *Periphylla periphylla*. Occasionally reference to the early-recognised species is used to clarify the size and bell shape of medusae (Russell, 1970). Jarms et al. (2002), however, has commented that more than one species may well exist within the genus *Periphylla*, although this has not yet been established.

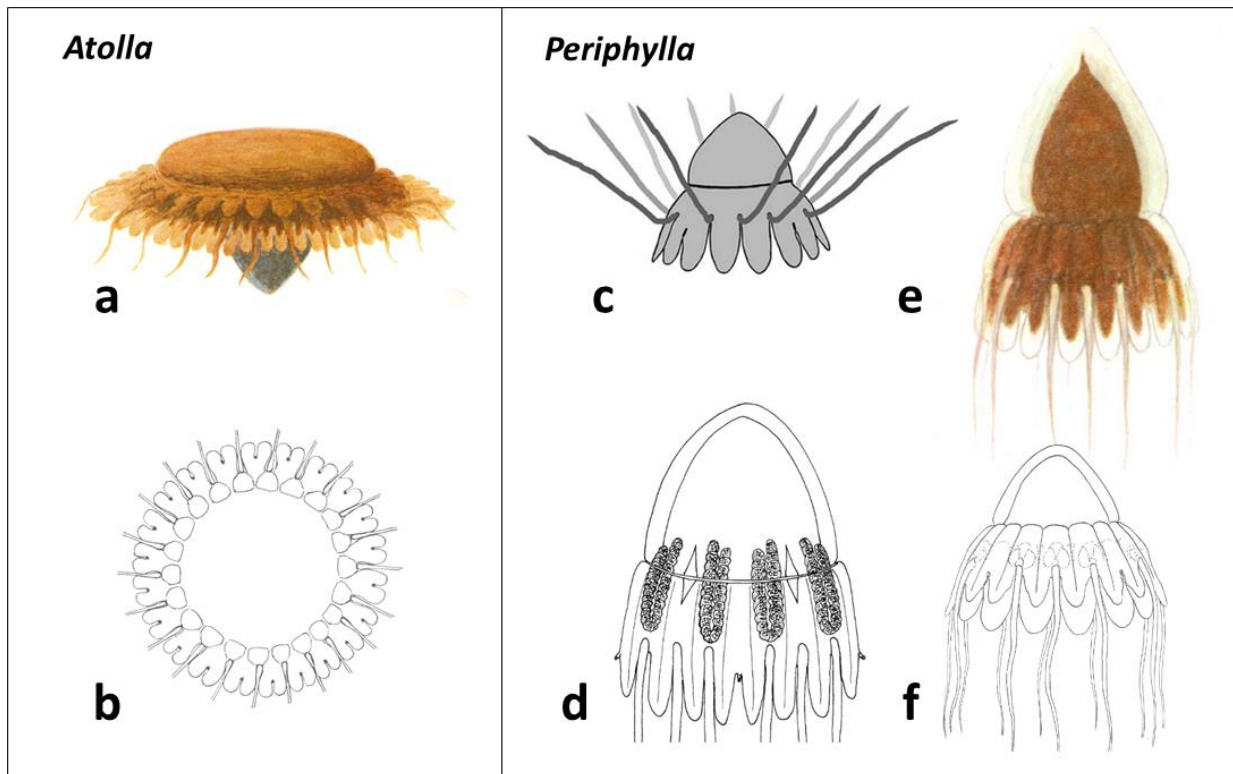


Figure 1.3 Diagrammatical representations of *Atolla* and *Periphylla* body shapes as found within the literature. *Atolla* is mostly depicted in dorso-ventral orientation due to its disc-like structure, with *P. periphylla* depicted in lateral orientation due to conical shape. a: *A. wyvillei* lateral view with pigmentation (Russell, 1970); b: *Atolla* genus dorso-ventral view (Russell, 1976); c: *P. periphylla* lateral view (Sötje et al., 2007); d: *P. periphylla* lateral view with gonads visible (Tiemann and Jarms, 2010); e: *P. periphylla* lateral view with pigmentation visible (Russell, 1970); f: *P. periphylla* lateral view (Russell, 1970).

Atolla

Atolla is currently recognised as having seven species: *A. vanhoeffeni* Russell, 1957, *A. wyvillei* Haeckel, 1880, *A. parva* Russell, 1958, *A. chuni* (Vanhöffen 1902), *A. russelli* Repelin, 1962, *A. tenella* Hartlaub, 1909, and *A. gigantea* Maas, 1897 (Russell, 1970). The cosmopolitan species, *A. wyvillei*, was formerly divided into three species, *A. wyvillei*, *A. verrillii* Fewkes, 1885 and *A. bairdii* Fewkes, 1886 (Vanhoeffeni, 1880; Maas, 1884). These three species were recognised in view of morphological variation on the upper part of the bell and the presence or absence of radial furrows on the crown when pressed with an instrument. However, Broch (1913) deduced that the distinguishing notches on the crown were simply related to contractions of the central disc and thus that at least *A. verrillii* and *A. bairdii* were the same species. When pressed, these notches would either manifest or not, depending on the state

of contraction when sampled. Larson (1986) noted that smaller specimens of *Atolla* were particularly hard to determine to species level due to their morphological similarities and thus large numbers of specimens were required to ensure species identity.

A visual representation of the respective *Atolla* species in diagrammatical and photographic form is presented in Figure 1.4 with key morphological descriptors. The key morphological descriptors are described in Table 1.1. The key features that were used to distinguish between the species were: *A. wyvillei* 22 tentacles, radial septa diverge towards the ends, clover-shaped stomach base, smooth marginal lappets; *A. gigantea* 24 and 28 tentacles, flat gonads, nearly straight radial septa, large species with mature medusae > 60 mm diameter; *A. chuni* 24 tentacles, endemic to Southern Ocean, marginal lappets have warts, scalloped margin of central disc; *A. russelli* 16-20 tentacles, radial septa straight, curving slightly at ends; *A. vanhoeffeni* 20 tentacles, base of stomach cross-shaped, eight black spots around the stomach ostia; *A. tenella* is endemic to the Arctic, with pairs of pigment spots around the margin of the umbrella. For *P. periphylla*, the medusae have 12 tentacles, 16 pedalial thickenings, and 4 marginal sense organs.

Early works by Haeckel (1881), Browne (1915), Stiasny (1934), Russell (1957, 1958, 1959, 1970), Kramp (1959; 1961; 1965) and Larson (1979, 1986) and Roe et al. (1984) have validated the specific characters of the deep-sea coronates (Table 1.1). Each subsequent piece of taxonomic work has built on the morphological descriptions, geographic distribution and functional biology of the previous. Larson (1986) undertook an extensive exploration of the Southern Ocean during the Eltanin cruises. Here 2390 specimens of *A. wyvillei*, 6 specimens of *A. vanhoeffeni*, 5 specimens of *A. parva*, 37 specimens of *A. gigantea*, 1168 specimens of *A. chuni* and 2305 specimens of *P. periphylla* were quantified and described, which has assisted not only the understanding of the various *Atolla* species, but also the distribution within a relatively poorly sampled area. More recent works on *Atolla* have focused predominantly on *A. wyvillei*, perhaps due to its broad geographic distribution and relatively large size. Such studies have included developments in the reproductive characteristics (Lucas and Reed, 2010), associated parasitism (Moore et al., 1993), bioluminescence (Haddock and Case, 1999) and habitats of mesopelagic scyphomedusae (Osborn et al., 2007).

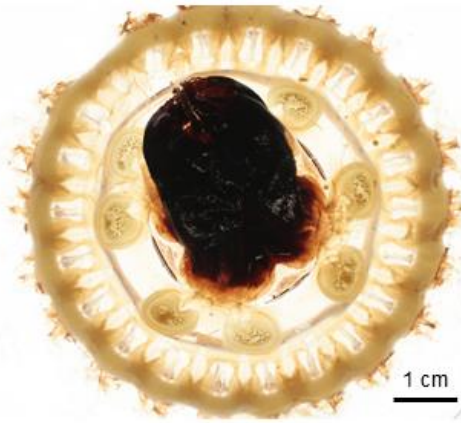
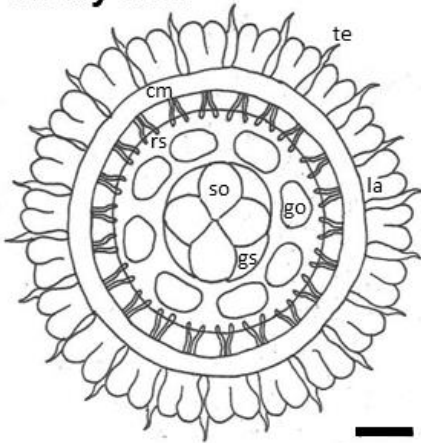
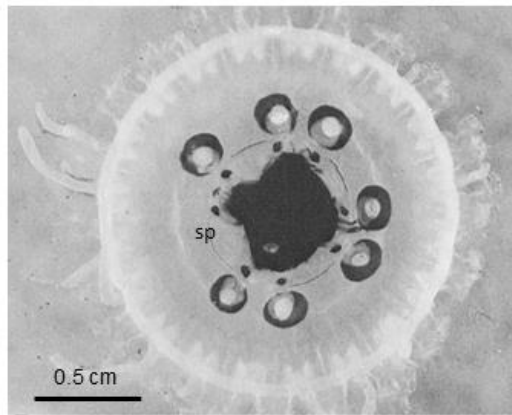
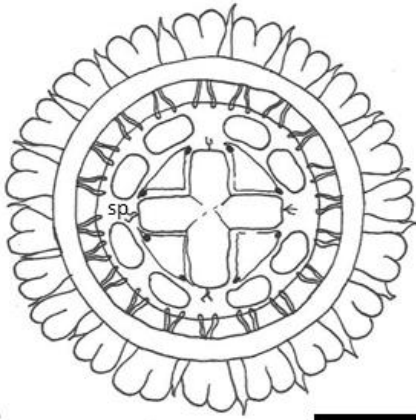
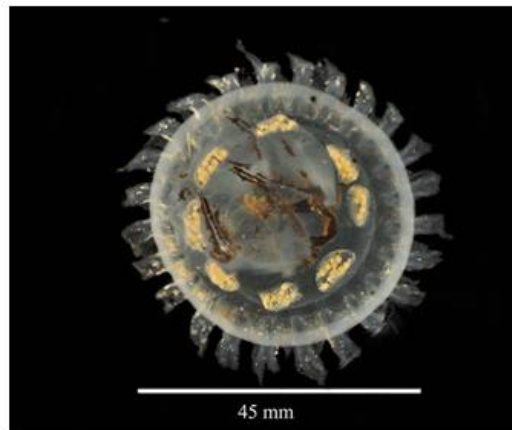
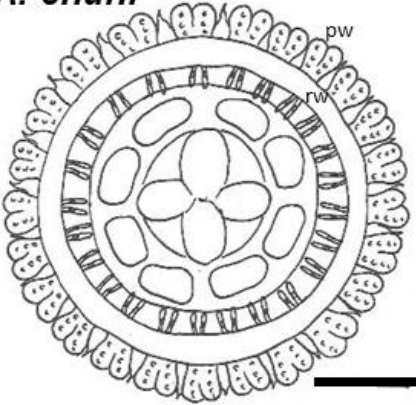
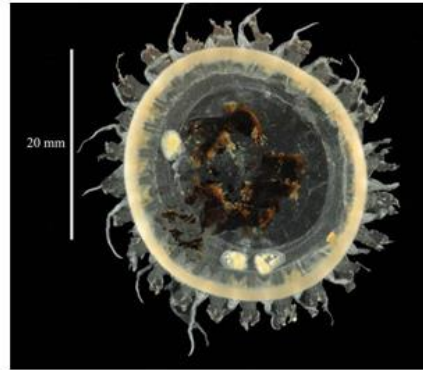
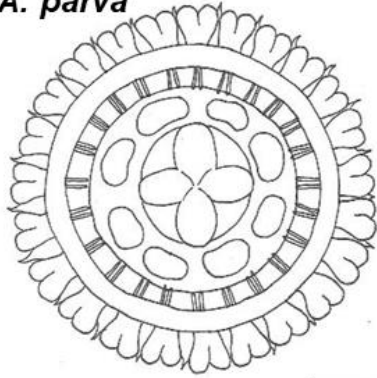
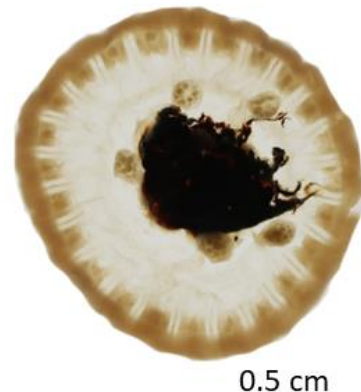
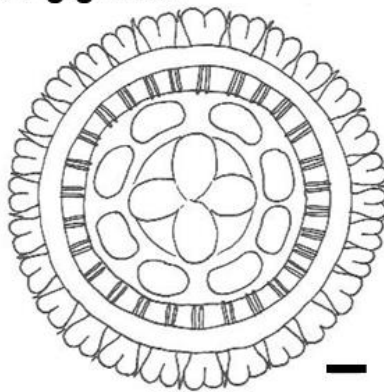
A. wyvillei***A. vanhoeffeni******A. chuni***

Figure 1.4 Composite drawings of *Atolla* specimens and photographs depicting key morphological landmarks for species differentiation. Scales marked for each species respectively. See accompanying table (Table 1.1) for further detail. Landmark key: *A. wyvillei* – te = tentacle, cm = coronal muscle, so = stomach ostia, gs = gastric sinus, go = gonad, rs = radial septa, la = marginal lappet; *A. vanhoeffeni* – sp = black spots around stomach ostia; *A. chuni* – pw = pedalial warts, rw = radial warts. Figure continued on following page. Photographs were available only for *A. tenella* and Super*Atolla* due to the paucity of data with which to draw composite drawings of the species. This species and potential species nova remain poorly understood and not yet fully documented. Drawings and photographs author's own with the exception of: *A. vanhoeffeni* photograph (Russell, 1970); *A. chuni* photograph (Smithsonian, available at: <https://www.gbif.org/occurrence/1320668521>);

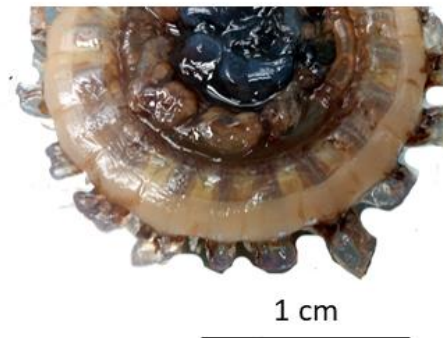
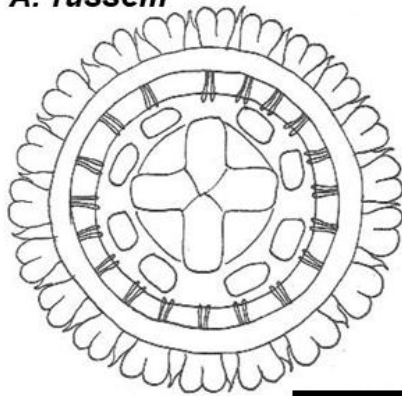
A. parva



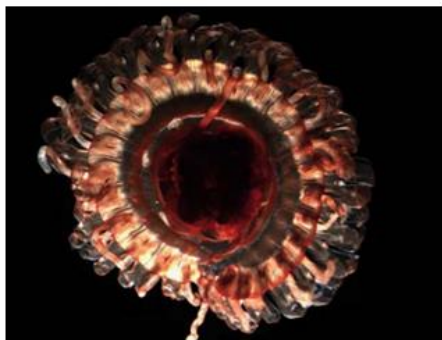
A. gigantea



A. russelli



A. tenella



'Super Atolla' (nov. sp.)



(Figure 1.4 continued.)

Table 1.1 Documented geographic occurrence, specific characters and key references for deep-sea coronates.

Species	Type locality (where known)	Holotype institute location (where known)	Documented geographic occurrence	Specific characters for identification	Key references	Additional identification comments.
<i>P. periphylla</i> Péron & Leseur 1810			Cosmopolitan distribution (Russell, 1970; Larson, 1984; Lucas and Reed, 2010).	12 tentacles. Size up to 350 mm diameter. 4 marginal sense organs (interradial, with 3 interjacent tentacles). 16 pedalial thickenings (12 tentacular, 4 thopalar).	Larson, 1984 Russell, 1970	Single species within the genus <i>Periphylla</i> . Previously described as consisting of the following species; <i>P.</i> <i>regina</i> Haeckel 1880, <i>P. mirabilis</i> Haeckel 1881, <i>P. dodechabostrycha</i> Haeckel 1880, and <i>P. hyacinthina</i> Steenstrup 1937. Larson (1984) noted that <i>P. periphylla</i> was cosmopolitan in deep oceans, except for the Arctic. Distinctive feature of the family is the interradial position of the four marginal sense organs, which differentiates it from the Paraphyllinidae which are perradial.
<i>A. vanhoeffeni</i> Russell 1957	Cape Basin, South Atlantic 47°S, 5.8°W	NHM London Catalogue number: 667130	Rockall Trough, NE Atlantic (Russell, 1957); Bay of Biscay; west coast of Africa (Repelin, 1962); Dutch East Indies (Maas, 1903); Cape of Good Hope (Stiasny, 1934); Pacific regions (Kramp, 1968).	20 tentacles, 20 marginal sense organs. Radial septa do not project centripetally beyond the coronal muscle margin, as with <i>A. parva</i> . Base of stomach cross-shaped, eight pigment spots on either side of each gastic ostium. Hypertrophied tentacle adjacent to an inward fold of the stomach.	Russell, 1958, 1970	Russell (1970) noted distribution is probably worldwide.
<i>A. tenella</i> Hartlaub 1909			Arctic Ocean (Raskoff et al. 2004).	Pairs of pigment spots round the margin of the umbrella.	Russell, 1970 Raskoff et al., 2004	Kramp (1961) listed as a synonym of <i>A.</i> <i>wyvillei</i> . However, Russell (1970) noted that is likely a separate species. <i>A. tenella</i> confirmed as separate species by Lindsay (2018, personal communication).

Species	Type locality (where known)	Holotype institute location (where known)	Documented geographic occurrence	Specific characters for identification	Key references	Additional identification comments.
<i>A. wyvillei</i> Haeckel 1880	Melbourne, 53°S, 108°E		Melbourne (53°S, 108°E) (Haeckel, 1880); Patagonia (42°S, 56°W) (Haeckel, 1880)	22 tentacles, 22 marginal sense organs. Mature specimens up to 150 mm diameter. Radial septa diverge widely towards the gastric sinus, with ends turning slightly in towards the end. Marginal lappets without warts. Hypertrophied tentacle adjacent to stomach interradius.	Russell 1959, 1970 Stiasny, 1934 Bigelow, 1913 Browne, 1910 Broch, 1913 Kramp, 1968	44 pedallial thickenings arranged in two series of equal number, the innermost being tentacular and the outermost rhopalial. Notches around the edge of the central disc, which if not apparent can be generated by pressing upon the central lens.
<i>A. gigantea</i> Maas 1897			Southern Ocean (Larson, 1986); Off coast of Brazil (Morandini, 2003).	24, 28 tentacles and marginal sense organs. Mature specimens over 60 mm diameter. Gonads flattened and nearly straight radial septa. Broad, flattened central disc.	Kramp 1961 Larson 1986	Previously regarded as a synonym of <i>A. wyvillei</i> (Larson, 1986).
<i>A. chuni</i> Vanhöffen 1902			Endemic to Southern Ocean (Russell 1970).	24 tentacles, 24 marginal sense organs. Marginal lappets have warts. Papillae present on exumbrellar side of rhopalial pedalia. Central disc vaulted, with scalloped margin. Mature gonads are trapezoidal, contiguous.	Russell, 1970 Stiasny, 1934 Browne, 1908 Mayer, 1910	Stomach margin with short, pigmented gastrodermal dendrites extending onto gastric septa (Larson, 1984).
<i>A. russelli</i> Repelin 1962			Japan Trench (Lindsay et al. 2004); Off coast of SW Africa (Russell, 1970).	16-20 tentacles and marginal sense organs. Radial septa straight, curving slightly at the ends, extending just to the end of the coronal muscle. Rectangular, bilobed gonads hang freely in the subumbrella cavity.	Russell, 1970	

(Table 1.1 continued).

incorporated into studies that served to further understand basic metazoan lineages (Medina et al., 2001), evolution amongst gelatinous zooplankton (Bayha and Dawson, 2010) and identify cryptic species and further the understanding of phylogenetics and speciation amongst jellyfish (Ortman et al., 2010). Relatively recent exposure of cryptic jellyfish species using molecular methods has increased the predicted scyphozoan species richness figures up to tenfold (Holland et al., 2004; Hamner and Dawson, 2009) (Figure 1.1).

1.3 Use of collections for ecological research

Museum collections offer an opportunity for macroecological investigations of deep-sea jellyfish. However, fixation of the material may alter the nature of the animals. In this section I review this issue. The primary aim of tissue fixation is to provide as much structural detail of the cells and cell components of the preserved specimen as possible. The maintenance of cell morphology is necessary so that maximum cellular detail may be observed in subsequent analyses (for example; staining for histological work; general morphological assessments). Historically, the most common fixative for specimen preservation is formalin, an aqueous solution of formaldehyde (CH_2O). A saturated solution contains 37% formaldehyde gas in water, plus a small amount of stabiliser (usually 10-12% methanol) to prevent polymerisation (Tucker and Chester, 1984). After fixation, the neutrality of formalin lasts only a short period; therefore buffers are required in order to maintain structural integrity of the specimens (Steedman, 1976). Different organisms require different preservatives and concentrations, and these may vary depending on the required period of preservation. Ethanol, Steedman's, gluteraldehyde and acrolein are other frequently used preservatives (Jones, 1976). Formaldehyde fixation for marine zooplankton is necessary for taxonomic and morphological studies, particularly when preserved for long periods of time (longer than 100 years) (Steedman, 1976). Formalin is the earliest form of preservative, and is used to a much lesser extent in present-day fixations due to the associated toxic properties (Fransway, 1991). As such, contemporary studies restrict formalin use to organisms that do not currently have a more suitable method of preservation.

During the 20th century studies on gelatinous zooplankton were limited to organisms that could be preserved in formalin (Haddock 2004). Purcell (1988) noted that in the case of fragile ctenophores, formalin preservation enabled more accurate and convenient sorting of species than studying and sorting the organisms live on-board a research vessel. Typically, the more robust species within the epipelagic zone undergo relatively little change with

preservation, with the more delicate deep-sea species presenting more of a challenge. The two deep-sea scyphozoan genera, *Periphylla* and *Atolla*, are atypically robust for their depth, which is perhaps attributed to their diel vertical migration. *Periphylla* and *Atolla* thus represent rare instances of cosmopolitan deep-sea jellyfish that can be analysed at surface level.

Atolla and *Periphylla* have been found to preserve well within various spirits. The bells of live *Atolla* and *Periphylla* adults have a very dark red or brown colouration, which changes to almost black upon preservation (Russell 1970). Vanhöffen (1902) and Stiasny (1934) noted that although these coronate medusae can be successfully preserved, it is rare to find a perfect specimen. The epithelium is very delicate and easily rubbed off, with fragments with pigments nearly always present at the bottom of preservation jars. The coronal muscle can also appear white or green in colour, but would normally be obscured on the subumbrella side by pigment (Russell, 1970). Russell (1970) established that specimens of *P. periphylla* retain their blackish colour after fifty years of preservation if kept away from light. Specimens kept in the light eventually become completely transparent.

Changes in medusa size and weight are documented to occur with formalin preservation (de Lafontaine & Leggett 1989). The mean umbrella diameter of *Staurophora mertensi* Brandt, 1835 and *Catablema vesicarium* Agassiz, 1862 respectively reduced to an average of 67.8% and 84.9% of the initial size after 154 days in 10% v/v formalin-seawater solution. Stabilisation in umbrella shrinkage occurred after 60 days, with no stabilisation in the mean wet weights after 154 days. Mean wet weights after the study period amounted to 30.5% and 37.9% of initial fresh weights of *S. mertensi* and *C. vesicarium*, respectively. Möller (1980) found that shrinkage in the umbrella diameter of *Aurelia aurita* varied between 15% and 28.6% after 42 days, and was greater for larger animals. Lucas (2009) noted that, the greatest reduction in bell diameter of specimens of *P. periphylla* preserved in gluteraldehyde was sustained in the largest individual (bell diameter = 42 mm fresh) at 28.6%, and that the medusae shrank by an average of 9.1% overall. There are no studies on how *Atolla* spp. change in size with preservation.

Chemical fixation of jellyfish is often essential for macro- and micro-scale analyses. Thus the degree of shrinkage is an important variable to consider when using preserved material for taxonomic and ecological studies. The value of morphometric studies will depend on the

accuracy and precision of measurements of the anatomy. Ideally, both pre- and post-fixation measurements would be taken, to eliminate error by shrinkage. Unfortunately, within museum collections, this is rarely possible. Therefore, care should be taken to standardise methods and preservatives so that the error associated with shrinkage and distortion is minimal (Tucker and Chester, 1984).

The means by which specimens are preserved will ultimately determine analyses that can be performed post-preservation. The study of nematocysts, for example, is hindered once preserved in ethanol, rendering the capsules opaque and hampering identification of nematocyst type (Mejía-sánchez et al., 2013). The use of buffers other than sodium glycerophosphate will dissolve the statoliths (calcium sulphate hemihydrate) when preserved in formalin (Petersen, 1976). A further concern may be whether formalin-fixed material is suitable for molecular analysis. Formalin is known to change the nucleoside content, especially deoxyguanosine (Bez-Ezra et al., 2010), and for the cross-linking of proteins, denaturation and methylation of nucleic acids (Bramwell and Burns, 1988). However, techniques for extracting DNA from formalin-fixed tissue are improving (see Palero et al., 2010; Taleb-Hossenkhani et al., 2013) and even fragmented DNA can be informative using new sequencing platforms, rendering museum collections potentially amenable for molecular analyses.

The robust nature of *P. periphylla* and *Atolla* spp. confers their long-term preservation in museum collections. Some shrinkage of specimens will ensue over time. However, all specimens within individual collections will typically experience the same conditions and thus the relative differences amongst specimens can be helpful for identifying taxa and gaining insights on relative size changes within taxa. Furthermore, experience gained by close inspection of extensive collections may also play an important role in identifying taxa and quantifying morphological change.

1.4 Aim and objectives of thesis

This thesis aims to investigate the comparative biology and macroecology of *Periphylla periphylla* Péron and Lesueur, 1810 and *Atolla* spp. coronate species across a global scale, using specimens from both oceanic and fjord environments. *P. periphylla* and *Atolla* spp. are the most recognised deep-sea jellyfish, and both have apparent cosmopolitan distributions. Little remains known about these genera beyond the early descriptions of the species, particularly relating to their macroecology and the expression of plastic traits according to varying environments. This study presents a large volume of morphological data using museum collections genera in order to better describe morphological variation on a global scale and to examine what factors might drive such variation. The Discovery Collections at the Natural History Museum London represent a vast and largely untapped ecological dataset. Russell (1953; 1970) utilised the Discovery scyphozoan collections material to produce early descriptions of *Periphylla* and *Atolla*. Few subsequent studies on coronate jellyfish have subsequently been undertaken and no studies have investigated the distribution and ecology of *Atolla* and *Periphylla* across large temporal and spatial scales. The following objectives are addressed:

- Take advantage of under-exploited museum collections to characterise broad scale patterns of morphological variation over space and time and identify drivers of morphological variation.
- Characterise the comparative biology of coronates along depth gradients using museum collections.
- Contrast the biology of coronates in fjord settings with that in oceanic environments using museum collections and newly sampled material.
- Explore a new method to determine the age of jellyfish.

The aim and objectives will be addressed through five chapters that focus on: distributions and morphological variation of coronates at a global scale (Chapter 2); morphological variation of *P. periphylla* and *Atolla* spp. over time within well-sampled regions (Iberian and Western European Basins; Chapter 3); depth-related variation in the morphology and reproduction of *P. periphylla* and *Atolla* spp. within one oceanic area (Porcupine Abyssal Plain; Chapter 4); comparing the biology of *P. periphylla* in unusual fjord conditions with that of oceanic populations at similar latitudes (Chapter 5). A final chapter (Chapter 6) explores

Chapter 1

a new method for inferring jellyfish ages based on sclerochronology of statoliths. Specific hypotheses that address the above over-arching objectives will be addressed within the individual chapters.

Chapter 2: Analysis of the global species distributions of the deep-sea coronate jellyfish, *Periphylla periphylla* and *Atolla* spp.

2.1 Abstract

Despite an increase in the number of marine macroecological studies in recent years, little remains known about the deep-sea pelagic fauna; with deep-sea jellyfish particularly poorly understood. The majority of ecological information collected on deep-sea jellyfish has been focused on contained, fjord environments. This study set out to generate a better understanding of the deep-sea coronate jellyfish *Periphylla periphylla* and *Atolla* spp. using museum collections from the Natural History Museum (NHM) London, the Smithsonian and the Global Biodiversity Information Facility (GBIF) to identify macroecological trends in distribution and morphology. Seven species of *Atolla* were found to occur, *A. gigantea*, *A. parva*, *A. russelli*, *A. wyvillei*, *A. chuni*, *A. vanhoffeni* and *A. tenella* as well as *P. periphylla*. The results of the study confirmed that *A. wyvillei* and *P. periphylla* have truly cosmopolitan distributions, which previously was largely speculative. *A. gigantea*, *A. parva*, *A. russelli* and *A. gigantea* exhibit broad global distributions, with *A. chuni* endemic to the Southern Ocean and *A. tenella* located within the Arctic only. All species exhibit broad vertical distributions within the water column, indicative of their diel vertical migration patterns, with *Atolla* species found at greater overall average depths than *P. periphylla* (*Atolla* spp. mean = 1007, n = 1234; *P. periphylla* mean = 645, n = 1596). No latitudinal gradient in the size of medusae was observed across the global dataset, however the occurrence of the larger species were found to be significantly correlated with variation in zooplankton diversity and chlorophyll-*a* levels. The development of new pedalia is observed within *Atolla*, which has not previously been described within the literature.

2.2 Introduction

Building up an understanding of the distributions of marine taxa is notoriously more difficult than within terrestrial environments due to the absence of conspicuous barriers with which to define species boundaries. Typically, marine distribution studies are more biased towards the benthic and shallow-water taxa due to the increased sampling ease and more conspicuous presence of the fauna. Benthic taxa distribution studies using quadrat-based sampling and ocean-floor mapping have increased the effects of climate change and ocean acidification on calcifying organisms such as the Mollusca (see Brandt et al., 1997; Olabarria, 2005). Determining the abundance and distributions of medusa populations is fundamental to understanding the roles of jellyfish within marine food webs and material cycling in the ocean (see Olesen et al., 1994; Purcell 2003; Lynam et al., 2005; Uye & Shimauchi 2005; Decker et al., 2007). The number of shallow-water distribution and abundance studies on jellyfish is proportionally higher than their deep-water counterparts (Mills, 2001; Graham et al., 2003). This is likely due to the number of anthropocentric interactions often with negative associated impacts that has furthered the knowledge (see Doyle et al. 2007; Purcell 2012). Such studies have increased the general understanding of the shallow-water medusae, including the presence of cryptic species (Lyake et al., 1997; Dawson and Jacobs, 2001), the colonisation of invasive species (Fuentes et al., 2010; Lehtiniemi et al., 2011; Bayha and Graham, 2014), and the phylogeography and phenology of various coastal species according to varying environmental conditions (Holland et al., 2004; Ramšak and Stopar, 2007).

P. periphylla and *Atolla* spp. are the most recognised deep-sea jellyfish, with both described as having cosmopolitan distributions (Youngbluth and Båmstedt, 2001; Tiemann et al., 2009; Tiemann and Jarms, 2010). The extent of these cosmopolitan distributions is yet to be described fully on a global scale, particularly for *Atolla*. Oceanic abundances of *P. periphylla* are estimated to be in the region of 1 ind 1000 m⁻³ to 2 ind 100 m⁻³ (Pages et al., 1996; Dalpadado et al., 1998; Youngbluth et al., 2008). Both genera are found at mesopelagic and bathypelagic depths (200 – 4000 m), participate in diel vertical migration for feeding and mating purposes (Kaartvedt et al., 2007; Youngbluth et al., 2008), and can be found as shallow as the surface during periods of darkness (Kaartvedt et al., 2007). Aside from the earlier work by Russell (1970), the majority of studies on deep-sea jellyfish have been centred on *P. periphylla* within Norwegian fjords, due to the mass aggregations found at a

number of localities. Studies within these fjords have increased the knowledge base on jellyfish as top predators (Klevjer et al., 2009); the diel vertical migration of zooplankton (Kaartvedt et al., 2007); the acoustic properties of gelatinous zooplankton (Klevjer et al., 2009); the distribution and behaviour of jellyfish (Youngbluth and Båmstedt, 2001) and the life cycle and biology of coronate medusa (Jarms et al., 1999; 2002). The genus *Atolla* isn't as well studied as *Periphylla* as it is restricted to the open ocean where deep-water sampling and *in situ* observations are more difficult (Lucas and Reed, 2010). Currently it is generally agreed that there are seven species of *Atolla* as available on the World Register of Marine Species (WoRMS); *A. chuni* (Vanhoffen, 1902), *A. gigantea* (Maas 1897), *A. parva* (Russell 1958), *A. russelli* (Repelin 1962), *A. tenella* (Hartlaub 1909), *A. vanhoffeni* (Russell 1957) and *A. wyvillei* (Haeckel 1880). Currently the most extensive descriptions of *Atolla* morphologies and distributions are from Russell (Russell, 1959, 1970) and Larson (1986).

The migration of *P. periphylla* fjord populations northwards has been noted as a result of climate change (Tiller et al., 2017). However, beyond this and the general consensus that *P. periphylla* is broadly cosmopolitan in distribution, there are currently no global studies determining the extent of deep sea coronate distributions and speciation.

There are inherent difficulties in obtaining high resolution datasets for macroecological studies. Therefore, it has been suggested to either enhance - or base entire studies on - citizen science and museum collections (Graham et al., 2014). Museum collections in particular; generally collected by scientists and preserved by experienced curators, are considered underexploited resources from an ecological perspective (Boakes et al., 2010; Beck et al., 2012). Furthermore, material collected on research expeditions may offer a large dataset that can be tapped with minimal expense. Using museum collections data, this study evaluates the extent of deep-sea coronate distributions worldwide. Using complimenting environmental data, this study analyses the morphological variation amongst *P. periphylla* and *Atolla* spp. over macroecological scales.

2.2.1 Aim and hypotheses

The objectives of this chapter are to map out global distributions of *Atolla* and *Periphylla* using museum collections both vertically and spatially to determine large scale distribution patterns; and to measure the morphological characters of *Atolla* and *Periphylla* to determine the expressed morphological variation of the genera according to different environmental conditions across the dataset.

The conceptual hypotheses being investigated within Chapter 2 are that *P. periphylla* demonstrates robust morphological characters and no expressed plasticity across the global dataset under a range of different conditions. A second hypothesis is that *Atolla* shows evidence of morphological responses to changes in environmental conditions resulting in speciation across the dataset. A number of species is exhibited within the genus *Atolla* across the global dataset in contrast to the single species of *P. periphylla* which is indicative of the fundamental phylogenetic distances between the two coronate genera. The justification of this is that the morphological characters of *P. periphylla* remain consistent within the literature, which is highlighted in Chapter 1.

2.3 Methods

2.3.1 Samples and study area

The samples used within this study were sourced from an extensive wet collection of deep-sea jellyfish held at the Natural History Museum London (NHM). Housed in the Discovery collections, which are a vast collection of benthic and pelagic samples taken from around the world, the jellyfish samples were initially sorted to determine the extent of the available deep-sea coronates. Aside from the registered samples within the NHM, no formal records of the available deep-sea jellyfish were present, so the samples were sorted initially to produce an assessment of data availability. Deep-sea coronates were located within 666 jars within the Scyphozoa and Residues collections and cross-referenced against the available station lists found at www.nhm.ac.uk to produce an initial dataset of available jellyfish specimens (see accompanying electronic material for full list of jars containing deep-sea coronates within the collection). Each jar logged contained a range of deep-sea jellyfish, from a single to hundreds of individuals. All material was formalin-fixed and stored in a temperature controlled warehouse in airtight jars away from sunlight to reduce degradation.

Samples from the NHM dataset were fixed at sea using 10% buffered formalin for 24 hours, which was subsequently diluted to 5% (White et al. 2013, personal communication). Ashore, specimens were then transferred into Steedman's, a formalin-containing preservation fluid commonly used with zooplankton samples (see Steedman, 1976 for description).

From the sample dataset of deep-sea coronate species available within the NHM *Discovery* collections, a sub-sample for morphological measurement and analysis was generated in order to reflect the distribution of *P. periphylla* and *Atolla* spp., dating between 1934 to 1990 (see Appendix A for full list of expedition vessels and cruise numbers included in this study (Tables 1 and 2)). The station lists determined that the majority of stations were along the low longitudes of the North and South Atlantic Oceans. In order to ensure maximum spread of data, individuals were randomly selected from the collections by grouping the stations into latitudinal increments of 10°. This was determined to be the optimal means of covering the greatest area. The sample locations for the study encompasses the entire globe, with the exception of the Pacific Ocean, which was not a sampled ocean of the *Discovery*

Expeditions. Due to the sample bias towards the Northern Hemisphere (92%), all specimens from the Southern Hemisphere stations were measured. One hundred individuals were measured per latitudinal increment of 10°, selected by inputting the station numbers into a random number generator. In instances with large numbers of specimens available, all individuals within the jar were laid out on a gridded tray and selected for analysis using a random number generator. Within each latitudinal area, 50 sample jars were selected at random for each genus from the stations and sub-stations lists, allowing for repeats. Each jar then corresponded to 1 individual to be measured, totalling 100 individuals per latitudinal 10° bracket. Individuals to be morphologically analysed were selected randomly within the jars by laying the specimens out on a gridded tray, and selected for measurement using a random number generator. Individual species were identified according to the key descriptors outlined in Chapter 1.

Cruise report data was located from the British Oceanographic Data Centre (BODC) online repository (https://www.bodc.ac.uk/resources/inventories/cruise_inventory/search/) whereby station numbers and associated sample locations were supplemented with depth, time, gear used and research objectives information. Cruise methodologies varied across the global historical dataset, using a range of plankton trawl nets including the Engel's Midwater Trawl (EMT), Isaac's-Kidd Midwater Trawl (IKMT) and Rectangular Midwater Trawls of various sizes (RMT 1+8, RMT 1, RMT 25) (see Appendix for full list of trawl gear types used and associated mesh sizes). Global depths sampled range between 0 to 4031 m below the surface. Where cruise report information was lacking using the online BODC repository, information was sought from the scientific personnel aboard the cruises (Thurston, 2014, personal communication, see Supplementary Information for data).

The primary dataset of the NHM was supplemented by distribution information from the Smithsonian National Museum of Natural History, USA (herein referred to as the Smithsonian) and the Global Biodiversity Information Facility (herein referred to as GBIF). This was in order to provide a more comprehensive assessment of the global distribution of the genera. The Smithsonian data was sourced from the Smithsonian Department of Invertebrate Zoology Collections online repository (<http://collections.nmnh.si.edu/search/iz/>) and includes cruises that sampled within the Pacific Ocean (see Appendix for full list of Smithsonian cruise information) to provide a more detailed assessment of global distribution. Deep-sea coronate samples held at the

Chapter 2

Smithsonian were collected from 1881 to 2007, from depths 0 to 4071 m below the surface. Extractable information for the purpose of this study from the Smithsonian dataset included sample locations, depth, collection method and date. The GBIF dataset formed a collection of various data sources, including that of the Smithsonian and NHM which were removed to eliminate data duplication. This data was more limited in terms of extractable information, with only latitude and longitude sampled available in many instances (see Appendix for full list of GBIF sourced material). Data from the Ocean Biogeographic Information System (OBIS) was considered as another secondary data source (<https://obis.org/data/>), however the majority of data entries for the deep-sea coronates were replicates of the Smithsonian and NHM data sources so was ruled out.

Table 2.1 Sample numbers of species collected across the various areas across the globe and split according to data source. *SuperAtolla* refers to a potential species nova, and Unknown refers to *Atolla* samples that were not identified to species level.

Sample area	Source	Atolla											Periphylla <i>P. periphylla</i>	Total location
		<i>A. wyvillei</i>	<i>A. parva</i>	<i>A. russelli</i>	<i>A. vanhoeffeni</i>	<i>A. gigantea</i>	<i>A. chuni</i>	<i>A. tenella</i>	SuperAtolla	Unknown				
Arctic	NHM					No data							11	
	Smithsonian GBIF					No data								
PAP	NHM	77	46	2	31	8		11		2		1205	1378	
	Smithsonian GBIF				1							6		
North Atlantic	NHM					No data							133	
	Smithsonian GBIF	20	2		1							110		
Iberian	NHM	155	400	44	45	7						114	778	
	Smithsonian GBIF		8		3							2		
Mid Atlantic	NHM	28	18	5	13	1			5	2		24	95	
	Smithsonian GBIF						No data					1		
South Atlantic	NHM					No data							45	
	Smithsonian GBIF	9	1			No data	14					21		
Indian	NHM	2											39	
	Smithsonian GBIF	6				No data	1	5				25		
North Pacific	NHM					No data							95	
	Smithsonian GBIF	41	6			No data						48		
South Pacific	NHM					No data							67	
	Smithsonian GBIF	22	5			No data		27				9		
Southern	NHM	38	10	1		2	1					21	209	
	Smithsonian GBIF	41	1	1			33					16		
Unknown location	NHM	16				9	19					13	19	
	Smithsonian GBIF	2				No data						4		
Total species		457	498	53	97	28	99	11	5	4		1619	2869	

Table 2.2 Sample numbers of species collected between 1880 to 2000 from the respective data sources. SuperAtolla refers to a potential species nova, and Unknown refers to *Atolla* samples that were not identified to species level.

Year		Source	Atolla							Periphylla	Total years		
			<i>A. wyvillei</i>	<i>A. parva</i>	<i>A. russelli</i>	<i>A. vanhoffeni</i>	<i>A. gigantea</i>	<i>A. chuni</i>	<i>A. tenella</i>	SuperAtolla'		Unknown	<i>P. periphylla</i>
1880	NHM						No data						
	Smithsonian	16										30	46
	GBIF						No data						
	NHM						No data						
1890	Smithsonian	3					No data					3	6
	GBIF						No data						
	NHM						No data						
	Smithsonian	38	2		1							25	66
1900	GBIF						No data						
	NHM						No data						
1910	Smithsonian						No data					2	2
	GBIF						No data						
	NHM						No data						
	Smithsonian						No data					2	2
1920	GBIF						No data						
	NHM						No data					5	11
1930	Smithsonian	3	2									1	
	GBIF						No data						
	NHM						No data						
	Smithsonian						No data						
1940	GBIF						No data					1	1
	NHM						No data						
1950	Smithsonian	1	1		1							4	
	GBIF	1										8	22
	NHM						No data						
	Smithsonian						No data						
1960	GBIF						No data						
	NHM	4	2	2				72				57	252
	Smithsonian	58	8									49	
	GBIF						No data						
1970	NHM	233	360	35	57	17	1			5	1275		2106
	Smithsonian	20	3	1			7				73		
	GBIF		9			2		1					
	NHM	39	97	10	27	1					26		
1980	Smithsonian										3		203
	GBIF						No data						
	NHM	20	12	5	4						22		88
	Smithsonian								8		1		
1990	GBIF	16											
	NHM						No data						
2000	Smithsonian	2										15	17
	GBIF						No data						
No date	NHM	2										13	57
	Smithsonian	2										2	
	GBIF	8	11					17	2				
Total species			466	507	53	89	21	97	11	5	13	1617	2879

2.3.2 Morphology

A range of morphological characters were recorded in order to determine large-scale patterns. Measurements were made using forceps, calipers a seeker, and for larger individuals, a 30 cm ruler. The following measurements and notations were taken from each individual: preserved wet weight, bell diameter (BD), bell height (BH), coronal diameter (CD), coronal height (CH), number of marginal lappets, number of tentacular muscular bundles (TMB), number of gonads, gonad shape, number of tentacles, gender, tentacle length and pigmentation (Figure 2.1).

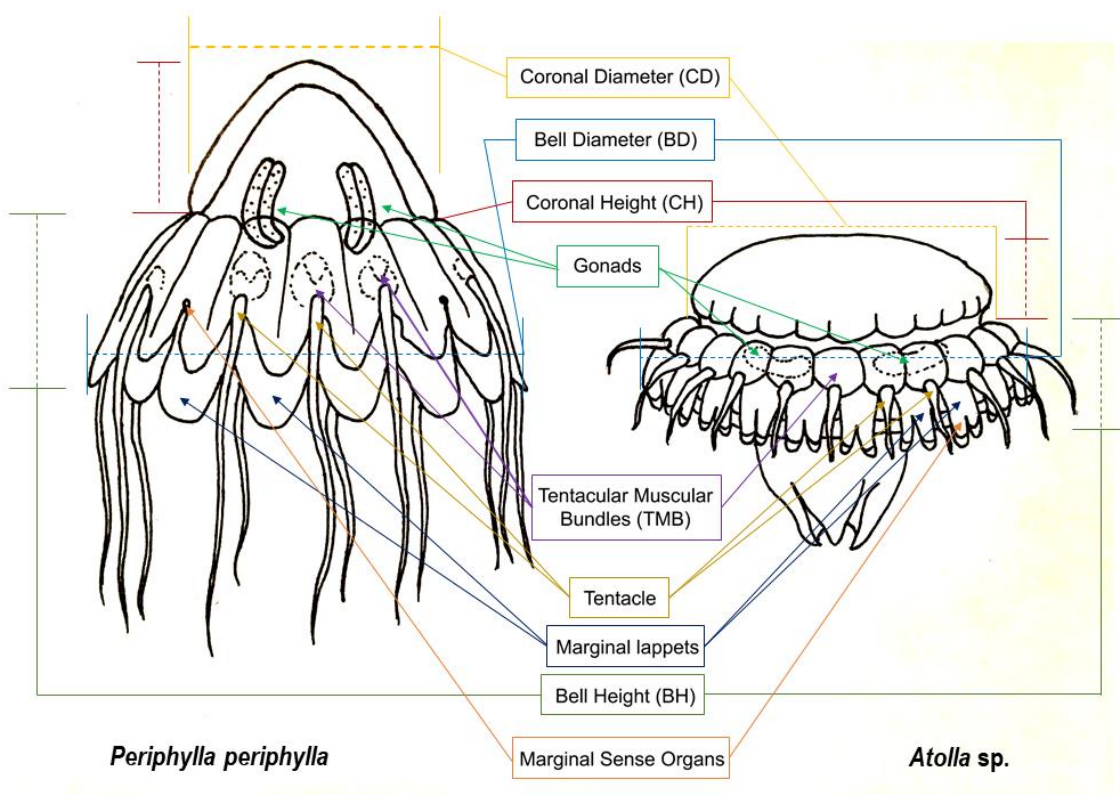


Figure 2.1 Depiction of *P. periphylla* and *Atolla* sp. to demonstrate key features and the landmarks used for the morphological analysis of both coronates. Illustrations by the author, adapted from Russell (1970).

Where possible, all specimens were analysed under a stereomicroscope, particularly when noting reproductive characteristics. *Atolla* specimens were measured in a dorso-ventral orientation, due to their disc-like bell. *Periphylla* specimens were laid in a lateral orientation to measure CD, CH, BD and BH, and in a dorso-ventral position for the remainder of the measurements. Tentacles were counted and measured by being spread out on a tray or petri dish depending on size. Forceps were then used to pull the tentacle taut against the callipers,

or ruler if length exceeded 15 cm. The length of *Atolla* tentacles could not be measured as the specimens were always damaged as a result of being trawled.

Measurements using the calipers were recorded to the nearest 0.1 mm, and to the nearest 0.5 mm using the ruler. Excess liquid was removed using paper towels, and the specimens were weighed using a nanogram-scale balance (Ohaus GA2000) where possible, and a milligram-scale balance (Ohaus CS2000) for larger specimens. Weights from both balances were recorded to the nearest decigram. Gonads of a number of specimens were then removed for histological analysis at a later date. Pigmentation is noted, despite the tendency to be either stripped off or faded when exposed to light. In the case of *Atolla*, differences in pigmentation, particularly of the stomach, can aid distinguishing between *A. wyvillei* and *A. vanhoeffeni*.

Information related to location, depth, time sampled, date and gear type were obtained from the cruise station lists held at the Natural History Museum London and the British Oceanographic Data Centre. A total of 3676 specimens were measured, with 2191 *Atolla* individuals and 1485 *Periphylla* individuals. There was a greater overall number of *Atolla* spp. specimens within the global dataset, accounting for the imbalance between the two genera in terms of measurements recorded.

2.3.3 Data analysis

The raw morphological measurements from the NHM data were combined with the cruise report data to provide a spatial and temporal context to the data. Data were organised in Microsoft Excel and Minitab. Exploration of the spatial information was done using ArcGIS 10.1, visualising the sample localities of the various coronate species. Key sample areas identified were the Porcupine Abyssal Plain region (PAP), the Iberian Basin, Southern Ocean, Mid-Atlantic and the Indian Ocean and were used to distinguish between large-scale geographic variation within the analyses of deep-sea coronate distribution. Size-frequency histograms were used to describe the variation between deep-sea coronate species. One-way analysis of variance (ANOVA) with Tukey's post-hoc test (as per Reed et al., 2013) was used to describe the variation in size and depths found for the various species, as well as seasonality in chlorophyll-*a* observed concentrations across the global dataset. Regression analysis with Pearson correlation coefficient test used to describe morphological

relationships between the various coronate species, latitudinal variation and the relationship between environmental variation (chlorophyll-*a*) with the size of medusae.

In order to analyse the extensive global spatial data, the latitude and longitude information was converted into a matrix for further analysis (see Sokal, 1979). Spatial autocorrelation was detected by creating a binary distance matrix and testing for spatial autocorrelation using Moran's *I*. Spatial autocorrelation was confirmed due to the presence of *p* values smaller than 0.05, and to remove this a further matrix was created using a geographical distance matrix calculation in R statistical package to produce 50 distinct distance groups within the global dataset (Rosenmai, 2014). A threshold limit of 172 km was set in order to produce the 50 distinct groups and address sampling bias. Generalised linear model (GLM) was used to identify the influence of environmental variation (chlorophyll-*a* and zooplankton diversity) on the global spatial occurrence of the deep-sea coronate species.

2.3.4 Environmental variables

i). Chlorophyll-*a*

Global chlorophyll-*a* data sourced from NASA Aqua moderate resolution imaging spectroradiometer (MODIS) satellite images were used as an index of phytoplankton biomass in order to model how changes in primary production effect deep-sea coronate morphology and distributions (accessible at <https://neo.sci.gsfc.nasa.gov/>).

Seasonal chlorophyll-*a* data was selected by matching the month and area of the sample with the corresponding coronate data from the primary NHM dataset. Aqua MODIS data was available dating back to 2002, which is why seasonal data was opted over an exact match for the historical data.

ii). Zooplankton

Zooplankton presence data was sourced from the OBIS Mapper data tool (accessible at <https://mapper.obis.org/>) as a proxy for food availability across the global dataset. Copepoda (Orders Calanoida, Cyclopoida, Harpacticoida, Monstrilloida, Mormonilloida, Poecilostomatoida and Siphonostomatoida), Ostacoda and Euphausiacea were selected to determine overall zooplankton availability. The zooplankton species were matched to the jellyfish samples according to month, year and depth for increased accuracy for inferring

potential patterns within the data. A Simpson's Diversity Index (see Schmera et al., 2017) was applied to the data to reflect the exhibited zooplankton diversity across the various sample areas; PAP, Iberian, Mid Atlantic, Indian and Southern Oceans.

2.3.5 Molecular analysis

Molecular methods were trialled to combine with the morphological work in order to investigate the population dynamics of the various coronate species, with the view to determining potential cryptic species within the dataset. Studies have suggested that cryptic speciation is likely highly underestimated amongst deep sea fauna (Danovaro et al., 2014). A range of molecular methods using formalin-fixed historic samples, fresh ethanol-fixed samples and frozen tissue were trialled (see Discussion chapter for full description of methods trialled and primers used), however none were successful due to the difficulty extracting DNA from formalin-fixed material (see Campos and Gilbert, 2012), especially jellyfish (Dawson, 2016; Lindsay, 2018, personal communications). As such, the molecular analyses trialled were omitted from this study.

2.4 Results

2.4.1 General distribution and species identification

The various species within the NHM dataset were identified by using the diagnoses and descriptions previously outlined by Kramp (1961), Russell (1970) and Larson (1986) (see Renner, 2016 for discussion on diagnoses). The previously observed distributions of the various species were also used to inform potential species occurrences of *A. chuni* (see Pages et al., 1996), *A. tenella* (see Raskoff et al., 2004), *A. russelli* (see Morandini, 2003), *A. wyvillei* and *P. periphylla* (see Lucas and Reed, 2010) and *A. vanhoeffeni* (Lindsay et al., 2004).

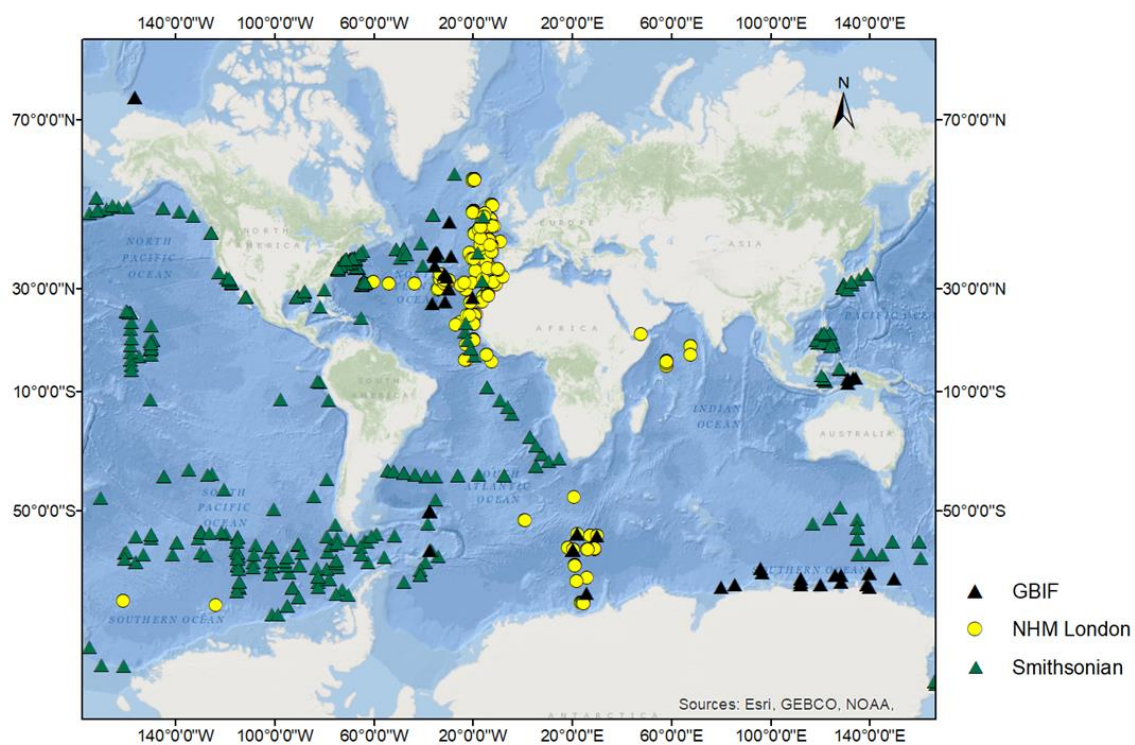


Figure 2.2 Distribution of all samples collated within this study, including the primary dataset of the NHM (yellow circles), Smithsonian (green triangles) and GBIF (black triangles).

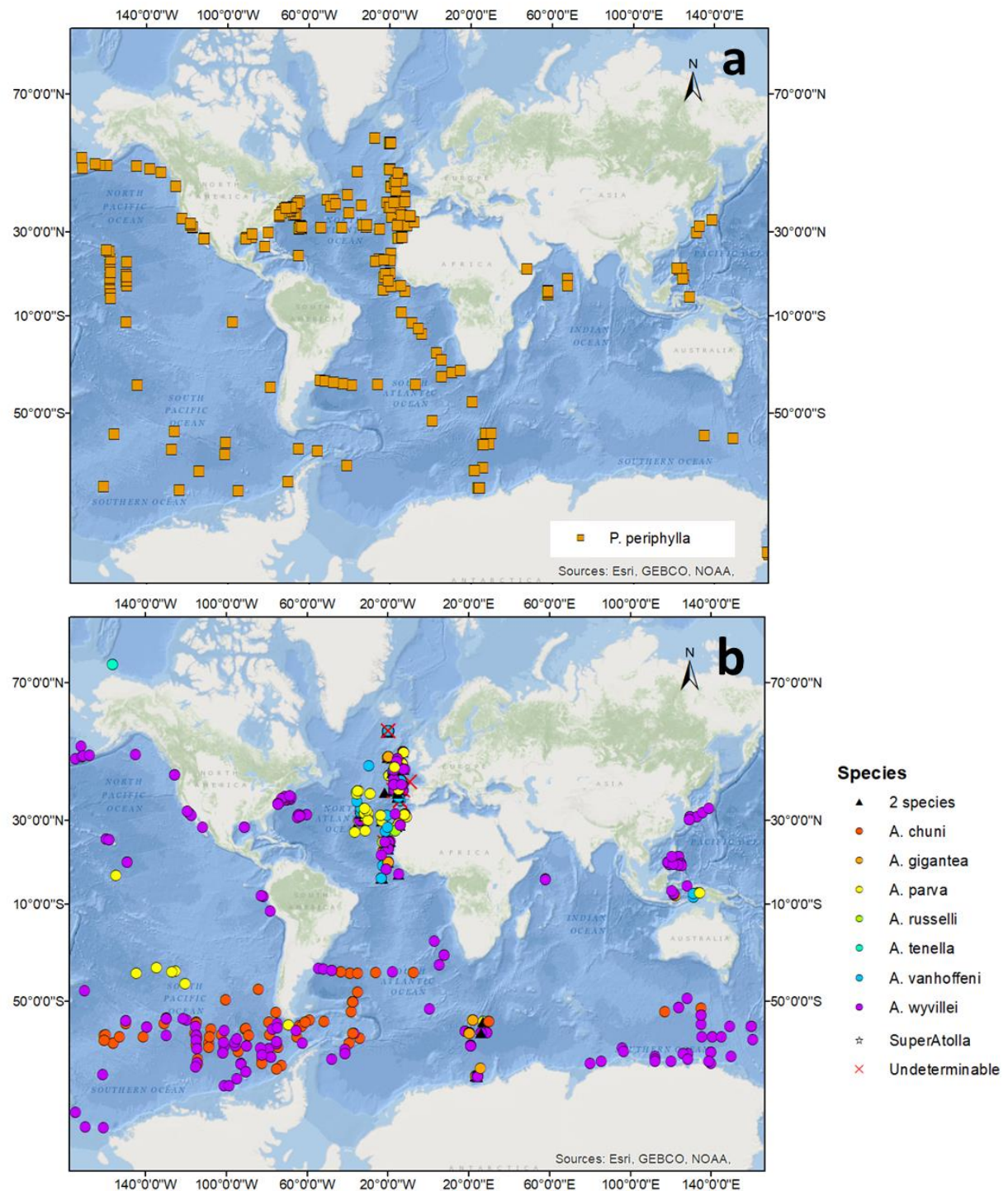


Figure 2.3 Distribution of deep sea coronates found within this study. a: *P. periphylla*; b: *Atolla* sp. Legend for *Atolla* show that in some instances there were two species possibilities for the sample. These were noted and removed from subsequent data analysis. All 7 described species of *Atolla* were found within the data, along with an additional potential species nova, referred to as 'SuperAtolla'. Undeterminable species are noted with a red cross and discounted from subsequent analyses.

Global distributions of both *Atolla* and *Periphylla* are demonstrated by combining available data from the NHM, Smithsonian and GBIF (Figure 2.2). The sample locations of the various data sources vary, with the NHM data mostly located in the Atlantic and low longitude Southern Ocean, the Smithsonian data from the Pacific, Southern and west Atlantic Oceans. GBIF data is mostly spread out across the Southern, Atlantic and Arctic Oceans. *P. periphylla* is the only species exhibits a cosmopolitan distribution, occurring in all oceans. This is in agreement with the current literature (see Collins, 2002; Dawson, 2004). A number of distinct sampling areas across the globe were identified from the NHM data to include the Porcupine Abyssal Plain (PAP) region, the Iberian Basin, the Mid Atlantic, the Southern Ocean, the

All seven described species of *Atolla* were found within the dataset, including *A. chuni*, *A. gigantea*, *A. parva*, *A. russelli*, *A. tenella*, *A. vanhoeffeni* and *A. wyvillei*. When measuring a number of individuals, particularly the smaller samples (<10 mm bell diameter), identification to species level was difficult, and was determined be two possible species. This was particularly common in *A. russelli*, *A. parva* and *A. wyvillei* samples. In this instance they were allocated as '2 species' (Figure 2.3b) and were omitted from subsequent data analyses. Three samples within the dataset were found to not comply with any of the current descriptions of *Atolla*. These samples were all found to have unusually high tentacle numbers (36), horse-shape gonads and papillae. The sample locations of these individuals was from the Mid Atlantic area. These samples are referred to as SuperAtolla, a potential species nova as described by Matsumoto and Lindsay (Lindsay, 2018, personal communication). Two example samples of SuperAtolla were provided by Lindsay, with varying sizes and sample locations; 1. 58 tentacles, 95 mm bell diameter, caught south of Tokyo; 2. 36 tentacles, 15 mm diameter, caught in the Caribbean. These two samples were incorporated into this global dataset.

Distributions of *Atolla* species exhibited a large degree of overlap within the dataset, particularly within the North Atlantic where *A. gigantea*, *A. parva*, *A. russelli*, *A. vanhoeffeni* and *A. wyvillei* are found. In accordance with the literature, *A. tenella* is found only in the Arctic Ocean (as per Raskoff et al., 2004) and *A. chuni* is found only in and around the Southern Ocean, and is described to be most numerous near the Antarctic Convergence (as

per Larson, 1986), which fits with what is shown in the distribution data of this study. *A. wyvillei* is the only species of *Atolla* found to exhibit a cosmopolitan distribution, with samples found across all oceans apart from the Arctic Ocean.

2.4.2 Morphological variation in *Atolla* and *Periphylla*

Linear regression analysis for all species within the *Atolla* and *Periphylla* genera demonstrate a highly significant relationship between bell diameter (BD) and coronal diameter (CD) (Figure 2.4) (Pearson correlation, *Atolla* species, $r = 0.968$, $p < 0.01$; *Periphylla*, $r = 0.982$, $p < 0.01$), with over 90% of the variation in BD explained by variation in CD (*Atolla* $r^2 = 0.9165$, *Periphylla* $r^2 = 0.95$). Positive relationships were also observed in the height and width of medusae. The disc-like appearance of *Atolla* renders the BD-bell height (BH) slope shallower than the CD- coronal height (CH) relationship in *Periphylla*. In medusae > 20 mm BD (*Atolla*) and > 30 mm CD (*Periphylla*), the diameter-height relationships aren't as strong, which may be indicative of the difference apex types in *Periphylla* (*hyacinthina*, *dodechabostrycha* and *regina*, as in Russell 1970). See Chapter 1 for visual representation of various apex types.

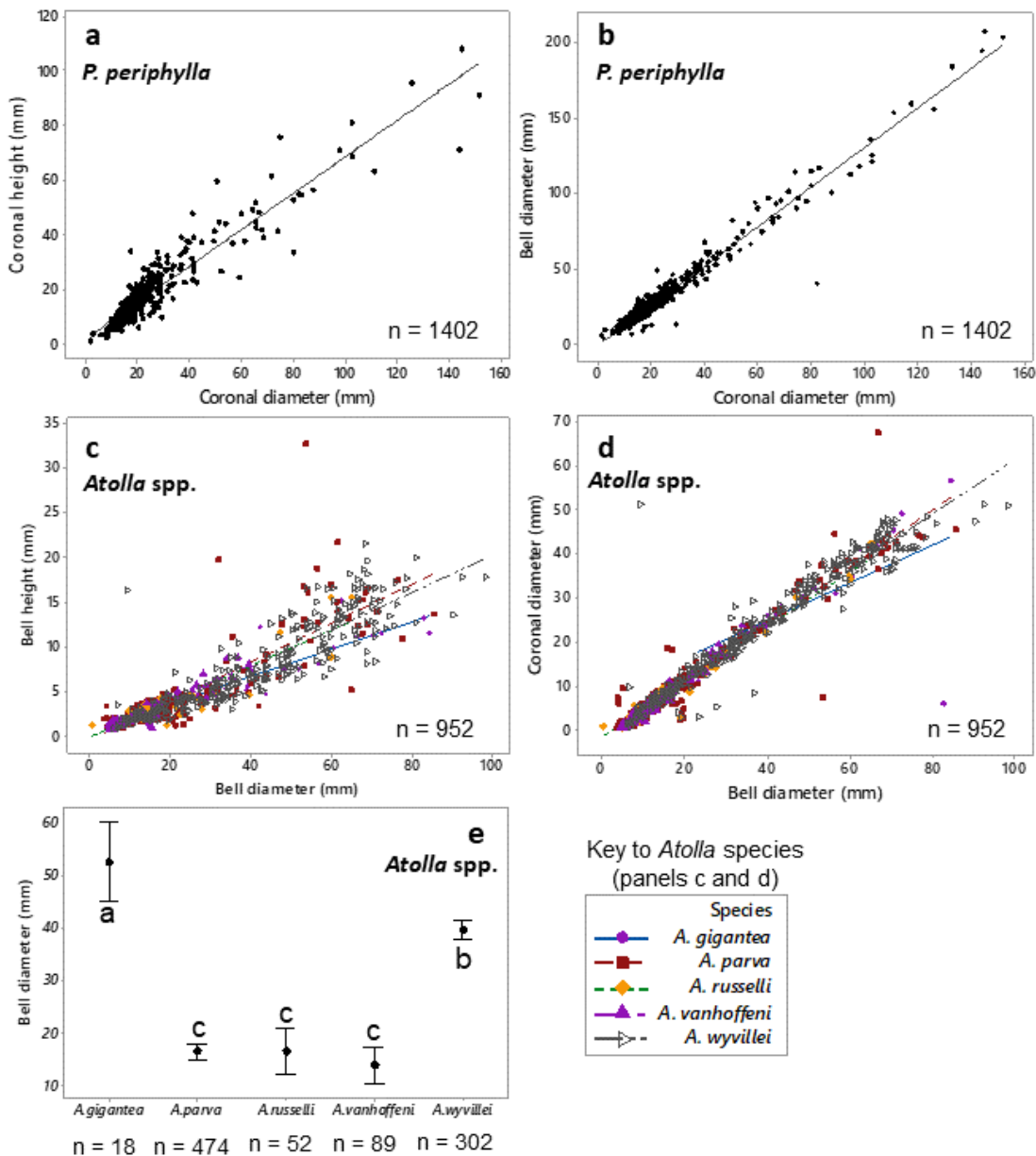


Figure 2.4 Morphological relationships for *P. periphylla* (a +b) and the species of *Atolla* (c – e) across the global dataset. e: *Atolla* mean bell diameter across the global dataset for the various species. Letters next to bars denote significantly different species sizes, Tukey's test, $p < 0.05$). Standard error bars to 95% confidence level.

Due to the damage to all *Atolla* tentacles after trawling, tentacle length was taken into account for *Periphylla* only. Significant positive relationships were observed between CD and average tentacle length, with 61% of the variation in tentacle length attributed to variability in CD (Pearson correlation, $r = 0.859$, $p < 0.01$). This value may be an under-representation due to trawl damage in some instances.

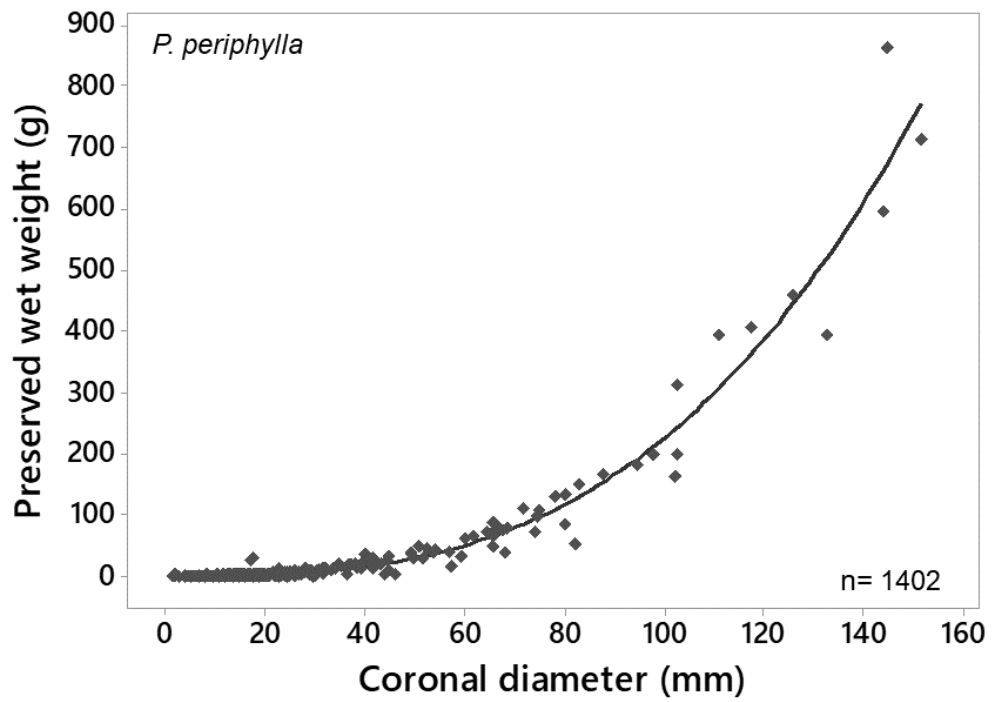


Figure 2.5 Cubic regression of *P. periphylla* length-weight relationship using preserved wet weight and coronal diameter, $p < 0.001$. Regression equation: The regression equation is: $\text{Weight} = -0.966 + 0.0795 \text{ CD} + 0.000158 \text{ CD}^2 + 0.000218 \text{ CD}^3$.

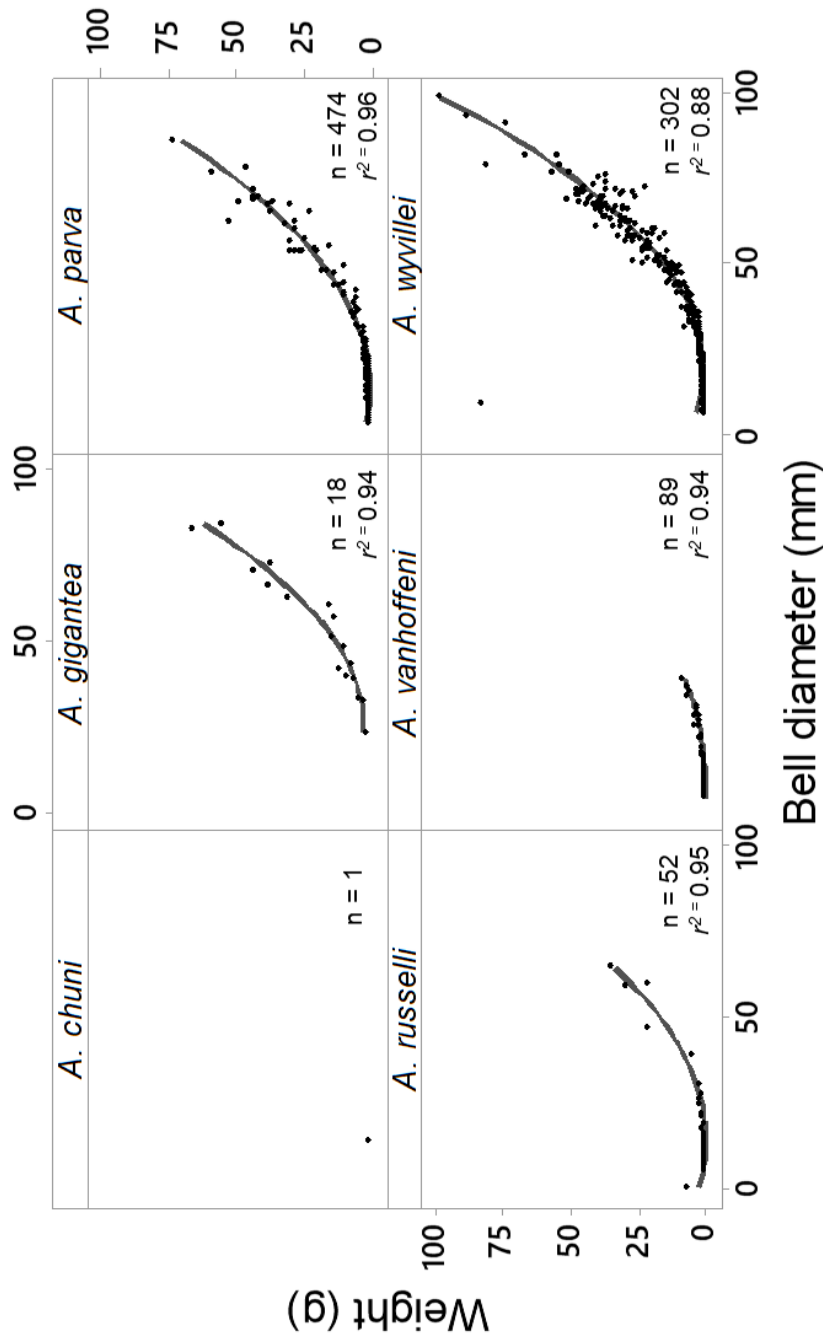


Figure 2.6 Cubic regression of *Atolla* length-weight relationship using preserved wet weight and coronal diameter. *A. chuni* was omitted from the dataset due to paucity of data. All regressions $p < 0.001$. Regression equations: *A. wyvillei*: $y = 8.043 - 0.718x + 0.018x^2 - 0.0002x^3$; *A. vanhoffeni*: $y = 0.121 - 0.003x + 0.0003x^2 + 0.0001x^3$; *A. russelli*: $y = 3.531 - 0.528x + 0.019x^2 - 0.00074x^3$; *A. parva*: $y = 1.772 - 0.2668x + 0.0103x^2 + 0.0002x^3$; *A. gigantea*: $y = 16.54 - 1.073x + 0.021x^2 + 0.00025x^3$.

Figure 2.5 demonstrates an exponential increase in weight according with coronal diameter for *P. periphylla*, with the majority of individuals < 20 mm in size. Previously, no length-weight information was available for *Atolla* species (Lucas et al., 2014). **Figure 2.6**

Chapter 2

demonstrates the various size-weight relationships amongst the species. No data was available for *A. tenella* within the NHM dataset, and *A. chuni* had insufficient data and size ranges to produce a regression ($n = 1$). *A. vanhoeffeni* and *A. russelli* are found to be smaller overall species, with *A. gigantea* overall larger in size. *A. parva* and *A. wyvillei* have the greatest spread of sizes of individuals according to weight.

Size frequency histograms were produced to represent the variation in overall body size between the various deep-sea coronate species. Multimodal distributions are observed in *A. parva*, *A. russelli*, *A. gigantea* and *A. wyvillei* (Figure 2.7), with *A. wyvillei* demonstrating a large range in size (range = 5 to 98 mm bell diameter; StDev = 21.04). *A. gigantea* does not indicate a clear size frequency relationship, however may be due to the mostly large specimen size (range = 48 to 84 mm) and the smaller sample number ($n = 18$). Specimens that were 'Undeterminable' to species level for *Atolla* were plotted to indicate that in all of these instances the individuals were small (< 30 mm diameter). Some of these samples were also damaged extensively

When analysing the data, it became apparent that the majority of individuals were small (< 20 mm diameter). In *P. periphylla*, there were 1111 individuals smaller than 20 mm coronal diameter which follows a normal distribution when separated out from the rest of the samples.

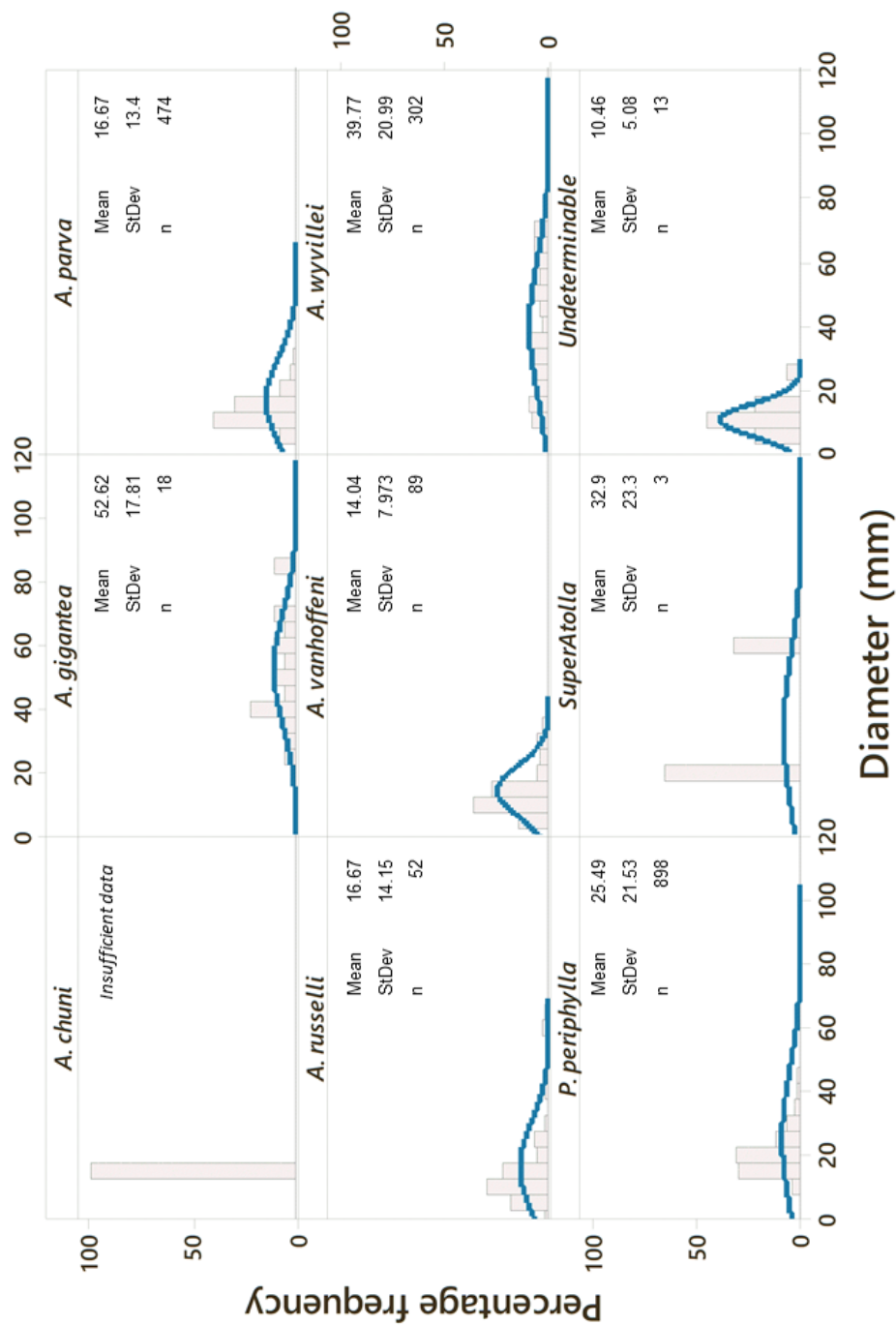


Figure 2.7 Size frequency histograms and distribution lines of fit for *Atolla* species across the global NHM dataset, excluding *A. chuni* due to lack of sufficient data. Mean, standard deviations (StDev) and number of individuals noted on each panel.

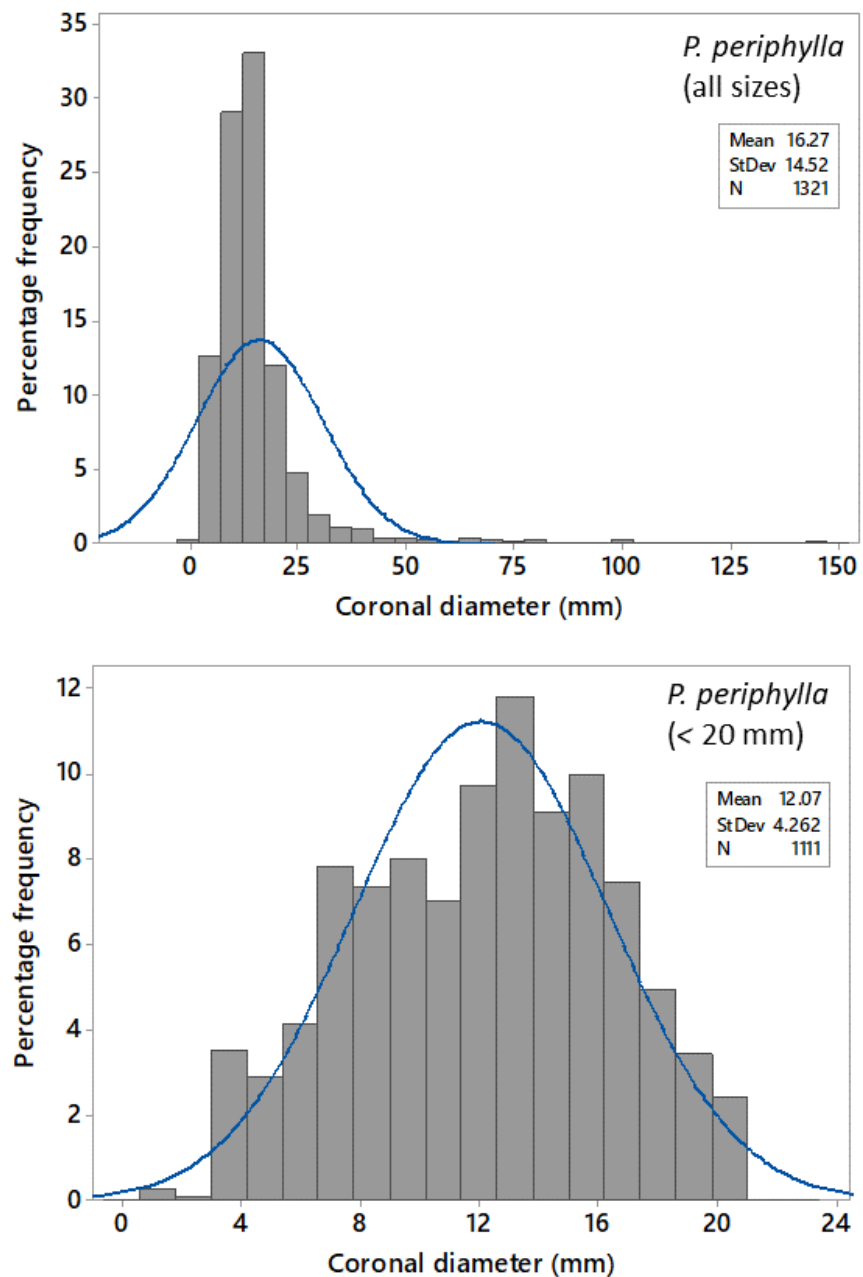


Figure 2.8 Size frequency histograms and distribution lines of fit for *P. periphylla* specimens within the NHM global dataset. Smaller specimens (<20 mm diameter) separated out in separate panel due to the large volume of smaller samples (n = 1111).

The number of tentacles observed within the various deep-sea coronate species varied according to species, with the exception of *P. periphylla* and *A. wyvillei*, which only had a single number of tentacles for all individuals recorded within this study (Figure 2.9).

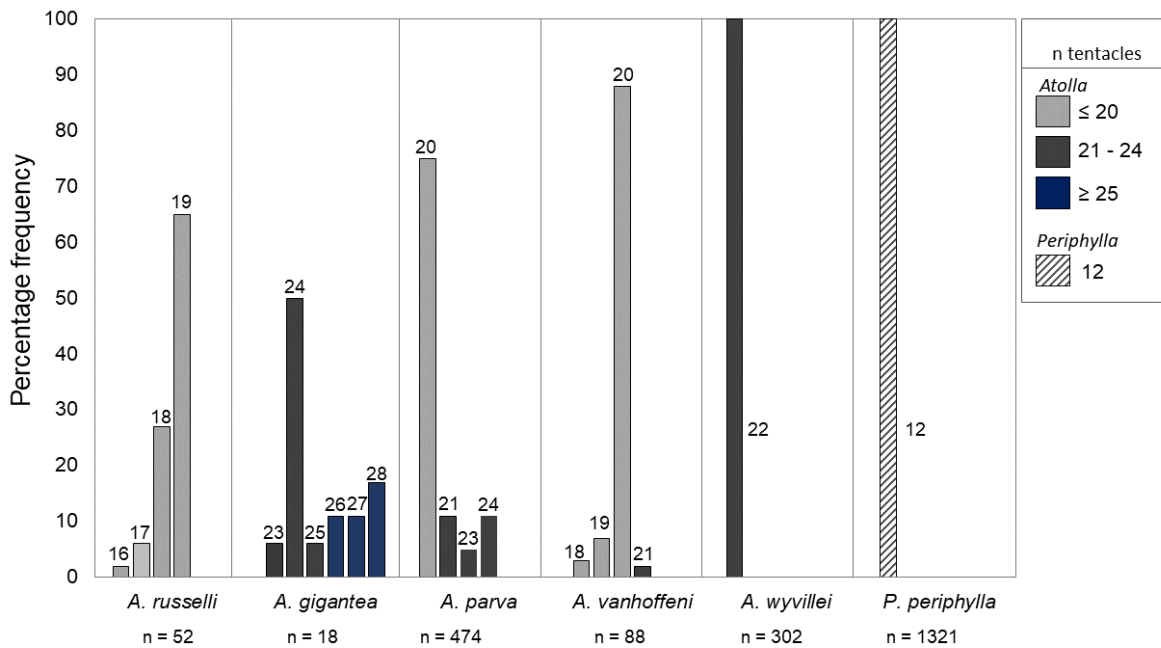


Figure 2.9 Percentage frequency variation in tentacle number observed across the global study area using NHM data for each deep-sea coronate species. Numbers above bars are the number of tentacles. Light grey bars are 20 tentacles and under, dark grey bars are 21 – 24 tentacles, and blue bars are 25 tentacles and over. Striped bar is 12 tentacles (*P. periphylla* only).

A. russelli all had a small number of tentacles (range = 16 – 19, $n = 52$), *A. gigantea* all had a higher number of tentacles, (range = 23 – 28, $n = 18$), 75% of *A. parva* had 20 tentacles (range = 20 – 24, $n = 474$) and 88% of *A. vanhoeffeni* also had 20 tentacles (range = 18 – 21, $n = 88$).

For the *Atolla* species with a range of tentacles, a GLM was used to identify whether the tentacle number varied according to spatial location, with the spatial location determined by using the assigned distance group values calculated from the geographic distance matrix. This was performed for *A. russelli*, *A. parva*, *A. gigantea* and *A. vanhoeffeni*, with the results presented in Table 2.3. Significant relationships were observed between geographical area (distance group) and *A. parva* and *A. gigantea*, but not for *A. russelli* and *A. vanhoeffeni*.

Table 2.3 GLM output of tentacle number variation according to spatial area (distance group) within the global study. *Atolla* species with tentacle ranges that incorporate 4 different number of tentacles are included.

	<i>n</i>	<i>DF</i>	<i>F</i>	<i>p</i>
<i>A. russelli</i>	52	11	1.06	0.419
<i>A. parva</i>	474	37	7.2	0.000***
<i>A. gigantea</i>	18	8	6.9	0.004***
<i>A. vanhoeffeni</i>	88	18	0.44	0.94

2.4.3 Development of new pedalia within *Atolla*

According to descriptions by Kramp (1961) and Russell (1970), variation in tentacle number has been observed in some of the species (e.g. *A. gigantea*, *A. russelli* and *A. parva*) with other species documented to never vary in tentacle number (e.g. *P. periphylla*, *A. wyvillei*). When analysing the NHM specimens, there were a number of *Atolla* samples ($n = 10$) whereby the apparent development of new pedalia was visible (Table 2.4). This is something that has not been documented previously in the literature. It is not certain whether the variation in pedial development is a reflection of stunted growth, or the development of new pedalia and tentacles.

Table 2.4 *Atolla* individuals within the NHM global study exhibiting developing pedalia, along with date and location sampled, weight (mm), total number of tentacles observed and description.

	Station	Date	Area	Bell diameter (mm)	Tentacles	Description of new pedalia
<i>A. parva</i>	9801.77	27/05/1978	Iberian Basin	64.4	21	1 very small developing tentacular pedalion.
	9966.18	21/02/1979	Southern	61.6	20	Multiple developing pedalia.
<i>A. russelli</i>	9798.20	13/05/1978	Iberian Basin	59.7	18	2 developing pedalia present.
	9801.66	14/06/1978	Iberian Basin	39.4	19	Multiple developing pedalia.
	9969.40	25/02/1979	Southern	64.9	19	Multiple developing pedalia.
	11095.10	20/04/1984	Iberian Basin	47.1	19	Multiple developing pedalia.
<i>A. wyvillei</i>	9801.24	17/05/1978	Iberian Basin	64.6	22	1 very small developing tentacular pedalion.
	9793.20	18/05/1978	PAP	49.8	22	All pedalia different sizes.
	9801.58	02/06/1978	Iberian Basin	57.5	22	All pedalia different sizes.
	9966.90	19/02/1979	Southern	56.4	22	Multiple developing pedalia.

2.4.4 Latitudinal variation in morphology

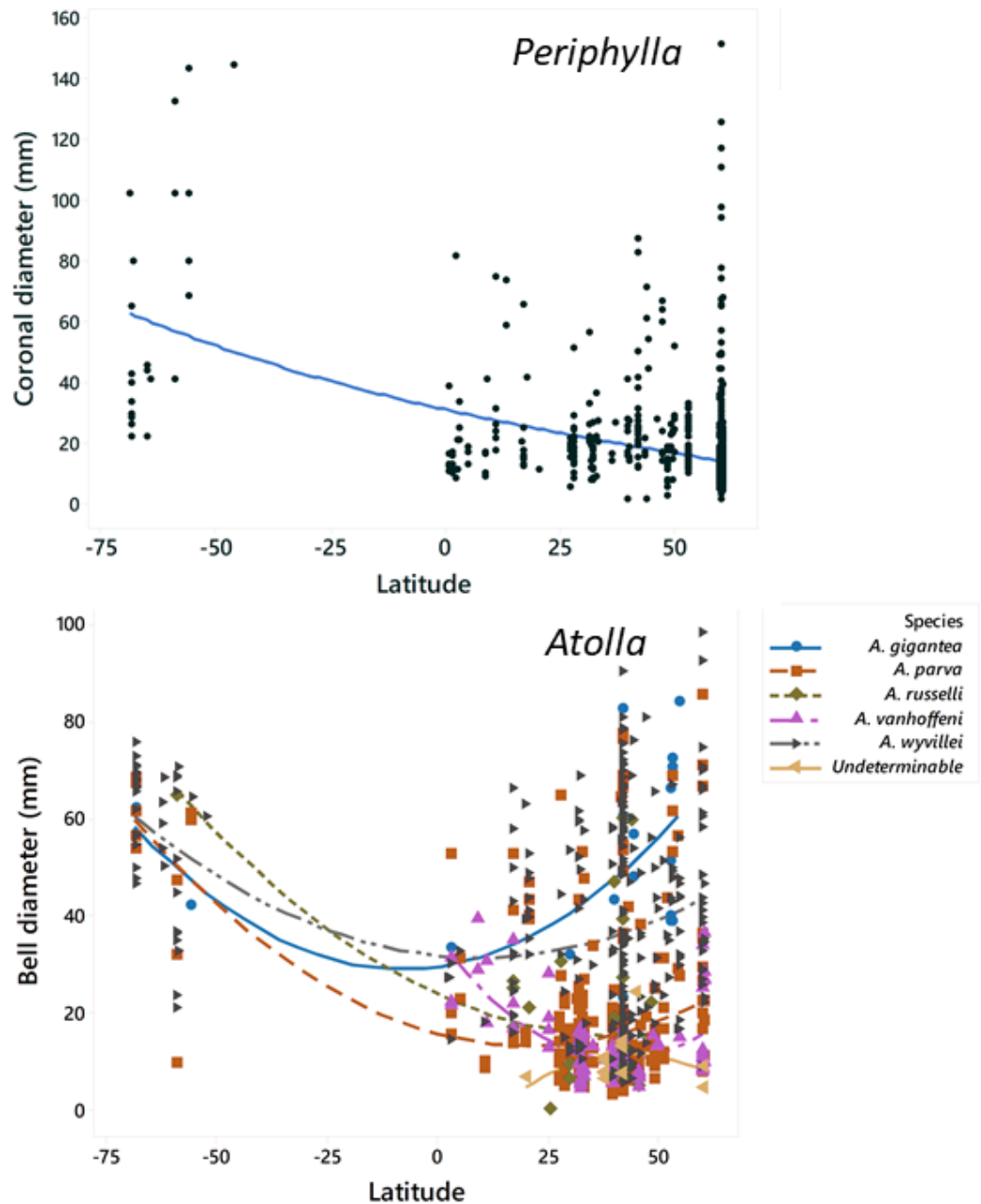


Figure 2.10 Quadratic regression analysis for change in body size (coronal diameter for *P. periphylla* $n = 1321$ and bell diameter for *Atolla* species $n = 934$) according to latitude, $p > 0.05$ for all species.

Bergmann's rule (1848), which posits that body size increases with age has been observed in a number of terrestrial, marine and freshwater faunal groups (see Partridge & Coyne 1997; Belk et al., 2002; Ashton & Feldman 2003; Olalla-Tárraga & Rodríguez 2007; Meiri 2011). Whilst variation in body size according to latitude has been documented for copepods

(Lonsdale and Levinton, 1985), isopods (Cardoso and Defeo, 2003) and mole crabs (Defeo and Cardoso, 2002), it remains undocumented in jellyfish and deep-sea pelagic fauna.

No significant trends were observed linking *P. periphylla* medusae size with latitude (Figure 2.10, $p > 0.05$), with latitude explaining just 19.5% of the variation. Overall, *Atolla* bell diameter was found to be slightly greater at higher latitudes (60 - 70°N, mean BD = 43 mm), then dropping to a mean diameter of 22 mm at 50°, and remaining near a mean of 27 mm for latitudes 10 - 40°N). There appears to be a pattern of larger individuals for both *P. periphylla* and *Atolla* towards the poles, with a stronger signal illustrated in *Atolla* spp. However, the sample bias towards smaller individuals and a lack of samples within the lower latitudes results in an inconclusive output.

2.4.5 Depths of deep-sea coronate species

A summary of the key depths and key morphological output for the various species of deep sea coronates within the global study is presented in Table 2.5. All the coronate species are found at depths ranging from the surface to approximately 3000 m deep, demonstrating large vertical distributions overall. *P. periphylla* represents the greatest depth range exhibited, from 0 to 5486 m. In all instances, *P. periphylla* had 12 tentacles across the global dataset. No depth or morphological information was available for the Arctic species *A. tenella*. The distribution of the various coronates according to depth is presented in Figure 2.11. Despite *P. periphylla* demonstrating the broadest recorded depth range within the dataset, the average overall depth observed is the shallowest (mean = 654 m, $n = 1596$), as displayed in Figure 2.12. The potential species nova, SuperAtolla, as described by Lindsay (2018) is found at an overall greater depth (mean = 2492), however also has a considerably small sample size ($n = 3$) so cannot be taken as indicative of its likely vertical distribution.

Table 2.5 Summary of key size and depth information for the various coronate species from the NHM and Smithsonian data. ND = no data available. Majority tentacle number is determined by the highest instance of that tentacle number. Diameter, weight and tentacle number information available from the NHM dataset only.

Genus	Species	N	Mean diameter (mm)	Mean weight (g)	Majority tentacle n	Min depth	Max depth	Average overall depth
Atolla	<i>A. wyvillei</i>	457	39.6	14.2	22	0	4901	905
	<i>A. chuni</i>	99	ND	ND	ND	4	4301	745
	<i>A. gigantea</i>	28	50.1	17.3	24	390	3100	1520
	<i>A. fenella</i>	11	ND	ND	ND	ND	ND	ND
	<i>A. parva</i>	498	15.9	2.1	20	0	4031	1108
	<i>A. russelli</i>	53	16.7	2.6	19	0	2700	1114
	<i>A. varhoeffeni</i>	97	15.0	1.1	20	0	3646	651
	<i>SuperAtolla</i>	2	41.74	7.8	36	ND	ND	ND
	<i>Undetermined</i>	4	10.5	0.2	ND	0	3760	1058
	<i>P. periphylla</i>	1619	38.1	31.9	12	0	5486	628

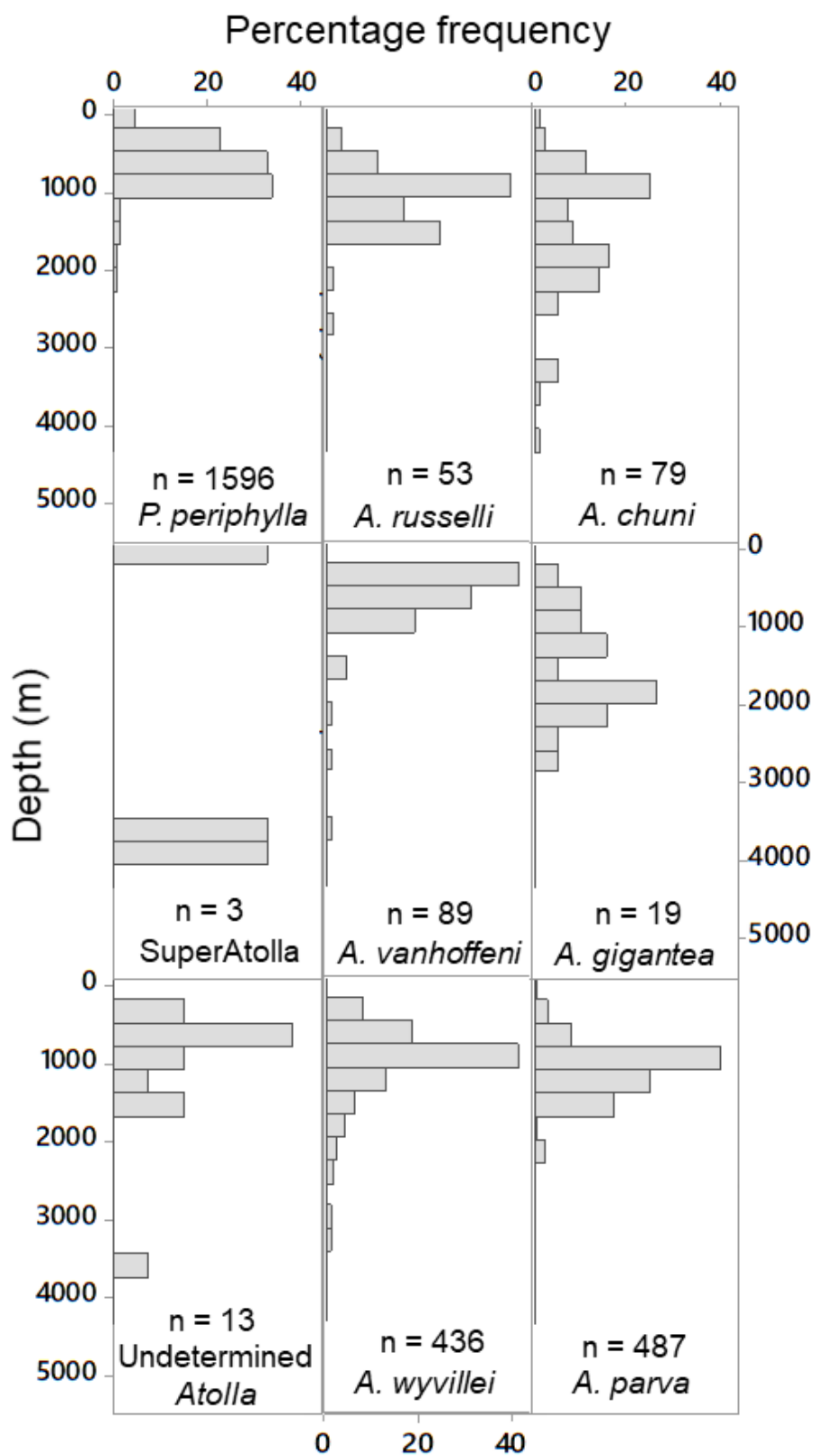


Figure 2.11 Depth distribution percentage frequency histograms of the deep-sea coronates within the global study using NHM and Smithsonian data. No data was available for *A. tenella*.

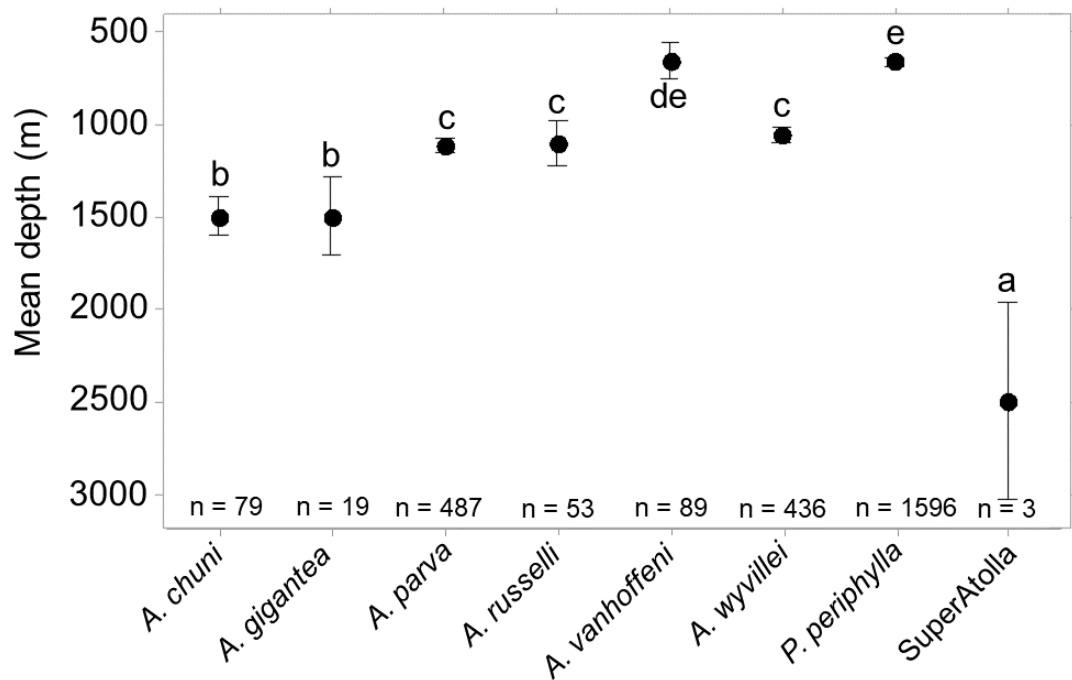


Figure 2.12 Mean depths of the deep-sea coronates within the global study, using data sourced from the NHM and Smithsonian. No data available for *A. tenella*. Significantly different groups indicated with letters above bars, Tukey test, $p < 0.05$.

2.4.6 Impact of environmental data on coronate species occurrence

Zooplankton data were collated as a proxy for food availability and to investigate whether availability is linked to the occurrence of the various deep-sea coronate jellyfish. Using Simpson's Index for Diversity, which remains a commonly used indicator of diversity throughout aquatic biology (Schmera et al., 2017), it was found that the area with the greatest diversity was the Iberian Basin (Simpson's Index = 0.93, $n = 12,768$), with the Southern and Indian Oceans giving the lowest diversity levels (Simpson's Index = 0.75 and 0.78 respectively). It would appear that sample number does not have an effect on the resulting diversity, as the Mid Atlantic has the smallest sample size ($n = 107$), but retains a high Simpson's Index.

Table 2.6 Zooplankton diversity (Simpson's Index) across the key global sampling areas within the NHM dataset study area.

Geographic area	Total n zooplankton species listed	Simpson's Index for Diversity
Iberian Basin	12,678	0.93
Mid Atlantic	107	0.88
Porcupine Abyssal Plain	13,247	0.83
Southern Ocean	219	0.75
Indian Ocean	618	0.78

Using global chlorophyll-*a* concentration data (mg m^{-3}) from the NASA MODIS satellite, the data were matched to sample season of the deep-sea coronates and divided according to global sample area. The spread of chlorophyll-*a* concentrations within the Mid Atlantic sample area displays the most normal distribution (Figure 2.13, StDev = 0.18), with the Iberian and PAP sites displaying the greatest spread of chlorophyll concentrations within their respective regions according to the . The Southern Ocean sample area displays the smallest degree of deviation from the mean (StDev = 0.014), with the majority of concentrations at 0.15 mg m^{-3} . Significantly lower chlorophyll-*a* concentrations were observed during the winter months (one-way ANOVA with Tukey's test, $F = 7.12$, $p < 0.001$).

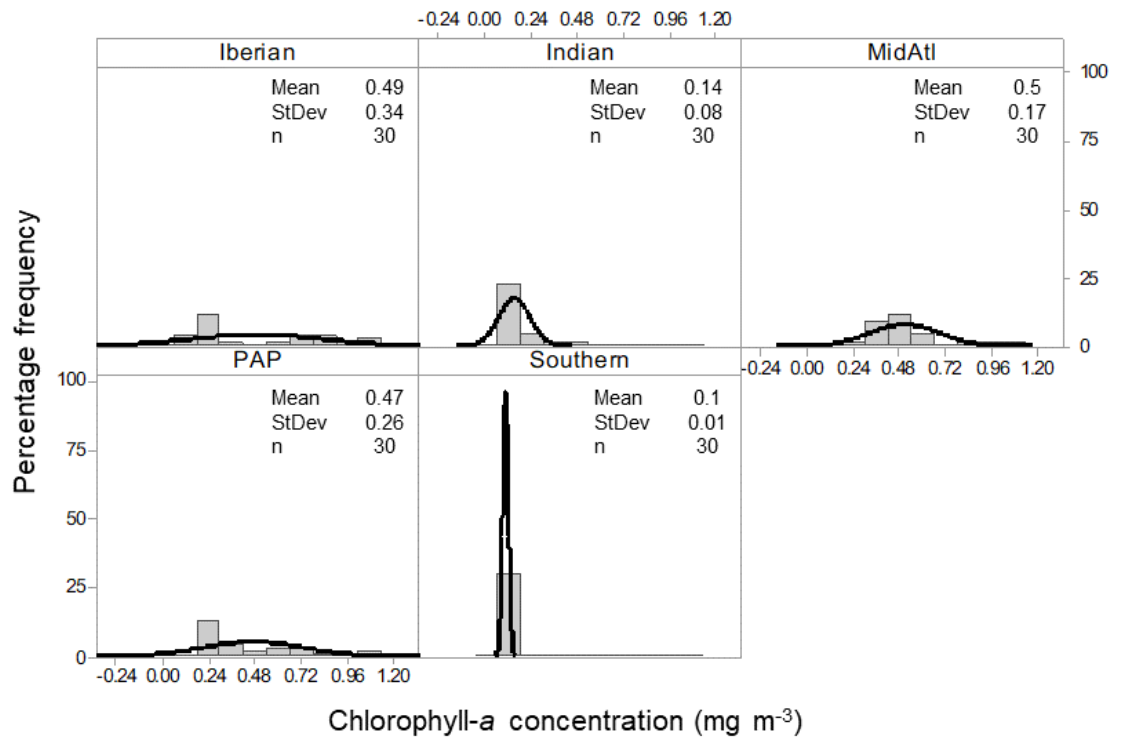


Figure 2.13 Chlorophyll-*a* percentage frequency concentrations according to geographical sample area within the global study area.

Due to the volume of seasonal data available for *P. periphylla*, it was used as a representative coronate species to investigate body size variation according to seasonal chlorophyll-*a* within each sample area (Figure 2.14). Globally, the size of *P. periphylla* individuals did not vary according to chlorophyll-*a* concentration (Pearson correlation $r = 0.03$, $p > 0.05$), however regional variation was observed, with a positive correlation between size and chlorophyll-*a* within the Iberian ($r = 0.39$, $p < 0.001$) and PAP ($r = 0.24$, $p < 0.01$) regions. A significant negative correlation was observed between *P. periphylla* medusa size and chlorophyll-*a* within the Southern Ocean ($r = -0.42$, $p < 0.01$). Globally, variation in *P. periphylla* medusa size was observed, with smaller individuals sampled during the winter months (one-way ANOVA with Tukey's test, $F = 5.73$, $p = 0.001$, $n = 392$). However, regional variation was apparent, with significantly larger medusae observed during the winter months within the Mid Atlantic sample region (one-way ANOVA with Tukey's test, $F = 13.1$, $p < 0.001$, $n = 94$) and significantly larger medusae observed within spring within the PAP region (one-way ANOVA with Tukey's test, $F = 16.02$, $p < 0.001$, $n = 120$). No significant variation was observed for medusa size and seasonality within the Southern Ocean or Iberian sample regions. Insufficient data was available for the Indian Ocean and as such was omitted.

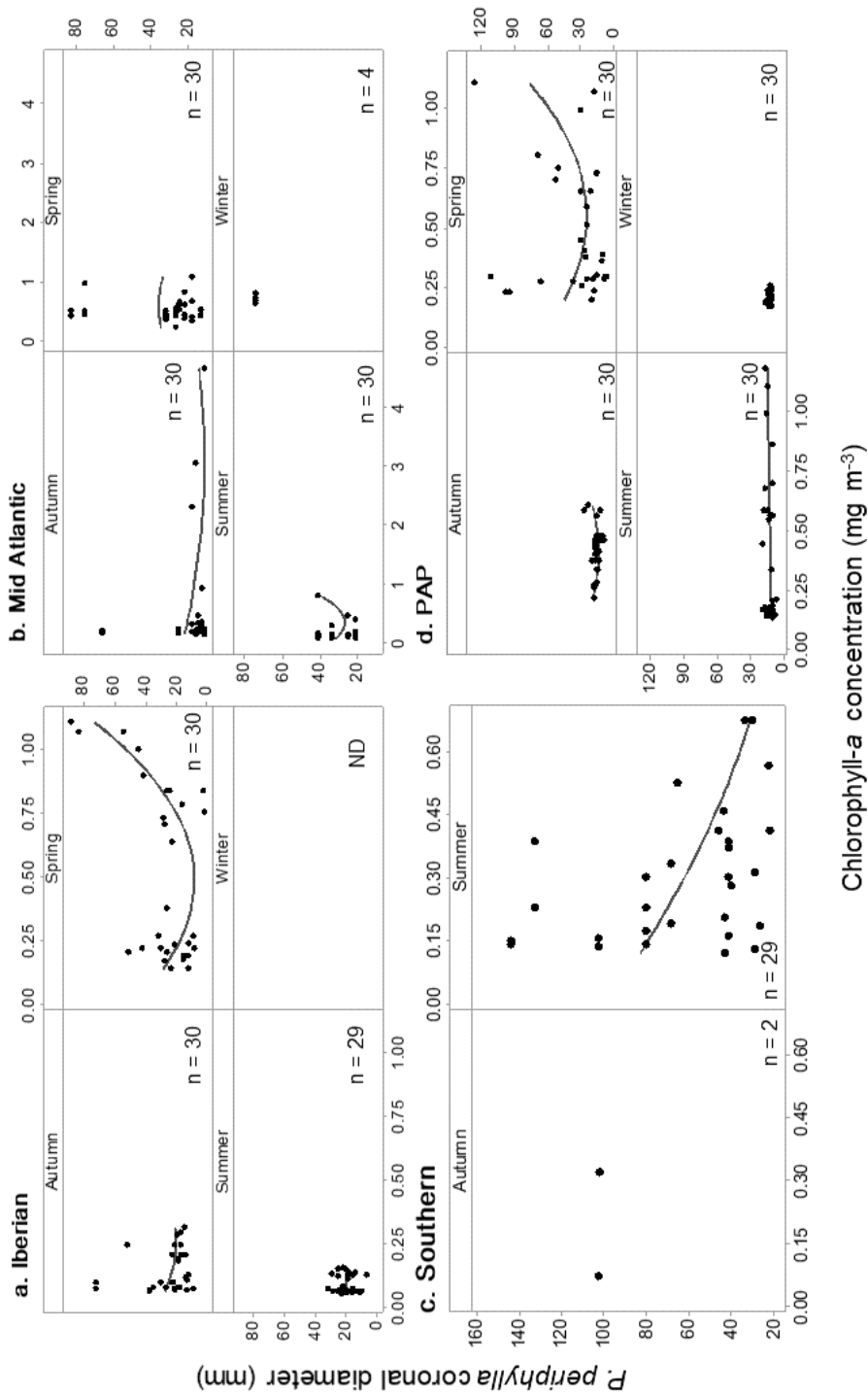


Figure 2.14 Relationships between *P. periphylla* coronal diameter and chlorophyll-*a* concentration (mg m⁻³) across seasons within the different sample areas across the global dataset. Winter and spring information was unavailable for the Southern Ocean, along with winter information for the Iberian region. Insufficient data was available for the Indian Ocean (n = 2 values in total) and as such was omitted.

2.4.6.1 Modelling environmental data

The spatial data were converted from latitude and longitudes to a geographic distance matrix whereby a distance group was assigned to 50 distinct areas within the global dataset. This was in order to remove the spatial autocorrelation and better determine large-scale patterns according to distance. A general linear model (GLM) was then applied to determine the spatial effects of species occurrence across the dataset when influenced by the environmental variables (zooplankton and chlorophyll-*a*).

Table 2.7 General linear model (GLM) output for the influence of environmental factors (chlorophyll-*a* and zooplankton diversity) on deep-sea corionate distribution according to global distance group generated by the geographic distance matrix for the global study area.

	<i>T</i>	<i>F</i>	<i>VIF</i>	<i>p</i>
Chlorophyll- <i>a</i> (mg m ⁻³)		4.33		0.038
Zooplankton diversity (Simpson's Index)		45.55		<0.001***
<i>A. chuni</i>	-1.31		11.1	0.191
<i>A. gigantea</i>	4.54		1.92	<0.001***
<i>A. parva</i>	-0.93		8.03	0.35
<i>A. russelli</i>	-0.65		2.16	0.515
<i>A. vanhoeffeni</i>	-8.05		2.72	2.72
<i>A. wyvillei</i>	-4.54		5.88	<0.001***
SuperAtolla	7.02		4.44	<0.001***
<i>P. periphylla</i>	-9.37		11.44	<0.001***

Zooplankton diversity indicates strong correlation with the geographic distance groups for the corionate species (Table 2.7). Species with widespread distributions such as *P. periphylla* and *A. wyvillei* demonstrate a significant negative relationship with the distance groups. Conversely, disparate specimens such as *A. gigantea* and SuperAtolla demonstrate significant positive relationships. The most significant relationships were observed within the larger species of deep-sea coronates (mean diameter > 30 mm) including *A. wyvillei*, *A. gigantea*, *P. periphylla* and SuperAtolla.

2.5 Discussion

2.5.1 Distribution of *Atolla* spp. and *P. periphylla*

The results of this study using museum collections have confirmed that deep-sea coronates exhibit cosmopolitan distributions throughout all large water masses and depth zones. *P. periphylla* is found within all areas of this extensive global dataset, both geographically and vertically in the water column (Figure 2.3a). Within the *Atolla* genus, the only species with a true observed cosmopolitan distribution was *A. wyvillei*, located within all regions apart from the poles (Figure 2.3b). By combining specimen resources from the NHM London, the Smithsonian and the GBIF, it was possible to map the species with poorer understood geographic occurrences, including *A. tenella* (Arctic region) and *A. chuni* (Southern Ocean region). Second to *A. wyvillei*, *A. parva* was also observed to exhibit significantly broad geographic spreads, located within all areas of the Pacific and Atlantic Oceans. *A. russelli* and *A. vanhoeffeni* were mostly clustered within the North Atlantic, the area with the highest data resolution. Previously only speculated in early literature (Russell 1970), this study confirms that on a global scale, the various species of *Atolla* are found at greater overall depths than *P. periphylla*, with mean depths of 905 m (*A. wyvillei*), 745 m (*A. chuni*), 1520 m (*A. gigantea*), 1108 m (*A. parva*), 1114 m (*A. russelli*), 651 m (*A. vanhoeffeni*) and 1058 m (potential species nova ‘SuperAtolla’) in comparison to 628 m (*P. periphylla*) (Table 2.5).

The spatial distribution of the various coronate species within this study provide no indication of change in size according to a latitudinal gradient (Figure 2.9). Latitudinal gradients have been well established in terrestrial and marine fauna with more documented distribution patterns, e.g. mammals (Blackburn and Hawkins, 2004), insects (Arnett and Gotelli, 2003), turtles (Ashton and Feldman, 2003), copepods (Lonsdale and Levinton, 1985) and fish (Belk et al., 2002). Although the mechanisms behind Bergmann’s rule have been frequently disputed since its inception (Scholander, 1955; Geist, 1987, 1990; Paterson, 1990), it remains recognised as a frequently observed general pattern in ecology. One such discussed mechanism is the starvation resistance hypothesis, whereby patterns in body size are skewed due to the resistance of the organism to seasonally scarce resources (Calder, 1984; Lindstedt and Boyce, 1985; Cushman, Lawton and Manly, 1993). The lack of a latitudinal response for the deep-sea coronates may be a result of jellyfish being plastic organisms that are able to shrink when food resources are scarce (Cary, 1915; Arai, Ford and

Whyte, 1989; Costello, 1998; Ishii and Båmstedt, 1998). It is also perhaps as a result of deep-sea coronates not being subject to the ‘temperature-size rule’, with deep-sea species not subject to the same seasonal fluctuations in temperature. However, the species within *Atolla* and *P. periphylla* are referred to as diel vertical migrating species (Thurston, 1977; Roe et al., 1984; Larson, 1986), and thus have an increased level of interaction with shallow water systems (Kaartvedt et al., 2007; Youngbluth et al., 2008). The position that the cell size of phytoplankton is also influenced by latitude (Sommer et al., 2017) would have an inevitable trophic effect on the marine food web and so in turn could have influenced such a display within this global jellyfish dataset.

2.5.2 Morphological variation in *Atolla* spp. and *P. periphylla*

Strong length-weight relationships were observed for all *Atolla* species and *P. periphylla* (Figure 2.4) as is a general assumption of overall growth in ecology. Strong relationships were also observed for both species between BD-BH in *Atolla* spp. and CD-CH in *P. periphylla*. The relationship between height and width within the *Atolla* genus isn’t as pronounced as *P. periphylla* due to the more disc-like appearance of the bell. Potential indicators of the three historical body forms in *P. periphylla* were observed in medusae > 30 mm diameter (Figure 2.4d). As discussed previously, *P. periphylla* was historically described as three separate species, *P. hyacinthina*, *P. dodechabostrycha* and *P. regina* due to the varied coronal morphologies. This may have ultimately be related to the environmental variables that have determined the growth of the organism, or the potential of morphological change after periods of shrinkage.

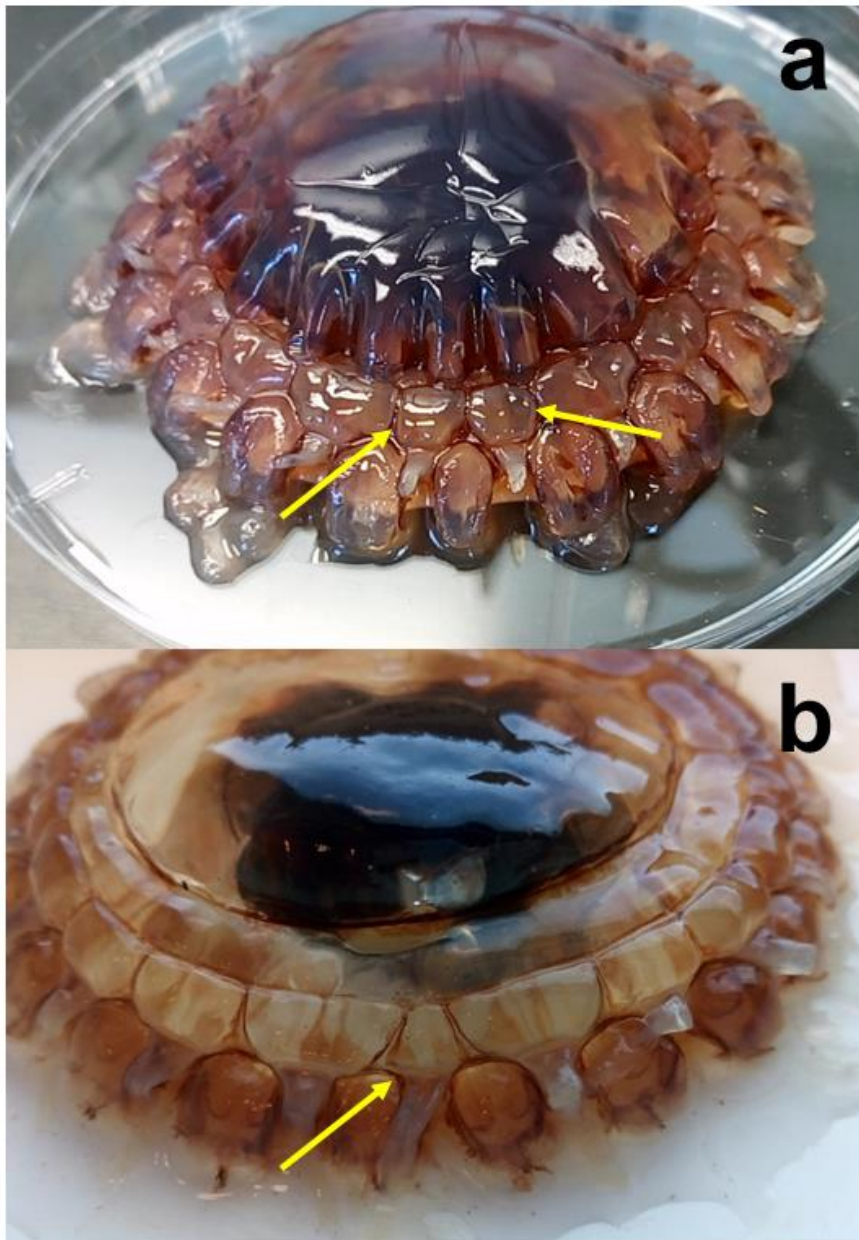


Figure 2.15 Photographs of developing pedalia and tentacles in **a:** *A. russelli* (bell diameter = 59.7 mm) and **b:** *A. wyvillei* (bell diameter 64.6 mm) from the museum collections used within this study.

In accordance with the descriptions by Russell (1970) and Larson (1986), *A. wyvillei* specimens within this study were found to have 22 tentacles in all instances, and *P. periphylla* with 12 tentacles in all instances. However, four other *Atolla* species were found to exhibit a range of tentacles which varied according to geographical area (Table 2.3). This variation may be a result of different prey types within certain regions requiring different levels of tentacular strength and in some instances, more tentacles. The tentacles of *Atolla* are significantly thinner than those of *P. periphylla*, and are much higher in number, therefore it is likely that the prey types vary. Studies documenting the behaviours such as

feeding and courtship using the tentacles for *Atolla* are minimal, however. Hunt and Lindsay (1998) observed the usage of the hypertrophied tentacle capturing the siphonophore *Nanomia* using *in situ* submersibles. This hypertrophied tentacle is noted to typically trail behind the main body of the medusa, and can reach lengths of up to 6 times the diameter of the bell. Repelin (1966) noted that this hypertrophied tentacle is always present, however whether it has any significance on the early development of the medusa is unknown (Russell, 1970). Repelin (1966) also notes that the position of the hypertrophied tentacle varies depending on species, with observed differences relative to the stomach pouch for *A. wyvillei*, *A. parva* and *A. vanhoffeni*. Hunt and Lindsay (1998) suggest that this observed behaviour may be indicative of a tentacle intended specifically for the capture of gelatinous prey such as *Nanomia*. Within this study, the identification of the hypertrophied tentacle was not possible due to extensive damage in particular to the finer *Atolla* tentacles following sampling.

Whilst gathering the morphological data, the development of new pedalia, and subsequent tentacles, was observed within *A. wyvillei*, *A. parva* and *A. russelli* (n = 10 total). This development has not previously been described, and could be as a result of a number of indeterminate factors. One possibility is that as the individual gains diameter, further tentacles are required in order to maximise prey capture and sustain its size. As the number of tentacles is positively correlated with size (all specimens > 30 mm diameter), it could also be an indication of a greater requirement for increased prey capture. As, although the size of an individual can reduce upon a scarcity of resources, there is no evidence to suggest that the number of tentacles would diminish. Tentacle number could therefore be a more robust proxy for age in certain regions, assuming that gradually over time the individual would gain subsequent tentacles. This is a novel approach which has not yet been discussed, and could have interesting implications for determining age in both deep sea jellyfish and gelatinous organisms in general. The age of individuals remains poorly understood, and could help understand ecological processes in time.

Environmental factors including zooplankton diversity and chlorophyll-*a* concentrations as proxies for food availability and primary productivity were collated on a global scale. The areas which displayed the greatest zooplankton diversity levels were the Iberian, PAP and Mid Atlantic (Table 2.6) which also represented the broadest chlorophyll-*a* frequency distributions (Figure 2.13). The Southern Ocean was observed as having the lowest

zooplankton diversity levels, which is in agreement with the lower observed zooplankton diversities within the literature (Hopkins and Torres, 1988; Siegel, 1996; Rombouts et al., 2009; Allcock and Strugnell, 2012) . Based on the results displayed during the spring months in the Iberian and PAP areas, it would suggest that an increase in tentacle number from the four species of *Atolla* is linked to greater food availability. This is further supported by the inverse relationship observed in the Southern Ocean.

2.5.3 Implications for marine macroecology

This study has demonstrated the value that historical museum collections can hold within macroecological studies. For organisms that are difficult to sample such as deep-sea jellyfish, making use of such a vast bank of specimen data and combining with modern contextual environmental data can provide valuable ecological insights into poorly understood fauna. Although inevitably the resolution of sample data is not as high as modern datasets, this study has established that macroecological patterns can nonetheless emerge.

The increased focus on the importance of gelatinous fauna in marine systems in recent years (Graham and Bayha, 2007; Pauly et al., 2009; Doyle et al., 2014) has resulted in a greater volume of scientific studies on jellyfish, however these are mostly focused on shallow-water, bloom-forming species (Parsons and Lalli, 2002; Bayha and Graham, 2014; Bosch-Belmar et al., 2017). The use of collections for deep-sea jellyfish research could therefore be a possible solution to answering some of the basic ecological questions that remain unknown. In general, marine macroecological studies are increasingly being undertaken as the value of ‘thinking big’ is better understood. However, the majority of deep-sea marine macroecology remains centred on benthic fauna, particularly bivalves (Macpherson, 2002, 2003; McClain, 2004; McClain, Boyer and Rosenberg, 2006; Kelly et al., 2010). These fauna may highlight the diversity of deep-sea benthic assemblages, however do not gain insights into the pelagic realm, which represents the greatest area of the oceans. Therefore, increasing the volume of macroecological studies focused on pelagic fauna could unlock some key insights into bathypelagic, mesopelagic and epipelagic systems, and using museum collections may be a means of doing this.

2.5.4 Conclusions

- This represents the first study to collate such a vast collection of material on *Atolla* spp. and *P. periphylla* using museum collections in order to better understand their distribution and morphology on macroecological scales.
- The spatial and vertical distributions of the deep-sea coronates is described, with *A. wyvillei* and *P. periphylla* exhibiting truly cosmopolitan distributions.
- No latitudinal gradient in body size is observed with any of the deep-sea coronates, indicative of their resilience as deep-sea species.
- No significant variation in the morphology of *P. periphylla* was observed within the global dataset (the data support the first hypothesis at the start of the chapter).
- The development of new pedalia within *A. wyvillei*, *A. parva* and *A. russelli* within mature medusae indicates that tentacle number is either reflective of age amongst the medusae, or reflective of a plastic response to changing environmental conditions requiring more tentacles for prey capture (the data support the second hypothesis at the start of the chapter).

Chapter 3: Investigating temporal morphological variation in deep-sea jellyfish within the Iberian Basin.

3.1 Abstract

With the exception of few long-term deep-sea research stations, there are minimal historical datasets on deep-sea pelagic taxa. Temporal change in deep-sea jellyfish physical characteristics is particularly poorly understood. As long-living taxa with broad spatial and vertical distributions within marine systems, the ecological significance of deep-sea jellyfish is likely underestimated. Any expressed morphological variation across spatial and temporal scales remains undocumented. This study investigated the use of historical collections data to identify comparative morphological variation in the widely distributed *Atolla parva*, *A. wyvillei* and *Periphylla periphylla* over a large temporal scale (1958 to 1983) within the Iberian Basin region in the North Atlantic. The North Atlantic Oscillation climatic index (NAOI) and fluctuations in chlorophyll-*a* were used to reflect environmental change within the study area across the temporal scale. Significant positive relationships for *A. parva* were observed between the tentacle numbers and depth located with the NAOI as well as the available phytoplankton. The outcomes of this study suggest that the expressed plasticity in *A. parva* and lack thereof in *P. periphylla* across this extensive study is a result of genetic distance between the two coronate genera, which molecular analyses could address in greater detail.

Chapter 3

The study of organismal features over time is fundamental to furthering our understanding of ecological processes and the ability to predict future change (Powell and Steele, 1995; Hunter et al., 2018). By examining biological data over time, it may be possible to better understand the mechanisms driving the population dynamics and spatial distributions of species, and understand how species respond to environmental perturbations. For example, Daufresne et al. (2009) provided evidence that fish body sizes have decreased over time in response to temperature in the North Atlantic. As is generally the case with macroecological data, extensive

Chapter 2

time series information is more abundant for terrestrial taxa, which are typically more conspicuous and easier to sample and document over extensive periods of time than marine taxa (Steele, 1995; Gotelli et al., 2017). The processes driving change between these two realms are also important to consider. For example, changes in air temperature and rainfall can impact terrestrial habitats on a day-to-day basis but will affect oceanic changes much more slowly. What constitutes a relevant time series for examining biological responses over time may thus vary depending on the taxa and habitat of interest.

Various long term temporal data are available from the marine environment. Commercially incentivised monitoring of fish stocks has to date provided the main source of information on the long-term variability of populations (Cushing, 1982). Such data have enabled categorisations of fish landing trends (as “steady, cyclical, irregular and stochastic”) (see Caddy & Gulland, 1983) because data over sufficient time scales can identify meaningful patterns. The bulk of routine marine time series data derive from the NE Atlantic, where data resolution is also greatest (Edwards et al., 2001). The Continuous Plankton Recorder (CPR), which was established in 1931, is the longest running and most widely recognised North Atlantic time series (Hardy, 1926; Warner and Hays, 1994; Beaugrand and Reid, 2003; H  laou  t et al., 2016). Other temporal datasets are available for the Atlantic Meridional Transect (AMT) (Aiken et al., 2000; Baker and Jickells, 2017), the Porcupine Abyssal Plain (PAP) (Iken et al., 2001; see Lampitt 2014 for cruise report example) and the European Station for Time Series in the Oceans (ESTOC) (Gonz  lez-D  vila et al., 2010).

Deep-sea temporal studies are on the increase due to appreciation of the high diversity of benthic species and the advent of cheaper and more effective sampling methods in pelagic and benthic habitats (see Larkin et al., 2009; McClain et al., 2009). Long-term deep-sea sampling has been conducted at the PAP (for almost 30 years) (Glover et al., 2010), Hausgarten in the Arctic (for 17 years) and Station M off the Californian coast (Soltwedel et al., 2016). Data repositories such as the British Oceanographic Data Centre (BODC) and the Ocean Biogeography Information System (OBIS) can also be used to generate time series information by combining data from various sources. Sustained observation of deep sea communities aids the understanding of deep-sea ecological processes, by capturing episodic events and associated faunal responses.

3.2.1 Temporal studies on gelatinous zooplankton

An increasing appreciation of the importance of gelatinous zooplankton as significant components of marine ecosystems has shifted the focus of a number of studies to focus on the macroecology – both spatially and temporally – of jellyfish populations. This is particularly apparent in shallow-water, bloom-forming species that are conspicuous in coastal environments, such as *Aurelia aurita* (Brotz et al., 2012). A long-term study conducted by Condon et al. (2013) compiled 37 datasets between 1874 and 2011 to better understand the temporal fluctuations in global jellyfish biomass. A conclusion of this unprecedented study was that shallow-water species are subject to periodic oscillations in abundance over 20 year intervals – a finding that challenged previous suggestions of global increases in jellyfish blooms. Time-series studies on gelatinous zooplankton have also analysed temporal data from sources such as the Continuous Plankton Recorder (CPR) (see Gibbons & Richardson 2009; Licandro et al., 2010) in relation to climatic indices, such as the North Atlantic Oscillation (NAO), to identify patterns of abundance (Lynam et al., 2004; Attrill and Edwards, 2008; Gibbons and Richardson, 2009; 2010). In other regions, a ten-year study in Monterey Bay compiled sample and video data of hydromedusae and found that the abundances of mesopelagic hydromedusae varied according to El Niño events observed within the time series (Raskoff, 2001). Temporal studies on gelatinous zooplankton have both focused on the drivers of jellyfish biomass and also

ess the bottom-

Chapter 3

Collections housed in various natural history museums (Natural History Collections, or NHCs) can offer complementary information to that of other data sources, such as OBIS and BODC. Some museums hold an array of global marine data, much of which is yet to be exploited for research (Lister et al., 2011). These NHCs can be used in conjunction with other data sources to produce valuable time-series insights that can either be analysed in their own right, or used as a baseline for future studies (Boakes et al., 2010; Graham et al., 2014). This study used NHC samples of *P. periphylla* and *Atolla* spp. from the Natural History Museum London to identify temporal trends in the comparative morphology and reproduction of deep-sea coronates.

3.2.2 Aims and objectives

This study aims to characterise temporal variability in the morphology and reproduction of *P. periphylla* and *Atolla* spp. within the Iberian Basin in relation to changes in climate and food availability. The objective of this chapter is to investigate the temporal variation in morphologies of *Atolla* and *Periphylla* using an extensive temporal dataset within the Iberian Basin.

The conceptual hypotheses being investigated within Chapter 3 are that *Atolla* spp. exhibit distinct morphological variation according to the fluctuations in the winter (Dec-Mar) North Atlantic Oscillation Index (NAOI). The second hypothesis is that the genus *Atolla* demonstrates a greater degree of morphological variation according to changes in chlorophyll availability as a result of the inherent phylogenetic distance between *Atolla* and *Periphylla*.

3.3 Materials and methods

3.3.1 Samples and study area

Samples of *Atolla* spp. and *P. periphylla* from the Iberian Basin were selected from historic wet collections of these taxa based at the Natural History Museum London (NHM). As described in Chapter 2, these samples were collected as part of the Discovery Expeditions. Material from the Iberian Basin was selected because these areas offered the greatest temporal resolution with unsorted deep-sea sample material available from 1937 and 1990. Following sorting for deep-sea coronates, the temporal dataset was reduced to a period of 26 years (1958 to 1983). Figure 3.1 depicts the sampling localities and provides dates of sampling.

As described in Chapter 2, this historic jellyfish material was fixed at sea at the time of sampling using 10% buffered formalin for 24 hours, which was subsequently diluted to 5% (White et al. 2013, personal communication). Ashore, specimens were then transferred into Steedman's, a formalin-containing preservation fluid commonly used with zooplankton samples (see Steedman, 1976 for description). All available *Atolla* spp. and *P. periphylla* specimens within the sample area were quantified and measured using the methodologies below.

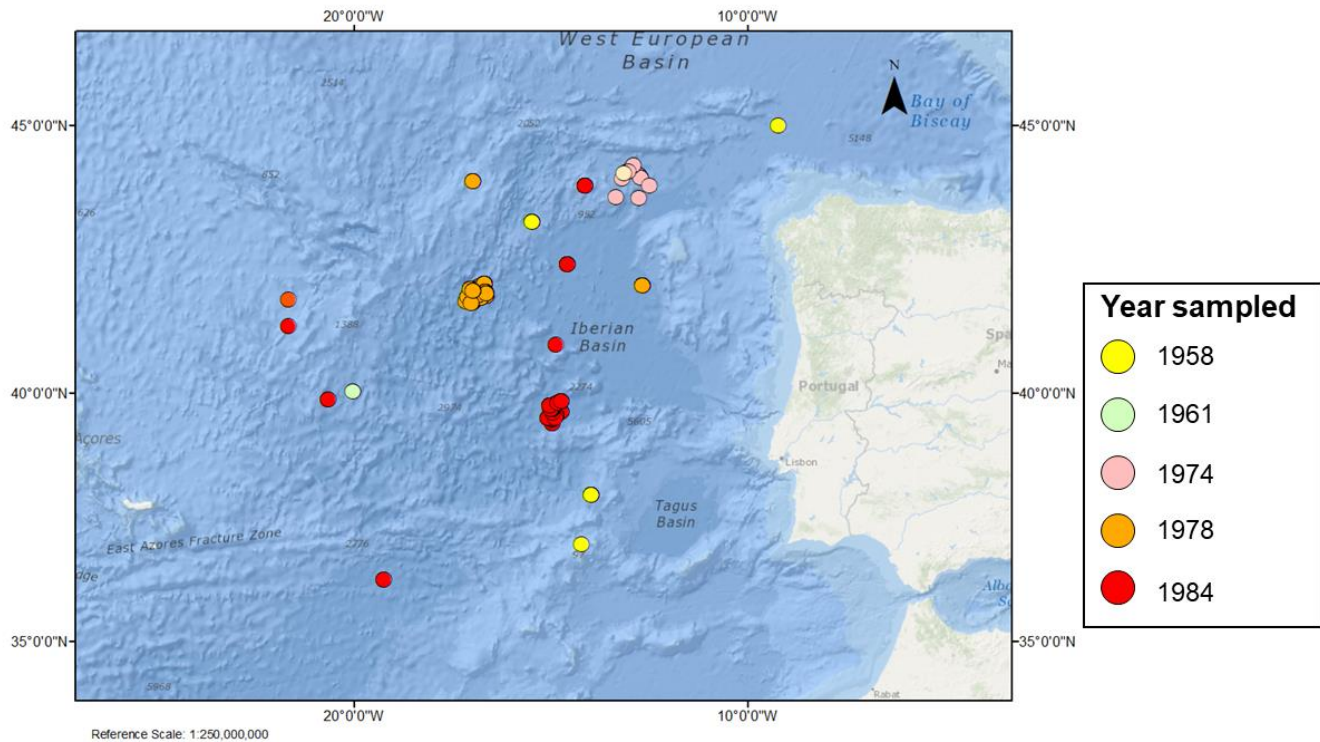


Figure 3.1 Distribution of the Iberian Basin sample area, with sample station locations of deep-sea coronate medusae within the NHM Discovery Collections dataset colour coded according to year collected. Base map source: ESRI.

3.3.2 Morphometric measurements of *Periphylla* and *Atolla*

Bell diameter, bell height, coronal diameter, coronal height and tentacle number were recorded for all specimens, along with preserved wet weight, using the morphometric methodology outlined in Chapter 2. Specimens smaller than 15 mm diameter were identified to species level and measured under a stereomicroscope. All individuals from the Iberian location were measured, with the exception of individuals that were extensively damaged following sample collection and storage.

3.3.3 Environmental variables

i). Chlorophyll-*a*

Global chlorophyll-*a* data (both surface and depth-specific) to compliment the historical sample dataset was sourced from the World Ocean Database of the National Oceanic and

Chapter 3

Atmospheric Administration (NOAA) data repository (<https://www.nodc.noaa.gov/cgi-bin/OC5/SELECT/dbsearch.pl>). Sample area and date were selected according to the station information for the sampled coronates. The chlorophyll-*a* data covered the period of 1957 to 1990 and was collected during research cruises from the Navy Instituto Hidrografico (Lisbon), the Institute of Oceanographic Sciences Deacon Lab (IOSDL) and the Woods Hole Oceanographic Institute (WHOI). The samples taken for chlorophyll-*a* determination covered a range of depths (0 – 2368 m). Due to the paucity of corresponding chlorophyll-*a* to sampled coronate data beyond 100 m, surface chlorophyll-*a* data were used to ensure the greatest resolution across the various year groups. Phytoplankton Colour Index data from the Continuous Plankton Recorder (CPR, available at <https://www.cprsurvey.org/data/map-data/>) was used in conjunction with the other chlorophyll data to provide a more comprehensive dataset, and reduce gaps within the data.

ii). Climatic indices data

The North Atlantic Oscillation Index (NAOI) was used as an indication of large-scale climatic forcing. This index developed by Hurrell (1995) is frequently used to analyse biotic interactions in both marine and terrestrial environments (e.g., Edwards et al., 2001; Ottersen et al., 2001). The NAO is the dominant mode of climatic variability in the North Atlantic, accounting for one third of the total variance in sea level pressure. Such pressures alternate between subtropical high surface pressures over the Azores (the 'Azores high') and sub-polar low surface pressures over Iceland (the 'Icelandic low') and are linked with fluctuations in the atmospheric pressures between the Icelandic low and the Azores high. Positive NAOI values represent the greatest difference in surface pressures between the two pressure systems. Data were obtained from the NOAA Earth System Research Laboratory Climatic Indices data repository at: <https://www.esrl.noaa.gov/psd/data/climateindices/list/> for data spanning 1937 to 1990.

Annual, monthly and seasonal NAOI values are calculated by normalising each station's raw sea level pressure data by the 1864-1983 long-term mean, subtracting the northern station (Reykjavik) from the southern station (monthly index) and creating seasonal/annual means of the raw sea level pressure data for each of the two stations, normalising the data by the 1864-1983 long-term mean, and subtracting the northern station (Reykjavik) from the southern

station (Lisbon for Dec-Mar) or Ponta Delgada for other seasons/annual (seasonal/annual indices). The winter NAOI (Dec-Mar) index is of particular interest (Lynam et al., 2004) for climatic studies relating to shallow-water jellyfish as it typically coincides with the period of ephyra production and development. Within this study dataset, all samples were taken during the spring and summer months, thus previous winter NAOI figures were used for analysing coronate and environmental data.

3.3.4 Data analysis

Following the morphological measurement of samples, robust characters including body size and tentacle number were selected for statistical analysis over the temporal dataset. These characters were determined to be consistent irrespective of trawl damage during sampling. One-way analysis of variance (ANOVA) and Tukey's post-hoc tests were used to determine significant differences between year groups. Significant differences between groups are highlighted with letter groupings *a* and *b*.

To test for correlation between two variables including variation in chlorophyll-*a* and the NAOI and its associated effects, a Pearson Correlation coefficient test and linear regression model were used, pooling morphological data across all time periods. For investigation into depths of sampled coronate medusae, data from specimens with broad depth records were removed prior to analysis. This included specimens whose depths were given in ranges exceeding 1000 m. To remove the influence of diel vertical migration, all depth records for analysis were taken during the day when sampling effort was greatest, omitting night and dusk samples. All depths were recorded in ranges and were sampled between 0 to 3450 m within the study area. There was no observed difference in using minimum, maximum or average depth readings for analysing morphometric data, thus the average depth sampled was used across the dataset.

3.3.5 Molecular methods

In an effort to understand the variation in species composition over time within the study area, DNA material was extracted from across the temporal dataset, using the landmarks with greatest DNA present within jellyfish (Dawson, 2016, personal communication). Tissue was removed from the formalin-fixed *Atolla* and *Periphylla* specimens held within the NHM

museum collections and processed using methodologies optimised for historical formalin-fixed material. See Chapter 7 (Conclusions) for full discussion of methods trialled.

3.4 Results

3.4.1 Temporal distribution of coronate species

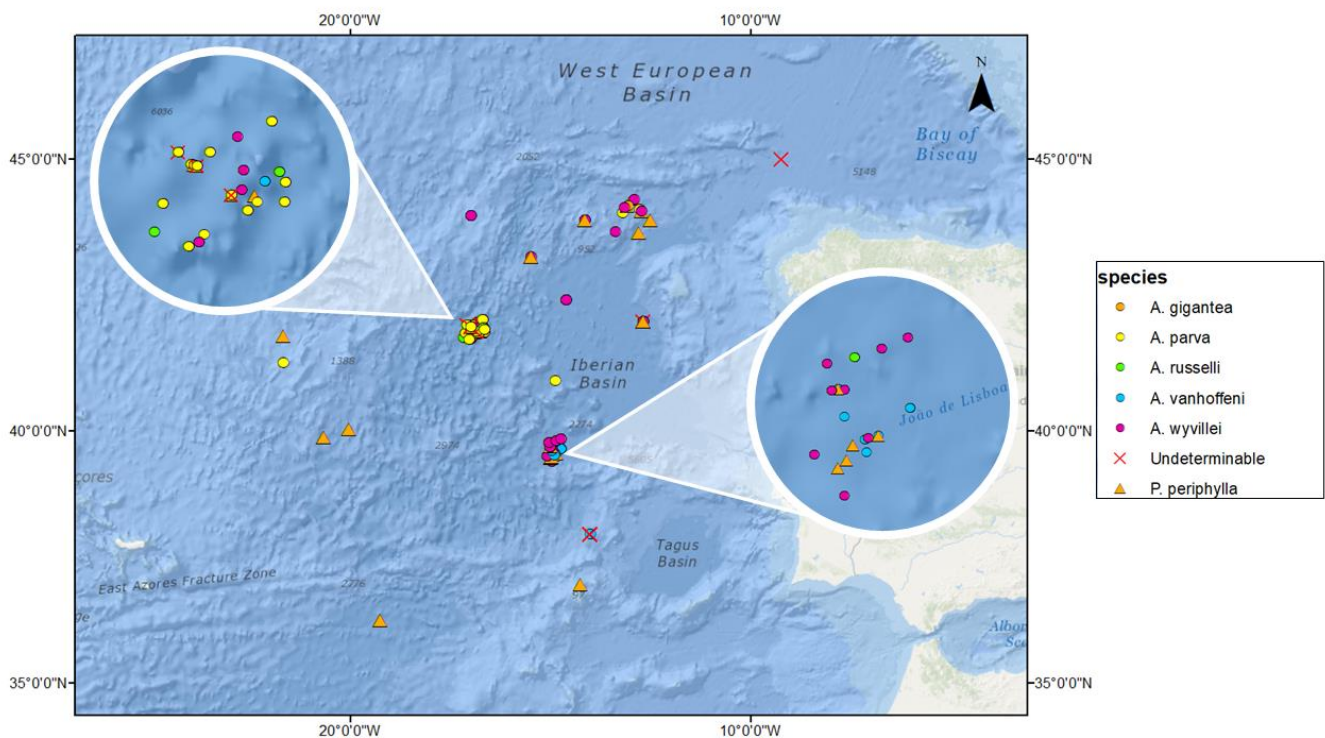


Figure 3.2 Distribution of the deep-sea coronate species found within the Iberian Basins study area. Clustered samples are depicted within the magnified circles. Base map source: ESRI.

Six deep-sea coronate species within *Atolla* and *Periphylla* were found following morphological analysis and identification to species level; *P. periphylla* ($n = 45$), *A. gigantea* ($n = 6$), *A. parva* ($n = 326$), *A. russelli* ($n = 39$), *A. vanhoffeni* ($n = 19$) and *A. wyvillei* ($n = 131$) (Figure 3.2). All samples were collected during the spring (Mar-May months). Species with low sample numbers ($n < 45$; *A. gigantea*, *A. russelli*, *A. vanhoffeni*) were removed due to their poor representation across the temporal scale. *P. periphylla* had relatively low sample numbers across the dataset, but was retained in order to identify potential comparative patterns to *Atolla* spp. reduced the temporal spread of the data to five sampled years and a 26-year range

(Table 3.1).

Table 3.1 Number of deep-sea coronates sampled following removal of species with poor temporal representation within the Iberian Basin collections. Figures highlighted in red represented too small a sample size for subsequent analyses and were removed. All deep-sea coronates sampled during the spring months of April and May.

Number of sampled deep-sea coronates			
Month and year	<i>A. parva</i>	<i>A. wyvillei</i>	<i>P. periphylla</i>
March 1958	1	1	4
March 1961			2
April and May 1974	3	5	4
May 1978	264	103	22
April 1984	58	22	13
Total	326	131	45

3.4.2 Morphological patterns over time

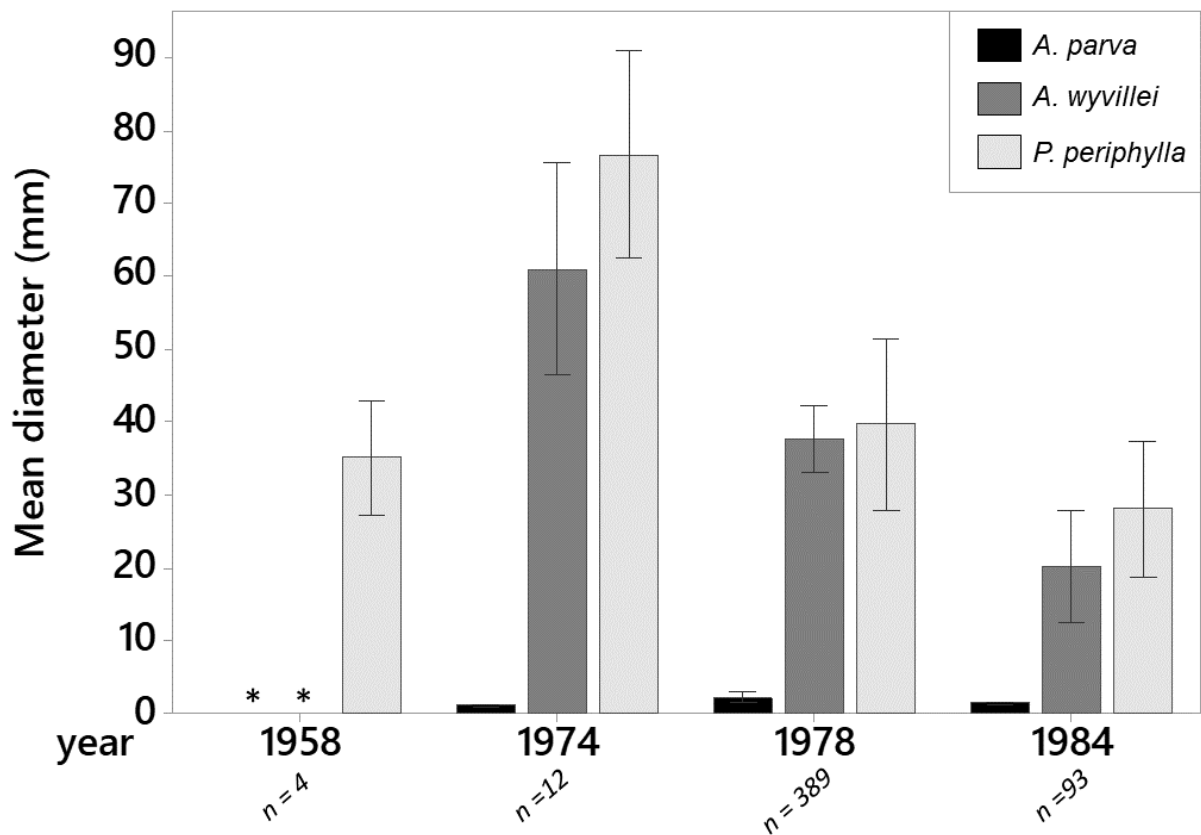


Figure 3.3 Mean diameter (bell diameter for *Atolla*, coronal diameter for *Periphylla*) and standard error (95% confidence) variation across the time series within the Iberian Basin study area. *A. parva*, $n = 325$, *A. wyvillei*, $n = 130$, *P. periphylla*, $n = 43$. Asterisks (*) = samples removed due to small size.

The sizes of the deep-sea coronate medusae retained within the dataset (*A. parva*, *A. wyvillei*, *P. periphylla*) demonstrate fluctuating body sizes across the time series, with apparent peaks for *A. wyvillei* and *P. periphylla* during 1974 (Figure 3.3). However, this is not significant to the 95% level for 1974 (one-way ANOVA with Tukey's test, $p > 0.05$) perhaps due to the small sample size for that year group ($n = 12$). Both *A. wyvillei* and *P. periphylla* are consistently larger than *A. parva*, with no significant difference between *A. wyvillei* and *P. periphylla* (one-way ANOVA with Tukey's test, $p > 0.05$). The relative body sizes of the various species are represented in Figure 3.4. No observed change in body size over time was apparent for *A. parva* (one-way ANOVA with Tukey's test, $p > 0.05$), despite the small sample size during 1974,

indicating that this smaller species remains a consistent size and not subject to much morphological change over time. For *P. periphylla* and *A. wyvillei* there is a significant difference in size between the earlier and later year groups, however the years themselves vary. In *P. periphylla* this is between 1974 (group a) and 1978+1984 (group b) (1958 is not statistically significant to either group), and for *A. wyvillei* this is between 1974+1978 (group a) and 1984 (group b) (one-way ANOVA with Tukey's test, $p < 0.01$). Due to the slight differentiation between *P. periphylla* and *A. wyvillei*, a further analysis was performed between the later years 1978 and 1984, due to the higher data resolution for these year groups (Figure 3.5). Still no observed difference was apparent for *A. parva*, however 1978 and 1984 were found to be significantly different for both *P. periphylla* and *A. wyvillei* (one-way ANOVA with Tukey's, $p < 0.05$).

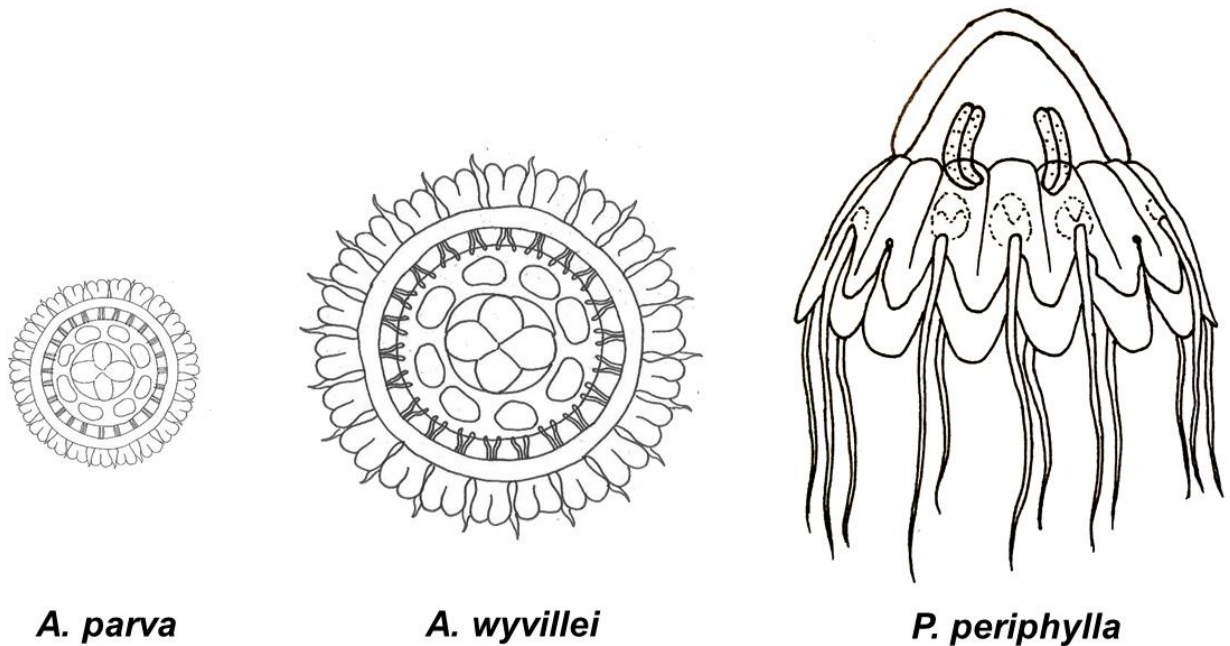


Figure 3.4 Relative body sizes of the species within the Iberian Basin dataset. Sizes illustrative of the mean sizes found (*A. parva* mean = 13 mm; *A. wyvillei* mean = 35 mm; *P. periphylla* mean = 38mm diameter). Illustrations drawn by author.

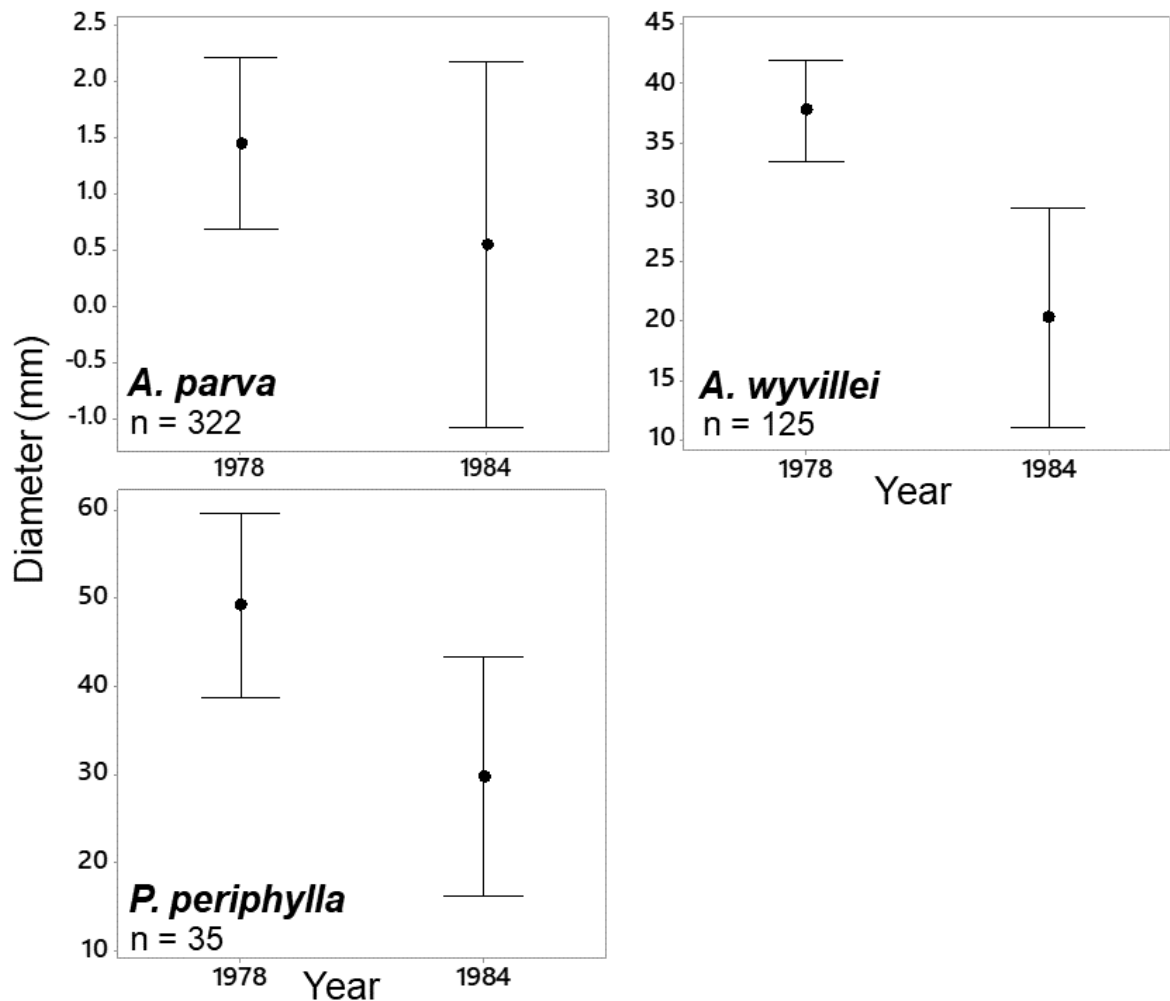


Figure 3.5 Variation in the corrected mean diameter of *A. parva*, *A. wyvillei* and *P. periphylla* within the Iberian Basin between 1978 and 1984. Significantly different groups indicated with letters above bars, one-way ANOVA, $p < 0.05$. Standard error bars to 95% confidence level.

Variation in tentacle number, however, was present for *A. parva*, ranging from 20 to 24 tentacles which is consistent with the descriptions of Russell (1970) (Figure 3.6). Variation observed alternated between fewer and larger numbers of tentacles between each year group. There was a significant difference in tentacle number between the heavier sampled 1978 and 1984 year groups (chi-squared test, $n = 322$, $chi-square = 108$, $p < 0.001$), with approximately 20 tentacles observed in 1978 and 21 tentacles in 1984. Tentacle number for *P. periphylla* was 12 tentacles across the dataset, with *A. wyvillei* having 22 tentacles consistently over time. This

contrast in body size versus tentacle number between the species could be indicative of varied expressed plasticity.

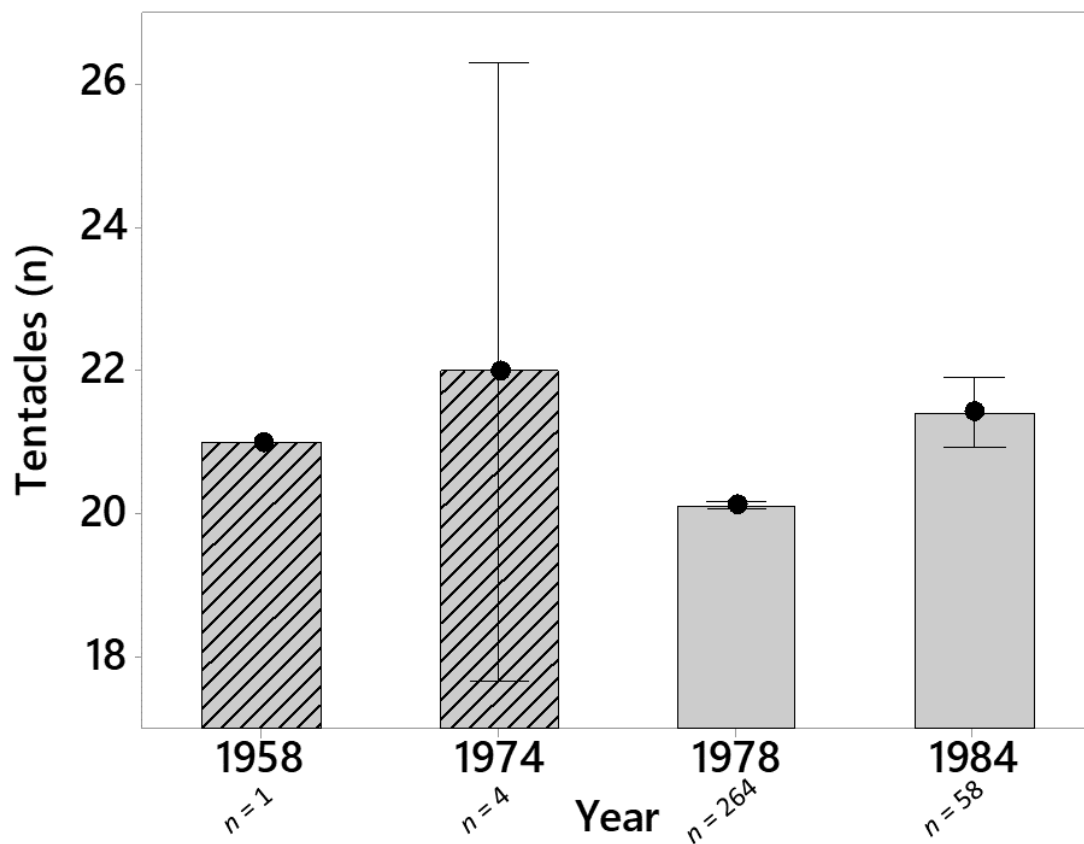


Figure 3.6 Mean tentacle number variation in *A. parva* between 1958 to 1984. Hatched bars represent small sample sizes that were not used for subsequent statistical analysis. Standard error bars to 95% confidence limits.

3.4.3 Chlorophyll-*a* fluctuations and influence on medusae

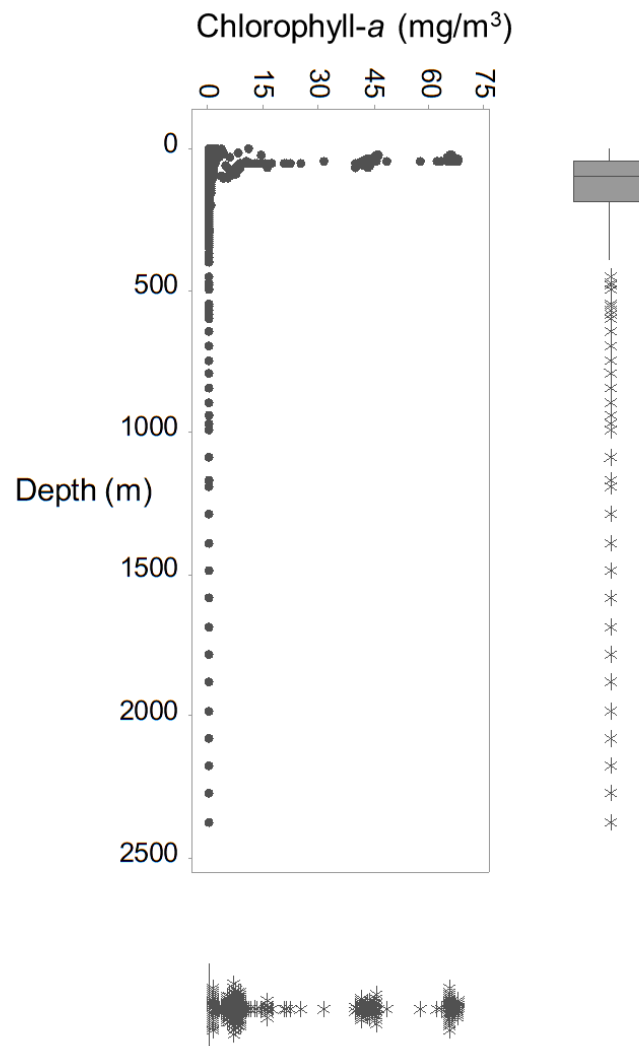


Figure 3.7 Relationship between depth and chlorophyll-*a* concentrations in the Iberian Basin overall (pooled years). Source of raw data: NOAA World Ocean Database.

Chlorophyll-*a* data sourced from the NOAA World Ocean Database produced concentrations from a range of depths between 1957 to 1990 within the Iberian Basin. As expected, the data show that the highest concentrations overall are within the top 20 m of the water column, with low levels of chlorophyll *a* ($< 0.2 \text{ mg/m}^3$) observed outside of the photic zone (200 m) (Figure 3.7). Analysis of the chlorophyll sampled within the top 20 m of the surface waters over time indicates that the levels remain quite consistent across the sample period, with the exception

of 1974 when chlorophyll concentrations reached up to 67.8 mg/m^3 , and may have been due to a combination of a greater sampling effort during that time ($n = 103$), as well as an apparent algal bloom at the time of sampling. (Figure 3.8).

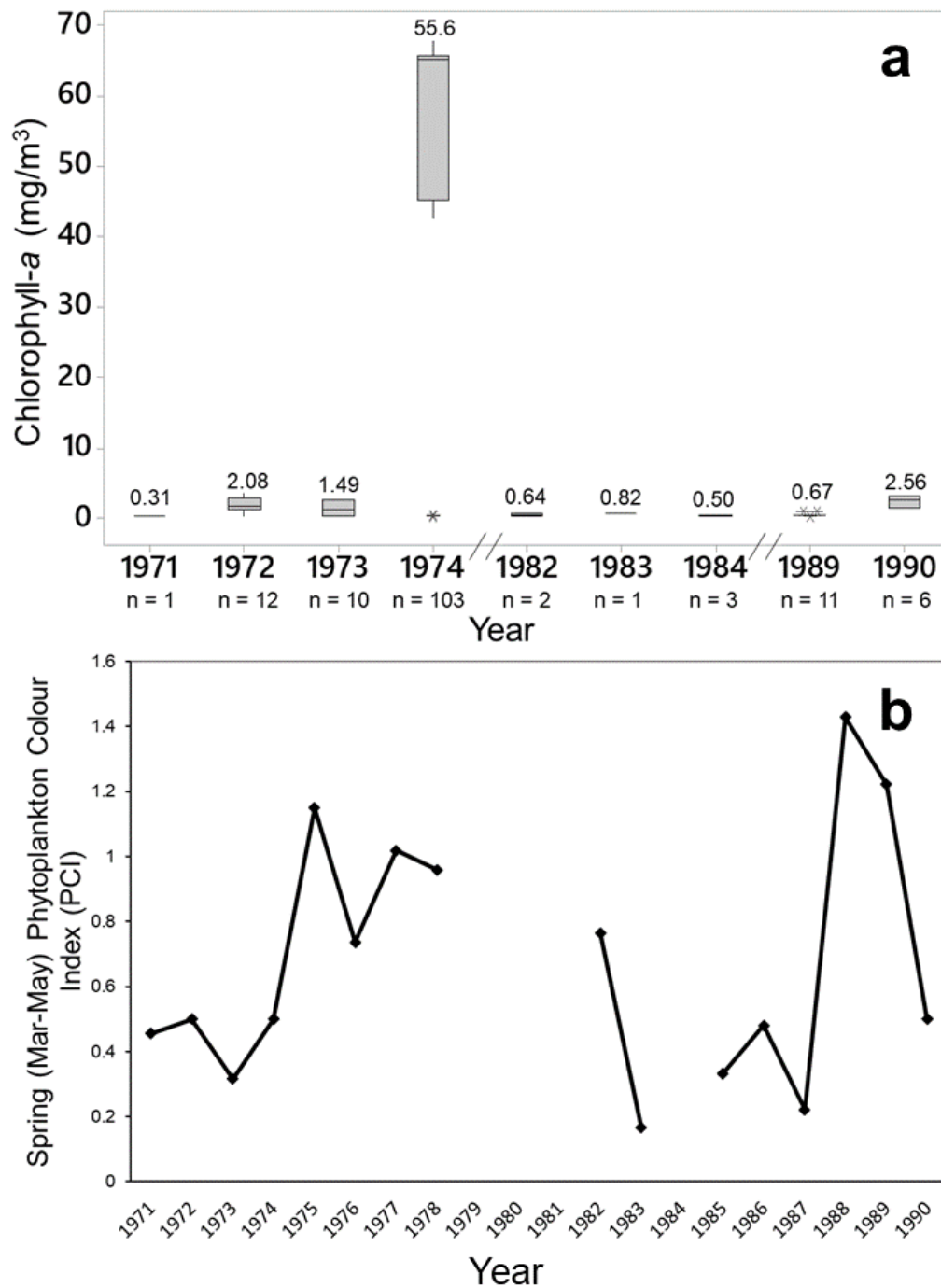


Figure 3.8 Spring (Mar-May) phytoplankton variation within the Iberian Basin 1971 to 1990. (a) Spring (Mar-May) near-surface (0 – 20 m below sea level) chlorophyll-*a* concentrations (mg/m³). Mean values noted above bars, with the exception of 1971 and 1983 as *n* = 1. Breaks in available data are marked on the x-axis (1974 to 1982; 1984 to 1989). Source of raw data: NOAA World Ocean Database. (b) Spring (Mar-May) Phytoplankton Colour Index (PCI) variation derived from the Continuous Plankton Recorder (CPR).

Due to the paucity of deep-water (>200 m) chlorophyll-*a* levels, surface chlorophyll-*a* data and the Phytoplankton Colour Index (PCI) from the CPR was used as a proxy for food availability against the deep-sea coronates found within the study area; irrespective of the depth at which the jellyfish were sampled. Figure 3.7 confirms that within this area the epipelagic photic zone is the area with the greatest chlorophyll-*a* variation and thereby the optimal area to use as a food availability proxy.

No significant trends were observed between body size and chlorophyll-*a* levels for all of the species across the dataset (Pearson's Correlation followed by linear regression, $r = 0.023$, $p = 0.679$ (*A. parva*); $r = -0.006$, $p = 0.947$ (*A. wyvillei*); $r = -0.08$, $p = 0.603$ (*P. periphylla*), Figure 3.9). Due to the range of observed tentacles in *A. parva*, tentacle number and chlorophyll sampled at the same time (PCI) were plotted against each other, however no observed trend was apparent (Chi-squared test, $r = 42.03$, $p > 0.05$, Figure 3.9). The years were pooled to increase resolution and despite the apparent chlorophyll-*a* bloom during 1974 (Figure 3.8a), the pattern is consistent with no observable outliers.

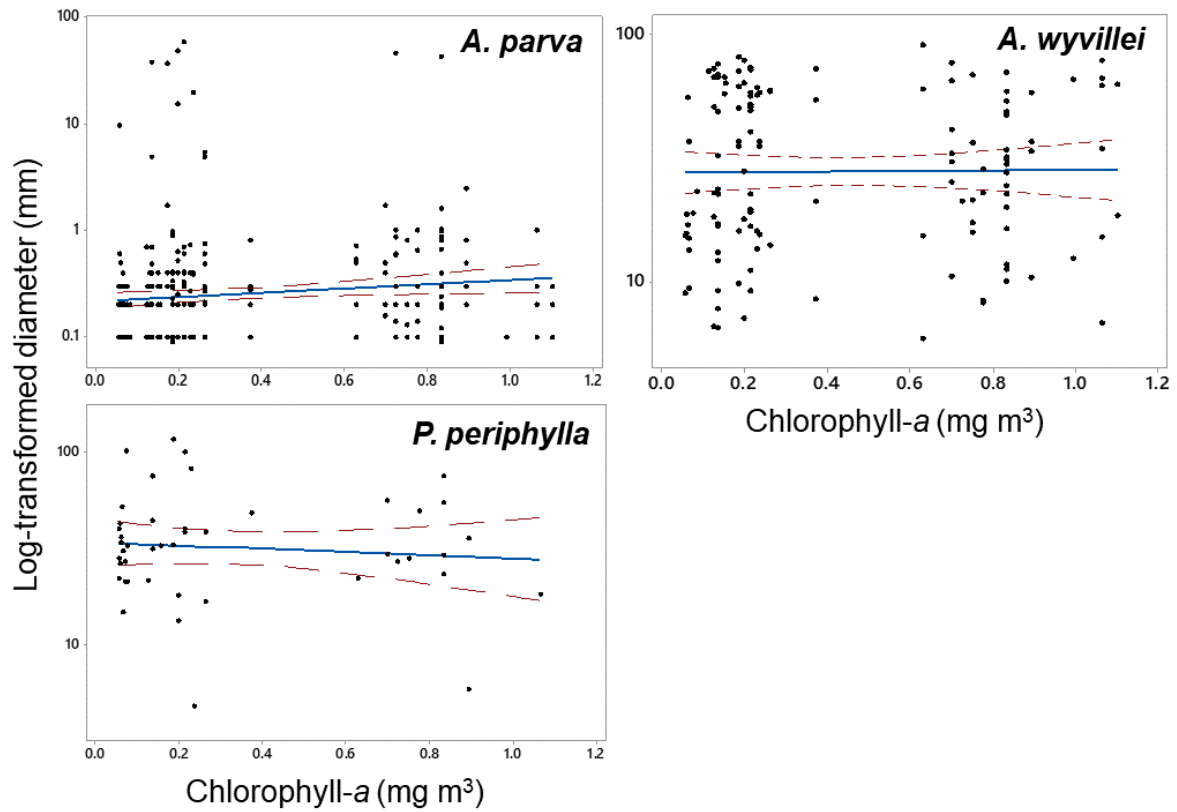


Figure 3.9 Log body size and surface spring (Mar-May) chlorophyll-*a* for *A. parva*, *A. wyvillei* and *P. periphylla* within the Iberian Basin study area, with linear regression line (blue) to 95% confidence interval (red dashed lines). Regression equations *A. parva* $y = 0.6575 + 0.1954x$, $r^2 = 0.016$; *A. wyvillei* $y = 1.441 + 0.01145x$, $r^2 = 0.01$; *P. periphylla* $y = 1.470 + 0.4945x$, $r^2 = 0.08$.

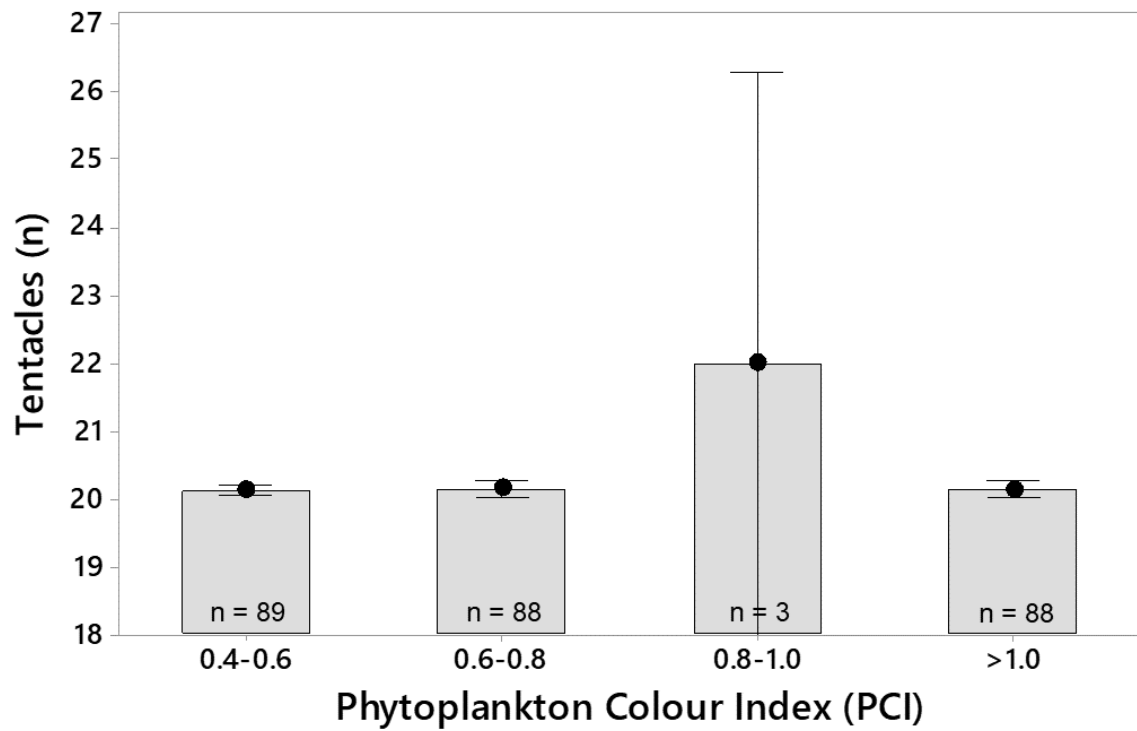


Figure 3.10 Phytoplankton Colour Index (PCI) and associated number of tentacles observed within *A. parva* within the study area. No PCI data was available for 1984 hence was omitted. Standard error bars to the 95% confidence limits. Source of raw PCI data: CPR.

3.4.4 Influence of climatic indices data

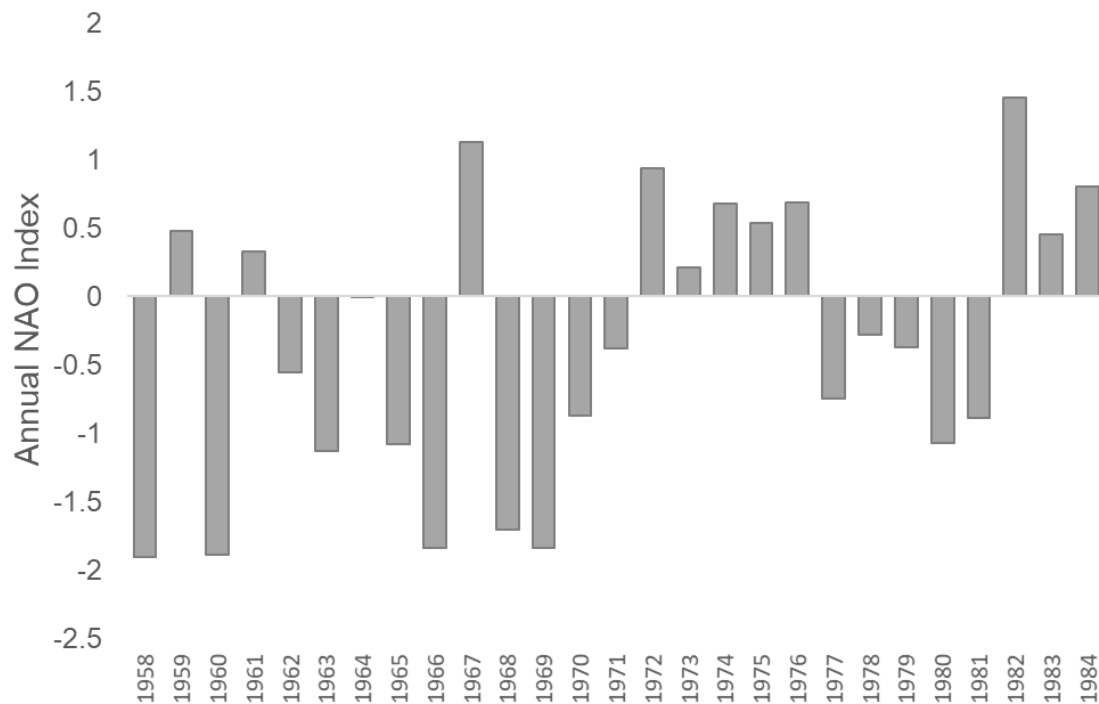


Figure 3.11 Annual NAOI fluctuations, displaying the difference of normalised sea level pressures between Ponta Delgada, Azores (high) and Reykjavik, Iceland (low) across the study sample period (1958 to 1984). Raw data source: NCAR, UCAR.

The NAOI over the study period is depicted in Figure 3.11, illustrating the cyclic positive and negative values associated with the climatic changes within the North Atlantic. Positive values represent the greatest difference between the Azores high and the Icelandic low.

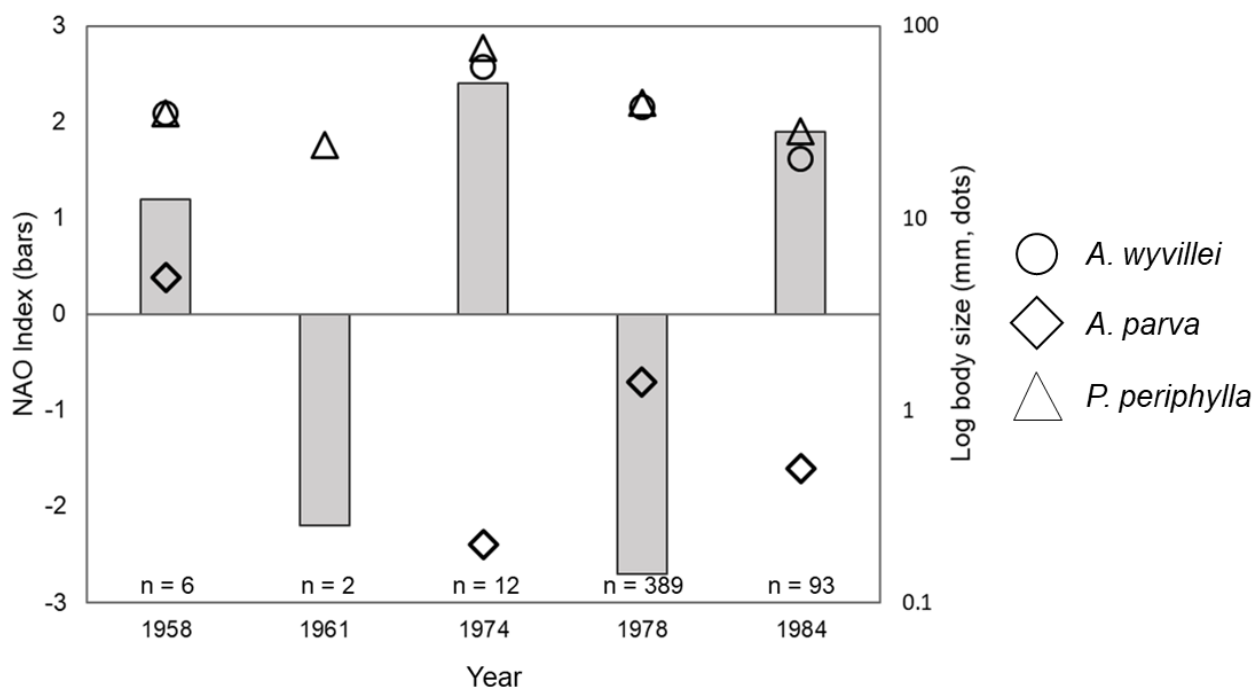


Figure 3.12 Normalised winter NAOI (December-March) Index (bars) and scaled log-transformed body size for *A. parva*, *A. wyvillei* and *P. periphylla* (dots). For ease of visual interpretation, the body size was log-transformed and plotted on the secondary axis. Small sample sizes present during 1958, 1961 and 1974, with $n = 1$ for *A. parva* and *A. wyvillei* during 1958.

No significant associations were found between the winter NAOI and log-transformed mean body size for all coronate species, (Figure 3.12, Pearson Correlation, *A. parva* $r = -0.54$, $p > 0.05$; *A. wyvillei* $r = -0.159$, $p > 0.05$; *P. periphylla* $r = 0.034$, $p > 0.05$). As with the influence of chlorophyll-*a*, the body size of all three species remains robust across a large temporal scale. The small sample set for NAOI figures during 1958, 1961 and 1974 could also be a contributor to this apparent lack of observed pattern.

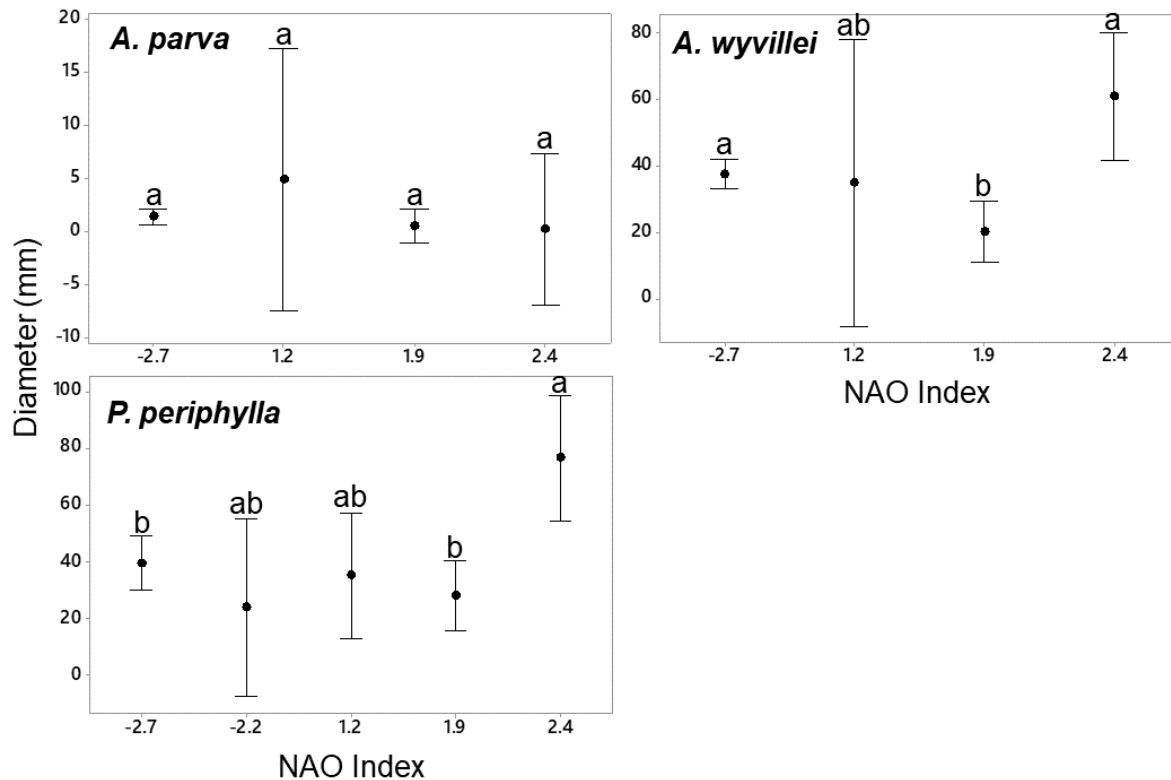


Figure 3.13 Variation in bell diameter with respect to NAO Index within the Iberian Basin study area, with year groups pooled. Significantly different groups indicated with letters above bars, Tukey test, $p < 0.05$. Standard error bars to 95% confidence limits.

Significant differences in overall body size and the winter NAOI were observed for *A. wyvillei* and *P. periphylla* (one-way ANOVA with Tukey's test, *A. wyvillei* $F = 6.26$, $p = 0.00$; *P. periphylla* $F = 4.05$, $p < 0.05$). However, there is no clear pattern in terms of relationships between diameter and positive or negative NAO indices (Figure 3.13).

Tentacle number in *A. parva* was found to be significantly associated with the winter NAOI (Chi-squared test, $\chi^2 = 108.31(9)$, $p < 0.05$), with a positive index representing the greatest difference between the Azores high and the Icelandic low resulting in an increase in the number of tentacles (Figure 3.14). This indicates that the greater the climatic response may result in subsequent morphological variation within *A. parva*.

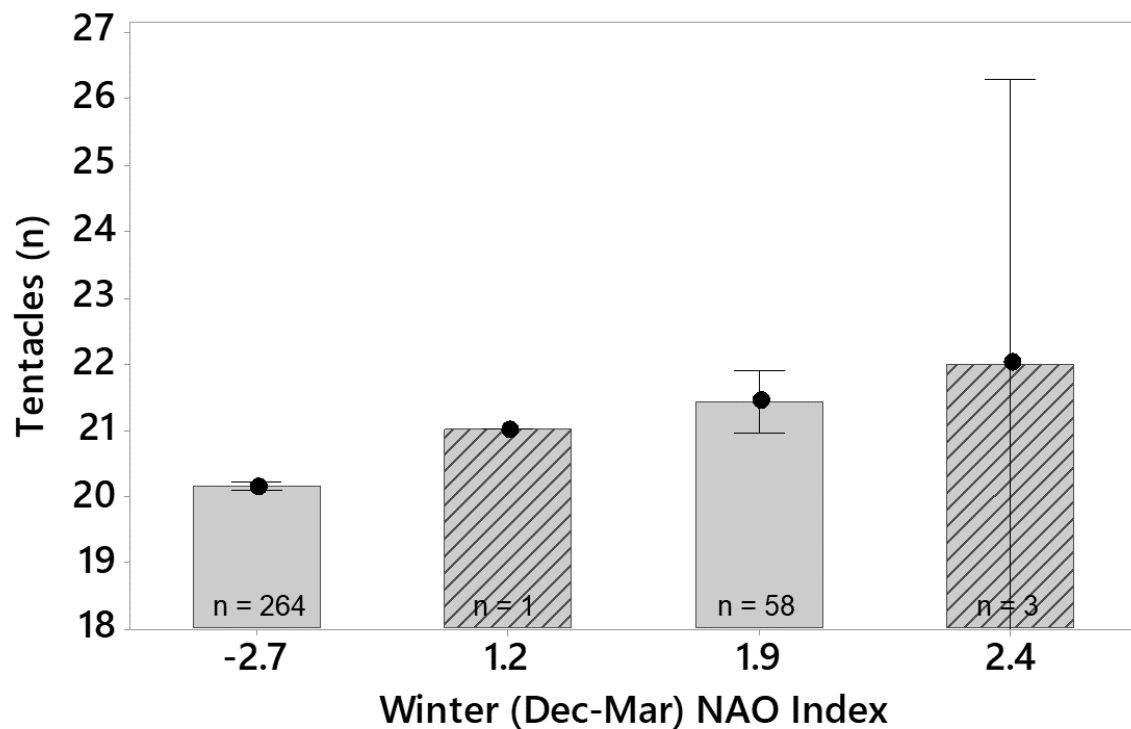


Figure 3.14 Winter NAO Index and associated tentacle number observed in *A. parva* within the study area, years pooled. Hatched bars represent low sample numbers. Standard error bars to the 95% confidence limit.

The influence of NAOI on depth that the deep-sea coronates were sampled was investigated to determine whether climatic forcing through systems such as the NAO could influence deep-dwelling medusae. Relatively few *P. periphylla* individuals were encountered in the daytime samples ($n = 25$) and the species was therefore discounted for statistical analysis. Significant patterns were observed between depth sampled and the NAOI index for *A. wyvillei* and *A. parva* (one-way ANOVA, *A. parva*, $F = 4.47$, $p < 0.05$, $n = 205$; *A. wyvillei*, $F = 8.66$, $p < 0.001$, $n = 90$, Figure 3.15). *A. parva* and *A. wyvillei* were found at deeper depths (bathypelagic) during periods of lower NAOI variance, and were both found at shallower depths (mesopelagic) during periods of greater NAOI change. Overall *A. parva* was found at overall greater depths during the day than *A. wyvillei* (mean = 1127.6 m and 983.8 m respectively, one-way ANOVA, $F = 11.45$, $p < 0.001$). Three NAOI values were available during the sample period for *A. wyvillei*, with only two available for *A. parva*. Based on the results it would indicate that the NAOI has influence on the depths that the various species migrate to within the Iberian Basin.

Chapter 3

To model the interaction of the various environmental factors on tentacle number in *A. parva*, a GLM was used, using the NAOI, PCI, average depth sampled and year as model terms (Table 3.2 General linear model (GLM) output predicting variation in tentacle number for *A. parva* within the Iberian Basin (1958-1984) (n = 226). Year, NAOI and average depth could not be estimated and were removed from the model. ***significant to > 99% confidence level.). Year, NAOI and average depth could not be estimated and were subsequently removed from the model. PCI indicates a strong relationship with tentacle number in *A. parva*, however the model summary nonetheless describes a large degree of uncertainty ($r^2 = 0.12$).

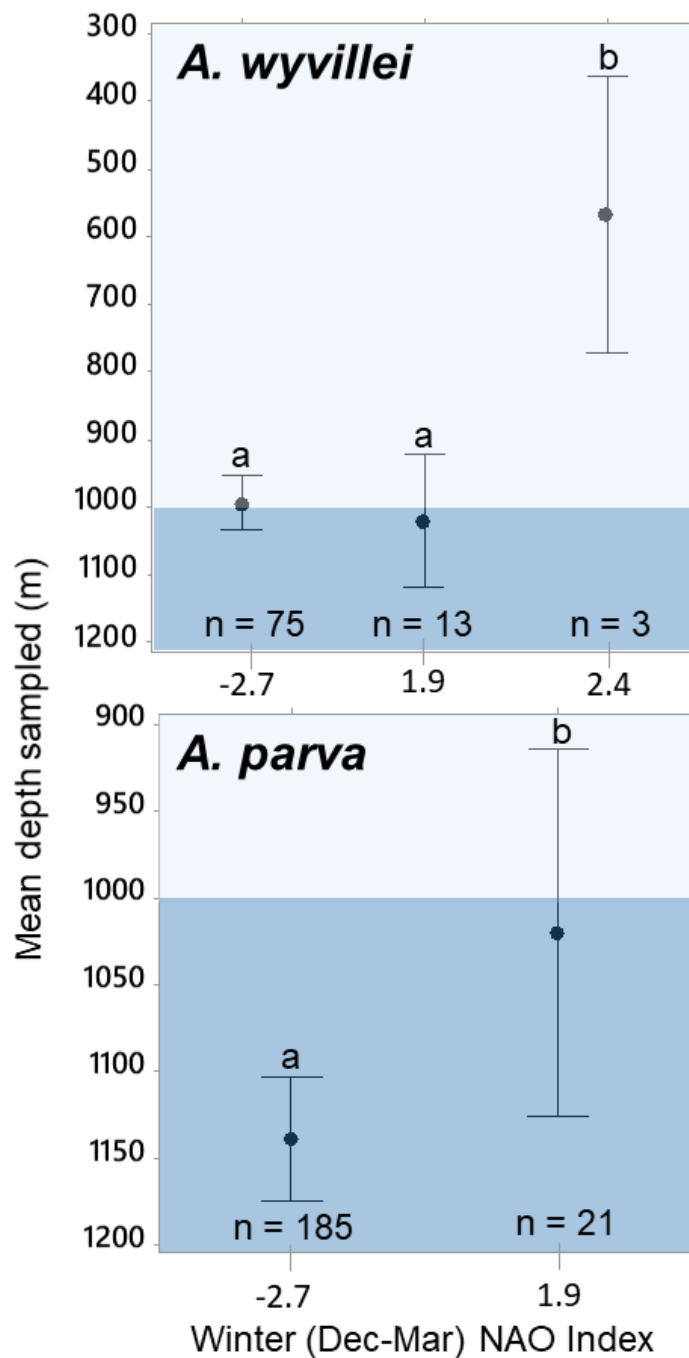


Figure 3.15 Mean depths of *A. parva* (n = 206) and *A. wyvillei* (n = 91) against the winter (Dec-Mar) NAO Index. All depths taken during day cruises. Coloured sections represent the mesopelagic (light blue) and bathypelagic (dark blue) depth zones at which coronates were sampled. *A. wyvillei* were sampled across a broader set of NAO indices and depths than *A. parva*. Letters above bars indicate significantly different groups (Tukey's test, $p < 0.01$). Standard error bars to 95% confidence limit.

Table 3.2 General linear model (GLM) output predicting variation in tentacle number for *A. parva* within the Iberian Basin (1958-1984) (n = 226). Year, NAOI and average depth could not be estimated and were removed from the model.
***significant to > 99% confidence level.

	<i>S</i>	<i>r</i> ²	<i>Adj SS</i>	<i>F</i>	<i>p</i>
<i>Factors</i>					
(Year)			*	*	*
(NAOI)			*	*	*
(Average depth (m))			*	*	*
PCI			11.11	9.33	0.000***
Model summary	0.54	0.12			

3.5 Discussion

Temporal studies on shallow-water jellyfish species are becoming more numerous, with the need to better understand periodic events such as bloom-forming scyphozoan genera such as *Aurelia* (Schroth et al., 2002), *Pelagia*, (Hamner and Dawson, 2009) *Cyanea* (Dong et al., 2010) and *Nemopilema* (Uye, 2008). Long-term datasets pooled from resources such as JeDI and across studies have helped build a better understanding of how gelatinous zooplankton within the photic zone fluctuate in abundance over time. Shallow-water environments are more heavily influenced by anthropogenic influences such as pollution and overfishing, resulting in subsequent alterations to marine food webs and species compositions. Parsons and Lalli (2002) hypothesised that bloom events – according to the definition of blooms related to an increase in reproduction - coincide with ‘low productivity’ food web systems, dominated by flagellates. This is in contrast to ‘high productivity’ systems, comprising more evolved fauna, dominated by diatoms (for example, in upwelling regions). The low productivity systems seem to favour the increase of jellyfish biomass, and would include areas subject to pollution and eutrophication. Parsons and Lalli (2002) stated that these two food webs are not mutually exclusive, but can fluctuate in dominance of an area or due to environmental perturbations. According to this theory, therefore, bloom populations can never occur in upwelling regions. Mills (1995), however, previously stated the converse, describing large volumes of jellyfish in the upwelling Angolan Benguela system. The hypothesis set by Parsons and Lalli (2002) is reinforced with the presence of mass volumes of jellyfish within a number of temperate fjords; systems that generally have low productivity, dominated by flagellate ecology. A number of Norwegian fjords contain mass aggregations of the study species *P. periphylla*, a typically oceanic species found at mesopelagic depths (Sørnes et al. 2007). While *P. periphylla* is not classed as a bloom-forming species as the high volumes of individuals within places such as Lurefjorden are a result of being physically contained within a semi-closed environment; it is nonetheless of significant interest how as a species it can adapt over time. *P. periphylla* is now known to be spreading in occurrence to the more northerly Norwegian fjords, thought to be as a result of warming waters with climate change (Tiller et al., 2017). Sighted first within Lurefjorden (60.4°N, 5.08°E) in 1999, *P. periphylla* has moved northerly to Trondheimsfjord (63.7°N, 11.31°E) and are predicted to move upwards to Holandsfjorden (66.7°N, 13.32°E),

Skjerstadvfjorden (67.2°N, 15.08°E) and Vestfjorden-Stordjupna (67.8°N, 14.17°E) (Tiller et al., 2017).

Condon et al. (2012; 2013) produced a meta-analysis of jellyfish data sources to produce an assessment of whether or not jellyfish are increasing in abundance. By using long-term empirical data, the study found that jellyfish blooms are subject to episodic, global oscillations; the periodicity of which being approximately 20 years. An exception to the peak-and-trough findings was a slight increase in abundances after 1970; a shift that cannot yet be explained without sustained monitoring over a longer timescale to infer the context of such a rise. The giant rhizostome jellyfish, *Nemopilema nomurai* Kishinouye, 1922 endemic to the East Asian Marginal Seas, is an example of a bloom-forming species that was particularly reported due to its vast size and subsequent disturbance to human activities particularly fishing (Uye, 2008; Dong, Liu and Keesing, 2010). In 2005 numbers of *N. nomurai* were as numerous as $3\text{-}5 \times 10^8$ medusae through the Tsushima Current, followed by a 'bloom and bust' (terminology coined by Pitt et al., 2014) event in 2006 whereby the numbers drastically dropped back to that of previous years. Uye (2008) reports that *N. nomurai* is subject to such cyclic bloom and bust events which is of ecological and climatic significance as well as a nuisance to various human activities.

Temporal studies on oceanic deep-sea jellyfish are limited, due to the inherent sampling difficulties and expense accrued by longer-term monitoring. The midwater ecology group at Monterey Bay Aquarium Research Institute (MBARI) has probably produced the most comprehensive long-term deep-sea jellyfish studies to date. Osborn et al. (2007) monitored the deep-water genera *Atolla*, *Periphylla* and *Poralia* within Monterey Bay using sampling, video and observation techniques. This covered a period of 9 years (1990-1998), and was able to identify specific water habitat affinities between the various genera. *Atolla* was found to inhabit the spicy (warm, salty) waters of the California Undercurrent within Monterey Bay, with *P. periphylla* more heavily associated with more variable, colder and fresher waters. *Poralia* were mostly associated with the densest, coldest waters. This fine-scale observation on differential water mass preferences may be prevalent in other oceanic areas, however would require replication over similar time scales in a number of different areas to capture this more holistically. Raskoff (2001) monitored the vertical distributions of mesopelagic hydromedusae over a period of ten years (1988 to 1998); during which two El Niño events occurred (1991-92 and 1997-98). Vertical species compositions were found to

vary, with *Mitrocoma cellularia* and *Colobonema sericeum* shifting their occurrences as a result of varied tolerances to the water mass changes associated with El Niño events.

3.5.1 Effects of climate and phytoplankton variation on deep-sea jellyfish

The Iberian Basin coronate dataset, selected as the region with the greatest temporal resolution is identified as a complex system with an array of eddies, buoyant plumes, upwelling filaments and fronts that have an undetermined influence on the ecosystem (Relvas et al., 2007). The Iberian Basin is also subject to changes in the North Atlantic Oscillation (NAO) climatic cycles, that are frequently linked to fluctuations in the density and diversity of biota within the North Atlantic on individual, population and community levels (Ottersen et al., 2001; Soltwedel et al., 2016). Fromentin and Planque (1996) identified that the NAO was positively related to abundances with the NAO suggested to explain apparent increases in gelatinous biomass over time. Attrill et al. (2007) identified a positive correlation of jellyfish with the NAO from 1958 to 2000, particularly during a regime shift during the 1980s in the North Sea. Lynam et al. (2004) investigated the correlation between the NAO and jellyfish abundances, and found that *Aurelia aurita* and *Cyanea lamarckii* were strongly inversely correlated with the NAO from 1971 and 1986. A number of other studies have supported these of climate-related findings for different regions (Brodeur et al., 2002; Kogovšek et al., 2010; Condon et al., 2012). This study sought to address the expression of plastic traits in gelatinous zooplankton, where previously only abundances have been correlated with the NAO climatic index. Lynam et al. (2004) were able to identify finer-scale temporal change within shallow-water jellyfish abundance and associations with the NAOI due to a greater level of data resolution that was unbroken in time between the period 1971 to 1986. The winter NAOI was selected as most significant for shallow-water jellyfish to coincide with important ephyrae production the following spring, with Lynam et al. (2004) revealing an inverse relationship and as such was also selected for this study to identify potential patterns.

This study has utilised available phytoplankton (chlorophyll-*a* and PCI) and NAOI data within the study area between the period 1958 to 1984. The NAOI climatic shift is documented to influence marine phytoplankton (Irigoien et al., 2000), whereby within the North Atlantic a positive produces warmer conditions that should result in an earlier onset of the spring bloom and subsequent higher productivity (Dickson et al., 1988). How this impacts the deep-

water fauna that rely on the transport of food from the epipelagic zone (Glover et al., 2010), however, is not yet understood. During 1974, a positive NAOI was observed (Figure 3.11), which also coincided with a significant observed phytoplankton bloom within the study area (Figure 3.8). Chlorophyll-*a* concentrations during this time reached up to 67.8 mg m³, which is significantly higher than what typically constitutes a bloom at anything in excess of approximately 10 mg m³ (Zeng et al., 2017). The chlorophyll-*a* within the dataset was sampled as part of the plankton investigations of Discovery Cruise 61 (see Angel, 1974 for cruise report), the results of which were subsequently published in Fasham and Pugh (1976). However, no indication of a significantly higher than typical spring bloom was described. Therefore, it is not possible to draw further conclusions regarding this significant bloom event. The potential responses by deep-sea coronates, and any associated lagged or immediate observed effects are also still uncertain.

3.5.2 Temporal variation in morphological traits within deep-sea coronates

Within the study area, *A. wyvillei* and *P. periphylla* were found to vary significantly between 1978 and 1984 (Figure 3.3), with no observed change in size at all within *A. parva* according to year, chlorophyll or NAOI variation. Tentacle number in *A. parva* was found to vary according to changes in environmental conditions, however the interactions of the various model terms remains uncertain. Chlorophyll (PCI) was most strongly linked to tentacle variation (Figure 3.10) and may be an indication that tentacle number is plastic within a species according to food availability. Little remains known about the genus *Atolla* overall. Russell (1959) speculated that tentacle number may increase as the medusa ages, due to high numbers of tentacles observed within small, mature specimens. This is merely speculative at this stage however and requires further analysis. *P. periphylla* was found to be robust across the temporal dataset, with no observed variation in tentacle number or arrangement. There are notably smaller sizes for *P. periphylla* however, which may have had an influence on this outcome.

This contrasting expression of morphological variation in *Atolla* and lack thereof in *Periphylla* aside from size highlights the genetic distance between the two deep-sea coronate genera. The coronate phylogeny remain poorly resolved due to lack of suitable deep-sea coronate sample data for molecular analysis (Collins, 2002; Bayha and Dawson, 2010; Bayha et al., 2010; Kayal et al., 2013) and so speciation and the evolutionary implications within

Coronatae remain poorly understood. The presence of various species within the genus *Atolla*, which are currently recognised to include *A. wyvillei*, *A. parva*, *A. vanhoeffeni*, *A. chuni*, *A. russelli*, *A. gigantea* and *A. tenella* (Russell, 1970) suggests an increased tendency to drive speciation or expressed plasticity driving radiation and speciation processes. DNA sequence diversity analysis in the deep-sea amphipod *Eurythenes gryllus* Mandt, 1822 identified genetically different cryptic taxa distributed at different depths (France and Kocher, 1996). *E. gryllus*, like *A. wyvillei* and *A. parva*, are found at broad depth distributions (184 to 6500 m). The results of the study highlight the importance of abiotic conditions leading to speciation over time within the group. Mitochondrial DNA analysis of four species of protobranch bivalves within the same area (*Nuculoma similis* Rhind and Allen, 1992, *Demincula atacellana*, *Malletia abyssorum* Verrill and Bush, 1898, and *Ledella ultima* Smith, 1885) revealed strong population-level divergence at bathyal depths, indicative of depth-related morphological divergence observed in deep-sea gastropods (Etter et al., 2005). Depth-related radiation within the bathyal zone may be significant in within the genus *Atolla*, however molecular analysis is required in order to address this. As little remains known about speciation in the deep-sea; with limited physical barriers resulting in genetic isolation, Davis et al. (2014) proposed that bioluminescence facilitates speciation in various fishes within the deep-sea. This was found to be the case in teleosts that exhibit species-specific bioluminescence. Bioluminescence is documented for *A. wyvillei*, *A. parva* and *P. periphylla* (Herring and Widder, 2004), with secretory bioluminescence observed in all three coronate species. However, inter-species differences in the luminescent capabilities for *Atolla* may be present beyond these descriptions.

Studies on shallow-water jellyfish population fluctuations are often based on abundance (biomass), in order to provide an assessment of the change in overall gelatinous volume within a usually coastal area (Lynam et al., 2010; Lilley et al., 2011; Lucas et al., 2014). This approach allows for the pooling of various data sources, as often this is the most pragmatic approach to field sampling. However, it comes with sampling difficulties as shallow-water jellyfish are delicate and are often unidentifiable when sampled with a net. Alternative approaches have been trialled, including acoustic methods, however as jellyfish are so close in density to the surrounding water and lack a reflecting organ, estimates of abundance are expected to be low (Mutlu, 1996; Monger et al., 1998; Brierley et al., 2001). Båmstedt (2003) tested a combination of acoustic and video methods to quantify *P. periphylla* within

Lurefjorden. While this provided important estimates of abundance and changes in vertical position of the population layers, uncertainties were still present relating to the sizes of individuals within the population. Museum collections provide the opportunity to study more robust gelatinous fauna over time, and thus gain a better understanding on any temporal fluctuations in morphology or distribution over considerable time scales (Lister et al., 2011). However, there are also limitations to this, as sampling methods often vary and are often not consistent, leaving large gaps in the dataset, particularly for deep-sea exploration. Gelatinous fauna are known to be subject to a degree of shrinkage upon preservation, however estimations of this vary significantly (9.1% (Lucas, 2009, *P. periphylla*) to 84.9% (de Lafontaine and Leggett, 1989, the hydrozoan *Staurophora mertensi*) observed shrinkage. In many instances it is therefore impossible to determine the level of shrinkage for historic samples, as the jellyfish are stored en masse in large jars with no indication of the original sample size. This study attempted to offset the limitations of using museum collections by using molecular methods to understand more about the phylogenetic dynamics of the deep-sea coronates. As jellyfish are known to exhibit plastic traits, morphological assessment of species is often not sufficient, with cryptic species subsequently known to emerge following molecular analysis (Dawson and Jacobs, 2001). Cryptic speciation within the deep-sea is predicted to be currently underestimated (Holland et al., 2004). The molecular methods trialled within this study unfortunately were not successful, likely as a result of a combination of jellyfish possessing lower quantities of DNA than many other metazoans, being historic samples and formalin-fixed.

3.5.3 Resilience of deep-sea jellyfish?

The lack of observed morphological change within *P. periphylla*, and minimal change within the genus *Atolla* is perhaps an indication of their resilience as deep-sea species. It may therefore be more prudent to establish comparisons between other deep-sea metazoans as opposed to drawing parallels between deep-sea coronates and shallow-water jellyfish. Although climate change within the deep-sea is increasingly becoming documented and noted for its importance (Levin and Le Bris, 2015), it may be that the deep-sea coronates are more resilient to change as they vertically migrate large vertical distances. Therefore, are perhaps comparably more tolerant to changes in environmental conditions than other species with more restricted habitat niches within the deep. Deep-sea organisms are

generally thought to live longer (Drazen and Haedrich, 2012), with studies on fishes able to determine ages of individuals by analysing the vertebral centra, fin rays and spines, other skeletal structures and otoliths (Cailliet et al., 2001). Deep-sea medusae are predicted to live up to 30 years (Båmstedt et al. unpublished data, see Jarms et al., 1999; Youngbluth and Båmstedt, 2001), however this has not been conclusively established via any testable methodology. Currently there is minimal understanding how long these jellyfish with significant vertical profiles and associated biotic interactions. The ability to determine age within the deep-sea coronates is therefore fundamental to understanding the potential rates that they respond to change.

3.5.4 Conclusions

The aim of this study was to utilise collections material in order to identify expressed morphological variation for the *Atolla* and *Periphylla* genera across a temporal dataset. Fluctuations in body size and tentacle numbers was observed for *A. wyvillei* and *A. parva*, with only body size change according to year within *Periphylla* which may be indicative of genetic distance within the Coronatae. Despite being the area with relatively high temporal resolution for a deep-sea study, there is nonetheless paucity of data. This investigation illustrates the potential of historical collections for areas of biology such as deep-sea research. The observed expressed plasticity over time in *A. parva* raises interesting evolutionary questions for the order Coronatae which molecular analyses could address.

- Over the temporal dataset within this study, variation in tentacle number was observed within *A. parva* according to fluctuations in the NAOI, indicative of potential plastic responses to climatic change (this data supports the first hypothesis).
- The NAOI appeared to contribute to the vertical distribution of some deep-sea coronate species, with *A. parva* and *A. wyvillei* found at deeper depths during periods of lower NAOI variance.
- No clear pattern was observed linking fluctuations in the NAOI with changes in the size of medusae.
- A phytoplankton bloom was observed within the study area during 1975, however resulted in no observable change to the size of medusae (this data goes against the second hypothesis).

Chapter 3

- This study highlights the importance of monitoring long-term change in deep-sea pelagic fauna, as there are currently large gaps in the available data with which to better understand the species dynamics.

Chapter 4: Population structure and reproduction of *Periphylla* and *Atolla* within the Porcupine Abyssal Plain (NE Atlantic)

4.1 Abstract

The population structure and reproductive traits of deep-sea coronate medusae remain poorly understood, due to the inherent sampling constraints and great depths that the species inhabit. This study used museum collections to develop understanding of the genera *Atolla* and *Periphylla*, members of which were collected during Discovery Cruise 92 in the Porcupine Abyssal Plain (PAP) during April and May of 1978. This study builds on previous reports by describing the population structure and distributions of the deep-sea coronates in more detail, and uses histology to describe reproductive traits. Six species of deep-sea coronates were found within the study area, *P. periphylla*, *A. parva*, *A. wyvillei*, *A. russelli*, *A. vanhoeffeni* and *A. gigantea*. Species of *Atolla* were found to inhabit greater depths overall than *P. periphylla*, with maximum mean depths of 1112 m and 802 m, respectively. The largest species of *Atolla*, *A. gigantea*, was found to inhabit the greatest overall depths (mean = 2622 m). Displacement volumes of twelve key zooplankton taxa (medusae, siphonophores, fish, polychaetes, mysids, pteropods, tunicates, euphausiids, decapods, amphipods, chaetognaths and cephalopods) were obtained from Cruise 92 to investigate potential variation in zooplankton associations between *Atolla* and *Periphylla*. Significant relationships were observed between the occurrence of zooplankton taxa and the representative species of each genus, *A. wyvillei* and *P. periphylla*, which is proposed to be a result of different preferred prey types. This is with the exception of amphipods, which were significantly correlated with both *A. wyvillei* and *P. periphylla*, and are suggested to be a display of parasitic relationships. The robust nature of *A. wyvillei* specimens enabled analysis of gonad development and fecundity. Large, mature oocytes (> 1 mm diameter) were observed within individuals smaller than 15 mm bell diameter, indicative of mature *A. wyvillei* individual across all size classes. Low fecundity was observed across all size classes (10 to 70 mm bell diameter). This study is an example of how museum collections can be used to further the ecological understanding of deep-sea fauna decades

after the original samples were collected, building on original work and conclusions that were reached shortly after the time of capture.

4.2 Introduction

4.2.1 Reproduction in deep-sea jellyfish

Deep-sea jellyfish are generally considered to have atypical life cycles for scyphozoans, involving either reduced and/or parasitic polyp stages or direct development. These life cycles thus completely bypass the free-living benthic polyp stage typically incorporated in other scyphozoan life cycles (Russell, 1953; Kramp, 1961; Osborn, 2000; Lucas and Reed, 2009). However, in deep-sea species other than *P. periphylla*, this is largely speculative (Lucas and Reed, 2010). Holopelagic development has also been described in the epipelagic scyphomedusan *Pelagia noctiluca* Forsskål, 1775 (Rottini Sandrini and Avian, 1991), providing support for the theory that a metagenic life cycle (i.e. the alternation between sexual (medusa) and asexual (polyp) generations (Ceh et al., 2015)) is not a requirement for bloom species (Hamner and Dawson, 2009). For both *P. periphylla* and *P. noctiluca*, oocytes across all stages of maturity are present throughout the year, with long incubation periods (Russell, 1970). However, egg sizes of *P. noctiluca* are tiny (0.25-0.32 mm in diameter) relative to those of *P. periphylla* (up to 2 mm (Rottini Sandrini and Avian, 1991; Lucas and Reed, 2010)).

Jarms et al. (1999; 2002) established that *P. periphylla* is the only known coronate jellyfish with a complete absence of the scyphistoma stage. They characterised the development from a yolky egg to medusa in terms of fourteen developmental stages and showed that *P. periphylla* possesses the largest eggs within the Cnidaria (egg diameter, 1280-1680 µm). The latter supported the hypothesis originally outlined by Berrill (1949), that taxa with large yolky eggs develop directly into medusae. Support for this hypothesis was later reinforced by Larson (1986), who used the large eggs of *P. periphylla* and *Atolla* species to indicate the link between egg size and direct development. The early development of *Atolla* spp. is not currently known, but as described by Russell (1970), is likely to have a stephanoscyphus (polyp) stage, reproducing at any time of the year (Russell, 1959). Sexual reproduction has been described

Chapter 4

for the coastal coronate species *Nausithoe aurea* Da Silveira & Morandini, 1997 (Morandini and da Silveira, 2001), *Nausithoe atlantica* Broch, 1914 and *Linuche unguiculata* Schwartz, 1788 (Eckelbarger and Larson, 1992). Polyp stages have been indicated for *Nausithoe racemosa* Komai, 1936 (Werner, 1970), *Atorella vanhoeffeni* Bigelow, 1909 (see Mills et al., 1987), *N. punctata* (Werner, 1973) and *L. unguiculata* (Arai, 1997). Jarms et al. (2002) describe the stephanoscyphistomae (periderm tubes of coronate polyps) of the Atorellidae and Nausithoidae coronate families, however note that such features are likely to be absent within the deep-water coronates.

Although scyphomedusae eggs are usually retained in the gastrovascular cavity or attached to the fringes of the oral tentacles, the coronate *L. unguiculata* sheds its eggs directly into the surrounding water (Berrill, 1949). Eckelbarger and Larson (1992) used *L. unguiculata* (an epipelagic species) to describe the ovarian ultrastructure of Coronatae. They deduced that coronates lack trophocytes (also known as nurse cells or paraovular bodies) - the specialised gastrodermal cells for the transfer of nutrients to the oocytes. Instead coronate oocytes develop freely in the mesoglea. However, subsequent studies have found that variation in reproductive development exists within the Coronatae. Tiemann and Jarms (2010) found that trophocytes were present in *P. periphylla*, and served to connect the oocytes to the genital epithelium. Those parts of the epithelium served to nourish the oocytes, and remained connected throughout oocyte development. The associated epithelial and trophocyte cells were suggested to be a necessary adaptation for the production of the large oocytes required for direct development. Lucas and Reed (2010), however, found no trophocytes in samples of *A. wyvillei* and *P. periphylla*. Instead early- to mid-vitellogenic oocytes break free from the gastrodermis and develop freely in the mesoglea without the aid of nutritive trophocytes. Nourishing cells containing dictyosomes and producing yolk granula, have been observed in the polypoid coronate species *Theoscyphus zibrowii* Werner, 1984 (Sötje 2003). Studies to date suggest that a variety of processes can be involved in yolk production and egg nourishment in coronates. For example, yolk within the large coronate eggs may originate solely from the activity of the Golgi-RER system (see Eckelbarger & Larson 1992) but nutrients may also be supplied by trophocytes (see Tiemann & Jarms 2010).

Differences in scyphozoan ovarian structure are viewed to reflect phylogenetic relationships rather than differences in habitat or rate of egg production (Eckelbarger and Larson, 1988).

This is reflected in the coronates, with ultrastructural studies revealing no differences in ovary development and vitellogenesis amongst species ranging from shallow waters (e.g. *L. unguiculata*) to the deep-sea (e.g. *P. periphylla*) (see Morandini & da Silveira 2001; Tiemann & Jarms 2010). However, the rate of egg production in coronates is linked to changes in environmental conditions, specifically depth inhabited. Larson (1986) speculated that mesopelagic coronates produce eggs very slowly (a few eggs per day), which would contrast greatly to the epipelagic *L. unguiculata*, which can produce over 100 eggs per day (Kremer et al., 1990). It is the large, slowly formed eggs of the deep-sea species that develop holopelagically from egg to medusa. It yet to be established whether *A. wyvillei* lacks a polyp stage. The oocytes in various stages of development in sampled medusae of a range of bell diameters, together with the apparent absence of spent gonads suggest that *A. wyvillei* and *P. periphylla* reproduce steadily and continuously from maturity until death (see Russell 1959; Larson 1986; Jarms et al., 1999; 2002; Lucas & Reed 2010).

4.2.2 Deep-sea research within the North Atlantic, including the Porcupine Abyssal Plain and Seabight

The Porcupine Abyssal Plain region (PAP) (16°30'W, 49°00'N) is an example of one of the most sampled regions of the deep-sea (Hartman et al., 2012). The PAP Sustained Observatory (PAP-SO) remains one of the two longest running abyssal research stations, hosting a multitude of disciplines over the past thirty years. The other is Station M in the north-east Pacific (34°50'N, 123°W, depth 4100 m), 220 km off Point Conception, California, an area subject to mesoscale and seasonal oscillations as well as tidal forcing (Smith and Druffel, 1998). Abyssal regions of the world represent over 50% of the Earth's surface (Gage and Tyler, 1991). However, due to their distance from land and significant depth, sampling abyssal regions is inherently difficult. This emphasises the importance of data collected from the PAP-SO and Station M sites which have been regularly sampled since 1989.

The PAP area is characterised as a vast, level stretch of seabed (4000 to 4850 m), with a muddy floor, rocky abyssal hills and submarine canyons (Summerhayes and Thorpe, 1996). The hydrography of the area is composed of the Iceland-Scotland Overflow Water, the Lower Deep Water, the Labrador Sea Water and the Mediterranean Sea Water. The North Atlantic Deep Water exhibits zonal trends of dissolved oxygen and nutrient mixing, due to cycling with the

Chapter 4

Lower Deep Water and mineralisation of organic matter (van Aken, 2000). Research at the PAP-SO site has largely focused on deep-sea particulate organic matter (POC) flux (Lampitt et al., 2010) and the associated benthic faunal responses over temporal scales (for examples see Billett et al., 2001, 2010 (megabenthos); Wigham et al., 2003 (holothurians); Gooday et al., 2010 (foraminifera); Soto et al., 2010 (polychaetes)) as well as furthering the understanding of surface processes and the link between shallow and deep water biogeochemical processes (Hartman 2010). Summaries of the benthic and time series research undertaken at the PAP-SO can be found in Glover et al. (2010), Lampitt et al. (2010) and Larkin et al. (2010).

Since the inception of the PAP-SO site in 1989, coordinated by the National Oceanography Centre Southampton (NOCS), increases in benthic megafaunal abundances were identified from 1989 to 2002 (Bett et al., 2001). The holothurians *Amperima rosea* Perrier, 1886 and *Ellipinion molle* Théel, 1879 particularly rapidly increased in abundance from 1997 to 1999, a time period now referred to as the '*Amperima* event' (Billett et al., 2010). This increase in these small holothurians as well as the larger *Psychropotes longicauda* Théel, 1882, *Pseudostichopus aemulatus* Solis-Marín and Billett, 2004 and *Oneirophanta mutabilis* Théel, 1879 resulted in more rapid cycling of phytodetritus deposits on the sea floor during that time (Billett et al., 2001). Significant shifts in faunal assemblages pre- and post-*Amperima* periods were apparent, including amongst the metazoan meiofauna (32-1000 µm) (e.g. nematodes and polychaetes; Kalogeropoulou et al., 2010). Ostracods exhibited significant decreases in abundance over the period, with copepods not demonstrating any notable change. Species richness and diversity decreased during this period, increasing the dominance of a select few species (Glover et al., 2010).

Community changes as a result of climatic forcing by the North Atlantic Oscillation (NAO) on the POC flux have also been observed, with a lagged effect to the sea floor community composition of a few months (Ruhl et al., 2008). Whilst commercial fish stocks within the area have been monitored and target species found to exhibit a decline, changes to the fish communities during and after periods such as the *Amperima* event and other natural temporal fluxes are not as clear (Basson et al., 2002). A study by Kemp et al. (2006) identified that seasonal fluctuations in temporal food availability to the abyss could affect the fish communities due to the associated trophic links (as opposed to feeding directly on the photodetritus).

Chapter 4

Overall, long-term monitoring within the PAP-SO has demonstrated that the inter-annual variability of POC to the deep-sea has significant impacts on the abyssal community structure. Currently studies that have featured gelatinous zooplankton at the PAP-SO have mostly focused on the transfer of carbon to the sea floor (Gage, 2003), general near-benthic population structure (Christiansen et al., 2010), and bioluminescence (Battle, and described in Martini and Haddock). While it is assumed that frequent sampling of gelatinous zooplankton has occurred since 1989, no studies have focused on jellyfish at the PAP-SO site.

Studies of the PAP region prior to the establishment of PAP-SO have also been undertaken. Bailey et al. (2009) monitored the diverse fish assemblages between the continental shelf edge and the abyssal plain from 1977 to 2002, identifying an overall decline in fish abundance from 800 to 2500 m (beyond that of the reach of commercial fisheries). The region was also regularly sampled as part of the extensive *Discovery* expeditions. Unlike the PAP-SO site, these cruises mostly involved sampling of the epipelagic and pelagic fauna such as the fishes, phytoplankton and zooplankton.

In addition to research conducted in the PAP itself, other studies provide further relevant insights on composition and changes in deep sea communities in the Northeast Atlantic. In April 1972, NW of the Canary Islands, Roe et al. (1974) investigated the diel vertical migrations of the planktonic community. This was done at a single depth in continuous hourly hauls for 24 hours, and established community-level diel vertical migration patterns of 104 planktonic species. This study was extended in April 1974 in the Charcot Seamounts region, between the Iberian Basins. This built on the 1972 study by extending the duration of trawling to 48 hours, obtaining samples from varying depths (ranging from 95 to 650 m), and incorporating temperature and salinity readings from 0 to 1000 m (for full description of the sampling strategies and objectives of the cruise see Roe et al. 1984). Outputs of this cruise included mapping the diel vertical migration patterns of mysids and crustaceans (Roe et al., 1984), ostracods (Angel, 1984), copepods (Roe and Badcock, 1984), fishes (Roe and Badcock, 1984), siphonophores (Pugh, 1984) and medusae, ctenophores, amphipods and euphausiids (Roe et al., 1984). A subsequent multivariate analysis of community structure was conducted by Domanski (1984). Medusae found at the study site included the deep-sea coronates *A. vanhoffeni*, *A. parva* and *A. wyvillei*, but no *P. periphylla* were detected. In agreement with Thurston (1977) *A. vanhoffeni* was found to have a distinct vertical migration over at least 200

Chapter 4

m and to reside at approximately 450 m during the day. *A. vanhoeffeni* was found to inhabit shallower depths than *A. parva* and *A. wyvillei*.

Discovery cruise 92 conducted by Angel et al. (1978) was carried out at three positions within the north-east Atlantic from the PAP along two transects south to the Iberian Basin, with the following specific research interests and principal investigators: holothurians (D.S.M. Billett and B. Hansen), fish (N.R. Merrett), bioluminescence (P.J. Herring), osmotic pressure of crustacean haemolymph (C. Durning), particle counting and phytoplankton fluorescence (P.R. Pugh), phytoplankton sampling (P. Domanski), CTD observations (M.J.R. Fasham) and midwater fishes (J.R. Badcock). A vast quantity of samples was collected and preserved, and subsequently added to the extensive *Discovery* collections. Preliminary results of the three key sample sites were published in Angel and Baker (1982), and grouped together the main taxonomic groups (euphausiids, fish, siphonophores, medusae, chaetognaths, decapods, mysids, salps and pteropods). Medusae were noted to increase steadily in importance with depth, until 900 to 1100 m where they constituted 70% of the biomass. In depths exceeding 1100 m medusae constituted 20-40% of the biomass. Due to the preliminary nature of this work, no information to species level was given. Angel (1984) described the vertical distribution of ostracods in the deeper part of the water column (1500 to 3900 m) at the three sample sites of cruise 92. Hargreaves (1985) described the vertical distribution of the decapods, euphausiids and mysids at the third station of Cruise 92 (station 9801) to investigate potential zonation within the bathypelagic realm.

The preservation of samples from these expeditions within the *Discovery* collections has allowed further study on the organisms that were caught within the north-east Atlantic during that time (Lister et al., 2011). A study by Cantero and Horton (2017) used *Discovery* collections material from a number of locations including the Porcupine Seabight and Abyssal Plain to further the understanding of the deep-sea benthic hydroid fauna and established that collections-based research can help answer fundamental ecological questions that weren't addressed at the time of sampling. Using museum collections, this study seeks to investigate the intra-species reproductive characteristics and population structure within a population of deep-sea coronates, using the samples from the PAP region collected during the 1978 *Discovery* Cruise 92. This study also seeks to build on the existing published works on

Chapter 4

zooplankton vertical distributions based on the same cruise by Angel and Baker (1982) by providing a specific focus on deep-sea coronates.

4.2.3 Aims and objectives

This study aims to describe the population structure and reproductive traits of the deep-sea coronate medusae *P. periphylla* and *Atolla* spp. within the Porcupine Abyssal Plain by examining material obtained during the 1978 Discovery Cruise 92. The objective of this study is to investigate the morphological characteristics and reproductive traits of *Atolla* spp. and *P. periphylla* according to food availability and different environmental conditions using museum specimens and data from Discovery Cruise 92.

The conceptual hypotheses being investigated within Chapter 4 are that the ovarian structure of both *P. periphylla* and *Atolla* spp. demonstrates consistently low fecundity and early maturation reflective of other deep-sea fauna such as mid-water decapods. The second hypothesis is that *P. periphylla* and *A. wyvillei* demonstrate evidence of associations in terms of relative abundance with different zooplankton taxa, indicative of their preferred prey types. A further hypothesis is that both genera exhibit diel vertical migration patterns, consistent with descriptions of the species discussed in Chapter 1.

4.3 Methods

4.3.1 Samples and study area

This study focused on deep-sea coronate jellyfish samples collected during the 1978 *Discovery* Cruise 92 and subsequently stored in the Natural History Museum (NHM) London *Discovery* collections. This Institute of Oceanographic Sciences (IOS) multi-disciplinary research cruise conducted by Angel et al. (1978) performed midwater and benthic sampling from the Porcupine Sea Bight (12°W, 50°N) up to the Iberian Basin (16°W, 41°N). For full details of Cruise 92 see Angel et al. (1978) cruise report in the Supplementary Information section. This study selected material collected from the early stations of the cruise (stations 9756 to 9791) within the Porcupine Sea Bight bathymetric feature and Porcupine Abyssal Plain (PAP) as these

Chapter 4

samples were located geographically close to each other in a high density. Figure 4.1 is a map of the sample locations within the Porcupine Sea Bight and the Porcupine Abyssal Plain (herein referred together as the PAP study site) used within this study. The study site was noted in published work by Angel and Baker (1982) to be inhabited by much larger volumes of medusae (unspecified species) than the lower latitudes of the cruise. The samples within this study were collected using a rectangular midwater trawl (RMT) 1+8 system (mesh size 4.5 mm, nominal mouth area 8 m²) between depths of 0 to 3500 m. Samples were fixed at sea in 5% formalin in seawater, and subsequently transferred into Steedman's preserving fluid. For full details of sampling methods on Cruise 92 see Angel and Baker (1982).

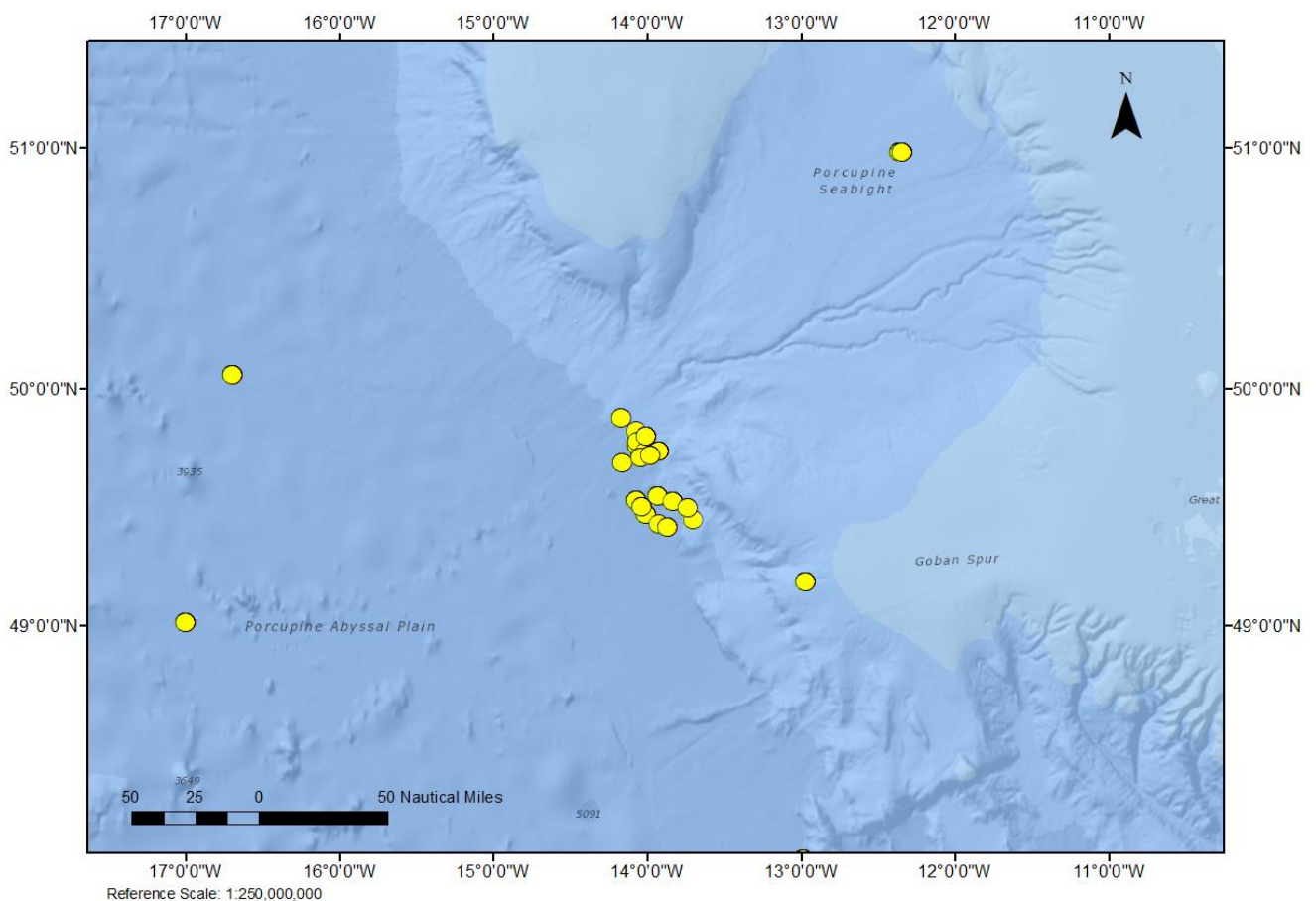


Figure 4.1 Map of the Porcupine Abyssal Plain and Seabight (PAP) study area and sample locations held within the *Discovery* collections from Cruise 92 (1978).

4.3.2 Data collection

All deep-sea coronates within jars corresponding to this early phase of Cruise 92 were quantified and identified to species level. The data within this study do not overlap with the data of chapters 2 and 3. Preserved wet weight, bell diameter (BD), coronal diameter (CD), bell height (BH) and tentacle number were recorded for all deep-sea coronates found within the specimen jars held in the collections. Body size was classified as bell diameter (BD) in *Atolla* spp. due to the disc-like appearance of the bell (see Russell 1970) and as coronal diameter in *P. periphylla* (Figure 4.2), which is the standard method according to previous studies (see Båmstedt 2003; Sørnes et al. 2008; Solheim 2012). See Chapter 2 for information on morphological landmarks of the deep-sea jellyfish. Measurements were made using callipers for smaller individuals (< 10 cm) and a ruler for larger individuals (> 10 cm). Where identifiable, gender and stage of maturity were described. Stage of maturity included describing the gonads as 'immature', crescent-shaped gonads in *Atolla* and thin straight gonads in *Periphylla*; 'developing', small, bean shape gonads in *Atolla* and J-shape gonads in *Periphylla* or 'mature', dense, bean-shaped gonads hanging from the subumbrella in *Atolla* and U-shaped folded gonads in *Periphylla*. Station and sub-station information for individual medusa, which included depth, gear and time, was sourced from the Cruise 92 cruise report (Angel et al., 1978).

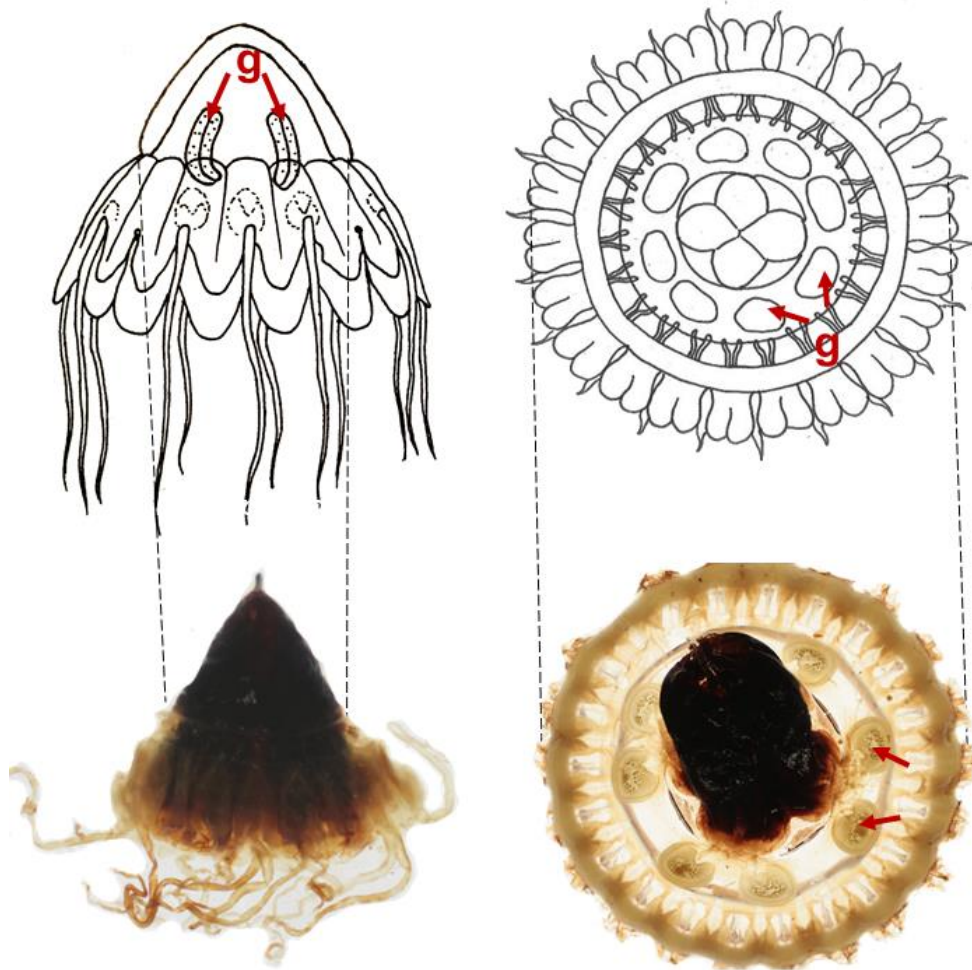


Figure 4.2 Drawings and photographs of museum specimens to illustrate measurement of body size on *P. periphylla* (lateral orientation) and *Atolla* spp. (here *A. wyvillei* subumbrella depicted in ventro-dorsal orientation). Gonads marked with red arrows. Drawings by the author, adapted from Russell (1970), photographs by author.

4.3.3 Histology

Histology was used to describe the reproductive traits of *A. wyvillei* and *P. periphylla* specimens. *A. wyvillei* was used as the species to represent *Atolla* due to its larger size and larger gonads for analysis. Gonads were taken from 50 *A. wyvillei* and 30 *P. periphylla* specimens, divided equally into male and female. *A. wyvillei* and *P. periphylla* individuals were selected at random by taking gonad tissue from every tenth individual measured in which

Chapter 4

gonads could be identified. Two out of the eight available gonads from each individual were removed, and stored in 10% buffered formalin. The second gonad was to act as a backup should the first be unsuccessful during embedding and sectioning.

To prepare for histological analysis the dissected tissue was dehydrated in graded isopropanol, increasing the concentration at hourly intervals from 40% to 60%, 70%, 80%, 90% followed by two washes at 100%. The dehydrated tissue was then cleared in HistoClear (CellPath) overnight before being dabbed dry and transferred into molten paraffin wax (Sigma Paraplast Plus) and into an oven at 60°C to embed. The wax was replaced after 4 hours to remove any HistoClear that may have bled into the wax. After a total of 8 hours in the oven, tissue samples were removed and placed into plastic moulds of varying sizes (5 x 5 mm, 10 x 10 mm and 15 x 15 mm), covered with plastic microtome cassettes, filled with fresh wax and left to harden. The wax blocks were then transferred into a freezer to chill before sectioning using a microtome.

Table 4.1 Protocol for staining with haematoxylin and eosin

Procedure	Time (min)
Dewax in HistoClear	5
Isopropanol (100%)	1
Isopropanol (70%)	1
Haematoxylin (CellPath, 'Z')	4
Water rinse (running water)	15
Eosin (BDH Technical)	2
Water rinse (running water)	1
Isopropanol (100%)	2
Isopropanol (100%)	2
Clear in HistoClear	2

Each gonad was sliced into 7 µm sections using a Reichert-Jung microtome and a tungsten carbide knife. Ribboned sections were transferred onto slides using a water bath, then left to dry overnight on a slide heater. Slides were stained in batches according to the haematoxylin and eosin (H&E) staining protocol described in Table 4.1. As with standard H&E staining, eosin

Chapter 4

stains basic structures such as cytoplasm, pink, with haematoxylin staining acidic structures such as nuclei, purple (see Fischer et al. 2008). Immediately after staining, slides were transferred to a fume cupboard and mounted with a cover slip using DPX mounting medium (Agar) before being left to set.

Histology image analysis

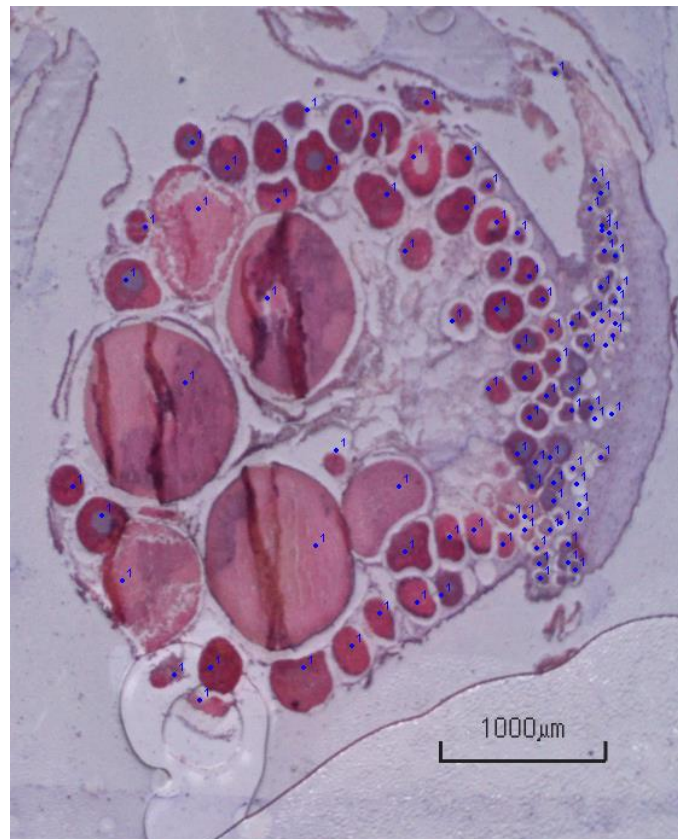


Figure 4.3 Example of sectioned mature *A. wyvillei* gonad with numbered oocytes using the ImageJ Cell Counter Tool.

Histology slides were photographed using a Nikon Shuttlepix digital microscope, using the in-built software to provide a reference scale (μm). Fecundity, or the total reproductive output of an individual over its lifetime (Bradshaw and McMahon, 2008), can also be split into ‘potential’ and ‘realised’ fecundity (Anger and Moreira, 1998). Here the realised fecundity is determined by quantifying the number of oocytes. Microscope images were imported into ImageJ image processing software for further analysis. Using ImageJ, oocytes were quantified and feret diameter and area measured using the Cell Counter and ROI Manager tools (Figure 4.3). Feret diameter was selected as the ideal measurement for particles non-uniform in diameter, as

Chapter 4

used in (Galley et al., 2005) for determining reproductive biology in echinoids. Oocytes were counted for *A. wyvillei* only. *P. periphylla* gonads did not section successfully, perhaps as a result of their weaker, more ribboned tissue structure than *Atolla*. This made measurements following sectioning less accurate and as such were used for descriptive purposes only and not for further cell counter analysis.

4.3.4 Accompanying data

Zooplankton displacement volume data as featured in Angel and Baker (1982) from Cruise 92 was provided by Phil Pugh (2014, personal communication). Displacement volumes were broken down into the following taxa: Medusae (MED), Siphonophorae (SIP), Fish (FIS), Chaetognatha (CHA), Polychaeta (POL), Amphipoda (AMP), Decapoda (DEC), Euphausia (EUP), Pteropoda (PTE) and Mysidae (MYS). Displacement volumes were produced two months after sampling during Cruise 92, and made by making the sample up to a known value then subtracting the volume of the fluid filtered off. The sample sizes were large enough for this to be accurate to the 1 ml level. Damage to specimens was kept to a minimum where possible, due to the intended identification to species level.

Environmental data (temperature, salinity, nitrate, oxygen, phosphate, silicate) from the PAP during April and May 1978 were sourced from Ocean Biogeographic Information System (OBIS) (available at <https://mapper.obis.org/>) and matched according to date and depth of the sampled coronate specimens.

4.3.5 Data analysis

Size frequency histograms were used to describe the population structure of the individual species of *Atolla* and *Periphylla* within the PAP study site, with certain species split into smaller and larger individual groups to reflect the intra-species size differences (this was done for *A. vanhoeffeni*, *A. parva*, *A. wyvillei* and *A. russelli*). One-way analysis of variance (ANOVA) with Tukey's pairwise comparison post-hoc test was used to determine variation in depth sampled between day and night hauls for each species, along with overall differences in depth sampled between coronate species (see Osborn et al., 2007). Multiple linear regression (forwards stepwise) was used to model the relationships between *A. wyvillei* and *P. periphylla* presence

Chapter 4

and associated zooplankton abundance, as well as identifying key environmental variables associated with occurrence across all depths (see Olabarria and Thurston, 2003). Often the depths from which samples were collected were imprecisely known or poorly understood and only broad depth ranges were reported. For example, a number of medusae were recorded to have been sampled between 0 to 1000 m deep. Cases where recorded depth ranges exceeded 200 m were excluded from all depth-related analyses ($n = 231$). All data analysed were checked for normality and log transformed where necessary.

4.4 Results

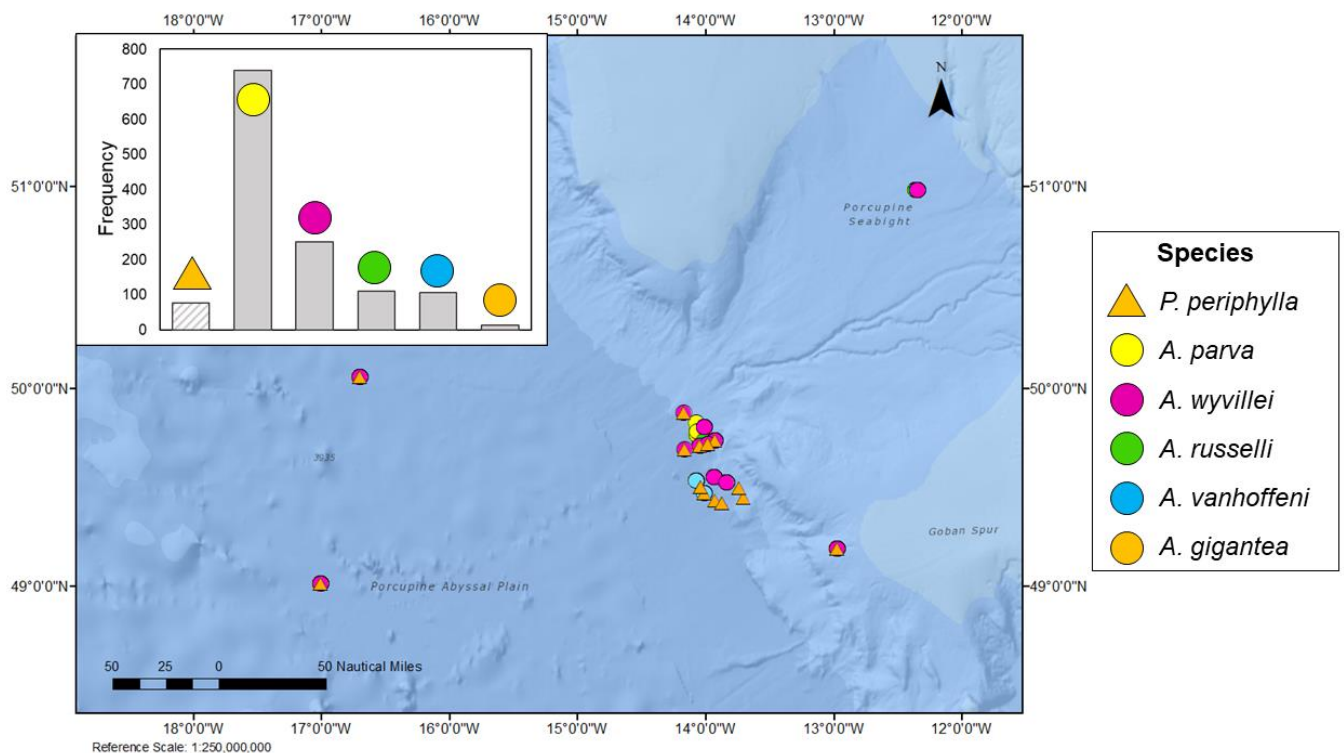


Figure 4.4 Deep-sea coronate species found within the PAP study area on map (samples overlapped when more than one species found within that location) and frequency chart with number of each species found: *P. periphylla* (orange triangles, $n = 77$), *A. parva* (yellow circles, $n = 740$), *A. wyvillei* (magenta circles, $n = 251$), *A. russelli* (green circles, $n = 111$), *A. vanhoffeni* (blue circles, $n = 107$), *A. gigantea* (orange circles, $n = 14$).

Six species of deep-sea coronates were found within the study area, *P. periphylla*, *A. parva*, *A. wyvillei*, *A. russelli*, *A. vanhoffeni* and *A. gigantea*. Overall there was a greater representation

Chapter 4

of *Atolla* spp. within the study area during 1978 than *P. periphylla*, with 6% of the specimens found to be *P. periphylla* (Figure 4.4). The species with the greatest number of individuals sampled is *A. parva* (n = 740), which is found distributed across the entire sample area, along with *A. vanhoeffeni* (n = 107) and *A. wyvillei* (n = 251). *P. periphylla* was only found to occur within the abyssal plain region of the PAP (n = 77) as opposed to the shallower Seabight (max depth of Seabight = 3000 m, (Dorschel et al., 2010)). *A. gigantea* (n = 14) was only found to occur at the conjunction between the Seabight and the abyssal plain region.

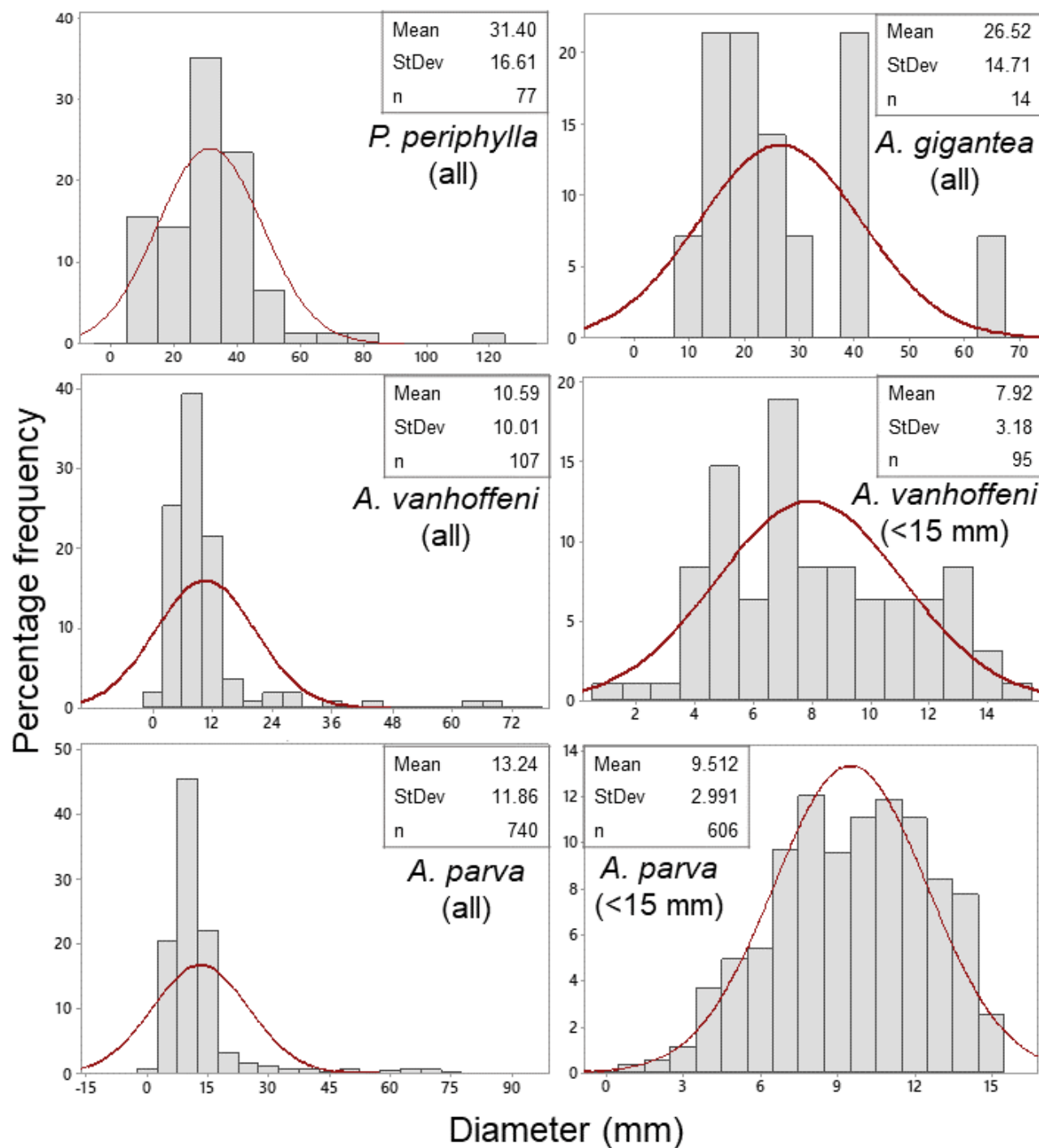


Figure 4.5 Size frequency histograms with normal distribution lines for deep-sea coronates within the sample area. Mean, standard deviation (StDev) and number of specimens within each species sample noted on respective charts. Histograms plotting smaller individuals (< 15 mm) were also produced for *A. parva* and *A. vanhoffeni* and for *A. wyvillei* smaller and larger than 40 mm diameter.

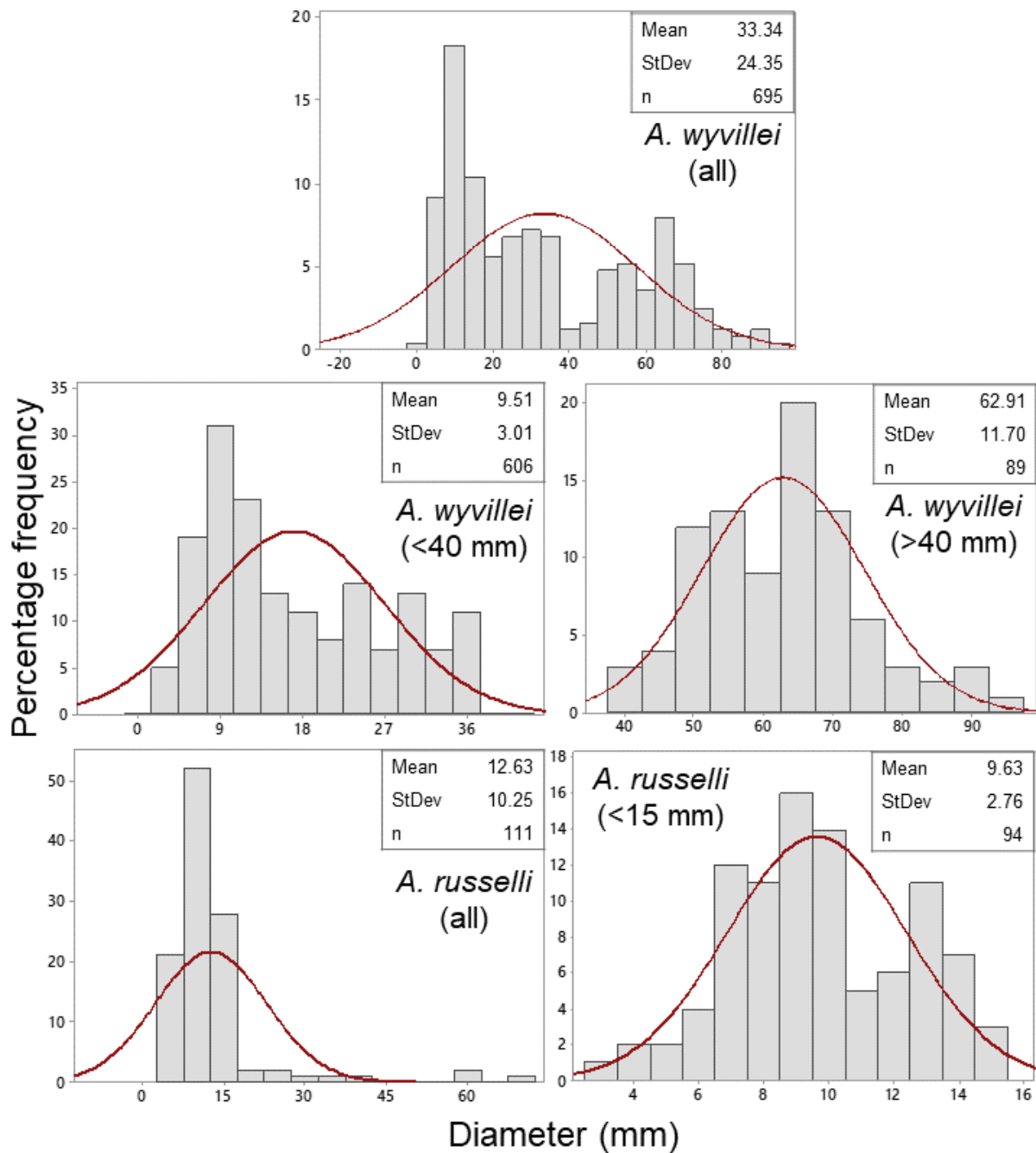


Figure 4.5 continued).

The *P. periphylla* population demonstrates a slightly positively skewed structure (*skewness* = 2.19, Figure 4.5) and with individual of a larger overall size than that of the *Atolla* species, with the exception of *A. wyvillei* which has a similar mean size (mean = 31.4 and 33.34 mm respectively). The standard deviation for *P. periphylla* is relatively large (StDev = 16.61) due to the presence of the 120 mm individuals. The *A. gigantea* specimens found within the study area are the second largest *Atolla* specimens in the study with peaks in abundance at 15, 20

Chapter 4

and 40 mm diameter. However, due to the small sample size ($n = 14$), no subsequent exploration of patterns was possible. For *A. parva*, *A. vanhoeffeni* and *A. russelli*, the majority of specimens were under 15 mm diameter. Two distinct peaks were observed in *A. wyvillei*, before and after 40 mm diameter (Figure 4.5). There were sufficient numbers to split the species into two sub-samples ($n = 606$ and 89), which may be indicative of two cohorts within the PAP site. When plotted separately, the skewness for both smaller and larger *A. wyvillei* individuals was found to be 0.33.

No significant difference was observed between the average depths of pooled coronate samples caught during the day and night (one-way ANOVA, $F = 0.13$, $p > 0.05$, mean = 933 m (day), 1488 m (night), total $n = 1299$) to investigate any overall vertical migratory pattern. The same insignificant pattern was observed for minimum and maximum depths sampled (one-way ANOVA, Min Depth, $F = 0.13$, $p > 0.05$; Max depth, $F = 0.93$, $p > 0.05$, $n = 1299$). When this was split according to coronate species, a significant contrast in maximum depth sampled between day and night sampling was observed for *P. periphylla* (Figure 4.6; Table 4.2), indicating that diel vertical migration was apparent (one-way ANOVA, $F = 12.97$, $p < 0.01$, $n = 50$). Accordingly, the minimum and maximum depth during the day was 933 m and during the night was 802 m (Table 4.2). No significant difference between day and night sampled and depth was observed for any species of *Atolla* (Figure 4.6; Table 4.2) (one-way ANOVA, $p > 0.05$, *A. parva* $n = 655$; *A. wyvillei* $n = 175$; *A. gigantea* $n = 13$; *A. russelli* $n = 98$; *A. vanhoeffeni* $n = 78$). 239 samples with broad depth ranges (> 200 m range) were removed from the dataset, reducing the dataset to 203 samples with ranges of 0-1000 m below the surface.

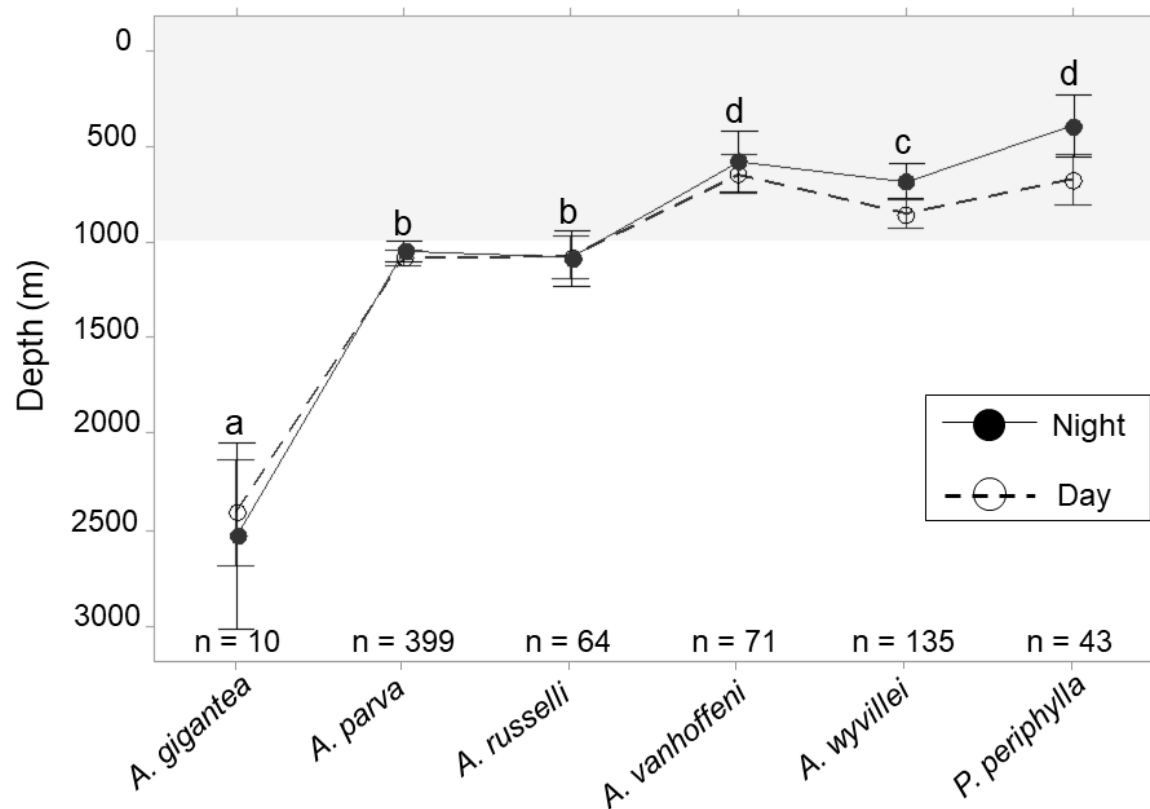


Figure 4.6 Depth distributions during the day and night for the coronate species within the PAP study area. Significantly different groups indicated with letters above bars, Tukey's test $p < 0.001$. Standard error bars to 95% confidence level. Samples that had depths reported in broad ranges of over 200 m were omitted from this study ($n = 203$), all of which were found from 0 to 1000 m deep.

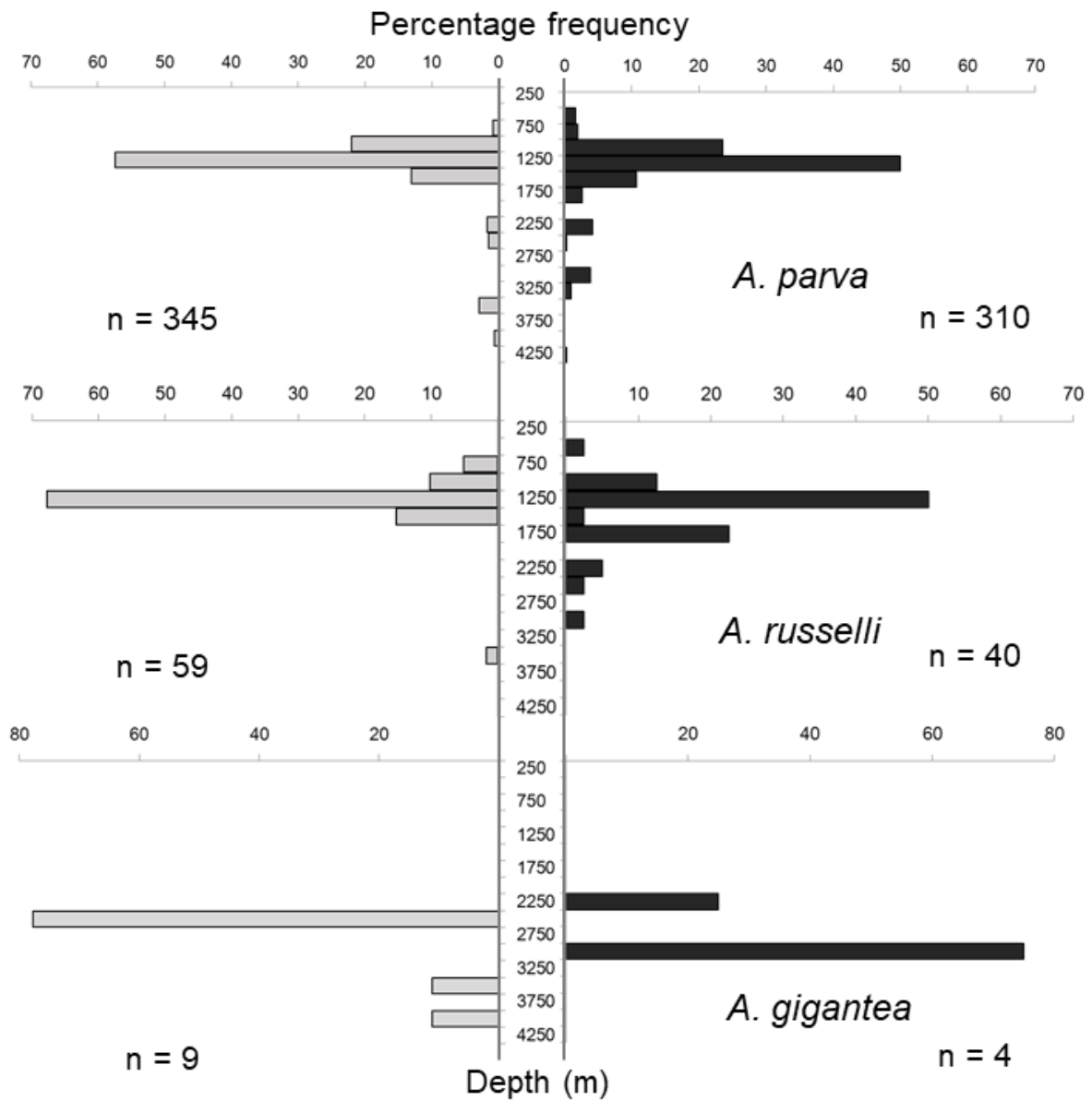


Figure 4.7 Percentage frequency depth distributions according to day (light grey bars) and night (dark grey bars) of deep-sea coricate species within the study area. Depths grouped into 250 m bins, from 0 – 250 m to 4000 – 4250 m.

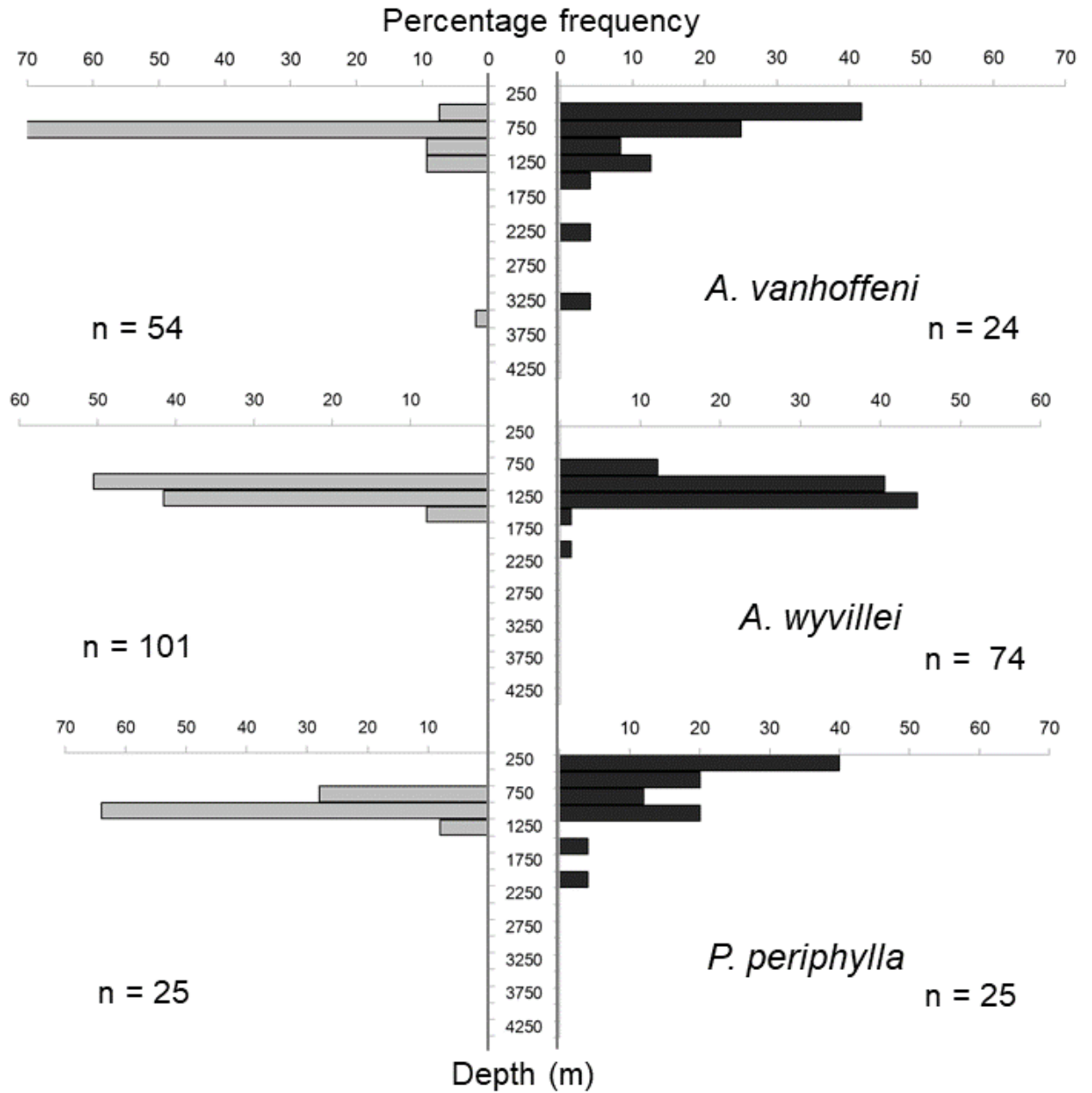


Figure 4.7 continued.

Table 4.2 One-way ANOVA output for variation in species depth sampled between day and night hauls within the study area. Mean depth values (in metres) during the day and night are within brackets. Significant results to the 99% confidence level are noted with ***.

Species	ANOVA output				Mean depth (m)	
	<i>n</i>	<i>r</i> ²	<i>F</i>	<i>p</i>	Day	Night
<i>P. periphylla</i>	50	0.11	13.12	0.000***	933.4	802.6
<i>A. parva</i>	669	0.001	0.07	0.79	1175.9	1186.8
<i>A. russelli</i>	120	0.29	2.86	0.09	1130.1	1276.40
<i>A. vanhoffeni</i>	101	0.004	0.33	0.565	691.9	763
<i>A. wyvillei</i>	201	0.009	2.74	0.1	975	933.4

4.4.1 Body size with depth

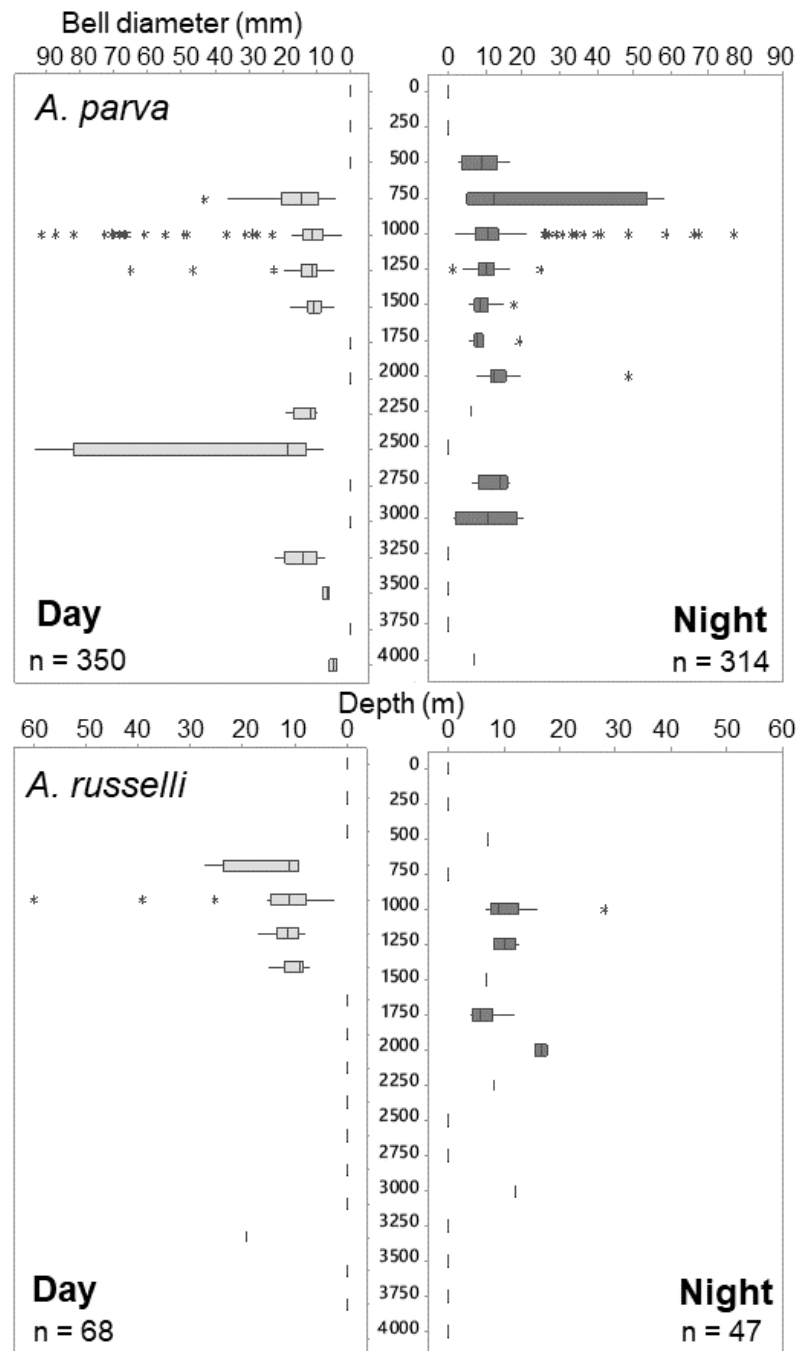


Figure 4.8 Depth distributions of coronate species within the PAP study area according to size (bell diameter in *Atolla* sp., coronal diameter in *P. periphylla*) from 0 to 4000 m during the day (left plots) and night (right plots). Continued on next page. Box plots demonstrate mean figures and interquartile range.

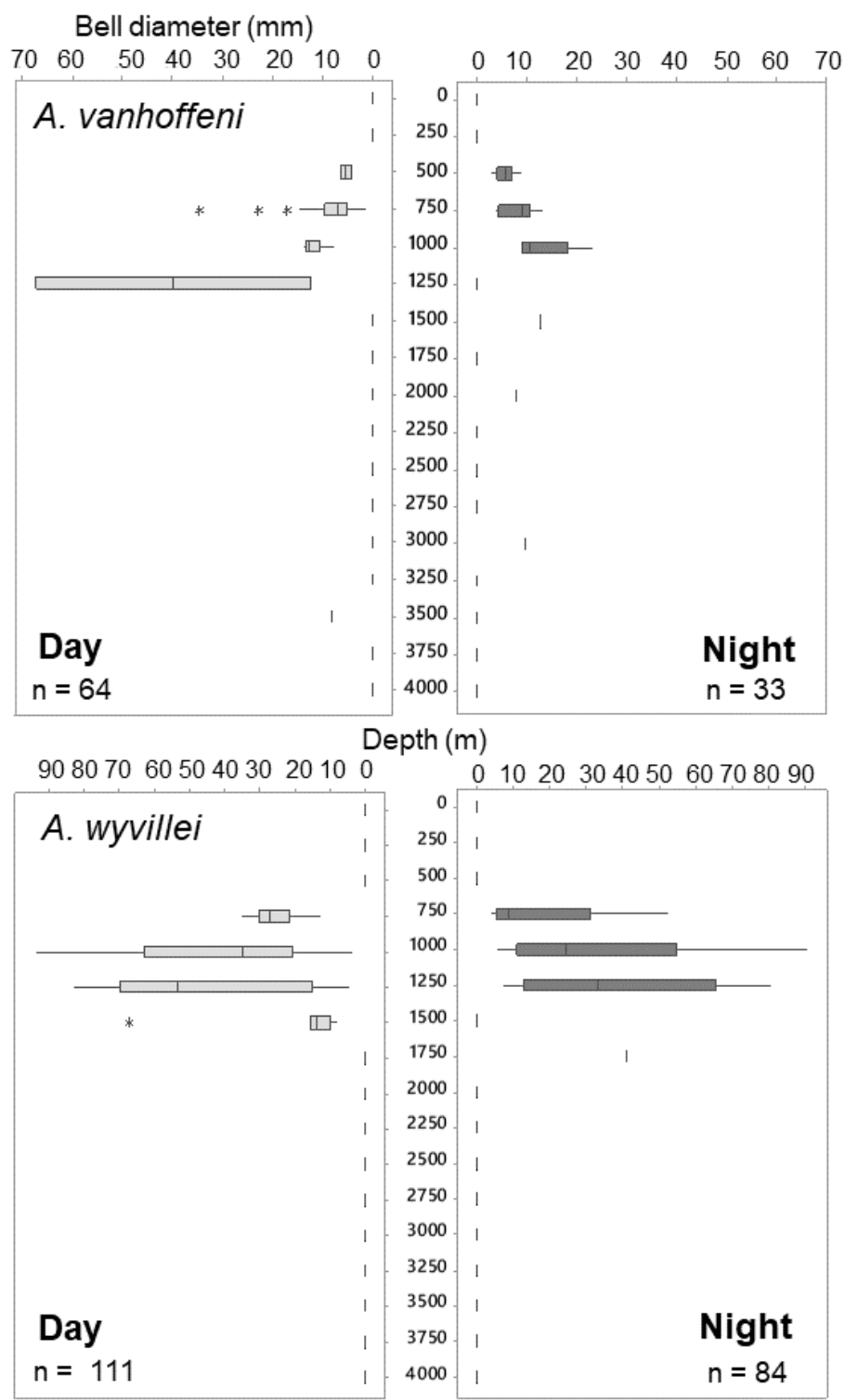


Figure 4.8 continued.

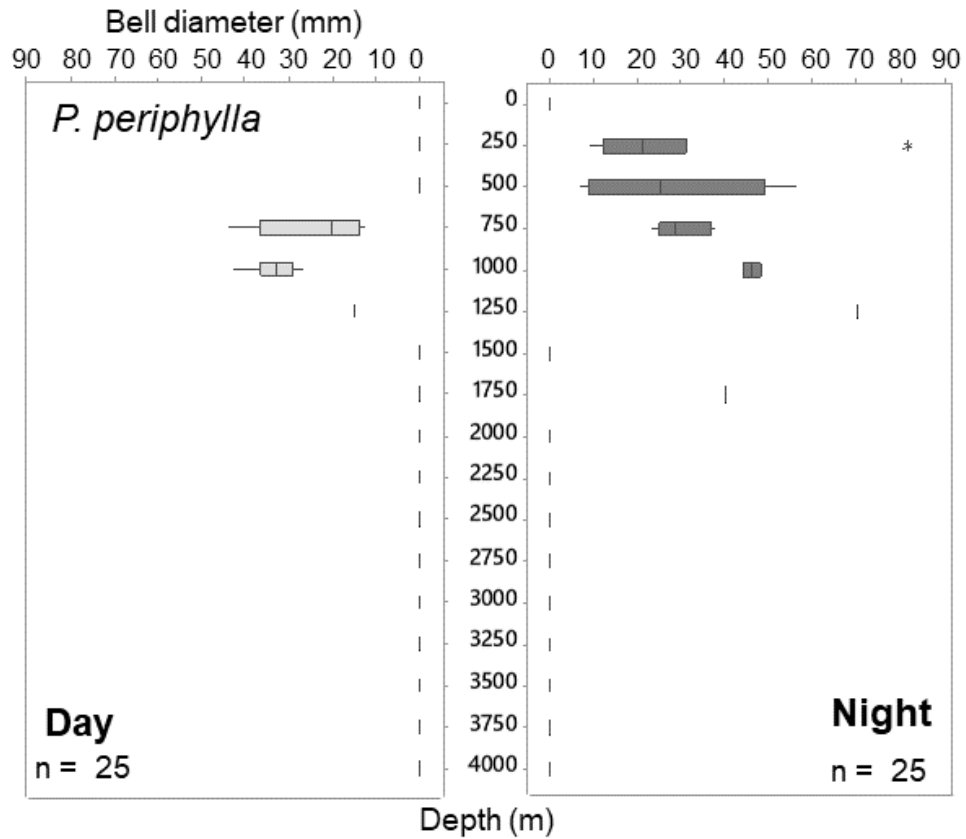


Figure 4.8 continued.

Table 4.3 Generalised linear model (GLM) output for body size according to depth across day and night sample hauls within the PAP study area. Significant results to 99% confidence level notated with ***.

Species			Depth		Day/Night	
	<i>n</i>	<i>r</i> ²	<i>F</i>	<i>p</i>	<i>F</i>	<i>p</i>
<i>P. periphylla</i>	50	0.241	24.58	0.000***	0.38	0.538
<i>A. parva</i>	669	0.01	3.17	0.08	4.8	0.03
<i>A. russelli</i>	120	0.08	10.25	0.002***	2.38	0.126
<i>A. vanhoffeni</i>	101	0.047	5.06	0.027	1.28	0.261
<i>A. wyvillei</i>	201	0.079	16.61	0.000***	2.44	0.12

P. periphylla demonstrated the most significant variation in body size according to depth, with larger individuals in shallower waters at night (Figure 4.8). Body size varied according to depth for *P. periphylla*, *A. russelli* and *A. wyvillei*, with larger individuals observed in deeper waters during the day, and shallower waters at night when modelled using GLM (*P.*

periphylla – $F = 24.58$, $p < 0.001$; *A. russelli* – $F = 10.25$, $p < 0.01$; *A. wyvillei* – $F = 16.61$, $p < 0.001$, Table 4.3).

Table 4.4 Multiple regression analysis predicting coronate body size according to different environmental variables sampled within the PAP study area. *P. periphylla* body size (coronal diameter) = $20.9 - 0.047 \text{ temperature} - 0.590 \text{ salinity} + 0.085 \text{ nitrate} + 0.94 \text{ oxygen} - 7.04 \text{ phosphate} - 0.0948 \text{ silicate}$. *A. wyvillei* body size (bell diameter) = $-26.59 + 0.2993 \text{ temperature} + 0.328 \text{ salinity} + 0.232 \text{ nitrate} + 2.187 - 0.69 \text{ phosphate} + 0.0030 \text{ silicate}$.

Independent variable		r^2	t	F	p
<i>A. wyvillei</i>	Temperature		-0.23	0.05	0.824
	Salinity		-0.85	0.73	0.403
	Nitrate		0.67	0.45	0.51
	Oxygen		0.68	0.47	0.502
	Phosphate		-0.83	0.69	0.415
	Silicate		-1.41	2	0.173
		11.68			
<i>P. periphylla</i>	Temperature		3.13	9.8	0.003***
	Salinity		2.62	6.8	0.002***
	Nitrate		2.19	4.81	0.01***
	Oxygen		3.11	9.66	0.03**
	Phosphate		-0.54	0.29	0.002***
	Silicate		1.83	3.36	0.069
		17.26			

A multiple regression was performed to investigate whether the various environmental factors (temperature, salinity, nitrate, oxygen, phosphate and silicate) could significantly predict a change in medusa body size. The results of the regression indicate that the model explained 11% of the variance for *A. wyvillei* and 17% of the variance for *P. periphylla*. None of the independent environmental variables were significant predictors of variation in *A. wyvillei* medusa size ($p > 0.05$). For *P. periphylla*, temperature ($F = 9.8$, $p < 0.01$), salinity ($F = 6.8$, $p < 0.01$), nitrate ($F = 4.81$, $p = 0.01$), oxygen ($F = 9.66$, $p < 0.05$) and phosphate ($F = 0.29$, $p < 0.01$) were all observed to be significant. Positive relationships were observed within all of these significant interactions for *P. periphylla* with the exception of phosphate, which was negatively correlated ($t = -0.54$).

4.4.2 Zooplankton biomass

Figure 4.9 depicts the vertical distribution of the total zooplankton taxa according to day and night collected as part of the Cruise 92 sampling effort. Species at overall shallower depths at night (indicating diel vertical migration) include the euphausiids (EUP), medusae (MED),

siphonophores (SIP), fish (FIS), chaetognaths (CHA) and amphipods (AMP); with significant differences between day and night hauls observed for the chaetognaths, euphausiids, medusae and siphonophores (GLM, CHA $F = 6.33$, $p = 0.03$; EUP $F = 6.27$, $p = 0.03$, MED $F = 6.96$, $p = 0.03$, SIP $F = 7.74$, $p = 0.02$). There was a greater number of zooplankton samples collected during the day than at night ($n = 65$ day, $n = 55$ night). Average zooplankton displacement volumes (ml per 1000 m³) were also greater during the day than at night (day: $mean = 53.52$ ml 1000 m⁻³, $SD = 82.27$; night: $mean = 47.27$ ml 1000 m⁻³, $SD = 73.0$).

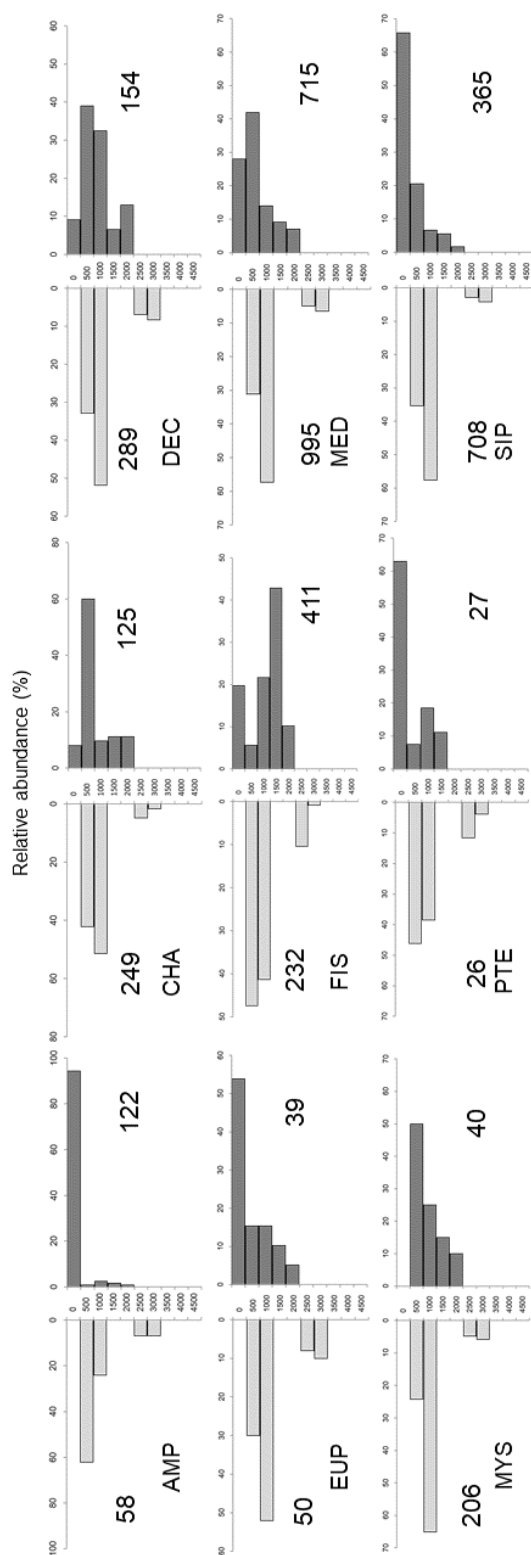


Figure 4.9 Percentage relative abundances of zooplankton taxa sampled during day (light grey bars) and night (dark grey bars) trawls at different depths during Discovery Cruise 92 within the PAP study area. Zooplankton samples were recorded as ml per 1000 m³ displacement volumes. Key to taxa: Medusae (MED), Siphonophorae (SIP), Fish (FIS), Chaetognatha (CHA), Polychaeta (POL), Amphipoda (AMP), Decapoda (DEC), Euphausia (EUP), Pteropoda (PTE) and Mysidae (MYS). Numbers on charts are the individual taxa sample volumes (ml 1000m⁻³) for day and night trawls.

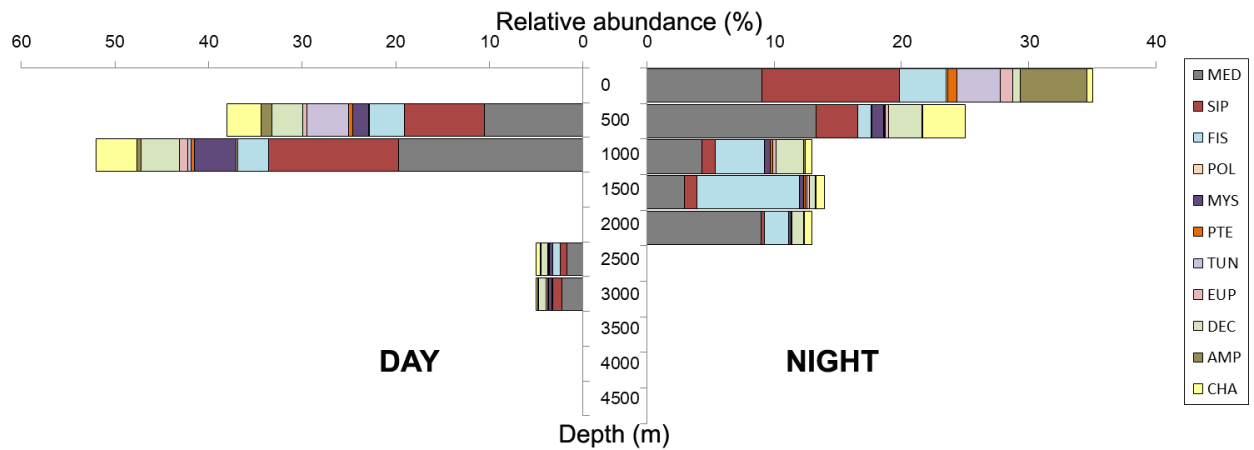


Figure 4.10 Relative abundances of all zooplankton taxa biomass sampled during day and night trawls. Taxa were recorded in ml per 1000 m³ displacement volumes. Relative abundances are according to depth, with individual taxa relative to the overall proportion sampled at that depth.

The relative abundance of all taxa at each depth increment illustrates that during both day and night periods the greatest represented taxa in terms of biomass displacement volumes are medusae and siphonophores (Figure 4.10). Overall the pattern of the combined taxa between day and night indicates that there is diel vertical migration present in the sample set, with 34% of the zooplankton biomass found at in the upper 500 m at night, and 25% found at a depth of 500 m. During the day, no zooplankton taxa were located in the upper 500 m, with 52% of taxa located at the start of the bathypelagic zone (1000 m).

The zooplankton taxa most strongly correlated with changes in medusa occurrence varied for *A. wyvillei* and *P. periphylla*. A forward stepwise regression analysis was performed to investigate whether the abundance of various zooplankton taxa (Medusae (MED), Siphonophorae (SIP), Fish (FIS), Chaetognatha (CHA), Polychaeta (POL), Amphipoda (AMP), Decapoda (DEC), Euphausia (EUP), Pteropoda (PTE) and Mysidae (MYS)) could significantly predict variation in the body size of *A. wyvillei* and *P. periphylla*. The results of the *A. wyvillei* regression indicated that the zooplankton taxa incorporated into the model explained 17% of the variance in medusa occurrence. Medusae (MED, $F = 14.93$, $p < 0.01$), fish (FIS, $F = 9.17$, $p < 0.01$), pteropods (PTE, $F = 62.76$, $p < 0.01$) and amphipods (AMP, $F = 22.70$, $p < 0.01$) significantly contributed to variation in *A. wyvillei* occurrence (Table 4.5). Polychaete abundance did not contribute to the model. For *P. periphylla*, polychaetes (POL, $F = 15.52$, p

< 0.01), euphausiids (EUP, $F = 16.61$, $p < 0.01$), decapods (DEC, $F = 14.53$, $p < 0.01$) and amphipods (AMP, $F = 12.77$, $p < 0.01$) were most strongly correlated with changes in occurrence in *Periphylla* (Table 4.5). Zooplankton taxa that did not result in statistically significant correlations were removed from the stepwise regression model. Significant relationships were observed with amphipods biomass predicting occurrence for both coronate species. However, for *A. wyvillei* this relationship was positive, and for *P. periphylla* it was negative.

Table 4.5 Model output from forward stepwise regression for predicting coronate occurrence with zooplankton biomass (displacement volume). Zooplankton taxa represent the independent variables that were retained within the model. Regression equation: *A. wyvillei* presence = $1.68 + 0.0166 \text{ MED} + 0.0053 \text{ FIS} + 0.013 \text{ POL} - 0.0095 \text{ PTE} + 0.023 \text{ AMP}$. Regression equation: *P. periphylla* presence = $4.175 + 0.614 \text{ POL} + 0.0033 \text{ EUP} - 0.0519 \text{ DEC} - 0.01578 \text{ AMP}$. *** indicates significant results to the 99% confidence level.

	Independent variable (zooplankton taxon)	r^2	t	F	p
<i>A. wyvillei</i>	MED		3.86	14.93	<0.01***
	FIS		3.03	9.17	<0.01***
	POL		0.49	0.24	0.627
	PTE		-7.92	62.76	<0.01***
	AMP		4.76	22.7	<0.01***
		0.17			
<i>P. periphylla</i>	POL		3.94	15.52	<0.01***
	EUP		4.08	16.61	<0.01***
	DEC		-3.81	14.53	<0.01***
	AMP		-3.57	12.77	<0.01***
		0.22			

4.4.3 Reproductive traits

Five *P. periphylla* and 184 *A. wyvillei* specimens possessed gonads that were identifiable as male or female (Figure 4.11). The majority of specimens overall were thus classified as 'unknown' because their gonad contents precluded sex determination or they lacked gonads ($n = 25$ for *P. periphylla*, $n = 228$ for *A. wyvillei*) (Figure 4.11). Unknown specimens were encountered across all size classes of *P. periphylla* (7 to 50 mm coronal diameter) and *A. wyvillei* (3 to 60 mm bell diameter), and no overall correlation between unknown specimens and size (Figure 4.11). There is no clear link between size of medusae and stage of maturity for *P. periphylla* (one-way ANOVA on mean medusa size and presence or absence of gonad

with Tukey's $F = 1.02$, $p > 0.05$), which may be due to the small sample size of 30. However, there is a clear relationship between stage of maturity and bell size in *A. wyvillei* (one-way ANOVA with Tukey's test $F = 30.23$, $p < 0.001$). Nevertheless, mature specimens with gonads were present throughout all size classes of *A. wyvillei* (Figure 4.11d).

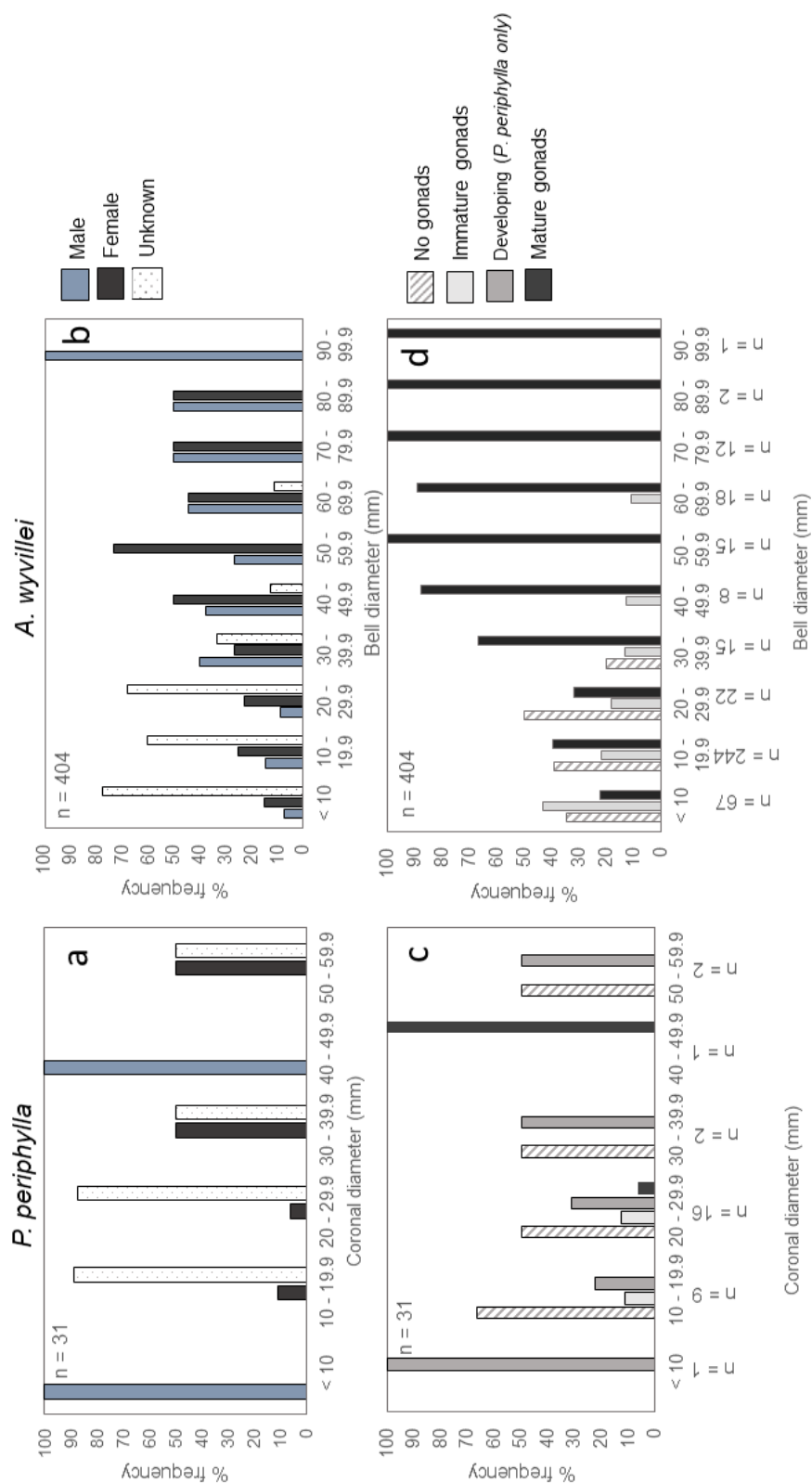


Figure 4.11 *P. periphylla* (a, c) and *A. wyvillei* (b,d) from the PAP study side split according to male, female and 'unknown' (see text) (a,b) and stage of maturity (c,d) according to size class. Coronal diameter used to determine size in *P. periphylla* and bell diameter in *A. wyvillei*.

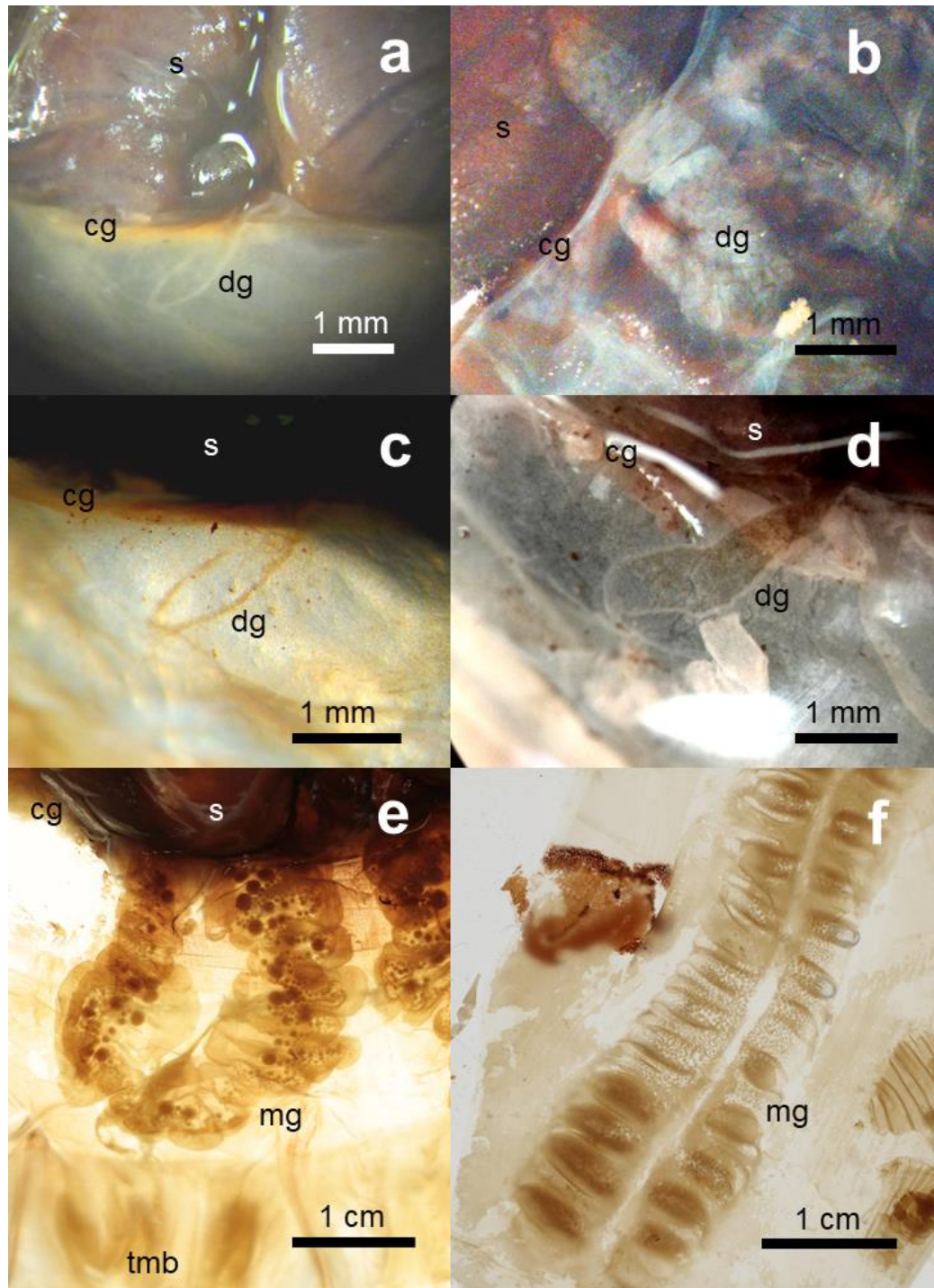


Figure 4.12 *P. periphylla* gonads at various stages of development from the PAP study area. First appearing as straight white ridges above the coronal groove, they become hooked and folded with the growth of the gastric sinus to form a J-shape (images **a – d**). The folds increase in volume as the medusa develops, producing a U-shape in maturity (images **e + f**). In the female gonad (image **e**) the young eggs originate at the point of origin of the fold and then migrate outwards, with the largest eggs > 1 mm diameter (Russell, 1970). The male gonads have secondary diverticula giving a more folded appearance (image **f**). Image **a** coronal diameter = 6.4 mm; image **b** = 7.1 mm; image **c** = 13.7 mm; image **d** = 9.2 mm; image **e** = 60 mm; image **f** = 82.7 mm. Key to images: s (stomach); cg (coronal groove); dg (developing gonad); tmb (tentacular muscular bundle); mg (mature gonad).

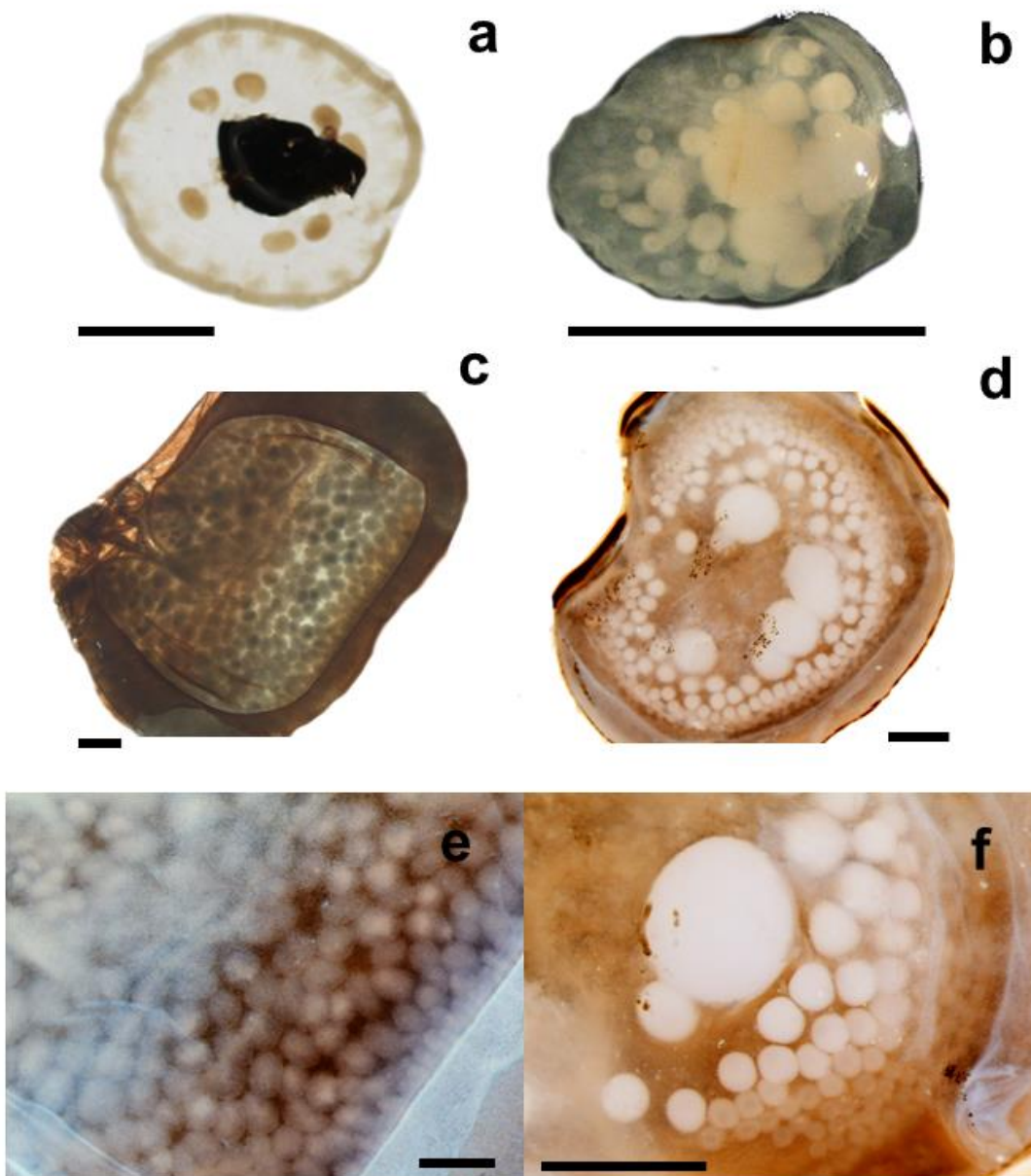


Figure 4.13 *A. wyvillei* gonads at various stages of development from the PAP study area. Gonads develop as crescent-shaped thickenings that are clearly visible at an early age (images **a** (entire specimen) + **b** (gonad only)). The gonads develop over time to form thick protrusions on the medusa subumbrella, with a mesogloal pad between the gastric endoderm and the germinal epithelium (Russell, 1970). The mesogloal pad is thinner in male gonads than female, with oval sperm follicles in a single layer next to each other, making the gonads appear dense (images **c** + **e**). In female gonads the mesogloal pad is dense, with oocytes originating near the periphery and migrating into the centre at maturity. The overall shape of the gonad in females resembles a bean shape (images **d** + **f**). Image **a** bell diameter = 2.2 mm; image **b** = 4.2 mm; image **c** + **e** = 45 mm; image **d** + **f** = 50.1 mm. Scale bars all 1 mm.

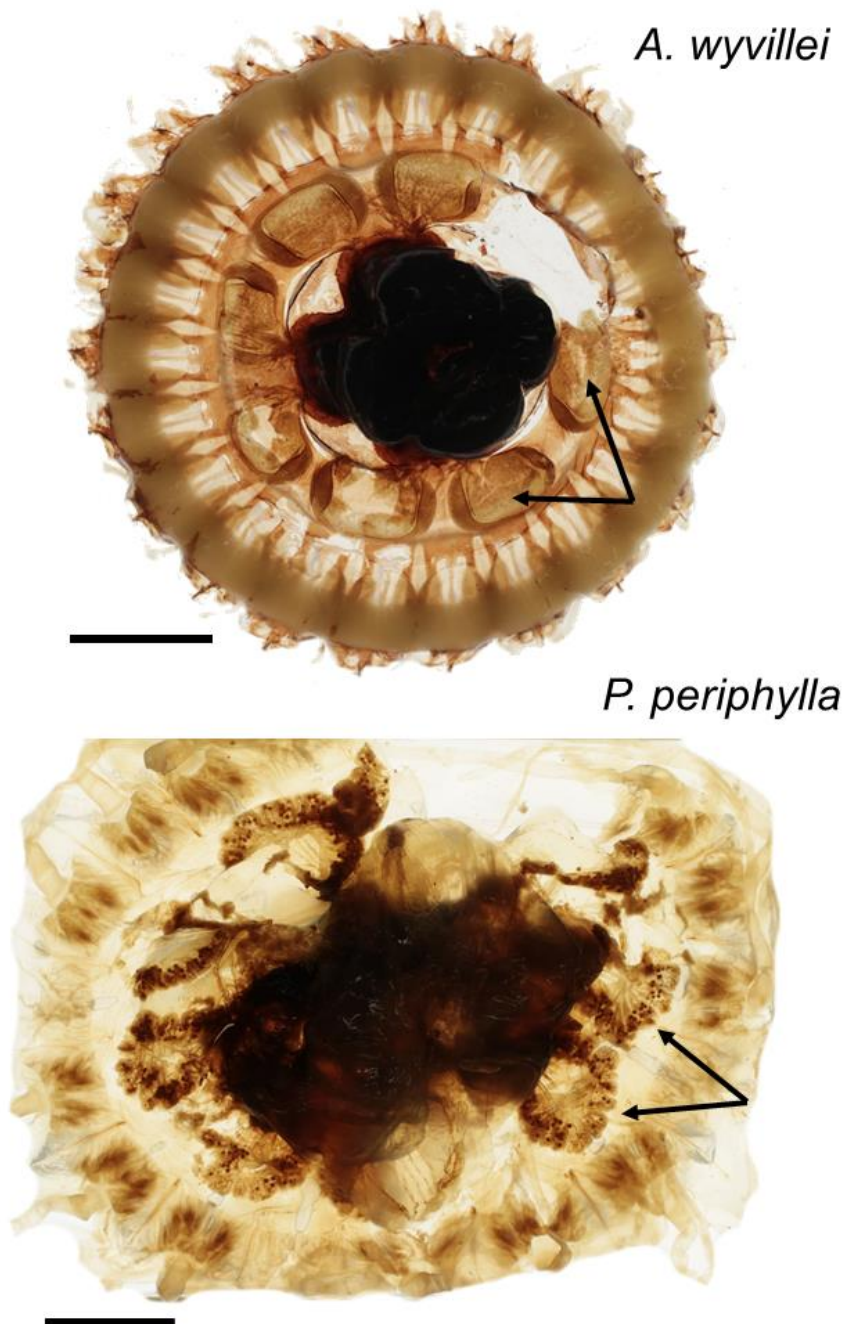


Figure 4.14 Subumbrella view of *A. wyvillei* (male) and *P. periphylla* (female) whole specimens with gonad locations (arrows). One gonad missing in *A. wyvillei*, one gonad damaged in *P. periphylla*. *A. wyvillei* specimen size bell diameter = 48.3 mm; *P. periphylla* specimen size coronal diameter = 32.3 mm. Scale bars all 1 cm.

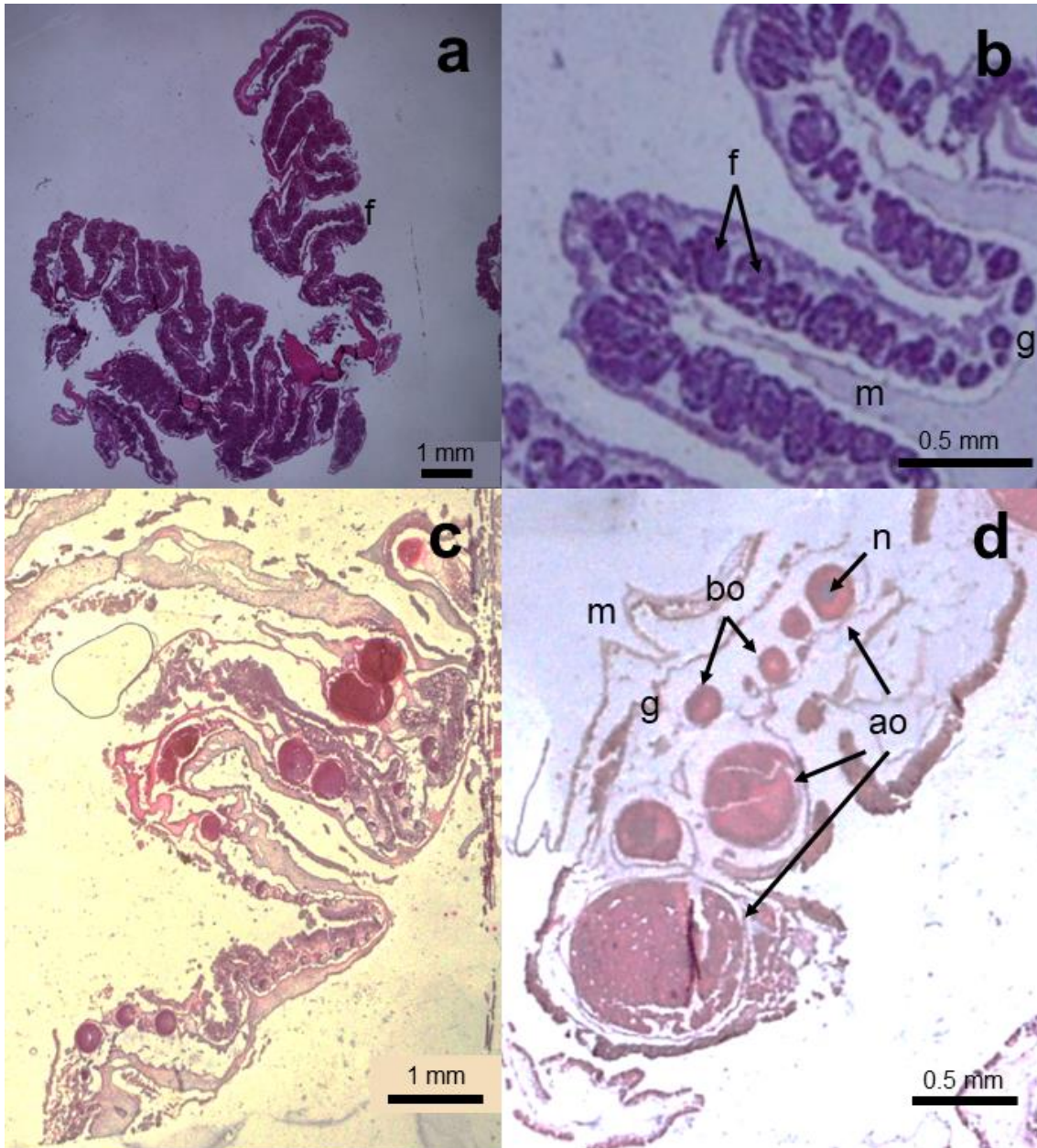


Figure 4.15 *P. periphylla* histology cross-sections of male (images a (whole gonad) + b (sub-section of a gonad)) and female (images c (whole gonad) + d (sub-section of a gonad)) gonads from specimens sampled from the PAP study area. Gonad folds are clearly visible in both male and female specimens, with the male sperm follicles more heavily stained than the female tissue overall. Key to images: f (sperm follicles); m (mesoglea); g (gastrodermis); bo (immature basophilic oocytes); ao (mature acidophilic oocytes); n (nucleus).

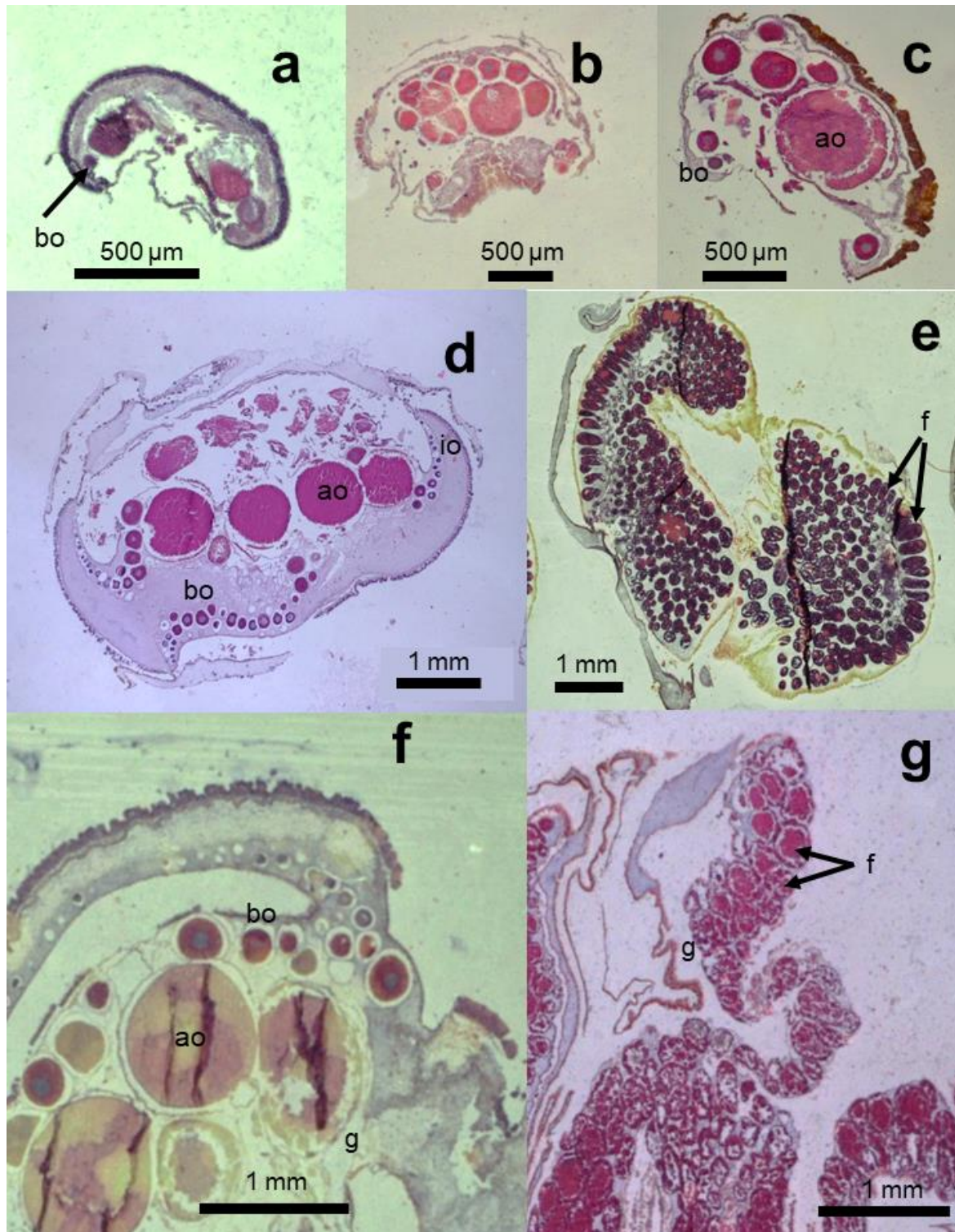


Figure 4.16 *A. wyvillei* histology cross-sections of developing (images a – c), mature female (images d + f) and mature male (images e + g) gonads from specimens sampled within the PAP study area. Sperm follicle arrangement (f) is indicative of the lobed mesogloal pad. Key to images: bo (basophilic oocytes); io (immature oocytes); ao (mature acidophilic oocytes); g (gastrodermis); f (sperm follicles).

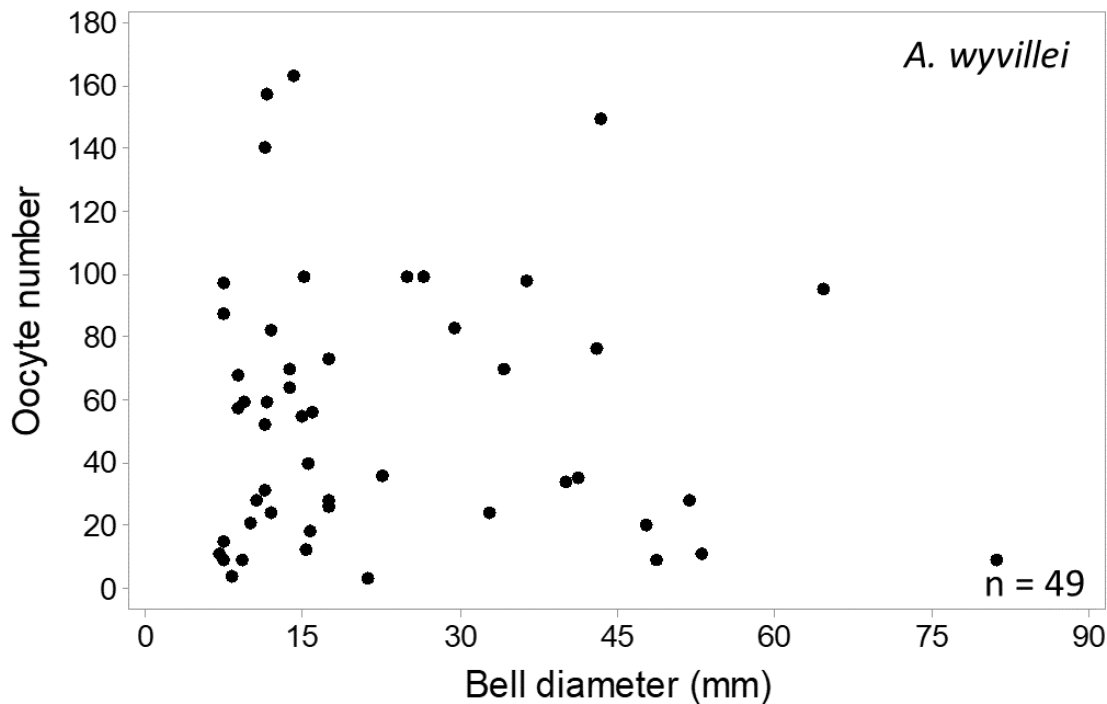


Figure 4.17 Number of oocytes against medusa bell diameter (mm) for *A. wyvillei* within the PAP study site.

Following the histological staining and sectioning of the coronate gonads, only *A. wyvillei* was suitable for analysing fecundity and egg size due to the more robust structure of the gonad that enabled retention of characters following embedding and sectioning. The histological analysis of the *A. wyvillei* female gonads illustrates the clear distinction between mature and immature oocytes (Figure 4.16). Within the larger medusae (bell diameter > 30 mm), the migration of the smaller, more immature oocytes from the periphery of the gonad for release into the mesoglea is apparent. Histological study demonstrates the development of these oocytes from immature stages at the periphery which then migrate into the gonad, appearing first as densely-stained basophilic oocytes and then becoming mature, lighter-stained acidophilic oocytes. Large nuclei are observed in mature oocytes and a granular cytoplasm with an air sac surrounds the oocyte. These mature oocytes show an increase in size from the small immature oocyte stages (approx. 800%). Mature oocytes were found in medusae as small as 9.4 mm diameter, and immature oocytes were observed in all medusa sizes.

There is no clear relationship between fecundity and medusa size (Figure 4.17), with a range of oocyte numbers found across all medusa sizes (Pearson Correlation, $r = 0.065$, $p > 0.05$).

The range in size of immature and mature oocytes observed was 73.3 to 234.7 μm and 154.8 to 1283 μm , respectively, as characterised for *A. wyvillei* ranging from 9.4 to 64.6 mm in bell diameter. The comparison between average depths for immature and mature oocytes illustrates that mature oocytes are found at an overall deeper depth than immature oocytes (one-way ANOVA, $r^2 = 2.64$, $F = 12.58$, $p < 0.001$).

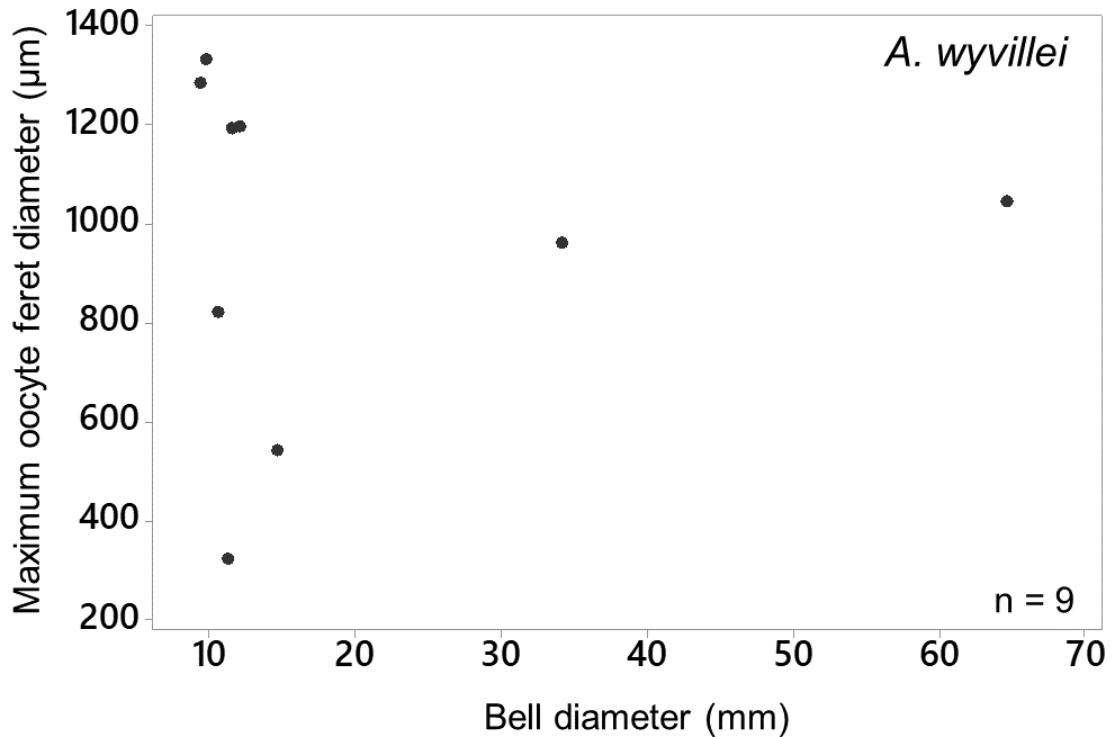


Figure 4.18 Variation in oocyte size with body size for *A. wyvillei* individuals sampled within the PAP study site.

Maximum oocyte feret diameter was quantified for individuals in which the largest oocytes were sectioned through the centre, providing accurate estimates of oocyte size ($n = 9$). Overall there is no relationship between maximum oocyte size (feret diameter) and medusa size for *A. wyvillei*, with the full range of oocyte feret diameters found within smaller individuals (approximately 10 mm bell diameter) (Pearson Correlation, $r = 0.036$, $p > 0.05$, Figure 4.18).

4.5 Discussion

The Porcupine Abyssal Plain (PAP) has been a relatively well-studied deep sea region since 1989 with investigations focusing on the links between surface processes, the transfer of particulate organic matter (POM) to the benthos, and benthic faunal communities. These studies have shown that the PAP site is a perennial CO₂ sink, with an average uptake of approximately 1.5 mmol m³ day⁻¹ (Frigstad et al., 2015). Studies at the PAP-SO have provided detailed biogeochemical assessments of the area over time, with sediment trap data tracking the flux of inorganic carbon and nitrogen to the deep ocean which drive benthic ecosystem processes (Hughes et al., 2011). The deep-sea benthic community at the PAP is recognised to be highly food limited, with the seasonal fluctuation of sinking detritus in May to June representing a major energy source that drives the system (Iken et al., 2001). Medusae, however, may compensate for fluctuations in food availability by prey capture and are thus interesting taxa for investigation within this area. In addition, increasing evidence that jelly falls represent export of organic matter from pelagic regions to the benthos highlights the importance of medusae as components of deep-sea benthic marine food webs (Lebrato et al., 2011, 2012; Sweetman and Chapman, 2011).

4.5.1 Coronate distributions and evidence for vertical migration

This study provides evidence that species of *Atolla* inhabit depths of 250 to 4150 m in the PAP, with *A. gigantea* found at deeper depths than other *Atolla* species (mean = 2603 m, Figure 4.6). Currently *Atolla* is thought to inhabit deeper waters than *P. periphylla*, however this speculation has not yet been fully tested within the same region, nor have distributions of *Atolla* species been considered at species level (see Russell, 1970; Osborn et al., 2007). Roe et al. (1984) note the minimal descriptions of the vertical distributions of *Atolla* species. The size of large species of *Atolla* such as *A. wyvillei* and *A. gigantea* inhabiting deeper overall waters is in agreement with the observation by Youngbluth and Båmstedt (2001) who noted that larger *P. periphylla* medusae were located at greater overall depths.

Within this study, diel vertical migration patterns are observed for *P. periphylla* only (Figure 4.7), however diel migration is still predicted for all of the species of *Atolla* in view of previous observations within the same region by Roe et al. (1984). 203 samples were omitted from the depth analysis because depths of sampling were poorly resolved. It is likely

that a number of shallow-water (< 250 m) samples were excluded from analysis and this may have contributed to lack of detection of diel vertical migration pattern for the various species of *Atolla*.

Angel and Baker (1982) concluded that the relative importance of medusae increased with depth based on samples examined from Cruise 92. Thus, medusae as a collective taxonomic group showed peaks of biomass at 900 to 1100 m, accounting for nearly 70% of the nekton biomass. The individual medusae in this case were not described to species level. However, medusae were assigned to species and quantified at a depth of 1000 m (Angel and Baker 1982). Medusae of eight recognised species (*A. parva*, *A. wyvillei*, *Aeginura grimaldi* Maas 1904, *Pontachogon haeckeli* Maas 1893, *Halicercera bigelowi* Kramp 1947, *Aegina citrea* Escholtz 1829, *Halicreas minimum* Fewkes 1882 and *Aglantha digitale* Müller 1776) accounted for approximately 31% of the total biomass of the sampled nekton at 1000m. While gelatinous organisms were estimated to account for approximately 68% of the total wet biomass at 1000m, the more delicate gelatinous constituents such as siphonophores and ctenophores were not quantified accurately due to disintegration during sampling. The study by Angel et al. (1982) did not include the coronates *P. periphylla*, *A. gigantea*, *A. russelli* and *A. vanhoeffeni*. Minimal variation in biomass was observed between day and night hauls of the various planktonic species at a depth of 1000 m, indicating that drivers of biomass variation did not include diel vertical migration but was more likely related to the particle flux of organic matter (Angel et al., 1982).

In a study of the same sample region sampled four years previous to Cruise 92 (April 1974), Roe et al. (1984) identified 15 species of medusae, but noted that the total number of medusae sampled was likely to be an underestimate due to sampling constraints. Diel vertical migration in the Roe et al. (1984) study was observed for two coronates, *A. vanhoeffeni* and mature *A. wyvillei*. *A. vanhoeffeni* exhibited a distinct vertical migration over at least 200 m, and mature *A. wyvillei* individuals were observed migrating from 600 m to 250 m at night. The study was limited to 250, 450 and 600 m depths and did not extend to bathypelagic depths. *A. parva* was reported to occur only at a depth of 600 m.

As outlined above, with the exception of *P. periphylla*, this study is limited in providing evidence for vertical migration of coronates in accordance with the inferences of Angel et

al. (1982) and Roe et al. (1984). The small samples sizes for species other than *P. periphylla* are likely to explain this discrepancy.

4.5.2 Body size variation in deep sea organisms

Variation in body size of deep sea animals is of interest as such phenotypic responses to environmental change may ultimately underlie in macroevolutionary trends (Hunt and Roy, 2006). Roy (2001) and Linse et al. (2006) identified potential patterns in body size according to latitude within deep-sea bivalves with larger sizes at higher latitudes. Shifts in body size over space of pelagic taxa such as gelatinous zooplankton is currently undocumented, particularly over macroecological (large spatial) scales. Body size varied according to depth for *A. parva*, *A. wyvillei* and *P. periphylla* (GLM, $p < 0.05$, Figure 4.8, Table 4.3), however the link between size and depth remains unclear. While it is predicted that larger coronate individuals are found at deeper depths (Russell, 1970; Roe et al., 1984), this was not strongly supported in this study although there was evidence that smaller individuals of *A. wyvillei* and *P. periphylla* were found near the surface at night.

It should be noted that due to their soft bodies, the specimens measured in this study may have undergone shrinkage during preservation. However, this potential margin of error was a consistent bias throughout the study, as all specimens were preserved similarly and over the same time period. A further consideration is that scyphozoan jellyfish can shrink and regrow depending on environmental conditions (Hamner and Jenssen, 1974; Lucas, 2001; Hopf and Kingsford, 2013). Such shrinkage and regrowth would further compromise identification of the effects of depth on medusa size. For many taxa substantial changes in body size may be precluded and thus size changes with depth may be relatively easily revealed.

Deep-sea fauna generally exhibit slow growth, low fecundity, and are long-lived (Drazen and Haedrich, 2012). In their study of gametogenesis and maturation of deep-sea coronate medusae Lucas and Reed (2010) described oocytes and gonads in all stages of maturity in medusae of all sizes. Jarms et al. (2002) suggested that oocytes of *P. periphylla* were not mature until they exceeded a diameter of 1 mm, however the histological interpretation of what defined mature oocytes was not described. In this study, four out of nine individual *P. periphylla* had gonads containing oocytes that exceeded this 1 mm size criterion of maturity.

These individuals were all less than 15 mm in diameter (Figure 4.18). Large mature oocytes may have already been released from the gonads of the larger individuals.

The consistently low fecundity (< 170 oocytes) across all size ranges indicates the high investment in eggs, with only one or two oocytes exceeding 1 mm diameter at a time before they are released. This is in contrast to shallow-water species such as the coronate *Nausithoe punctata*, which was documented by Morandini and da Silveira (2001) to possess up to 485 oocytes. Lucas and Lawes (1998) used the number of planula larvae held by *Aurelia aurita* medusae as an indicator of fecundity, and found that medusae of 115 m could contain up to 100,000 planula larvae. A following study by Lucas (2001) on *A. aurita* found that the fecundity significantly varied according to environmental conditions, ranging from < 5000 to 65,000 planula larvae depending on favourability. While the ultrastructure and gametogenesis within deep-sea coronates has been discussed previously (Eckelbarger and Larson, 1992; Lucas and Reed, 2010), the fecundity of *A. wyvillei* has not previously been documented. Due to the limited time period during which samples were collected (April and May), it was not possible to determine whether a distinct spawning period was apparent. Russell (1959) stated that mature specimens of *A. wyvillei* were observed all year round, but noted that increased spawning may occur during the summer months in more northerly latitudes. Mature gonads were observed in *P. periphylla* individuals sampled from Lurefjorden throughout the year (Jarms et al., 2002), with no distinct spawning period.

4.5.3 Zooplankton relationships – prey or parasitism?

The occurrence of *A. wyvillei* and *Periphylla* was differently impacted by zooplankton taxa biomass. *A. wyvillei* exhibited stronger links with medusae, fish and pteropods, while *P. periphylla* exhibiting stronger links with polychaetes, euphausiids and decapods (Table 4.5). Amphipoda are the only taxon that was strongly associated with sizes of both species. The correlation of medusa occurrence with the different taxa may relate to preferred prey types. If so the data would support *A. wyvillei* preferring the medusae, fish, pteropods and amphipods, and *P. periphylla* preferring polychaetes, euphausiids, decapods and amphipods.

As highlighted by Childress (1995) and Choy et al. (2017), prey capture amongst deep-sea faunal groups is poorly understood. Assessing stomach contents as an indication of diet was dismissed from this study as trawl-caught medusae were found to give unreliable estimates

of realistic gut contents. For example, Youngbluth and Båmstedt (2001) noted that within trawl nets, coronate medusae shed atypically high quantities of nematocysts and engulfed all available prey encountered within the net.

P. periphylla has been observed *in situ* using submersibles to prey upon certain crustaceans, squid, fish, copepods, ostracods and chaetognaths in other studies (Larson, 1979; Fosså, 1992; Youngbluth and Båmstedt, 2001). No reliable assessments of the prey of any species of *Atolla* have been made to date. *P. periphylla* possess 12 strong tentacles that can easily coil around active prey (Klevjer et al. 2009), whereas *A. wyvillei* possess approximately 22 finer tentacles that are subject to damage more readily (Russell, 1959). Hunt and Lindsay (1998) noted the presence of a single hypertrophied tentacle (3-6 times the bell diameter in length) in all *in situ* observations of *A. wyvillei* which was used to ensnare other gelatinous prey (specifically the siphonophore *Nanomia*). Hypertrophied tentacles were not found in this study perhaps due to damage during trawling. Prey capture techniques may thus vary between *Atolla* and *Periphylla*. In both genera the main tentacles may be used to capture the majority of prey (fish, crustaceans for instance), and the hypertrophied tentacle reserved for gelatinous prey only in *Atolla*. This interpretation is supported by the positive link between *A. wyvillei* occurrence and overall medusae biomass observed.

Gelatinous organisms including medusae are associated with a number of parasitic species. In shallow waters, parasites of medusae include digenean trematodes (Martorelli and Cremonese, 1998; Martorelli, 2001), cestodes (Vannucci-Mendes, 1944), isopods (Barham and Pickwell, 1969), nematodes (Svendsen, 1990), barnacles (Pagès, 2000) and sea anemones (McDermott et al., 1982). Parasitism is predicted to be in such volumes within shallow-water medusae that the parasitic species are considered to be significant contributors to population crashes within jellyfish blooms (Pitt et al., 2014). Martorelli (2001) identified the parasitic infection of cnidarians and ctenophores by digenean trematodes ranged between 1.4 to 30% prevalence within the southern Atlantic. Associations between decapod crustaceans and jellyfish are also documented, including the crab *Libinia ferreirae* Brito Capello 1871, *Libinia spinosa* Guérin 1832, the cleaner shrimp *Periclimenes paivai* Chace 1969 and *Leander paulensis* Ortmann 1897 (Diniz-Filho and Bini, 2008; Gonçalves et al., 2016; de Moraes et al., 2017). Within this study, the significant link between the Amphipoda (AMP) and both *P. periphylla* (negative association) and *A. wyvillei* (positive association) (Table 4.5) could be indicative of potential parasitism. Hyperiid amphipods are well

documented to exhibit parasitism on medusae (Laval, 1980; Dittrich, 1988), with most species depending on gelatinous hosts for some stage of their life cycle (Arai, 2005). In some instances, 100% of the jellyfish population may be infected (Towanda and Thuesen, 2006). The zooplankton taxa were not described to species level, however may be an indication of potential parasitic species within the dataset. While it is not possible to confirm parasitism on individual museum specimens due to preservation and subsequent sorting, the significant relationship between amphipods and both *A. wyvillei* and *P. periphylla* could be an indication of parasitic association between deep-sea coronates and hyperiids.

4.5.4 Conclusions

This study built on the existing information generated from Cruise 92 in April and May of 1978 by Angel et al. (1978) by using samples collected during the cruise and subsequently preserved within the Discovery collections at the Natural History Museum London. Deep-sea coronate species such as *P. periphylla*, *A. russelli*, *A. gigantea* and *A. vanhoeffeni* were not described in the original outputs of the cruise. This may have been a result of the broad focus of the cruise, which sampled at least 194 planktonic species. Following fixation in formalin, the samples from the cruise were then available for analysis decades later, adding to the contributions of the original cruise for posing different ecological questions at a later time. The deep-sea coronate genera *Atolla* and *Periphylla* have robust mesogleal structures, which is both beneficial during the time of sampling and also following years of preservation, retention of key physical landmarks (with the exception of damaged and missing tentacles). No conclusions could be drawn with respect to the potential use of the hypertrophied tentacle in *A. wyvillei* for predation on other medusae, which it was found to be significantly correlated with in this study. The significant associations with the different zooplankton for *A. wyvillei* and *P. periphylla* confirm the hypothesis that the prey types vary for the respective genera, likely as a result of their different tentacle numbers, strengths and spacing. Further work is required on in-tact specimens to confirm this, preferably by observing prey capture *in situ*. Because gut content analysis was not considered to reliably estimate of prey a combined approach using museum specimens and observations of live specimens is suggested might reveal better insights into prey of deep-sea coronates. Amphipods were found to be associated with both *A. wyvillei* and *P. periphylla*, which is suggested to be an example of parasitism of hyperiid amphipods on scyphozoan medusae; something that is

well documented within shallow-water species however not within deep-water species. However, further *in situ* observations on these deep-sea species is required in order to confirm this hypothesis.

- Six deep-sea coronate species were found within the study area.
- Diel vertical migration patterns were observed for *P. periphylla* (day mean = 933 m, night mean = 802 m), which is in agreement with current studies.
- No observed diel vertical migration patterns were apparent for *Atolla* spp. and as such remains not fully documented within the literature.
- *P. periphylla* exhibited changes in medusa size according to variation in environmental conditions (temperature, salinity, nitrate, phosphate).
- The occurrence of both genera was significantly linked to the available zooplankton biomass, with different zooplankton taxa (with the exception of amphipods) linked to each genus. This is inferred to be an indication of the variation in preferred prey types between *Atolla* and *Periphylla* as a result of their varied morphologies, particularly the tentacles (the data supports the second hypothesis).
- Both species were significantly linked to amphipod biomass, which could be indicative of potential parasitism on the deep-sea coronate medusae.
- Gonads containing mature oocytes exceeding 1 mm diameter were found in specimens of *Atolla* of all sizes, ranging from 10 mm to 90 mm bell diameter.
- Mature gonads were observed in *P. periphylla* from 20 mm to 50 mm coronal diameter.
- There was no indication of spent gonads in larger (presumed to be older) medusae within the study.
- Low oocyte numbers within *A. wyvillei* ($n = 170$ maximum) are evidence of low fecundity which until now has not been documented within *Atolla* (data supports the first hypothesis).

Chapter 5: A comparison between fjord and oceanic populations of *Periphylla periphylla*

5.1 Abstract

Periphylla periphylla is an oceanic mesopelagic species well adapted to the deep-sea environment. However, mass occurrences of *P. periphylla* have been discovered within various Norwegian fjords. Densities within these fjords have been compared to the mass occurrences of *Mastiagas* sp. in Palau and *Mnemiopsis leidyi* in the Black Sea as opposed to opportunistic blooms as a result of reproduction events. A number of these narrow inlets of water along the west coast of Norway have been found to possess certain characteristics for the proliferation and retention of *P. periphylla*. Lurefjorden, the most researched study site, has a low exchange rate of water masses, so the jellyfish can proliferate and remain *in situ*. The sizes of *P. periphylla* are believed to be larger within fjord environments, however until now this has been undocumented. This study describes the population structures of oceanic and fjord samples using data from the Iceland Basin and Lurefjorden, and confirms that there is a significant difference between sizes of medusae between systems (fjord mean = 80.34, SD = 16.82, n = 662; ocean mean = 13.89, SD = 11.10, n = 1121). This variation is proposed to be a result of shrinkage in oceanic environments that is absent in the more stable fjord environments where *P. periphylla* represent the apex predators. This study highlights the importance of using macroecological data from a number of sources in order to obtain accurate representations of species distributions, particularly for the poorly understood deep sea coronates.

5.2 Introduction

There are few studies of the life history and ecology of deep-sea coronates from oceanic samples beyond the early works of Russell (1959; 1970). Studies on oceanic populations of deep sea coronates such as *Atolla* spp. and *P. periphylla* are constrained by problems in retrieving intact samples and expense. Our knowledge is therefore generally based on studies conducted over short periods of time and inferences that are often based on small sample sizes. Despite such constraints, investigators have managed to gain various insights

into the ecology and biology of oceanic coronate medusae. Specifically, these include insights on reproductive traits of *A. wyvillei* and *P. periphylla* (Lucas, 2009; Lucas and Reed, 2010), prey capture in *A. wyvillei* (Hunt and Lindsay, 1998), predator-prey relationships of *A. wyvillei* (Moore et al., 1993), sperm longevity within species of *Atolla* (Himes, 2007) and comprehensive anatomical descriptions of *Atolla* and *Periphylla* (Russell, 1959, 1970). Oceanic deep-sea coronates have also featured in studies focusing on scyphomedusan habitats (Osborn et al., 2007), bioluminescence (Haddock and Case, 1999; Battle, 2004) and scyphozoan species occurrence in the Southern Ocean (Larson, 1986).

Much of our understanding of the biology of deep-sea coronates derives from studies focusing on populations in Norwegian fjords. Such studies take advantage of the mass occurrences of *Periphylla periphylla* in fjords such as Lurefjorden, Halsafjorden, Sognefjorden, Trondheimsfjord and Vefsnfjorden (Sötje et al., 2007; Solheim, 2012; Tiller et al., 2014). These mass occurrences are unlike jellyfish blooms within shallow-water systems which are a result of opportunistic periods of mass breeding under certain conditions (Parsons and Lalli, 2002). Fjord populations proliferate and are retained within relatively enclosed fjords as a consequence of optical control (Sørnes et al., 2007) and basin topography (Gorsky et al., 2000). Studies of such fjord populations were instigated when high densities of jellyfish began impeding local fishing activities (Fosså, 1992). The relative ease of access and reduced effort of sampling fjord populations in comparison to those in the open ocean greatly facilitated the feasibility of investigating the biology of deep-sea jellyfish. Studies on *P. periphylla* and other coronates in fjords have focused on jellyfish as top predators (Klevjer et al., 2009), how jellyfish-dominated systems affect microbial activity (Riemann et al., 2006), diel vertical migration (Kaartvedt et al., 2007), jellyfish distribution and behaviour (Youngbluth and Båmstedt, 2001), the life cycle and biology of coronate medusae (Jarms et al., 1999; 2002) and the impacts of jelly falls and particle flux on scavenger communities (Sweetman and Chapman, 2011; 2014).

Limited investigations suggest there may be differences between oceanic and fjord populations of *P. periphylla*. Population densities within the fjords are documented to be two to three orders of magnitude higher than within open ocean environments, with as many as 2.5 individuals m⁻³ (Sørnes et al., 2007). In addition, the diameters of individuals caught within Lurefjorden reach greater maximum sizes than some oceanic individuals. For example, fjord individuals of *P. periphylla* reach up to 160 mm in diameter whereas

diameters of individuals reach up to 80 mm in the Gulf of Mexico and 60 mm in Cape Hatteras in the north-western Atlantic (Lucas & Reed 2010). However, oceanic specimens from other regions, such as offshore Japan and the Southern Ocean, have similar diameters to *P. periphylla* in various Norwegian fjords (Larson, 1986; Lucas and Reed, 2010). In general, there are few studies of oceanic populations relative to those in Norwegian fjords (see Child & Harbison 1986; Mills & Goy 1988; Pages et al., 1996; Osborn et al., 2007; Lucas & Reed 2010) and these have been conducted on populations widely separated geographically from Norway.

The aim of this study is to compare morphological traits of fjord and oceanic populations of *P. periphylla* from the same latitudinal range in the northern hemisphere. Morphological variation may signify that *P. periphylla* can adjust traits according to contrasting environments - high density fjord environments and relatively low density open ocean habitats. An alternate explanation would be that fjord and oceanic populations are comprised of cryptic species perhaps as a result of retention over time and local adaptation to fjord environments.

5.2.1 Aim and objective

This study aims to determine whether there is morphological variation between fjord and oceanic populations of *P. periphylla* from the same latitudinal range and thus to contribute to our general understanding of the biology of *P. periphylla*. The objective is to investigate the morphological characteristics of *P. periphylla* within two contrasting populations; the oceanic Iceland Basin and the fjord Lurefjorden, Norway using a combination of fresh samples and preserved specimens held at the Natural History Museum London.

The conceptual hypothesis is that there is a significant difference in morphological characteristics between oceanic and fjord populations, which is predicted to be reflective of the varied trophic interactions and environmental conditions between the oceanic and fjord populations.

5.3 Methods

5.3.1 Samples and study area

Fjord samples

Mass occurrences of *P. periphylla* in Lurefjorden have been widely documented (Fosså, 1992; Youngbluth and Båmstedt, 2001; Klevjer et al., 2009; Sötje et al., 2011; Sweetman et al., 2014). Populations of *P. periphylla* are consistently large throughout the year in fjords, as observed by Youngbluth and Båmstedt (2001) during February, August and December, and by Sørnes et al. (2007) during April, June and October.

P. periphylla samples were collected from Lurefjorden, Norway (60°41.7'N, 05°08.5'E) aboard the 'MS Solvik' during a 'Jelly Farm Project' multi-disciplinary research cruise (see <http://jellyfarmproject.blogspot.com> for further information) in August 2015 (Figure 5.1). The primary objective of the cruise was to photograph the sea floor for evidence of jelly falls and to set sediment traps to monitor particle flux within the fjord. The specimens for this study were collected at the end of each day on the 1st and 2nd August 2015. The sample collection, measurements of individuals and subsequent analyses were not part of the Jelly Farm Project but were conducted for this thesis alone.

Samples were collected from the deepest part of the main basin (440 m) using a 2 m diameter vertical tow net (10 mm mesh) hauled from the sea floor to the surface, twice daily over 2 days. Physical damage to medusae was minimised by hauling the nets slowly (10 m min⁻¹). Specimens were weighed (wet weight) immediately upon collection, and the following morphological measurements (dependent on extent of trawl damage) were made using forceps as per the methods described in previous chapters in this thesis; coronal diameter, coronal height, bell diameter, bell height, male/female, tentacle number and tentacle length. The same methods for morphological measurement were used on fresh and preserved museum specimens.

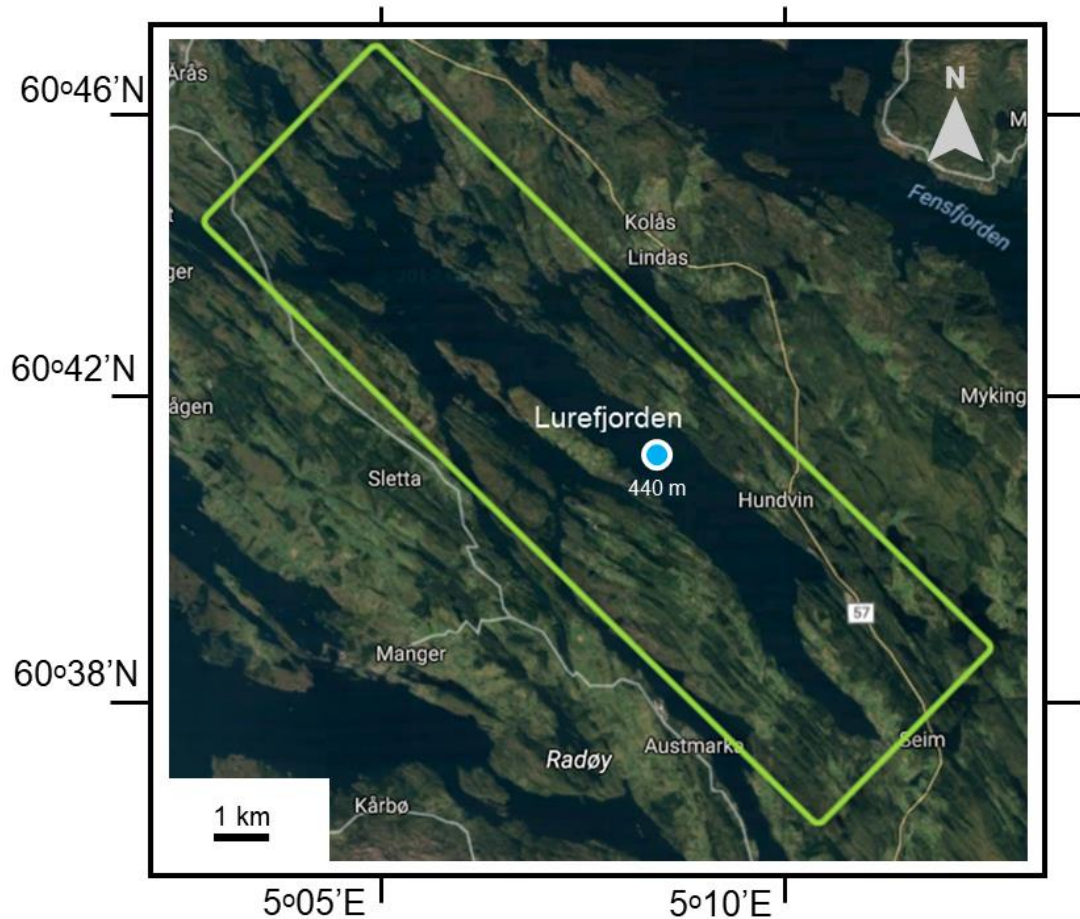


Figure 5.1 Sample site for the collection of fresh *P. periphylla* samples, Lurefjorden, Norway (60°41.7'N, 05°08.5'E). Lurefjorden is outlined with yellow rectangle, and sample site is marked with blue dot (depth = 440 m).

Gonad tissue samples were extracted from each individual for subsequent histological analyses post-cruise. Two out of a possible eight gonads were dissected and transferred into 100% ethanol for subsequent embedding in paraffin for histological analysis as outlined in Chapter 4. Gonad, coronal muscle and tentacular tissue were also dissected from every individual for molecular analysis. Marginal sense organ tissue was dissected from every individual for subsequent sclerochronological analysis as described in Chapter 6. 100% ethanol was used as a fixative and short-term preservative in order to retain all of the necessary structure for histological, molecular and sclerochronological work (see Quicke et al., 1999 and Williams and Syoc, 2007 for ethanol usage for histology). The usage of formalin, the typical fixative for gelatinous fauna (see Purcell, 1988; Haddock, 2004) is not ideal for DNA extraction (see Taleb-Hossenkhani et al., 2013) and would compromise the bassanite structure within the marginal sense organs (Petersen, 1976). The histological and molecular

analyses were precluded due to failure to embed in the paraplast wax and problems with DNA sequencing. For full description of molecular methods see Chapter 7.

An 'OPENROV' remotely operated vehicle (ROV) was taken to Lurefjorden in order to document *P. periphylla* individuals *in situ*. The ROV used was small in size (40 cm x 30 cm) with a 20 m wire connected to the device controller and was therefore only suitable for near-surface recording. The ROV was deployed during the day and night. Perhaps due to the summer month of sampling with light conditions throughout the night, no *P. periphylla* individuals were sighted and as such no ROV data was included in this study. See Appendix B for images of the equipment used.

Supplementary coronal diameter data were obtained from three other Jelly Farm Project cruises to Lurefjorden during 2010, 2011 and 2016 in order to provide a larger sample set across multiple sample seasons.

Oceanic samples

Comparative oceanic samples were identified in the formalin-fixed *P. periphylla* collections held at the Natural History Museum, London. The samples were based on material collected in 1971 from the Iceland Basin in the North Atlantic (60°N, 20°W) and were thus taken from the same latitude (60°N) as Lurefjorden. Samples were a combination of material collected as part of RRS Discovery Cruise 39 (April to June 1971, Foxton et al., 1971) and an unknown cruise number (July to December 1971) (Figure 5.2). Information on sample location, depth, time of day and gear used was available for all specimens included in this study. Morphological information was recorded for all available *P. periphylla* specimens within the collections from the Iceland Basin during 1971, using the same methods as described for the fjord specimens and in previous chapters. As with the fjord specimens, tissue samples were taken from a number of medusae (n = 80) for histological, molecular and sclerochronological analysis. Medusae were selected at random for the extraction of tissues by laying all individuals within specimen jars onto a gridded tray and selecting every tenth individual morphologically measured. This resulted in collecting data for medusa that ranged in size, sex and stage of maturity (n = 80 individuals). However, as described above, the histological and molecular work was omitted from this study as a result of failure to successfully embed and lack of successful DNA sequences.

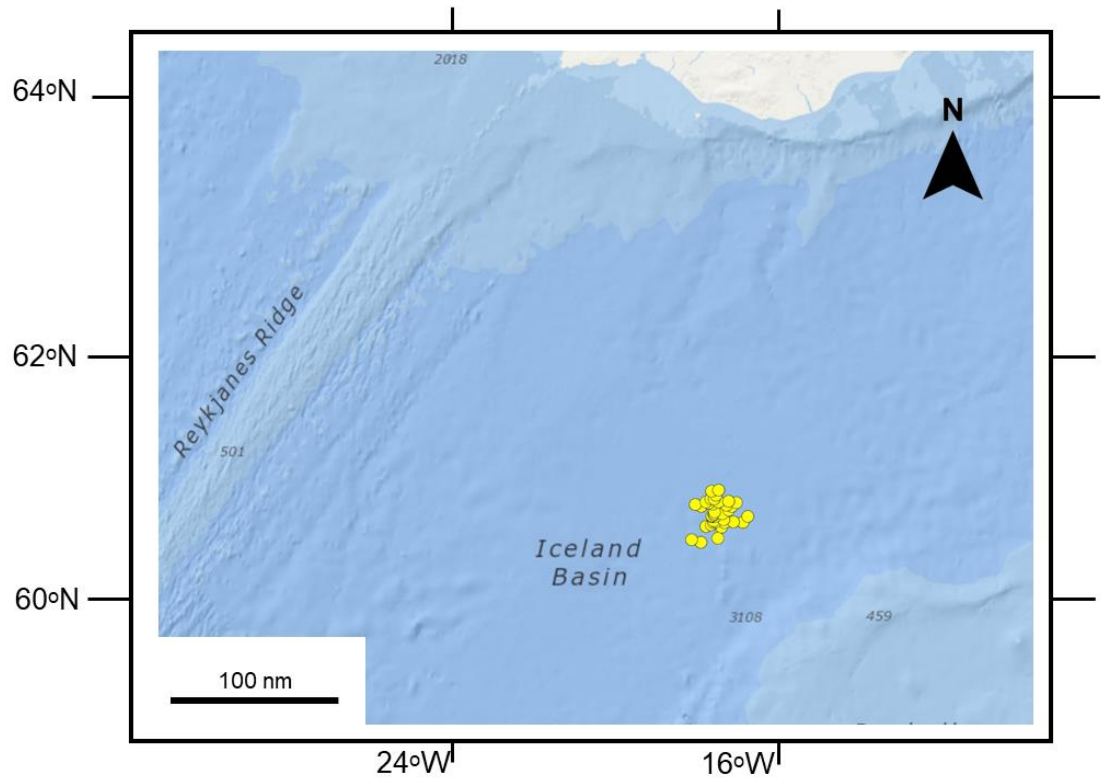


Figure 5.2 Sample stations (station numbers 7709, $n = 28$) within the Iceland Basin for the oceanic specimens used within this study held within the Discovery Collections at the Natural History Museum London. All samples collected during 1971.

5.3.2 Data analysis

The Lurefjorden and Iceland Basin data were tested for normality using the Kolmogorov-Smirnov test in Excel. Histograms were produced to describe population structure based on size frequency distributions of the two populations. One-way analysis of variance (ANOVA) was used to determine the variation in mean coronal diameters between the areas, as well as documenting any seasonal variation and the male and female splits.

5.4 Results

5.4.1 Morphological comparisons between oceanic and fjord environments

Table 5.1 Numbers of *P. periphylla* measured following fieldwork in Lurefjorden, Norway and sampling of museum collections from the Iceland Basin. Supplementary information from the Jelly Farm Project 2010, 2011 and 2016 cruises listed.

Fresh samples, collected Lurefjorden, Norway (60°N, 05°E)			
Year	Month	Depth range (m)	n sampled
2010	Dec	0-440	127
	Mar	0-440	273
2011	Jul	0-440	60
	Dec	0-440	127
2015	Aug	0-440	72
2016	Jun	0-440	18
2010-2016	Mar-Dec	0-440	677

Museum specimens, Iceland Basin, NE Atlantic (60°N, 20°W)			
Year	Month	Depth range (m)	n sampled
1971	Apr	72-952	59
	May	77-1125	404
	Jun	152-905	246
	Jul	350-905	159
	Aug	650-905	85
	Sep	650-905	60
	Oct	650-905	57
	Nov	650	30
	Dec	650	21
1971	Apr-Dec	72-1125	1121

A total of 72 *P. periphylla* individuals were sampled and measured during fieldwork on the 1st and 2nd of August 2015 within Lurefjorden (herein referred to as the fjord population). With work on further material collected during other time periods a total of 677 fjord specimens were measured (Table 5.1). 1121 individuals were measured within the Iceland Basin sample area (herein referred to as the oceanic population). Both fjord and oceanic regions were sampled during multiple seasons. The fresh and museum specimens differ in terms of appearance due to the degradation of the porphyrin pigment over time. However, the key landmarks could still be recognised after long-term preservation due to the robust structure of the deep-sea coronates. See Figure 5.3 for examples of specimens caught within Lurefjorden, 2015.

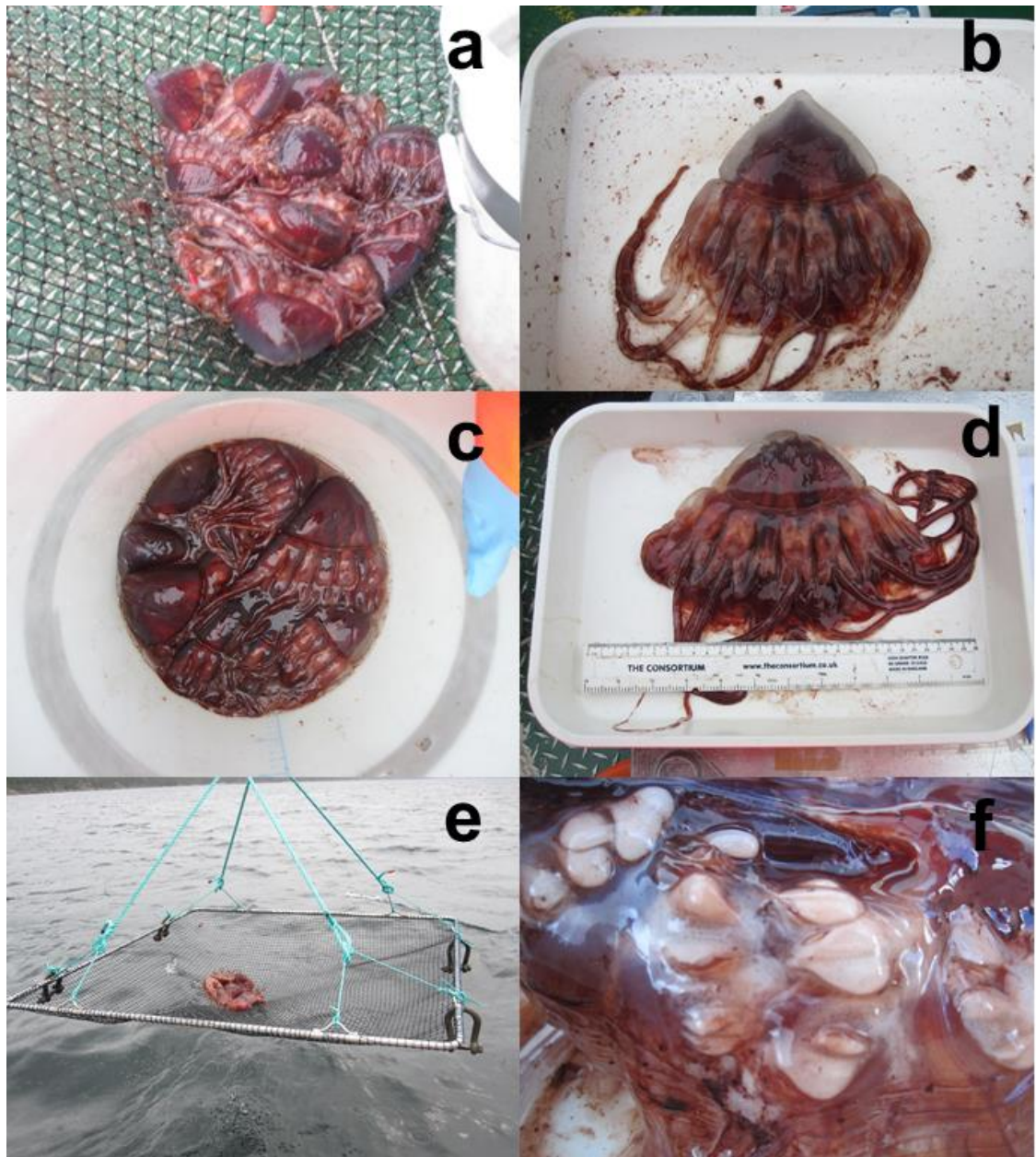


Figure 5.3 Examples of *P. periphylla* caught during the Lurefjorden field work, August 2015 aboard 'MS Solvik'. a + c + e: example of hauls following vertical tows; b: example of the rapid extent of porphyrin pigmentation degradation following the exposure to light and handling (note red flecks against white tray); d: additional *P. periphylla* specimen with 30 cm ruler for scale; f: mature male specimen with gonads (white) clearly visible on the subumbrella.

There is a higher proportion of smaller individuals (< 20 mm diameter) in the oceanic population, with a skewness of 6.09 (SD = 11.10). The fjord population demonstrates an overall larger proportion of medusae when compared on the same scale, with a skewness of -0.37 (SD = 4.62) (Figure 5.4).

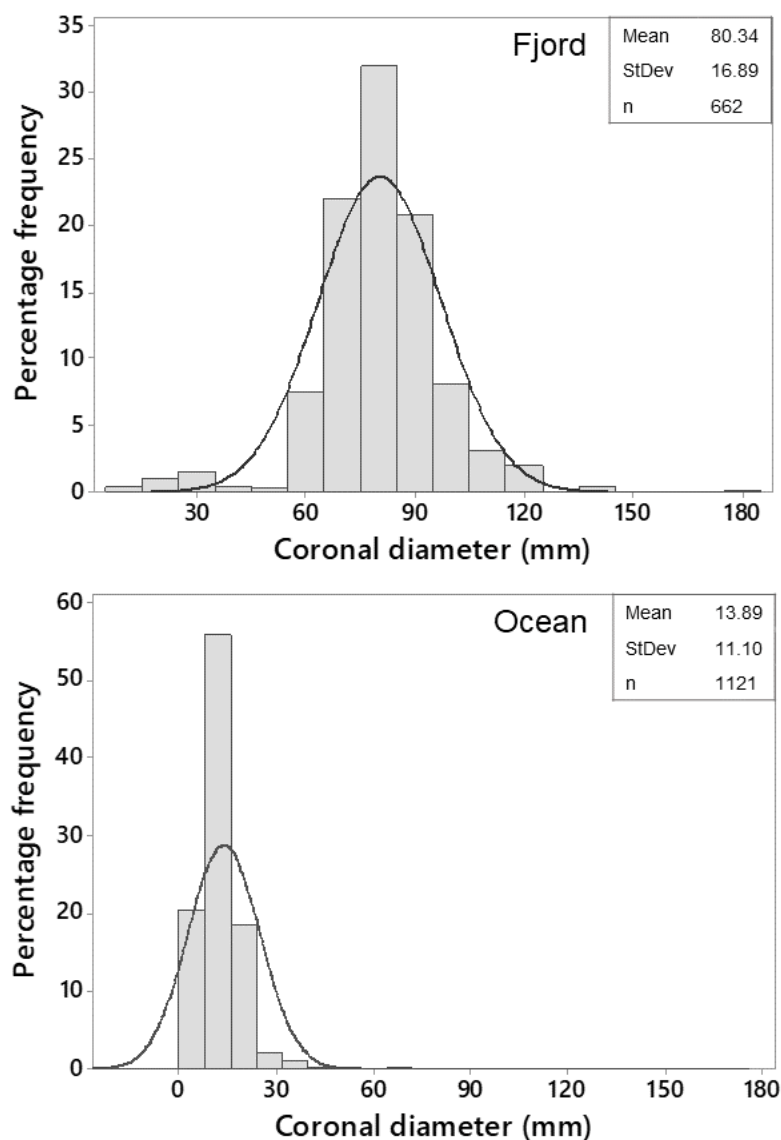


Figure 5.4 Size frequency histograms for the oceanic and fjord populations within the fjord and ocean study sites.

The mean size of fjord medusae (80.3 mm) is significantly larger than the oceanic samples (13.9 mm) (one-way ANOVA , $F = 9594.6$, $p < 0.001$, Figure 5.5). There is strong sexual dimorphism within the oceanic population compared with the fjord population. The sizes of male, female and undetermined (sex unknown) medusae are consistently larger in the fjord samples than the oceanic samples (Figure 5.6). Within the fjords, the size of males is slightly greater than females (mean = 109 mm for males, 104 mm diameter for females). A more pronounced variation is apparent within the oceanic population, which had larger females

than males (mean = 66 mm for females, 26 mm for males). The relatively large numbers of undetermined specimens reflect the presence of smaller immature individuals with straight or early J-shaped gonads, as described by Russell (1970).

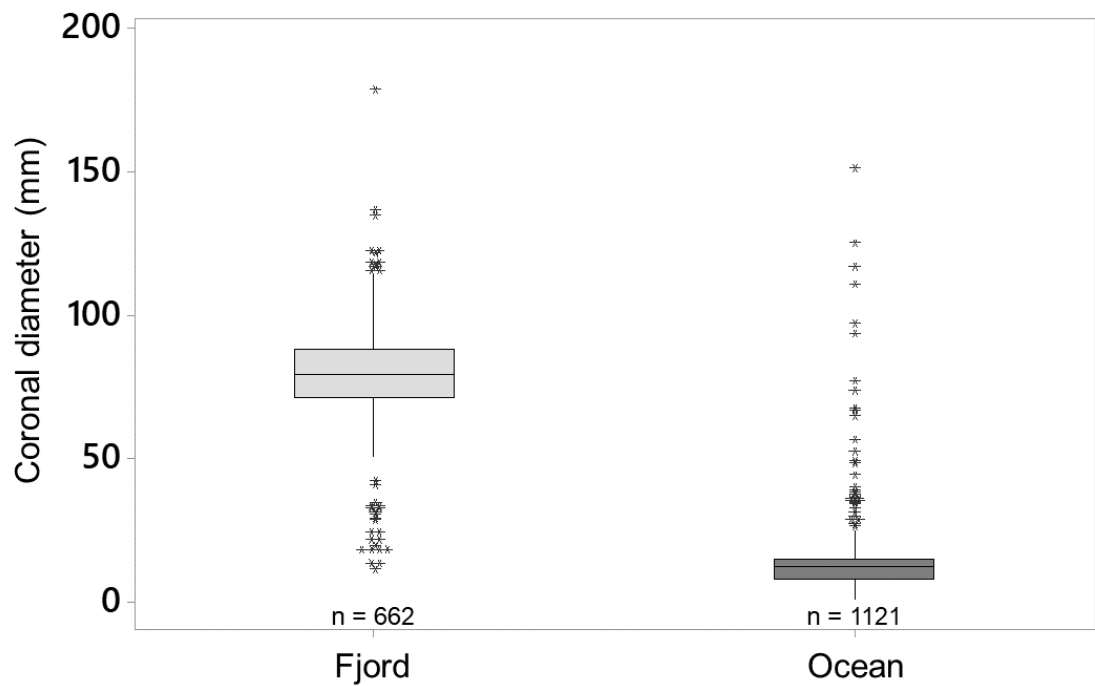


Figure 5.5 Mean coronal diameters of *P. periphylla* medusae in fjord and ocean sample areas. Boxplots depicting interquartile range and outliers of the observed coronal diameters within each area.

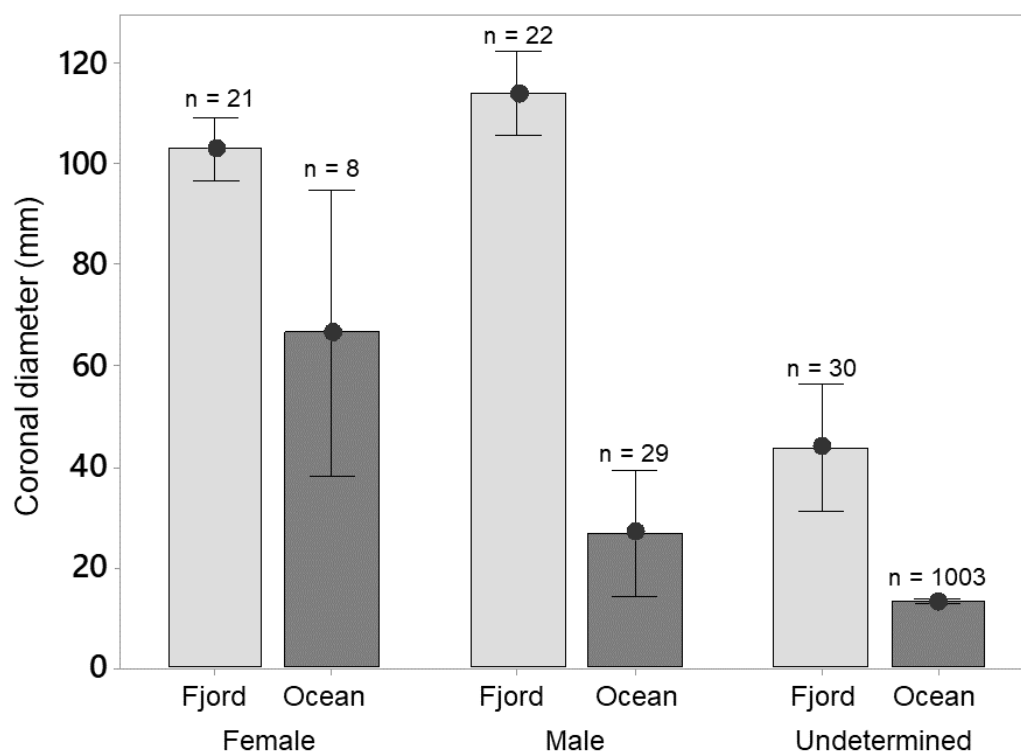


Figure 5.6 Mean coronal diameters of male, female and undetermined specimens from the oceanic (lighter bars) and fjord (darker bars) sample areas. Bars represent two standard errors.

There is a more pronounced seasonal variation in medusa size for the fjord samples than the oceanic sample group Figure 5.7, with significant differences between summer and winter medusa sizes (one-way ANOVA with Tukey's, $F = 19.16$, $p < 0.001$).

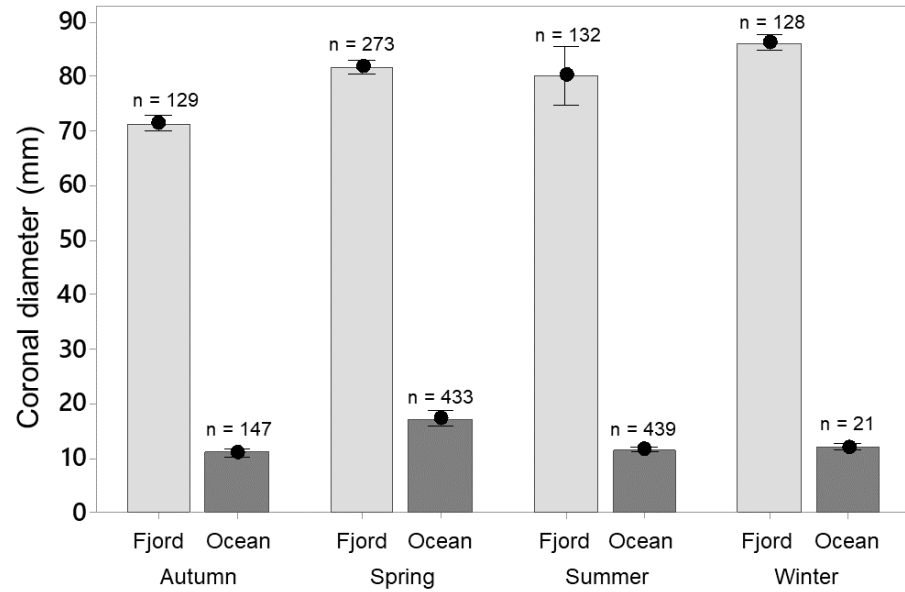


Figure 5.7 Variation in *P. periphylla* body size according to sample season within the fjord and oceanic study areas. Bars represent two standard errors.

Due to the lack of available histological data, gonad length was used as an indicator of maturity. The regression analysis of body size and gonad length revealed a much steeper slope for the oceanic population (Figure 5.8a). The oceanic samples are thus characterised by an overall greater gonad length to body size ratio. The oceanic data exhibit a broad spread of gonad lengths relative to the range of coronal diameters and in the upper range these lengths exceeded those measured in fjord material. No significant difference was observed between gonad length of oceanic (mean = 8.4 mm, SD = 6.9, $n = 11$) and fjord populations (mean = 8 mm, SD = 2.3, $n = 25$) (one-way ANOVA, $F = 0.07$, $p = 0.79$).

The relationship between coronal diameter and tentacle length was similar for oceanic and fjord populations (Figure 5.8b), with no observed significant difference in this relationship between the two areas (Pearson correlation, $r = 0.02$, $p > 0.05$). Observed tentacle lengths were typically greater in fjord specimens due to their larger overall size (fjord mean = 179 mm, SD = 84.1, $n = 36$; oceanic mean = 41 mm, SD = 30.8, $n = 74$). Tentacle length was unavailable for a number of oceanic specimens due to evident damage as a result of trawling or preservation.

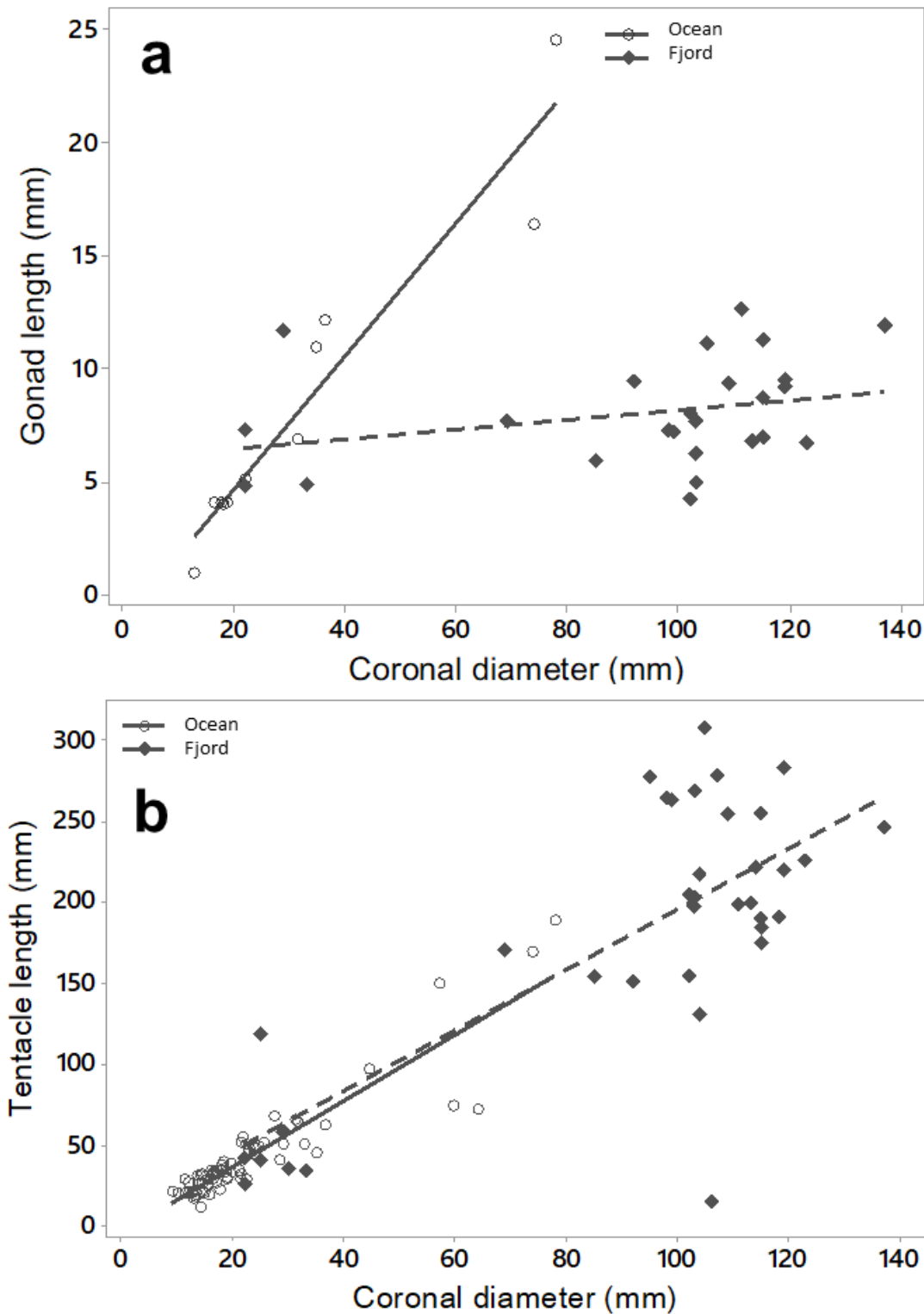


Figure 5.8 Relationship between *P. periphylla* medusa size and gonad length and tentacle length for fjord and oceanic samples within the study. **a:** Regression equations: Oceanic $y = -1.214 + 0.2946 x$, $r^2 = 91.7\%$, $F = 98.97$, $p < 0.001$, $n = 9$; Fjord regression equation: $y = 6.069 + 0.02117 x$, $r^2 = 8.5\%$, $F = 0.33$, $p > 0.05$, $n = 25$. **b:** Regression equations: Oceanic regression equation, $y = -4.052 + 2.036 x$, $r^2 = 83.7\%$, $F = 370.5$, $p < 0.01$, $n = 76$; Fjord $y = 8.87 + 1.86 x$, $r^2 = 57.5\%$, $F = 35.4$, $p < 0.01$, $n = 36$.

5.5 Discussion

5.5.1 Sizes of individuals in oceanic and fjord populations

The fjord population of *P. periphylla* was comprised of larger individuals than those from an oceanic environment at a similar latitude. This relationship applied across all seasons and was characteristic of both sexes. This finding is in agreement with previous studies which noted larger sizes of *P. periphylla* medusa within Norwegian fjords relative to oceanic populations (Youngbluth and Båmstedt, 2001; Lucas and Reed, 2010), but this is the first study to make a direct comparison across seasons. The results support the suggestion by Thuesen et al. (2005) that hypoxic conditions within Norwegian fjords do not limit the size of *P. periphylla*. It should nevertheless be appreciated that oceanic *P. periphylla* may also grow to relatively large sizes. For example, Larsen & Harbison (1990) noted specimens in the Southern Ocean with coronal diameters that exceeded those measured in this study (up to 350 mm in coronal diameter).

A number of factors might explain the size disparity between fjord and oceanic populations of *P. periphylla*, including variation in food availability, reproduction, age or shrinkage. For example, Lurefjorden may be a more stable environment offering more constant conditions. Stable conditions and/or greater food availability may promote longevity and hence growth to larger size. Such conditions may also minimise shrinkage. On the other hand, the size profiles could simply reflect greater reproduction in oceanic populations with consistently larger recruitment of young medusae throughout the year. The greater apparent investment in sexual reproduction of oceanic individuals (exemplified by relatively greater gonad length to coronal diameters) may provide support for this latter scenario. A further scenario relates to competition with high densities in fjords diminishing investment in sexual reproduction in these population and hence perhaps more energy is allocated to somatic growth.

It seems most likely that oceanic individuals in general do not reach the same consistently large sizes as those within fjords due to periodic shrinkage during extreme conditions over time (e.g. food shortage (for example see Hopf and Kingsford, 2013)). A complex population structure may thus characterise oceanic samples. The relatively high ratio of gonad length to coronal diameter for specimens from the oceanic sample site may provide evidence for this scenario (i.e. if oceanic individuals diminish in diameter but retain gonad dimensions

typical of larger individuals). However, the relationship is based on few data points and potential impacts of outliers.

A final scenario explaining size disparity is shrinkage of formalin-preserved oceanic material. Formalin-induced shrinkage of tissue has been documented previously, with medusae shrinking from 9.1% to 84.9% of their initial size after approximately 100 days in preservation fluid (Lucas 2009; De Lafontaine 1989) respectively). Shrinkage is documented as greater in larger medusae (Moller 1980).

5.5.2 Other life history comparisons and differences between oceanic and fjord populations

The regressions of tentacle length and coronal diameter do not discriminate between fjord and oceanic material and revealed a strong linear relationship for the two traits. This provides evidence of the importance of maintaining isometry for e.g. prey capture across the range of body size regardless of environment.

Jarms et al. (1999) suggested that large Norwegian specimens of *P. periphylla* may be over 30 years old, although age and size relationships of *P. periphylla* at present remain obscure. Chapter 6 discusses the development of sclerochronology for *P. periphylla* that would enable age to be inferred on the basis of statolith secretions and not body size.

It has been suggested that cryptic species of *P. periphylla* may be present in different regions (Jarms et al., 2002), and it is possible that cryptic speciation might occur as a result of retention within fjord environments. The possibility that fjord and oceanic populations represent cryptic species would best be resolved by genetic analysis and pilot studies were undertaken to determine feasibility. Unfortunately none of the methods trialled were successful in extracting DNA from the formalin-fixed material – a notoriously difficult problem that is widely recognised (Palero et al., 2010; Bucklin, Steinke and Blanco-Bercial, 2011; Campos and Gilbert, 2012). The similar regressions of tentacle length and coronal diameter do not discriminate between fjord and oceanic material and hence provide no evidence for cryptic species. However, the opposite trends in body size according to sex between fjord and oceanic populations could be consistent with cryptic speciation with males being relatively larger in fjord environments. This observation suggests that genetic studies and further sampling of sexes in the two environments are warranted.

5.5.3 Conclusions

As is clear, there are many factors that might contribute to variation in size in the oceanic and fjord samples. Post-fixation shrinkage is very likely to have generally reduced the size of the oceanic material as this was all formalin-fixed. However, other data suggest this may not have acted in isolation in explaining size disparity. The smaller mean sizes of the oceanic populations are likely also to be explained by the higher proportion of immature and hence small individuals. Environmentally-induced shrinkage (e.g. poor ecological conditions) requires further study but is hinted at by the different regression profiles for gonad length vs. coronal diameter. The possibility that favourable fjord conditions promote growth and avoid shrinkage requires further investigation. Other issues requiring further investigation are sex ratios, cryptic speciation and aging. I return to the latter in the next chapter.

- The sampling of fresh *P. periphylla* specimens from Lurefjorden, Norway allowed for the first fully documented comparison between oceanic and fjord populations
- The sizes of *P. periphylla* medusae within the fjord were consistently larger than oceanic medusae, across all sampled seasons (fjord mean = 80.3 mm, oceanic mean = 13.9 mm) (data supports the hypothesis).
- The length of gonads, used as an indication of maturity, was larger within smaller sizes of oceanic medusae, indicating the prioritisation of reproductive outputs over size within variable oceanic conditions.

Chapter 6: Sclerochronology of *Periphylla periphylla* statoliths

6.1 Abstract

Jellyfish, as a significant component of the zooplankton, form important and often conspicuous components of the marine ecosystem. However, they still remain poorly understood, particularly outside of epipelagic, coastal environments where apparent ‘bloom populations’ tend to occur. The ability to age organisms is fundamental to understanding the demographics of populations, and for providing a temporal context for ecological processes. Lack of adequate ageing techniques has so far limited the scope for jellyfish research. This report discusses the development of determining age in jellyfish medusae, specifically within the cnidarian classes Cubozoa and Scyphozoa. Currently, classifying the age of cubomedusae is a well-documented and established process, perhaps as a result of the structural similarities of the focal tissue with fish otoliths for sclerochronological research. Scyphozoan ageing, however, is still in the developmental stages, despite being a more cosmopolitan class. Statocysts were dissected from a number of *Periphylla periphylla* medusae, and statoliths liberated by trialling a number of novel methods (proteinase K, pancreatin, bleach and manually using needles). Manually extracting the statoliths using fine needles was found to be the most effective and pragmatic approach. Numbers of statoliths, as well as size and morphology were observed to vary across a range of *P. periphylla* body sizes. The statoliths were imaged and analysed using a range of novel scanning electron microscope (SEM) and computed tomography (CT) methods. This study has produced body size:statolith relationships, which if combined with specimens reared in a laboratory to provide a benchmark for age would significantly further the understanding of the age and longevity of medusae overall, particularly for the long-lived coronates.

6.2 Introduction

Investigations on *P. periphylla* within fjords such as Lurefjorden, Halsafjorden, and Sognefjorden have enhanced our understanding of the biology of deep-sea jellyfish and gelatinous zooplankton in general, as a result of increased sampling ease within fjord

environments. Nevertheless, substantial knowledge gaps persist including determining the age of individual medusae (Tiemann, Sötje and Jarms, 2002; Hopf and Kingsford, 2013). Determining age in jellyfish is relevant for understanding the development and persistence of shallow-water bloom-forming populations and for contextualising ecological processes in time. Sclerochronology is the study of physical and chemical variations in the accretionary hard tissues of organisms, and the temporal context in which they were formed (Buddemeier and Taylor, 1978).

Gelatinous fauna by definition have very few hard structures incorporated in their soft bodies. However, medusae house small calcium concretions, called statoliths, within their marginal sense organs (Chapman, 1985). In Cubozoa and Scyphozoa, these statoliths are composed of calcium sulphate hemihydrate, or bassanite ($\text{CaSO}_4 \cdot 0.5\text{H}_2\text{O}$) (Tiemann et al., 2002; Becker et al., 2005). The function of statoliths is to determine the position of the jellyfish within the water column. This information is gained because statoliths brush against cilia lining the inside the rhopalial bulb that houses the statoliths, called the statocyst, according to gravity (Spangenberg and Jernigan, 1994; Arai, 1997; Winans and Purcell, 2010). Statoliths are formed during strobilation and can be used to generate a timeline of the medusa life cycle (Spangenberg, 1968; Becker et al., 2005). Unlike the Cubozoa and Scyphozoa, the statoliths of Hydrozoa are composed of calcium magnesium phosphate ($\text{CaMg}[\text{PO}_4]_2$) which is suggested to be representative of their different development origin (see Chapman 1985, Tiemann et al., 2006).

Currently, the sclerochronology of Cubozoa is well documented. Box jellyfish accrete layers on a single statolith over time, much in the way that otoliths develop and grow in vertebrates (Campana and Neilson, 1985; Natsukari and Komine, 1992). One layer of the statolith can be approximated to one day (Ueno et al., 1995) with the expected life span to be up to approximately one year. The study of statoliths with the Cubozoa has furthered the understanding of the evolution of the group (Kawamura et al., 2003; Tiemann et al., 2006; Gordon and Seymour, 2012; Gershwin et al., 2013). Scyphozoans, however, house numerous statoliths within the rhopalial statocyst bulb, and how they are produced remains poorly understood. Statolith structure was proposed to enable differentiation between genera (Holst et al., 2007, Gershwin et al., 2013). Holst et al. (2017) reported that statoliths of *Rhizostoma octopus* increased in size and number from ephyra to medusa.

While bell diameter has been the traditional proxy for scyphozoan age, it has now been deemed to be too inaccurate due to the ability of jellyfish to shrink and regrow depending on temperature, salinity or food availability (Lucas, 2001; Lilley et al., 2014; Goldstein and Riisgard, 2016). Hopf and Kingsford (2013) produced the first study to use statolith numbers as a proxy for age in *Cassiopea* sp. and identified that for medusae over 65 days old, the size as well as number of liths may be significant in determining age. Sötje et al. (2011) used calcein as a fluorescent marker to identify the growth of bassanite statoliths in *Aurelia aurita*, confirming the previous prediction of Hopf and Kingsford that the statoliths are produced at regular temporal increments (2013). The composition of *P. periphylla* statoliths has been used to determine evolutionary relationships within Cnidaria (Tiemann et al., 2002; Sötje et al., 2011). However, the statoliths of *P. periphylla* are yet to be considered for their sclerochronological potential. This study addresses this knowledge gap and uses a range of different techniques to investigate whether statoliths may be used for aging *P. periphylla* whose life span has predicted to be some 30 years based on observations of various cohorts within Lurefjorden (Båmstedt et al. unpublished data, see Jarms et al., 1999; Youngbluth & Båmstedt 2001). Contextualising ecological processes in time may then enable better insights on the structure and demography of fjord and oceanic populations.

6.2.1 Aims and Objectives

This study aims to further the knowledge of sclerochronology within Scyphozoa using statoliths as a proxy for age, and to establish general morphological comparisons between oceanic and fjord populations of *P. periphylla*. The objective of this study is to document the numbers and sizes of statoliths of *P. periphylla* using morphological techniques on both preserved and fresh specimens. The conceptual hypothesis for this study is that individuals of *P. periphylla* exhibits distinct differences amongst its sense organ characteristics, which is indicative of different age groups within the dataset.

6.3 Materials and methods

6.3.1 Study samples

The *P. periphylla* samples examined here were collected from Lurefjorden, Norway in August 2015. For further details on the fieldwork and associated sample methods, see Chapter 5. A total of 76 *P. periphylla* specimens were collected within Lurefjorden from a maximum depth of 440 m. The coronal diameter of each specimen was recorded. Two marginal sense organs taken from each specimen and fixed in 100% ethanol to retain the structure of the bassanite crystals within the rhopalial tissue. A number of methods were trialled in order to determine the optimal approach to quantify statolith numbers and sizes. Two sense organs from the same individual were used in some instances. For a full list of the *P. periphylla* specimens used within this study ($n = 83$), see Appendix (Table 5). During this study, efforts were made to obtain some recently hatched juvenile medusae in order to rear a batch and cull individuals after a number of specified intervals (Bozman, 2015, personal communication). This would have allowed the number of statoliths to be directly traceable to the known age of the individual medusae, and for the relationship between known age, coronal diameter and statolith number to be mapped. However, it was not possible to obtain such live specimens and as such was not investigated within this study.

6.3.2 Liberation of statoliths and preparation of statoliths for scanning electron microscopy

Statoliths within the preserved tissue samples were found to be completely degraded due to the absence of sodium glycerophosphate in the formalin preservation fluid, which retains the structural integrity of the concretions (see Petersen 1976 for discussion). The rhopalial tissue was therefore examined exclusively using the fresh fjord specimens. A range of methods were trialled to liberate statoliths from the statocyst rhopalial bulb (Table 6.1). These methods were tested because the bassanite comprising the statoliths rehydrates to gypsum and degrades when exposed to moisture (Becker et al., 2005).

For scanning electron microscopy, statoliths were extracted from the statocyst by transferring from 100% to 50% ethanol in 10% stages in order to soften the statocyst tissue. Statocysts were washed and transferred immediately into each subsequent concentration

to mitigate degradation of statoliths. The statocyst was then transferred onto a microscope slide with a concave well, and liths were liberated from the tissue using fine needles under a light microscope. Liths were then pipetted onto a cover slip and left to dry. Exploratory images of statolith structures were obtained using back scatter detection on a LEO 1455 VP scanning electron microscope (SEM), (chamber 20 Pa, EHT = 20.00, Spot size = 550) (Figure 6.1). Automated scans of entire stubs to capture all liberated statoliths were performed using backscatter detection on a FEI Quanta 650 FEG SEM in high vacuum mode. MAPS software was used for tiling and stitching together the high resolution images together. Cell Counter and ROI Manager tools in ImageJ were used to count and produce measurements of statoliths. Linear regression was conducted to examine whether statolith numbers and lengths were correlated with the size of medusae.

Table 6.1 Methods trialled to isolate statoliths from statocyst tissue (preserved in 100% ethanol) for SEM analysis.

Trialled method	N samples	Description
Critical Point Drying (CPD)	2	This method was trialled to dehydrate the rhopalial tissue surrounding the statoliths. Samples were transferred from 100% ethanol into drying baskets within the CPD, and dried using 100% CO ₂ at graduated intervals. Statocysts were then mounted on carbon SEM stubs (no coating). This method kept the statolith concretions intact but loosely housed within the rhopalial tissue so concretions could not be quantified.
Weak bleach	5	Statocyst tissue was dissolved in a weak bleach and deionised water solution (15%) and left overnight. Samples were pipetted onto an SEM cover slip and left to dry, and then coated with a gold-palladium sputter coat. This method resulted in the degradation of the statoliths.
Pancreatin	2	A 10 mg/ml dissolution of pancreatin grade enzyme complex (as described in Hormiga et al. 2008) was used to dissolve the statocyst, and was left overnight to expose the statoliths. Examination under a light microscope revealed total degradation of liths and so was not transferred to SEM stubs for subsequent microscopy.
Proteinase K	2	Samples were washed in TE buffer and transferred into Proteinase K at room temperature for 2 days, then incubated at 55°C for 1.5 hours. Using this method, statoliths completely degraded and as such were not imaged using the SEM.

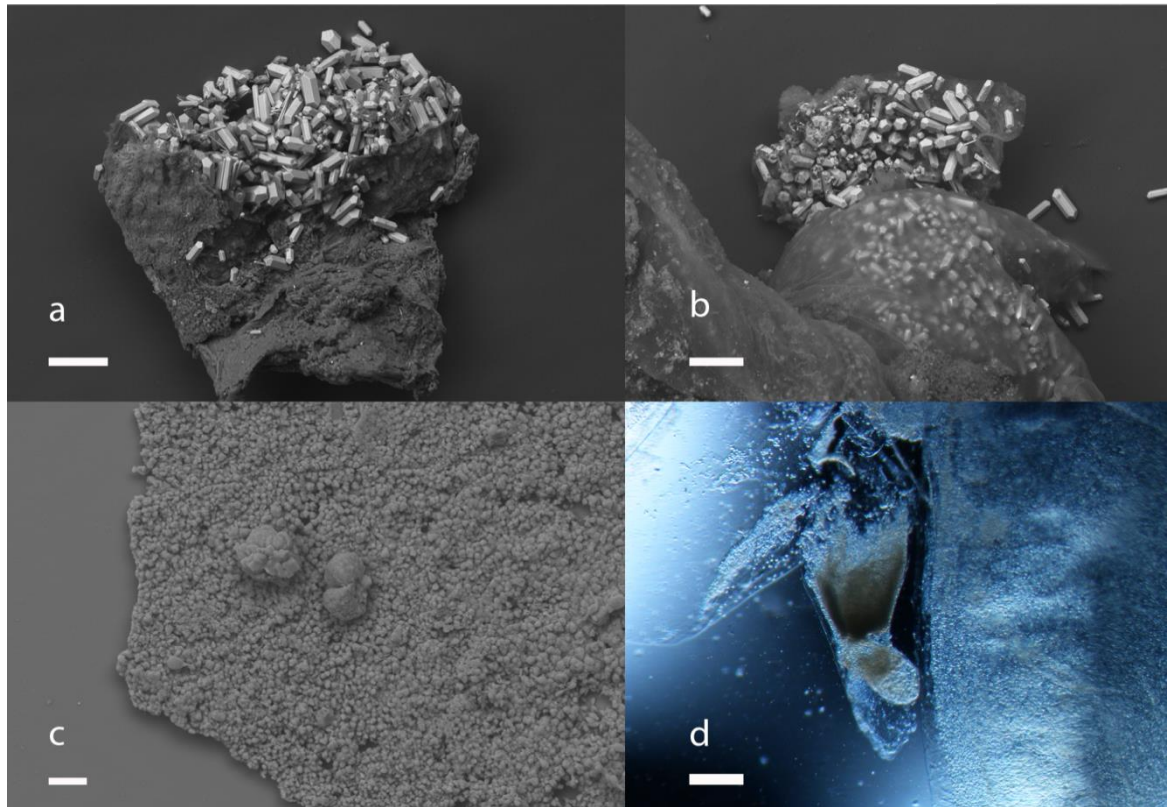


Figure 6.1 Scanning electron and light micrographs depicting methods trialled to liberate statoliths. **a + b:** Scanning electron micrographs of critical point dried specimens, with statoliths seen spilling out of the thin dried rhopalial tissue. Scale bars = 100 μm . **c:** Scanning electron micrograph of statocyst tissue dissolved in weak bleach and mounted on SEM stub, illustrating the degradation of the liths. Scale bar = 20 μm . **d:** Light micrograph of rhopalial bulb from formalin-fixed tissue. Here the statocyst bulb and hood remain intact, but the statoliths are completely dissolved as a result of the lack of glycerophosphate buffer within the preservation fluid. Scale bar = 1 mm.

6.3.3 Preparation of statoliths for micro-computed tomography

To complement the analysis of statoliths liberated destructively from the rhopalial cyst and captured using SEM, a non-destructive method was trialled to produce a 3D visualisation of the statoliths within the cyst. A test scan was performed using formalin-fixed material, confirming the complete degradation of the bassanite concretions. Six samples were selected for micro-CT. This number was determined by sample availability and equipment scan time constraints. Four statocyst bulbs were prepared using London Resin (LR) white medium, as described in Holst et al. (2016). Statocysts were transferred to increasing ethanol:LR white concentrations as follows: 2:1 EtOH:LR white (2 hours); 1:1 EtOH:LR white (2 hours); 1:2 EtOH:LR white; 100% LR white (overnight to embed). Two samples were then transferred to gelatin capsules filled with LR white and sealed, and two samples were transferred into half a gelatin capsule filled with LR white and covered with a 2 mm square

of dental wax (Figure 6.2). Bowling et al. (2008) suggest this to be a more efficient way of polymerising the LR white, as the hardening occurs in a bottom-up direction. Samples were then left to polymerise in an oven for 24 hours at 55°C. A further 2 samples were transferred from ethanol into a low-density tube containing glycerol immediately before scanning to mitigate bassanite degradation. Glycerol was trialled in order to determine whether glycerol is a sufficiently viscous medium for scanning as the sample is rotated in the chamber. All samples were scanned within Pasteur pipette tubes that maintained the samples in an upright position in a Zeiss Xradia 520 Versa 3D X-ray microscope (source setting 50kV 80µA, 4.03 optical magnification, 10 sec exposure time, LE2 source filter). ImageJ 3D Viewer was used to stack the sliced scan data for visualisation. The Classic Watershed plugin tool was used to set threshold limits to isolate each statolith within the cyst and compute their volumes. Morphometric data were then exported into Excel for analysis.

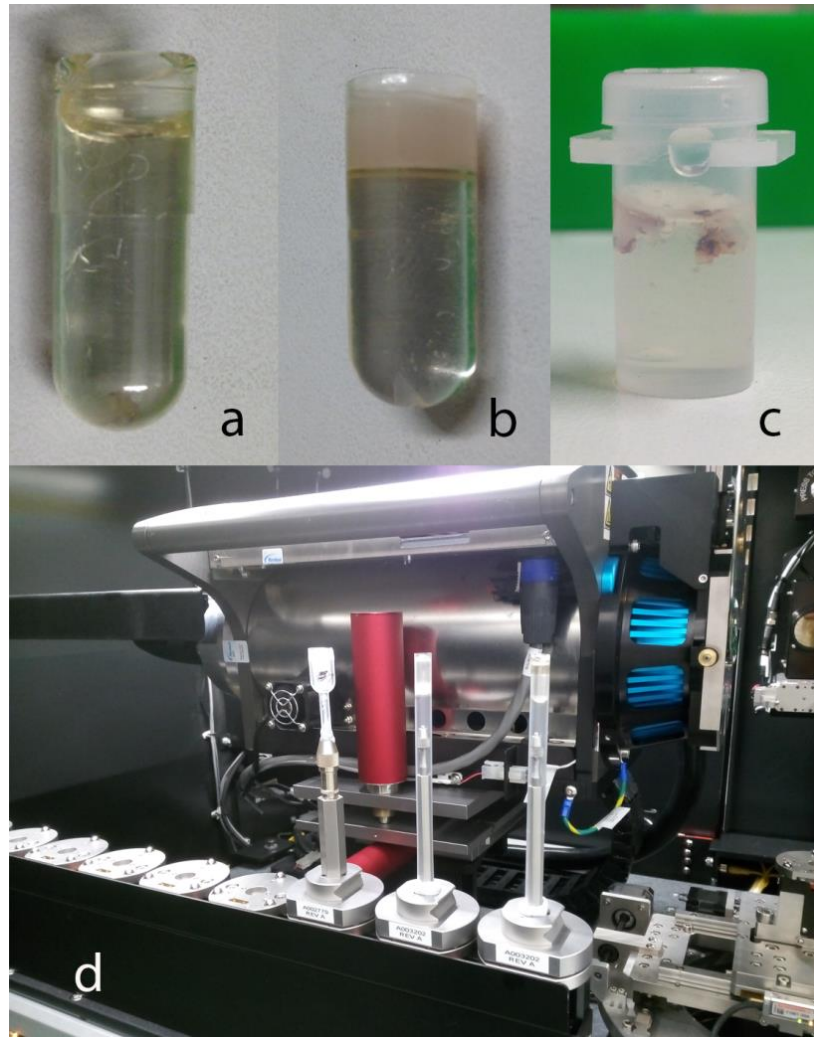


Figure 6.2 Samples prepared for micro-computed tomography for 3D visualisation of statoliths. a: Statocyst embedded in polymerised LR white in sealed gelatin capsule. b: Statocyst embedded in polymerised LR white in gelatin capsule and sealed with dental wax. c: Statocysts in low density tube containing glycerol. d: Samples loaded into X-ray chamber and held in place with Pasteur pipettes for scanning.

6.4 Results

6.4.1 Initial observations on *P. periphylla* statolith structures

As described in previous studies on scyphozoans (Tiemann, Sötje and Jarms, 2002; Becker et al., 2005), the statolith structures of *P. periphylla* exhibit a trigonal crystalline shape, composed of calcium sulphate hemihydrate (bassanite) (Figure 6.3).

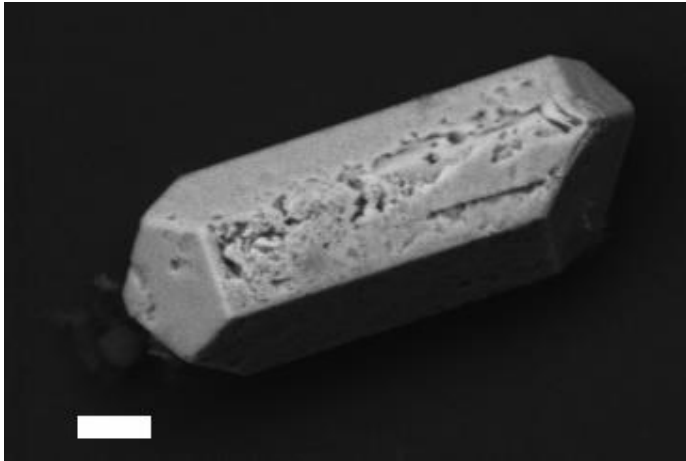


Figure 6.3 Scanning electron micrograph of a single *P. periphylla* bassanite crystal, depicting its trigonal structure. Scale bar = 10 μm .

Various methods of extracting the statoliths were trialled in order to determine the most effective way of liberating the intact statoliths from the rhopalial bulb. Methods using bleach, pancreatin and proteinase-K dissolved the crystals (Figure 6.1c). Critical point drying produced effective structural detail of the statoliths, however the presence of dried tissue made it difficult to visualise and quantify all liths following drying.

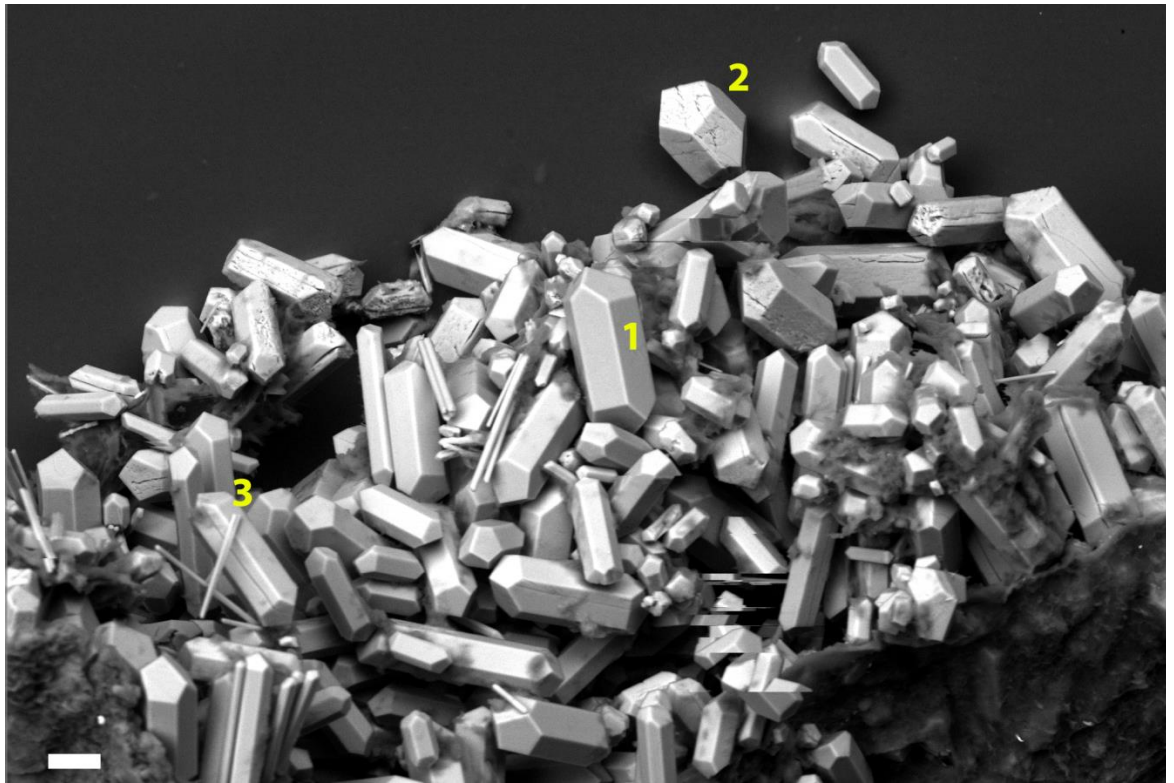


Figure 6.4 Scanning electron micrograph of statoliths retained within a critically point dried statocyst bulb, illustrating the various crystal formations (1,2,3). Scale bar = 20 μm . (Note: slight distortion of image during scanning).

The scanning electron micrographs provided an insight into the structure of the statolith crystals (Figure 6.3). Statoliths of *P. periphylla* ranged in size and shape, but maintained their trigonal structure (Figure 6.4). The shapes included three crystalline forms documented previously (a standard trigonal shape (number 1 in image), followed by short and squat (2) and long and thin variants (3)) (Becker et al., 2005; Tiemann et al., 2006b; Hopf and Kingsford, 2013).

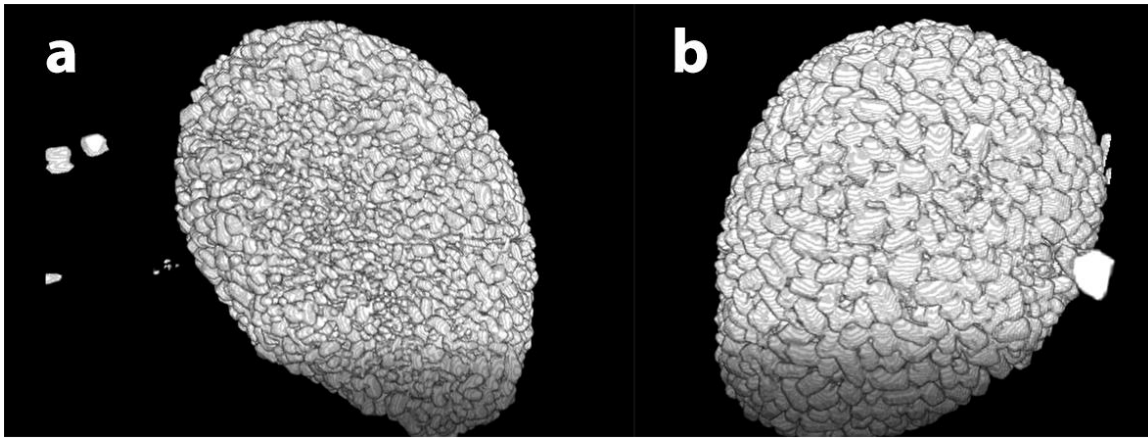


Figure 6.5 Computed tomography image of statoliths housed within intact statocyst bulb (rhopalial tissue was not stained and so is not detectable in the micro-CT chamber). The distribution of statoliths within the cyst is visible, with smaller crystals located at the origin of the rhopalial bulb (a), and larger crystals migrating towards the opposite edge of the statocyst (b).

Computed tomography was used to investigate the microstructure of statoliths housed within the intact statocyst. Two sample preparation media were trialled; LR White and glycerol. The LR White produced a negative result whereas the glycerol produced a strong signal within the micro-CT chamber. Based on the results of the scan data, it is clear that the smaller crystals are present at the origin of the statocyst bulb (Figure 6.5a), and that larger crystals migrate to the anterior end of the statocyst bulb (Figure 6.5b), presumably indicating that the statoliths accrete over time as previously suggested in Prymak et al. (2005).

6.4.2 *P. periphylla* statolith analysis

Scanning electron micrograph images between 1 -1.3 $\mu\text{m}/\text{pixel}$ resolution were stitched together to produce an overall view of the statoliths per stub, with each stub representing an emptied statocyst. The most effective method of retaining the structure of the bassanite crystals was by manually extracting the crystals from the surrounding tissue with needles. Complete statoliths were then quantified in terms of lengths and numbers using ImageJ for 72 specimens (Figure 6.6).

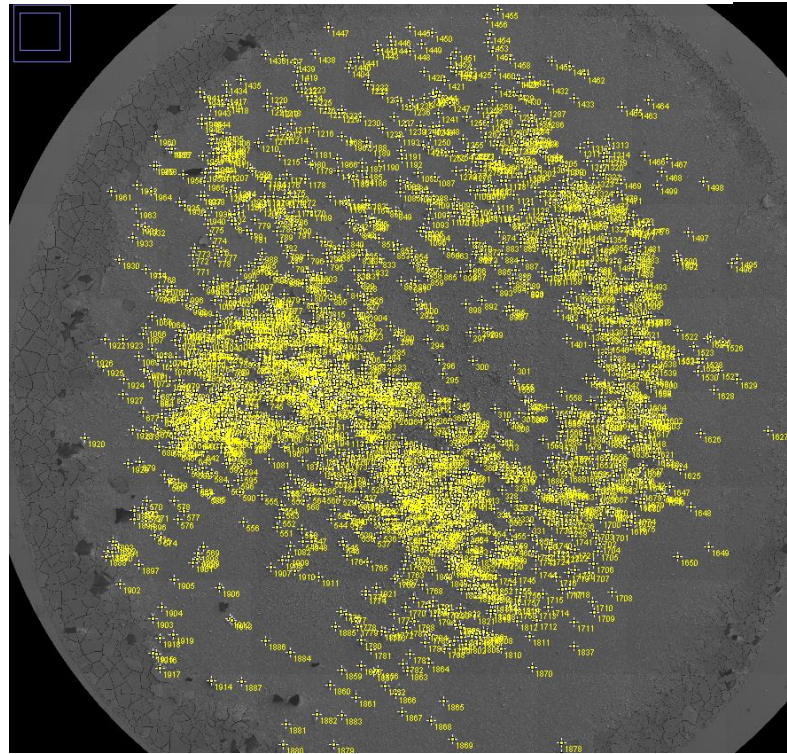


Figure 6.6 Labelled statoliths on SEM stub using ImageJ Particle Counter.

Regression analysis of the data indicates a slight increase in the number of statoliths with coronal diameter of the medusa ($r^2 = 8.9\%$, Figure 6.7d), with no trend observed between coronal diameter and mean statocyst length ($r^2 = 0.0\%$, Figure 6.7b) when taking into account all lengths. However, there is a slight positive trend when plotting the maximum statolith length against coronal diameter ($r^2 = 2.5\%$, Figure 6.7a). Two distinct groups are observed when comparing the relationship between statolith length and width (Figure 6.7c), which was observed in initial observations of the scan data (Figure 6.4). Based on the 3 clear crystal structures within the dataset, it is likely that a third distinct group is present amongst the noisy data.

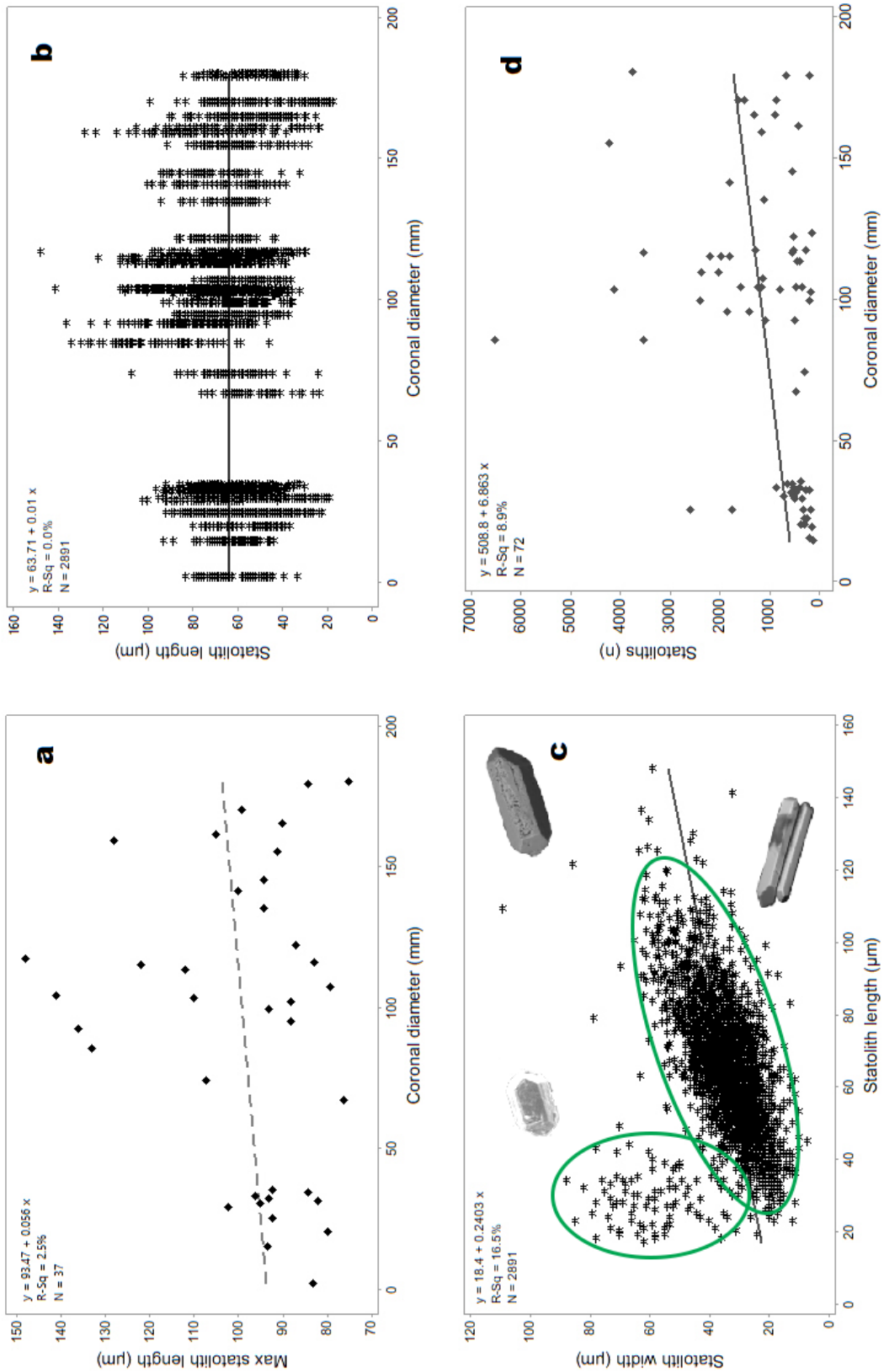


Figure 6.7 Regression analysis of statolith composition from scanning electron data. a: max statolith length against coronal diameter; b: total statolith lengths against coronal diameter; c: statolith length against statolith width; d: number of statoliths against coronal diameter.

Table 6.2 General linear model results describing changes in statolith numbers and morphometrics as a function of changes in the coronal diameter.

<i>Response</i>	<i>r</i> ²	<i>t</i>	<i>F</i>	<i>p</i>
Statolith n	79.56	106.00	322.46	< 0.001
Statolith length (μm)	27.82	207.00	32.83	< 0.001
Statolith width (μm)	21.66	174.5	22.55	< 0.001

Variation in coronal diameter is significantly associated with statolith number, statolith length, and statolith width ($r^2 = 79.56\%$, $F = 322.46$, $p < 0.01$, Table 6.2), which is expected following the initial assessment of the small and large crystals within the statocyst bulb.

6.4.3 Statocyst computed tomography

Following Watershed analysis in ImageJ 3D Viewer, the micro-CT statolith data was labelled to isolate each statolith housed within the statocyst. From this, individual volumes were calculated. The crystals were tightly packed within the rhopalial bulb, with a degree of overlap which restricted the clarity of the watershed analysis and the scan data therefore do not exhibit the trigonal crystalline structure (Figure 6.9).

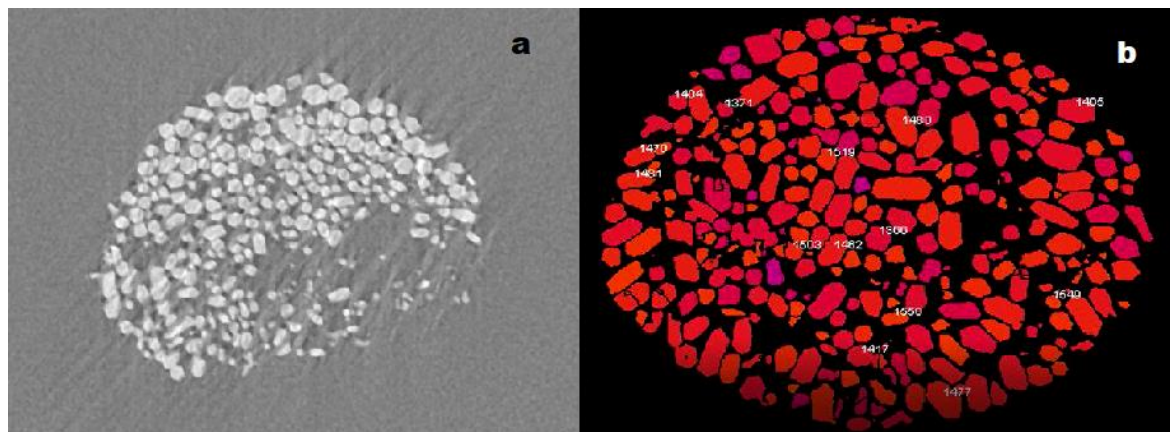


Figure 6.9 Micro-CT slices of statocyst containing statolith crystals. a: raw micro-CT data; b: Labelled and quantified statoliths following Watershed analysis, with loss of trigonal definition due to crystal overlap.

The frequency histogram of statolith volumes indicates a normal distribution, reflecting the range of statolith volumes associated with the various crystal morphologies observed using

the SEM. Although there was overlap between the crystals which had an impact on the efficacy of statolith morphometric analyses, the number of statoliths identified ($n = 3331$, Figure 6.10) is in line with statolith quantities of a similar size *P. periphylla* specimen (coronal diameter = 96 mm) in the SEM sample dataset (Figure 6.7d).

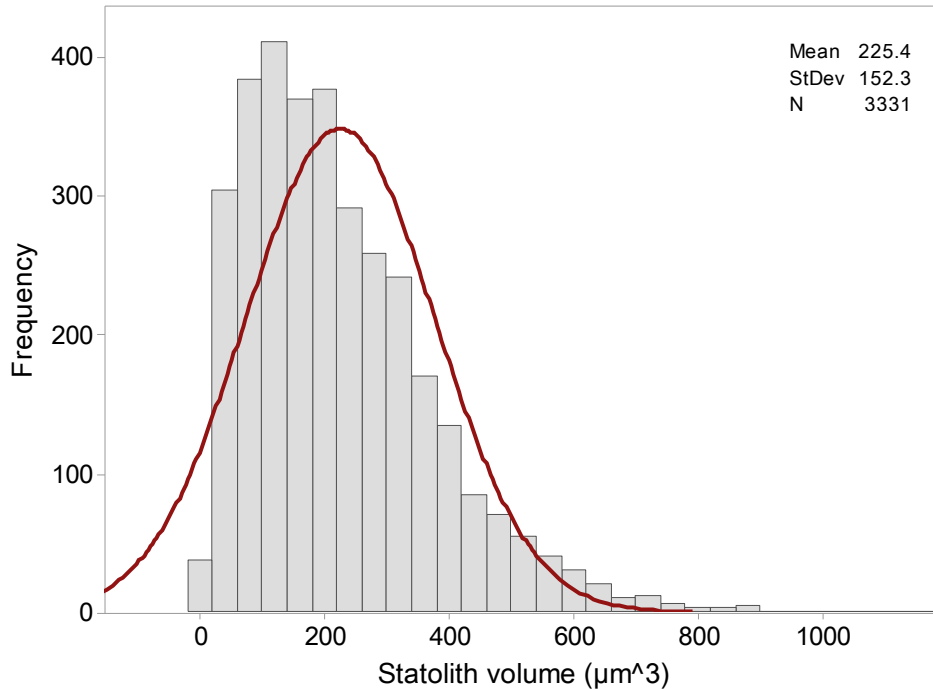


Figure 6.10 Frequency histogram of statolith volumes within scanned statocyst bulb. Coronal diameter of medusa = 96 mm.

6.5 Discussion

6.5.1 Statoliths of deep-sea medusae and elucidating age

An aim of this study was to further the basic understanding of deep-sea jellyfish by investigating the sclerochronology of their only hard structures, statoliths. Båmstedt et al. (unpublished data, see Jarms et al., 1999) proposed that *P. periphylla* could live up to 30 years, however this has yet to be demonstrated. Two imaging methods were used in this study to investigate whether statoliths vary within the statocyst; their number according to the size of the medusa; and whether the crystals accrete over time. Both methods provided useful insights. Scanning electron microscopy and subsequent regression analyses provided an indication that statolith numbers and maximum lengths increase with medusa size, although the trends were not significant. However, regression modelling indicated that

coronal diameter explained a significant amount of variation in statolith numbers and sizes. It is possible that environmentally-induced shrinkage of jellyfish could complicate the relationship between statolith numbers and sizes and jellyfish age, thus resulting in the weak trends observed. Jellyfish are plastic organisms that can shrink and regrow. Further studies based on growth in a controlled laboratory over long periods are required to disentangle the relationship between jelly size and age and the numbers and sizes of statoliths. If such studies demonstrate a strong relationship then statolith numbers and dimensions could provide a much more robust measure of jellyfish age than that based on bell diameter (Hopf and Kingsford, 2013).

The micro-CT results demonstrate that smaller statoliths originate from the base of the rhopalial bulb (Figure 6.5). They then grow and migrate to the anterior end of the statocyst. This is a new finding for *P. periphylla*. Previously it was assumed that crystals were a set size due to their trigonal structure (Becker et al., 2005), although Prymak et al. (2005) recognised the potential of bassanite accretion. The drivers of variation in statolith crystal morphologies in *P. periphylla* remain unclear. Further micro-CT investigations examining size variation and positions of the statoliths within the statocysts of multiple specimens of different inferred ages, however the overlap of crystals will impair visualising fine details. A combination of micro-CT and SEM might therefore be most suitable for such studies.

Specimens of *Cassiopea* sp. of a known age were reared in order to develop insights on the numbers of statoliths present at regular intervals (Hopf and Kingsford, 2013). The study concluded that bell diameter was a more accurate indicator of age under constant laboratory conditions, however in varying conditions statolith number was a more robust indicator of age.

Attempts were made throughout this study to rear specimens of a known age, culling at regular intervals in order to obtain an age benchmark. It was not possible to locate and rear *P. periphylla* specimens within this study, however as noted above, it is something that could be attempted in future sclerochronological investigations. This, however, may prove to be challenging as *P. periphylla* is notoriously difficult to rear (Widmer, 2015) and has only been kept alive for a maximum for six weeks (Jarms et al., 1999).

6.5.2 Conclusions



Figure 6.11 Light micrograph of liberated statolith crystals from the statocyst bulb, with the trigonal structure visible.

This study investigated a number of methods to liberate and quantify the number and morphometrics of *P. periphylla* statoliths. The most effective method of liberating the statoliths was to manually extract the liths from fresh statoliths using fine needles (Figure 6.11). Statoliths in formalin-fixed material were found to be degraded. Micro-CT offers insights into the distribution of the statoliths within 3D space, something that has previously been investigated in Scyphozoa by Holst et al. (2016). The technique enables inferring how the statoliths first develop and then migrate and accrete. However, for future sclerochronological investigations, the constraints of micro-CT (crystal overlap) must be appreciated. Nevertheless, the technique could be suitable for gross 3D examination of growth and migration of statoliths within statocysts over time based on examination of material from specimens of known or inferred ages. SEM and subsequent imaging analysis proved to be most useful for quantifying statolith numbers and sizes. This study acts as a benchmark for future *P. periphylla* sclerochronological studies.

- A number of methods were trialled to liberate the statoliths from the statocyst bulb within *P. periphylla* medusae. The optimal method was found to be simply manually

bursting the bulb and extracting the liths using needles over more complicated and expensive methods.

- Coronal diameter maintains the strongest impact on the various statolith response variables. Although the specific age of medusae could not be validated without rearing specimens of a known age, this study highlights the variation in statolith morphology and number which are an indication of medusa age (data supports the hypothesis).
- This represents the first study to attempt to understand the most pragmatic approach of determining age amongst the presumed long-lived deep-sea coronates.

Chapter 7: Conclusions

7.1 The macroecology of globally-distributed deep-sea jellyfish

The investigation presented here is the most extensive study on the distributions of deep-sea coronate jellyfish over both spatial and temporal scales to date. A full depiction of sample locations and *in situ* observations for this and other studies on *Atolla* and *Periphylla* is given in Figure 7.1. Previous studies on *Atolla* and *Periphylla* used small sample sets from a number of isolated locations that served to answer specific questions relating to the ecology and biology of taxa in the poorly studied order Coronatae. Beyond the early works of Russell (1959; 1970), studies based on relatively small sample sizes of *Atolla* and *Periphylla* have furthered understanding of the life cycle of holopelagic jellyfish (Jarms et al., 1999; 2002); coronate trophic ecology and functional morphology (Sötje et al., 2007); the biochemical composition of coronates (Clark et al., 1992; Tiemann et al., 2002; Lucas, 2009); the habitat of mesopelagic scyphomedusae (Osborn et al., 2007); the diel vertical migration of gelatinous zooplankton (Roe, 1984; Riemann et al., 2006; Kaartvedt et al., 2007; Bozman et al., 2017); general coronate behaviour and ecology (Larson et al., 1991; Sötje et al., 2007; Sørnes et al., 2008); bioluminescent properties of jellyfish (Haddock and Case, 1999; Herring and Widder, 2004) parasitism in jellyfish (Child and Harbison, 1986) and coronate reproduction and gametogenesis (Lucas and Reed, 2010).

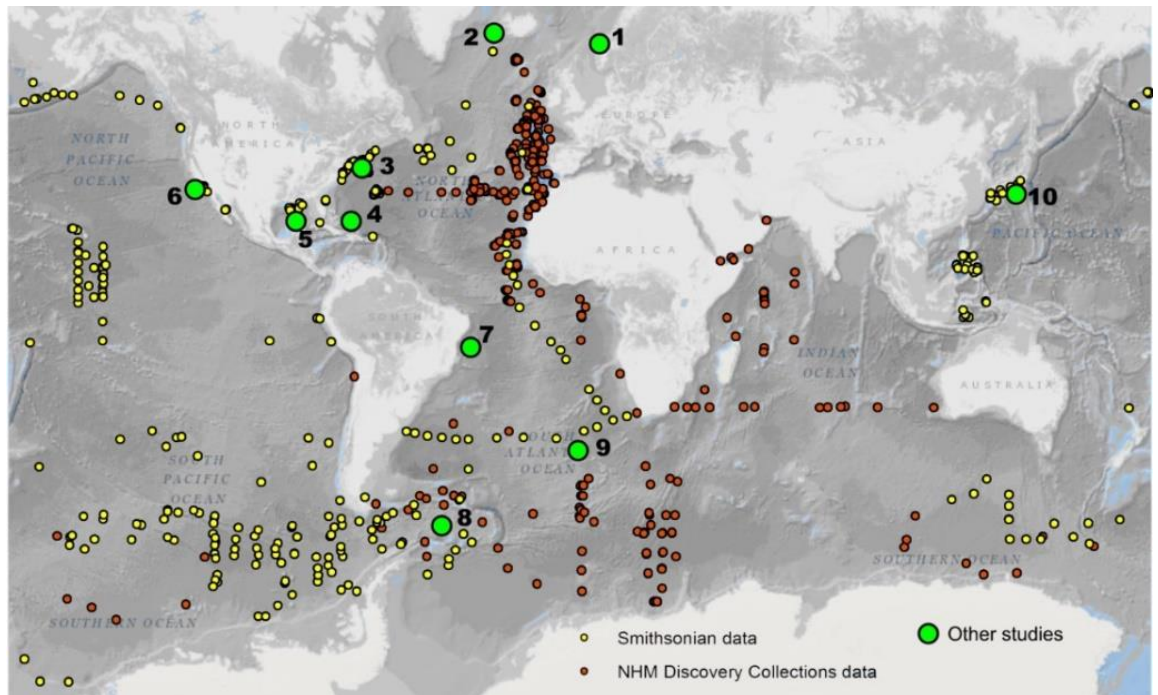


Figure 7.1 Map illustrating the global extent of this study. Red dots represent sample locations of *Atolla* and *Periphylla* from the NHM Discovery collections where morphometric and histological data was gathered; yellow dots represent sample locations of *Atolla* and *Periphylla* from the Smithsonian Collections which were used to confirm cosmopolitan distributions of the taxa; green circles represent other isolated studies as follows:

- 1 **Lurefjorden:** Fosså 1992; Jarms et al. 1999; 2002; Herring & Widder 2004; Kaartvedt et al. 2007; Sötje et al. 2007; Bozman et al. 2017 (and others).
- 2 **Rockall Trough:** Mauchline & Harvey 1983; Roe 1984.
- 3 **Cape Hatteras:** Lucas & Reed 2010.
- 4 **Bahamas:** Child & Harbison 1986; Larson et al. 1991; Haddock & Case 1999.
- 5 **Gulf of Mexico:** Lucas 2009; Lucas & Reed 2010.
- 6 **Monterey Bay:** Osborn et al. 2007.
- 7 **Brazilian coast:** Jarms, AC Morandini, et al. 2002.
- 8 **Scotia Sea:** Clarke et al. 1992; Pages et al. 1996.
- 9 **Southern Atlantic:** Mianzan & Cornelius 1999.
- 10 **Sagami Bay:** Hunt & Lindsay 1998.

The aims of this study were to investigate morphological and ecological plasticity amongst the two coronate taxa across global (Chapter 2), temporal (Chapter 3) and regional scales (Chapters 4 and 5). It also addressed the possibility of determining age in medusae using the accretion of hard tissues (Chapter 6) This was done by using understudied collections materials and field-collected fresh material from fjord environments. Collating a large volume of morphometric data from collection material has enabled identification of unique

macroecological patterns for the two coronate taxa with cosmopolitan distributions. For example, regional variation in tentacle numbers in *Atolla* spp. but not in *P. periphylla* suggests differences in phenotypic responses between the two coronate species which may be indicative of genetic variation. In addition, analyses of Iberian Basin material revealed temporal changes in body size with the species of *Atolla* exhibiting distinct variation in bell diameter from 1937 to 1990. In contrast, *P. periphylla* exhibited no overall change in size (Chapter 3). However, there is a clear difference in sizes of *P. periphylla* between oceanic and fjord populations. This may reflect a trade-off with fecundity in the smaller oceanic specimens (Chapter 5). Nevertheless, tentacle number in *P. periphylla* was constant regardless of body size and environment. Collectively these results suggest that *Atolla* spp. demonstrate environmentally-induced plasticity in growth and morphology unlike *P. periphylla* which presents relatively constant phenotypes throughout its distribution.

7.2 Deep sea macroecology

The shift of marine studies from isolated, small scale investigations to larger temporal and spatial scales has furthered our understanding of the processes driving marine ecosystems. This represents the largest study of coronate morphological information to date using historical and field data. However, the collections data are a pooled resource from a number of research cruises each with their own methods of specimen collection and storage (see Appendix A for list of cruises and stations included in this study). This inevitably has an effect on the quality of data produced and the number of conclusions that can be reliably drawn. Edgar et al. (2016) note the increase in marine macroecological studies are as a result of advances in macroecological and statistical approaches combined with more readily available data, however they also stress that in order to produce reliable scientific output, a more systematic, standardised methods of collating data is required.

The synthesis of macroecological data and investigations serve to not only identify patterns and novel avenues of investigation to pursue, but also as a means of generating baseline information for further studies. For example, Condon et al. (2013) and Lucas et al. (2014) used an array of data and metadata sources to generate a macroecological dataset of gelatinous zooplankton abundances spanning 1934 to 2011 by using an array of data and metadata sources. By collating this large number of individual studies, it was possible to identify worldwide oscillations of jellyfish abundance with an approximate 20 year

periodicity. This highlights the value of such studies and their potential for revealing temporal and spatial macroecological patterns- whose drivers may be then investigated.

7.3 Deep-sea jellyfish macroecology: evidence of plasticity to environmental variation over space and time?

The manifestation of phenotypic plasticity according to changes in environmental conditions illustrates the ability for species to adapt when conditions vary. Variation in the abiotic environment is the most common trigger for plasticity amongst marine fauna (Padilla and Savedo, 2013). The responses of deep-sea fauna to climate change have been addressed in recent studies, particularly for fauna exposed to broad depth ranges, and therefore temperatures, including in diel vertical migrators. Warming waters and changes in the energy available in the photic zone have resulted in observed responsive adaptation in the deep sea (Gambi et al., 2017). Nevertheless, the physiology of deep-sea fauna remains poorly understood along with their general responses to environmental change.

This study observed variation in tentacle number in *A. parva* between oceans (Chapter 2) and variation in body size of *P. periphylla* between ocean and fjord environments. This variation may represent morphological responses to the varying conditions within and between exhibits a morphological response to open and closed systems, including varying food web assemblages, zooplankton abundances and chemical compositions and patterns of light attenuation. The observed variation in morphologies of deep-sea coronates across the global dataset examined here confirms the relatively recent understanding that there are complex ecosystem interactions outside of the epipelagic zone, and that the deep sea is not simply a homogenous system. Some of the phenotypic variation linked with environmental conditions observed in this study may in some cases be indicative of genetic distance between the two deep-sea coronate genera.

Further studies on the phylogenetic relationships within the Scyphozoa would aid understanding of the occurrence and drivers of phenotypic plasticity and potential speciation (Dawson et al., 1998; Dawson and Jacobs, 2001; Holland et al., 2004; Dawson, 2004; Mianzan et al., 2008). A further understanding of the ontogeny of deep-sea coronates, particularly in *Atolla* spp., would also assist in confirming plastic traits. Currently the early

developmental stages have been documented for *P. periphylla*. only (Jarms et al., 1999), and no plastic traits were noted here during these early development stages. Morphogenesis of *Aurelia aurita* has been shown to vary with changes in fluid dynamics according to temperature variation (Nawroth et al., 2010). This may be the case for the various species of *Atolla* which exhibit a range of morphological traits according to environmental variation, particularly *A. parva*, *A. russelli* and *A. gigantea*. A further understanding of the early life cycle stages of *Atolla* spp. would therefore promote understanding of how variation in tentacle number may relate to locomotion and feeding. Such insights require gaining access to larger sample sizes than were available within this study.

7.4 Scyphozoan phylogeny

The use of molecular methods to facilitate understanding how organisms respond to environmental change is a growing theme within both deep-sea and gelatinous zooplankton research (see Dawson 2004; 2005; Bayha et al., 2010; Danovaro et al., 2017). Better understanding of the phylogenetic relationships within the Scyphozoa would help to understand of the occurrence and drivers of phenotypic plasticity and speciation. Scyphozoan phylogeny is subject to debate, with Coronatae in particular being poorly resolved due to small sample sizes and a sample bias towards the shallow-water genera *Linuche* sp. and *Nausithoe* sp. (Collins, 2002; Bayha and Dawson, 2010; Bayha et al., 2010; Kayal et al., 2013). Currently four of the six recognised coronate families are monophyletic (Atollidae, Periphyllidae, Paraphyllinidae, Linuchidae, (Ortman et al., 2010)). Family Nausithoidae is considered to be genetically distinct (Bayha et al., 2010). Approaches to further understand scyphozoan phylogeny include using of rhopalia (sense organs) as an evolutionary indicator. Sötje et al. (2011) note that the rhopalial bulb and statocyst, which are essential for orientation, developed together with the pelagic stage in cnidarians. Inclusion of the rhopalia and statocyst in phylogenetic analysis has suggested that Cubozoa developed from a scyphozoan ancestor (Sötje et al., 2011). In other cases, rhopalia have been used as descriptors between species has furthered the understanding of scyphozoan species (Han et al., 2016).

This study explored a range of molecular methods using specimens within this study in an effect to better understand the relationships amongst coronate lineages. This was of particular interest as it could enable determining whether observed variation in morphology

may result from phenotypic plasticity or whether it might reflect potential cryptic species. The methods trialled are described in Table 7.1. The negative output from all trialled methods is indicative of the inherent difficulties associated with extracting DNA in sufficient quantities and qualities in jellyfish. Gelatinous zooplankton possess low quantities of DNA material for extraction (Hwang et al., 2014). In addition, formalin-fixed material is also recognised to restrict extraction and amplification as a result of cross-linking the sample proteins (Shibata, 1994; Fang, Wan and Fujihara, 2002). DNA extraction was possible on formalin-fixed deep sea lithoids (Decapoda: Anomura: Lithodidae) (Palero et al., 2010), however has not yet been possible to date using formalin-fixed gelatinous zooplankton samples.

Table 7.1 Summary of molecular methods trialled in the study. Sample sources used include historical collections (formalin-fixed *Atolla* spp. and *P. periphylla*), fresh tissue (ethanol-fixed *P. periphylla*) and fresh tissue (frozen *Rhizostoma*, control).

Extraction Method	Description	Subsequent methods
EZNA Kit 'EaZy Nucleic Acid Isolation' EZNA Mollusc DNA Isolation Kit	Gonad, coronal muscle and tentacle tissue used separately to determine optimal tissue selection. Column-based kit lysing DNA in guanadine-detergent lysine solution.	1. Quantities of DNA determined using a ThermoScientific Nanodrop 8000 and Qubit. 2. Polymerase Chain Reaction (PCR) using 16S and COI primers. Primers used:
CTAB Method Amended from Campos & Gilbert, (2012).	Gonad, coronal muscle and tentacle tissue used. Tissue lysed in Polymerase K and also by manually grinding with pestle and mortar. DNA cleaned using Illustra GFX PCR DNA and Gel Band Purification Kit (GE Healthcare).	(Cunningham and Buss, 1993): 16S primers for Hydractiniidae 16SAR TCGACTGTTTACCAAAAACATAGC 16SBR ACGGAATGAACTCAAATCATGTAAG (Folmer et al., 1994): Universal COX I primers
Qiagen All-Prep DNA/RNA Formalin-Fixed, Paraffin-Embedded Kit (FFPE).	Gonad, coronal muscle and tentacle tissue used.	LCO1490: 5'-ggtaacaaatcataaagatattgg-3' HC02198: 5'-taaactcagggtgacaaaaaatca-3' 1. Electrophoresis (agarose) and DNA sequencing (Sanger Sequencer).

7.5 Exploiting museum collections for macroecological studies

This study exemplifies a shift in scientific approaches to maximise the use of existing specimen data rather than undertake destructive sampling of wild populations. In this case museum specimens of notoriously difficult to sample gelatinous zooplankton provided baseline information on the distribution and biology of understudied deep sea populations to gain insights on how deep sea jellyfish respond to their environments over space and time. While museum collections are often used to complement field-collected data (see

Larson & Harbison 1990; Hobson & Sease 1998; Gershwin 2005 for examples), they are rarely used on a macroecological scale (Lister et al., 2011).

Atolla spp. and *P. periphylla* provided ideal gelatinous zooplankton for study because their robust structure enables trawling from considerable depths with little damage to individuals. While preserved museum specimens vary in appearance in comparison to live specimens, morphological characteristics are retained with the exception of pigmentation and the number of tentacles in *Atolla* sp. which were damaged in all instances (Table 7.1). The fixation and preservation of jellyfish using formalin is known to result in shrinkage over time (Angel and Baker, 1983; Tucker and Chester, 1984; de Lafontaine and Leggett, 1989) and this can reach up to a 75% reduction in overall size (see Hamner & Jenssen 1974; Costello 1998). However, because the collection of data was standardised in this study the observed patterns are real as they result from analyses of comparable data.

Previous studies on coronate reproduction have used fresh specimens (Eckelbarger and Larson, 1992; Arai, 1997; Lucas and Reed, 2010), however this study has illustrated that museum specimens of *Atolla* sp. can be used to characterise gonad development and the production of both gametes. If the ability to age individual medusae could be achieved, this could assist to contextualise the reproductive development of deep-sea medusae. The gonads of *P. periphylla* analysed in this study, however, did not retain their structural integrity during histological analysis.

The ability to gain macroecological insights into the deep sea coronates examined here suggests that there is great scope for gaining such insights on other deep sea denizens (e.g. crustaceans, annelids, fish). Future studies focusing on animals that are more easily collected, less prone to damage and may be sampled in greater numbers could reveal complementary, more robust and new insights on the macroecology of deep sea animals without entailing the costs and expenses of collecting new material.

7.6 Deep-sea jellyfish macroecology: evidence for determining age in medusae?

Assigning definitive age of individual scyphozoan medusae based on physical descriptors is currently impossible. Nevertheless, there is some appreciation of the potential longevity of certain shallow-water species such as *Aurelia aurita* due to their conspicuousness and

anthropogenic impacts (Spangenberg, 1968; Miyake, Iwao and Kakinuma, 1997; Lucas, 2001). In addition, shallow-water species are relatively easy to culture in a laboratory environment as they are photophilic. This study sought to further the understanding of the age of individual coronates. It was discovered during this study that the bassanite statoliths found within the rhopalial tissue of *P. periphylla* are subject to rapid degradation in water or formalin if not fixed with a sodium glycerophosphate buffer. The use of museum specimens to elucidate age based on statolith structure and counts was not possible, and fresh material was required. Study of this material produced baseline data from a range of sizes of field-collected *P. periphylla* specimens. If combined with data from specimens of a known age, it would be possible to determine a reliable estimate of age that is not subject to shrinkage in adverse conditions.

7.7 Future studies on jellyfish macroecology and deep-sea medusae.

This study has significantly developed our understanding of the global macroecology of deep-sea jellyfish. Insights from this and other studies suggest that species complexes and cryptic species may characterise the taxa investigated here but that morphological variation according to environmental conditions can also occur. Future molecular work using field-collected material could resolve these issues as well as providing insights into whether morphological variation within the species of *Atolla* reflects speciation or phenotypic plasticity. Further studies should also investigate whether plasticity has an effect on speciation either by enhancing or suppressing the selection of phenotypic traits which have become genetically controlled by isolation distance.

The results from this study also suggest the following further areas for future research:

- Further collection of deep-sea coronates coupled with accurate depths of collection would provide a dataset that could be analysed to obtain more precise insights on macroevolutionary patterns. The data analysed were based on depths reported in broad ranges.
- Insights into ontogeny and the potential for plasticity of *Atolla* spp. through rearing in controlled laboratory conditions would provide baseline data on e.g. age, statolith formation, onset of reproduction, phenotypic plasticity and a context for interpreting macroevolutionary patterns. The collection of fresh *P. periphylla* and *Atolla* spp.

from oceanic and fjord environments throughout the year would assist interpreting age for both species and provide material for molecular analysis. This would further the understanding of phenotypic plasticity, species complexes and cryptic species in the poorly resolved coronate order.

Appendices

Appendix A

Table 1 Station list of all deep sea coronate samples used within this study. Samples used are held within the Discovery Collections at the Natural History Museum London, with collection dates spanning from 1934 to 1990. Stations listed includes both Atolla and Periphylla genera. Discovery collections lists available on <http://www.nhm.ac.uk/discover/collections.html>, with supplementary information available from the British Oceanographic Data Centre (BODC) cruise inventory at https://www.bodc.ac.uk/resources/inventories/cruise_inventory/. Stations ordered from oldest to newest.

Station	Date	Longitude	Latitude	Sampling Gear	Min Depth (m)	Max Depth (m)	Start time of trawl	End time of trawl	Description
1299	02/03/1934	-123.95	-68.76	N 100 B	0	86	43	2302	Eastward ice-edge cruise in South Pacific Ocean
2065	04/05/1937	-12.51	2.13	N 450 B	1400	1600	1007	1107	34° S, 0° E to Canary Islands
2066	06/05/1937	-14.78	4.94	N 450 B	0	1550	1010	1118	34° S, 0° E to Canary Islands
2229	19/02/1938	-161.33	-68.16	N 100 B	200	330	265	2234	Zig-zag off ice-edge from 164° W to 79° W
2313	12/04/1938	0.49	-52.45	N 70 V	500	750	625	2015	50° S to 65° S in Greenwich meridian
2378	22/07/1938	20.70	-46.34	N 100 B	250	450	350	2320	First cruise of repeated series in area W and S of Capetown
2986	24/02/1939	0.99	-52.49	N 100 H	0	5	2.5	2235	Seventh cruise of repeated series in area W and S of Capetown
3658	12/03/1958	-15.50	43.25	IKMT	0	1500			Off West Spain
3700	09/04/1958	-14.25	37.00	IKMT	0	1000			Off SW Spain
3702	10/04/1958	-14.00	38.00	IKMT	0	700			Off SW Spain
3710	17/04/1958	-9.25	45.00	IKMT	800	1600			North of Spain
4767	11/10/1961	-20.03	40.03	BOVT	0	82			From 40° 02' N, 20° 02' W to 40° 09.5' N, 19° 52.5' W
4921	31/05/1962	-16.20	33.37	IKMT	0	950			From 33° 22' N, 16° 12' W to 33° 12.4' N, 16° 15.6' W
5101	19/08/1963	47.63	13.17	IKMT	300	625	1800	2048	South East Arabian Upwelling Region
5272	18/03/1964	57.87	2.23	IKMT	0	400			Aden to Mauritius - Indian Ocean
5368	03/05/1964	67.55	4.86	Bact.	0	200			Mauritius to Cochlin, Carlsberg Ridge, Indian Ocean
5372	05/05/1964	67.70	8.55	IKMT	0	180			Mauritius to Cochlin, Arabian sea, Indian Ocean
5413	02/06/1964	57.99	1.49	IKMT	0	80	1930	112	Cochlin to Seychelles, Indian Ocean, E of Somali Republic
5411	03/06/1964	58.02	2.51	IKMT	1200	4901	1736	2336	Cochlin to Seychelles, Indian Ocean, E of Somali Republic
5415	03/06/1964	58.06	0.65	IKMT	0	100			Cochlin to Seychelles, Indian Ocean, E of Somali Republic
5792	12/10/1965	-14.10	28.05	IKMT	620	950			Fuerteventura
5795	15/10/1965	-14.15	28.09	IKMT	0	1050			Fuerteventura
5797	17/10/1965	-14.16	28.08	IKMT	650	775			Fuerteventura
5799	19/10/1965	-14.16	28.08	IKMT	0	675			Fuerteventura
5801	21/10/1965	-14.16	28.08	IKMT	0	800			Fuerteventura
5805	02/11/1965	-14.18	28.08	IKMT	0	380			Fuerteventura
5806	03/11/1965	-13.98	27.83	IKMT	0	150			Off NW Africa
5809	08/11/1965	-14.08	28.09	IKMT	630	750			Off NW Africa
5810	07/11/1965	-13.85	28.07	IKMT	0	800			Off NW Africa
5823	25/11/1965	-14.80	28.09	N 113 H	800	960			Off NW Africa
6170	10/11/1966	-14.06	28.08	EMT	0	570	2036	233	Canary Islands
6178	11/11/1966	-13.95	27.98	IKMT	0	1200	2020	256	Canary Islands
6186	17/11/1966	-8.00	34.29	EMTB	0	510			Off NW Africa
6199	22/11/1966	-10.00	36.50	EMTB	0	510	1941	2102	Off NW Africa
6200	22/11/1966	-10.20	36.81	EMT	0	550			Off NW Africa
6363	24/07/1967	-14.08	28.08	N 113 H	0	860	627	1850	Fuerteventura
6397	02/08/1967	-14.15	28.10	TMT8	0	790	212	900	Fuerteventura
6425	12/08/1967	-14.32	27.90	TMT8	0	970	845	1555	Fuerteventura

Table 1: NHM stations continued.

Station	Date	Longitude	Latitude	Sampling Gear	Min Depth (m)	Max Depth (m)	Start time of trawl	End time of trawl	Description
6441	16/08/1967	-13.95	27.92	EMT	0	240	1836	100	Fuerteventura
6662#22	17/02/1968	-19.96	10.96	RMT8	610	680			NE Atlantic (off NW Africa)
6662#23	18/02/1968	-19.89	10.89	RMT8	310	415			NE Atlantic (off NW Africa)
6662#21	24/02/1968	-19.84	10.86	RMT15	0	700			NE Atlantic (off NW Africa)
7080#3	03/11/1969	-27.05	16.69	RMT1	0	500	2341	115	Off NW Africa, Canary Islands, NE Atlantic
7089#1	11/11/1969	-25.46	17.82	RMT1	910	990	1457	1839	Off NW Africa, Canary Islands, NE Atlantic
7060#1	26/11/1969	-22.65	20.54	TMT8 B	0	1000	2215	40	Off NW Africa, Canary Islands, NE Atlantic
7709#1	25/04/1971	-19.98	60.05	RMT8	110	200	1045	1245	Biology: NE Atlantic (Iceland Basin,Rockall)
7709#2	25/04/1971	-20.03	60.19	RMT8	205	300	1431	1631	Biology: NE Atlantic (Iceland Basin,Rockall)
7709#3	25/04/1971	-19.98	60.06	RMT8	495	590	2331	131	Biology: NE Atlantic (Iceland Basin,Rockall)
7709#16	26/04/1971	-20.03	59.96	RMT8	50	95	2236	36	Biology: NE Atlantic (Iceland Basin,Rockall)
7709#4a	26/04/1971	-19.97	60.19	RMT8	105	200	226	426	Biology: NE Atlantic (Iceland Basin,Rockall)
7709#5	26/04/1971	-19.95	60.04	RMT8	290	390	722	922	Biology: NE Atlantic (Iceland Basin,Rockall)
7709#7	26/04/1971	-20.02	60.04	RMT8	410	500	1740	1940	Biology: NE Atlantic (Iceland Basin,Rockall)
7709#21	27/04/1971	-19.89	60.17	RMT8	710	800	1634	1834	Biology: NE Atlantic (Iceland Basin,Rockall)
7709#22	27/04/1971	-19.98	60.04	RMT8	800	900	2231	37	Biology: NE Atlantic (Iceland Basin,Rockall)
7709#23	28/04/1971	-20.08	60.16	RMT8	405	500	208	408	Biology: NE Atlantic (Iceland Basin,Rockall)
7709#24	28/04/1971	-20.01	60.04	RMT8	910	995	657	857	Biology: NE Atlantic (Iceland Basin,Rockall)
7709#25	28/04/1971	-20.20	60.13	RMT8	810	900	1101	1301	Biology: NE Atlantic (Iceland Basin,Rockall)
7709#26	28/04/1971	-20.31	60.14	RMT8	600	700	1436	1636	Biology: NE Atlantic (Iceland Basin,Rockall)
7709#28	28/04/1971	-19.90	60.27	RMT8	705	800	2238	38	Biology: NE Atlantic (Iceland Basin,Rockall)
7709#33	29/04/1971	-20.12	60.17	RMT8	55	100	847	1047	Biology: NE Atlantic (Iceland Basin,Rockall)
7709#36	29/04/1971	-19.94	60.23	RMT8	600	700	2250	50	Biology: NE Atlantic (Iceland Basin,Rockall)
7709#17	30/04/1971	-19.97	60.08	RMT11	900	1000	156	356	Biology: NE Atlantic (Iceland Basin,Rockall)
7709#37b	30/04/1971	-19.72	60.17	RMT8	205	300	150	350	Biology: NE Atlantic (Iceland Basin,Rockall)
7709#44	01/05/1971	-19.66	60.13	RMT9	1250	1500	648	1048	Biology: NE Atlantic (Iceland Basin,Rockall)
7709#61	01/05/1971	-19.46	59.98	RMT8	0	1000	1155	1335	Biology: NE Atlantic (Iceland Basin,Rockall)
7709#63	02/05/1971	-20.12	59.95	TSD	1000	1250	2307	308	Biology: NE Atlantic (Iceland Basin,Rockall)
7709#71	05/05/1971	-19.80	60.01	RMT8	0	1000	313	532	Biology: NE Atlantic (Iceland Basin,Rockall)
7709#76	05/05/1971	-19.63	59.99	RMT8	1250	1500	2240	240	Biology: NE Atlantic (Iceland Basin,Rockall)
7709#74	07/05/1971	-19.37	60.04	RMT10	310	400	1636	1836	Biology: NE Atlantic (Iceland Basin,Rockall)
7709#83	07/05/1971	-19.83	60.06	RMT8	430	700	247	348	Biology: NE Atlantic (Iceland Basin,Rockall)
7709#27	08/05/1971	-20.00	60.15	RMT18	300	400	1751	1951	Biology: NE Atlantic (Iceland Basin,Rockall)
7709#92a	08/05/1971	-20.22	59.81	RMT25/10	800	1000	612	912	Biology: NE Atlantic (Iceland Basin,Rockall)
7709#93	08/05/1971	-20.38	59.83	RMT25/10	615	800	1117	1417	Biology: NE Atlantic (Iceland Basin,Rockall)
7709#93a	08/05/1971	-20.38	59.83	RMT25/10	615	800	1117	1417	Biology: NE Atlantic (Iceland Basin,Rockall)
7709#92	09/05/1971	-20.22	59.81	RMT25/11	800	1000	612	912	Biology: NE Atlantic (Iceland Basin,Rockall)

Table 1: NHM stations continued

Station	Date	Longitude	Latitude	Sampling Gear	Min Depth (m)	Max Depth (m)	Start time of trawl	End time of trawl	Description
7710	15/05/1971	-15.38	52.50	RMT8	25	1000	1701	2105	Biology, NE Atlantic (Iceland Basin,Rockall)
7711#5	17/05/1971	-19.97	52.99	RMT8	800	650	951	1011	Biology, NE Atlantic (Iceland Basin,Rockall)
7711#1	18/05/1971	-20.21	52.76	RMT8	505	600	1340	1540	Biology, NE Atlantic (Iceland Basin,Rockall)
7711#10	18/05/1971	-20.21	52.76	RMT8	505	600	1340	1540	Biology, NE Atlantic (Iceland Basin,Rockall)
7711#8	18/05/1971	-20.03	52.94	RMT8	700	805	721	921	Biology, NE Atlantic (Iceland Basin,Rockall)
7711#9	18/05/1971	-20.16	52.84	RMT8	605	700	1037	1237	Biology, NE Atlantic (Iceland Basin,Rockall)
7711#13	19/05/1971	-20.01	52.92	RMT8	800	900	35	237	Biology, NE Atlantic (Iceland Basin,Rockall)
7711#15	19/05/1971	-20.16	52.87	RMT8	110	200	607	807	Biology, NE Atlantic (Iceland Basin,Rockall)
7711#23	19/05/1971	-20.00	52.95	RMT8	200	300	2342	142	Biology, NE Atlantic (Iceland Basin,Rockall)
7711#24	20/05/1971	-20.07	52.87	RMT8	50	102	210	310	Biology, NE Atlantic (Iceland Basin,Rockall)
7711#29	22/05/1971	-19.95	53.06	RMT9	610	700	201	401	Biology, NE Atlantic (Iceland Basin,Rockall)
7711#31	22/05/1971	-20.00	52.99	RMT8	100	200	145	345	Biology, NE Atlantic (Iceland Basin,Rockall)
7711#33	23/05/1971	-20.08	52.97	RMT1	410	800	159	359	Biology, NE Atlantic (Iceland Basin,Rockall)
7711#35	23/05/1971	-20.08	52.86	RMT8	1525	2000	1056	1555	Biology, NE Atlantic (Iceland Basin,Rockall)
7711#39	24/05/1971	-20.16	52.80	RMT8	1520	2000	634	1034	Biology, NE Atlantic (Iceland Basin,Rockall)
7711#28	25/05/1971	-20.08	52.97	RMT3	410	800	159	359	Biology, NE Atlantic (Iceland Basin,Rockall)
7711#40	25/05/1971	-20.37	52.91	RMT9	1005	1250	1408	1808	Biology, NE Atlantic (Iceland Basin,Rockall)
7711#65	28/05/1971	-20.14	53.10	RMT8	1020	1250	2247	247	Biology, NE Atlantic (Iceland Basin,Rockall)
7711#72	30/05/1971	-20.13	52.93	RMT25/10	1020	1500	1643	2043	Biology, NE Atlantic (Iceland Basin,Rockall)
7711#77	31/05/1971	-20.06	53.05	RMT25/10	1500	2010	35	438	Biology, NE Atlantic (Iceland Basin,Rockall)
7712	02/06/1971	-15.82	51.79	RMT8	20	1000	2020	2313	Biology, NE Atlantic (Iceland Basin,Rockall)
7711#67	02/06/1971	-20.02	53.17	RMT25/14	605	800	958	1358	Biology, NE Atlantic (Iceland Basin,Rockall)
7716#1	04/06/1971	-13.13	51.03	RMT8	800	1000	50	120	Biology, NE Atlantic (Iceland Basin,Rockall)
7709#29	14/07/1971	-20.02	60.26	RMT84	300	400	153	356	Biology, NE Atlantic (Iceland Basin,Rockall)
7709#92b	27/10/1971	-20.22	59.81	RMT25/182	810	1000	612	912	Biology, NE Atlantic (Iceland Basin,Rockall)
7799#2	17/02/1972	-21.76	20.42	RMT8	0	1000	1730	1850	NE Atlantic (Off NW Africa, Canary and C. Verde Isles)
7824#13	08/03/1972	-20.16	10.76	RMT9	1000	1250	2103	103	NE Atlantic (Off NW Africa, Canary and C. Verde Isles)
7824#44	10/03/1972	-20.31	10.96	RMT8	240	265	2100	2300	NE Atlantic (Off NW Africa, Canary and C. Verde Isles)
7824#46	11/03/1972	-20.15	10.89	RMT1	220	260	204	404	NE Atlantic (Off NW Africa, Canary and C. Verde Isles)
7824#65	13/03/1972	-20.01	10.98	RMT8	205	300	233	433	NE Atlantic (Off NW Africa, Canary and C. Verde Isles)
7856#48	12/04/1972	-23.01	29.81	RMT16	1005	1250	1005	1250	NE Atlantic (Off NW Africa, Canary and C. Verde Isles)
7982	21/07/1972	-16.33	25.60	RMT1	0	1000	0091	1044	NE Atlantic (Off NW Africa)

Table 1: NHM stations continued

Station	Date	Longitude	Latitude	Sampling Gear	Min Depth (m)	Max Depth (m)	Start time of trawl	End time of trawl	Description
8263	25/02/1973	-20.44	32.10	WB7.4	0	1000	2111	2325	N Atlantic (32' N Section, Bermuda)
8264	26/02/1973	-23.80	32.15	WB7.4	0	1000	2216	19	N Atlantic (32' N Section, Bermuda)
8272	03/03/1973	-43.62	31.96	RM78	0	1000	2313	127	N Atlantic (32' N Section, Bermuda)
8276	06/03/1973	-54.08	31.93	RM78	0	1000	2345	148	N Atlantic (32' N Section, Bermuda)
8279	09/03/1973	-60.39	32.36	WB7.5	0	1000	2336	135	N Atlantic (32' N Section, Bermuda)
8281#1	13/03/1973	-63.87	31.92	RM78	905	1000	405	606	N Atlantic (32' N Section, Bermuda)
8281#6	13/03/1973	-63.73	31.81	RM78	800	900	2342	142	N Atlantic (32' N Section, Bermuda)
8281#7	14/03/1973	-63.67	31.89	RM78	700	800	321	522	N Atlantic (32' N Section, Bermuda)
8281#8	14/03/1973	-63.58	31.97	RM78	605	700	704	904	N Atlantic (32' N Section, Bermuda)
8281#9	14/03/1973	-63.74	31.95	RM78	805	900	1144	1344	N Atlantic (32' N Section, Bermuda)
8281#14	16/03/1973	-63.74	31.85	RM79	1010	1250	1200	1600	N Atlantic (32' N Section, Bermuda)
8281#32	18/03/1973	-63.54	31.59	RM78	205	300	33	233	N Atlantic (32' N Section, Bermuda)
8281#33	18/03/1973	-63.34	31.50	RM78	1490	2000	500	900	N Atlantic (32' N Section, Bermuda)
8507#27	03/04/1974	-13.20	44.05	RM78	400	500	121	321	NE Atlantic (44'N, 13'W)
8508#10	13/04/1974	-12.78	44.11	RM78	610	690	2347	47	NE Atlantic (44'N, 13'W)
8508#13	14/04/1974	-12.74	44.07	RM78	590	610	551	651	NE Atlantic (44'N, 13'W)
8508#32	15/04/1974	-13.09	44.18	RM78	405	500	2347	147	NE Atlantic (44'N, 13'W)
8508#78	20/04/1974	-12.95	44.27	RM78	2500	3100	2118	718	NE Atlantic (44'N, 13'W)
8509#23	25/04/1974	-12.91	44.28	RM78	500	600	2051	2252	NE Atlantic (44'N, 13'W)
8509#15	27/04/1974	-13.06	44.18	RM78	2000	2500	126	626	NE Atlantic (44'N, 13'W)
8516#4	10/05/1974	-13.38	43.71	RM78	500	600	2108	2308	NE Atlantic (44'N, 13'W)
8516#13	12/05/1974	-13.17	44.15	RM78	0	1000	1220	1354	NE Atlantic (44'N, 13'W)
8517#6	15/06/1974	-12.51	43.91	RM78	503	400	205	405	NE Atlantic (Passage from UK, off NW African continental margin)
8563#1	31/07/1974	-22.71	2.94	RM78	805	900	1206	1406	Equatorial East atlantic
8565#5	01/08/1974	-23.24	3.05	RM71	700	800	845	1045	Equatorial East atlantic
8567#1	02/08/1974	-23.46	2.95	RM78	505	600	835	1035	Equatorial East atlantic
8568#1	04/08/1974	-23.24	3.05	RM74	700	800	845	1045	Equatorial East atlantic
8604	22/08/1974	-23.17	9.00	RM78	100	200	34	234	Eq. E Atlantic (8'N,23'W)
8614	23/08/1974	-22.68	8.95	DN	500	600	554	654	Eq. E Atlantic (8'N,23'W)
8633#1	25/09/1974	-12.79	43.68	RM78	300	405	2103	2303	NE Atlantic (Canary Islands)
8948#07	25/07/1976	-11.79	32.39	RM78	0	3273	2120	2220	NE Atlantic (Canary Islands)
8948#32	28/07/1976	-11.77	32.41	RM78	395	500	0005	0105	NE Atlantic (Canary Islands)
8964	31/07/1976	-14.61	28.61	RM78	900	1100	1734	1934	NE Atlantic (Canary Islands)
8968	03/08/1976	-11.03	31.58	OTS814	1767	1846	0524	0625	NE Atlantic (Canary Islands)
8973	04/08/1976	-11.33	32.03	BN2.4/4.5	3003	3008	1154	1241	NE Atlantic (Canary Islands)
8976	05/08/1976	-11.67	32.91	BN2.4/4.5	3610	3646	1244	1505	NE Atlantic (Canary Islands)
9000	15/08/1976	-16.06	27.26	RM78	300	400	136	336	NE Atlantic (Canary Islands)
9002	15/08/1976	-15.87	27.38	RM78	1200	1300	0731	1031	NE Atlantic (Canary Islands)
9131#19	21/11/1976	-21.79	20.24	RM78	3500	3760	2016	116	NE Atlantic (Off NW Africa)
9131#23	23/11/1976	-21.73	20.07	RM78	3000	3500	53	453	NE Atlantic (Off NW Africa)
9132#5	25/11/1976	-18.93	20.84	OTS815	3089	3109	1408	1530	NE Atlantic (Off NW Africa)

Table 1: NHM stations continued

Station	Date	Longitude	Latitude	Sampling Gear	Min Depth (m)	Max Depth (m)	Start time of trawl	End time of trawl	Description
9541#22	20/04/1977	-21.42	20.15	RMT8	3740	3870	945	1545	NE Atlantic (off NW Africa, 20°N, 21°W, passage to UK)
9541#25	21/04/1977	-21.94	20.39	RMT8	41		1123	1723	NE Atlantic (off NW Africa, 20°N, 21°W, passage to UK)
9541#30	22/04/1977	-21.33	20.03	RMT1	995	1500	1921	2321	NE Atlantic (off NW Africa, 20°N, 21°W, passage to UK)
9756#2	10/04/1978	-14.17	49.88	RMT8	1000	1500	2306	306	NE Atlantic (Porcupine Seabight, along 13°N and 17°W, around 42°N, 17°W)
9756#4	11/04/1978	-14.17	49.69	RMT8	1500	2000	2033	33	NE Atlantic (Porcupine Seabight, along 13°N and 17°W, around 42°N, 17°W)
9750#3	29/04/1978	-12.69	42.06	RMT8	10	1000	533	1702	NE Atlantic (Porcupine Seabight, along 13°N and 17°W, around 42°N, 17°W)
9791#10	06/05/1978	-14.01	49.48	RMT8M/3	500	600	2320	21	NE Atlantic (Porcupine Seabight, along 13°N and 17°W, around 42°N, 17°W)
9791#17	07/05/1978	-13.74	49.50	RMT8M/1	895	1100	1226	1426	NE Atlantic (Porcupine Seabight, along 13°N and 17°W, around 42°N, 17°W)
9791#21	07/05/1978	-13.99	49.72	RMT8M/2	700	800	2223	2323	NE Atlantic (Porcupine Seabight, along 13°N and 17°W, around 42°N, 17°W)
9791#12	08/05/1978	-13.88	49.42	RMT8M/3	100	200	218	318	NE Atlantic (Porcupine Seabight, along 13°N and 17°W, around 42°N, 17°W)
9791#4	08/05/1978	-12.69	42.06	RMT1M/5	800	905	1340	1440	NE Atlantic (Porcupine Seabight, along 13°N and 17°W, around 42°N, 17°W)
9792#3	11/05/1978	-16.70	50.06	RMT10	10	1000	957	1114	NE Atlantic (Porcupine Seabight, along 13°N and 17°W, around 42°N, 17°W)
9798#2	13/05/1978	-17.00	44.00	RMT9	10	1000	204	441	NE Atlantic (Porcupine Seabight, along 13°N and 17°W, around 42°N, 17°W)
9801#5	13/05/1978	-16.66	41.86	RMT8M/3	800	900	956	1056	NE Atlantic (Porcupine Seabight, along 13°N and 17°W, around 42°N, 17°W)
9801#16	14/05/1978	-16.78	41.88	RMT1M/2	100	200	247	347	NE Atlantic (Porcupine Seabight, along 13°N and 17°W, around 42°N, 17°W)
9801#27	14/05/1978	-16.84	42.05	RMT8M/1	600	700	2254	2354	NE Atlantic (Porcupine Seabight, along 13°N and 17°W, around 42°N, 17°W)
9801#3	14/05/1978	-16.73	41.92	RMT8M/2	600	700	754	856	NE Atlantic (Porcupine Seabight, along 13°N and 17°W, around 42°N, 17°W)
9793#2	15/05/1978	-17.01	49.02	RMT14	10	10000	2058	2239	NE Atlantic (Porcupine Seabight, along 13°N and 17°W, around 42°N, 17°W)
9796#2	15/05/1978	-17.00	46.01	RMT5	10	1000	415	606	NE Atlantic (Porcupine Seabight, along 13°N and 17°W, around 42°N, 17°W)
9801#26	15/05/1978	-16.95	42.01	RMT1M/4	990	1010	2019	2119	NE Atlantic (Porcupine Seabight, along 13°N and 17°W, around 42°N, 17°W)
9801#20	16/05/1978	-17.08	42.00	RMT1M/5	1280	1500	1023	1223	NE Atlantic (Porcupine Seabight, along 13°N and 17°W, around 42°N, 17°W)
9801#58	17/05/1978	-16.71	42.10	RMT1M/2	990	1010	3	103	NE Atlantic (Porcupine Seabight, along 13°N and 17°W, around 42°N, 17°W)
9801#65	17/05/1978	-16.83	41.90	RMT1M/3	990	1010	1121	1221	NE Atlantic (Porcupine Seabight, along 13°N and 17°W, around 42°N, 17°W)
9801#72	18/05/1978	-16.77	41.86	RMT8M/1	990	1010	46	146	NE Atlantic (Porcupine Seabight, along 13°N and 17°W, around 42°N, 17°W)
9801#76	18/05/1978	-16.99	41.74	RMT8M/1	990	1010	820	920	NE Atlantic (Porcupine Seabight, along 13°N and 17°W, around 42°N, 17°W)
9801#77	19/05/1978	-17.04	41.73	RMT1M/3	990	1020	920	1022	NE Atlantic (Porcupine Seabight, along 13°N and 17°W, around 42°N, 17°W)
9801#83	19/05/1978	-17.02	41.97	RMT8M/3	1900	2100	203	408	NE Atlantic (Porcupine Seabight, along 13°N and 17°W, around 42°N, 17°W)
9801#66	20/05/1978	-16.68	41.95	RMT1M/4	990	1010	1432	1532	NE Atlantic (Porcupine Seabight, along 13°N and 17°W, around 42°N, 17°W)
9801#84	20/05/1978	-17.17	41.76	RMT8M/4	2500	2700	1736	1936	NE Atlantic (Porcupine Seabight, along 13°N and 17°W, around 42°N, 17°W)
9801#87	20/05/1978	-16.98	41.76	RMT8M/3	3100	3800	434	634	NE Atlantic (Porcupine Seabight, along 13°N and 17°W, around 42°N, 17°W)
9801#24	21/05/1978	-17.03	41.97	RMT1M/8	975	1010	1819	1919	NE Atlantic (Porcupine Seabight, along 13°N and 17°W, around 42°N, 17°W)
9801#60	21/05/1978	-16.82	41.95	RMT1M/5	985	1010	424	524	NE Atlantic (Porcupine Seabight, along 13°N and 17°W, around 42°N, 17°W)
9801#64	21/05/1978	-16.87	41.88	RMT1M/6	990	1010	1021	1121	NE Atlantic (Porcupine Seabight, along 13°N and 17°W, around 42°N, 17°W)
9801#79	22/05/1978	-17.13	41.85	RMT8M/5	1500	1710	2207	8	NE Atlantic (Porcupine Seabight, along 13°N and 17°W, around 42°N, 17°W)
9791#3	25/05/1978	-12.69	42.06	RMT8M/21	700	800	1238	1340	NE Atlantic (Porcupine Seabight, along 13°N and 17°W, around 42°N, 17°W)
9801#73	26/05/1978	-16.80	41.84	RMT1M/10	990	1000	146	246	NE Atlantic (Porcupine Seabight, along 13°N and 17°W, around 42°N, 17°W)
9801#81	02/06/1978	-17.02	41.97	RMT8M/17	1900	2100	203	408	NE Atlantic (Porcupine Seabight, along 13°N and 17°W, around 42°N, 17°W)
9801#19	13/06/1978	-17.00	41.96	RMT8M/32	1100	1280	823	1023	NE Atlantic (Porcupine Seabight, along 13°N and 17°W, around 42°N, 17°W)
9801#71	13/06/1978	-16.66	41.92	RMT1M/30	995	1010	2148	2248	NE Atlantic (Porcupine Seabight, along 13°N and 17°W, around 42°N, 17°W)

Table 1: NHM station list continued

Station	Date	Longitude	Latitude	Sampling Gear	Min Depth (m)	Max Depth (m)	Start time of trawl	End time of trawl	Description
9960#03	11/02/1979	29.95	-55.99	RMT8M/2	0	510	255		Indian and Southern Oceans
9961#2	11/02/1979	28.99	-58.90	RMT8M/2	500	1000			Indian and Southern Oceans
9959#03	12/02/1979	27.18	-55.95	RMT8M/4	1000	2000	1500		Indian and Southern Oceans
9962#02	14/02/1979	26.13	-58.99	RMT8M/4	490	1000	745		Indian and Southern Oceans
9961#3	15/02/1979	28.97	-58.94	RMT8M/7	1000	2000	1500		Indian and Southern Oceans
9964#2	15/02/1979	25.79	-64.33	RMT8M/2	500	990	745		Indian and Southern Oceans
9966#15	18/02/1979	23.75	-68.42	RMT8M/1	325	410			Indian and Southern Oceans
9967#2	19/02/1979	21.57	-64.94	RMT1M/1	325	380			Indian and Southern Oceans
9966#1	20/02/1979	24.27	-68.46	RMT8M/5	350	395	372.5		Indian and Southern Oceans
9968#2	20/02/1979	20.98	-62.16	RMT8M/2	500	980	740		Indian and Southern Oceans
9968#3	20/02/1979	20.96	-62.11	RMT8M/3	980	1990	1485		Indian and Southern Oceans
9966#18	21/02/1979	23.33	-68.45	RMT8M/4	390	450			Indian and Southern Oceans
9966#12	23/02/1979	24.10	-68.44	RMT8M/6	290	380	335		Indian and Southern Oceans
9969#18	23/02/1979	18.11	-58.71	RMT8M/2	1800	2000	1900		Indian and Southern Oceans
9969#4	25/02/1979	20.34	-58.94	RMT8M/6	1000	1205	1102.5		Indian and Southern Oceans
9966#9	26/02/1979	24.45	-68.47	RMT8M/9	270	320	295		Indian and Southern Oceans
9994#4	18/03/1979	25.74	-59.07	RMT8M/3	500	1000			Indian and Southern Oceans
10000#4	23/03/1979	21.80	-55.59	RMT8M/3	1000	1800	1400		Indian and Southern Oceans
10105#2	31/08/1979	-12.48	54.58	RMT8M/2	1090	1290	2153	2353	NE Atlantic (Rockall Trough, Porcupine Seabight, and NW African coast)
10105#7	01/09/1979	-12.36	54.53	RMT8M/3	800	900	1255	1355	NE Atlantic (Rockall Trough, Porcupine Seabight, and NW African coast)
10105#1	02/09/1979	-12.28	54.40	RMT8M/4	500	600	1729	1829	NE Atlantic (Rockall Trough, Porcupine Seabight, and NW African coast)
10105#12	02/09/1979	-12.55	54.59	RMT8M/2	700	810	2	141	NE Atlantic (Rockall Trough, Porcupine Seabight, and NW African coast)
10105#18	02/09/1979	-12.66	54.66	RMT8M/2	1700	1900	1529	1729	NE Atlantic (Rockall Trough, Porcupine Seabight, and NW African coast)
10105#13	03/09/1979	-12.68	54.61	RMT8M/4	770	900	141	241	NE Atlantic (Rockall Trough, Porcupine Seabight, and NW African coast)
10109#1	06/09/1979	-12.41	49.33	RMT1M/1	60	100	1814	1914	NE Atlantic (Rockall Trough, Porcupine Seabight, and NW African coast)
10109#2	06/09/1979	-12.46	49.31	RMT1M/2	1110	1150	1914	2014	NE Atlantic (Rockall Trough, Porcupine Seabight, and NW African coast)
10109#5	06/09/1979	-12.41	49.33	RMT1M/1	10	900	2029	2124	NE Atlantic (Rockall Trough, Porcupine Seabight, and NW African coast)
10110#3	07/09/1979	-11.76	49.28	RMT8M/1	10	810			NE Atlantic (Rockall Trough, Porcupine Seabight, and NW African coast)
10115#12	12/09/1979	-14.18	49.87	RMT8M/1	295	400	148	248	NE Atlantic (Rockall Trough, Porcupine Seabight, and NW African coast)
10147#37	07/10/1979	-21.29	25.14	RMT8M/1	500	605	532	632	NE Atlantic (Rockall Trough, Porcupine Seabight, and NW African coast)
10222#01	29/10/1980	-30.04	33.06	RMT1M/1	800	900	2016	2116	NE Atlantic (UK/Azores, Madeira abyssal Plain)
10222#09	30/10/1980	-30.07	33.12	RMT8M/3	700	800	1118	1218	NE Atlantic (UK/Azores, Madeira abyssal Plain)
10228#20	02/11/1980	-31.45	33.13	RMT8M/3	650	1000	1804	1851	NE Atlantic (UK/Azores, Madeira abyssal Plain)
10228#28	03/11/1980	-31.52	32.98	RMT8M/1	800	900	926	1026	NE Atlantic (UK/Azores, Madeira abyssal Plain)
10228#30	03/11/1980	-31.45	33.01	RMT8M/3	995	1100	1540	1640	NE Atlantic (UK/Azores, Madeira abyssal Plain)
10228#8	03/11/1980	-31.48	33.06	RMT8M/5	1000	1100	2216	2316	NE Atlantic (UK/Azores, Madeira abyssal Plain)
10233#26	16/11/1980	-31.49	32.05	RMT8M/1	800	910	1149	1249	NE Atlantic (UK/Azores, Madeira abyssal Plain)
10233#28	16/11/1980	-31.57	32.04	RMT8M/3	0	1000	1349	1449	NE Atlantic (UK/Azores, Madeira abyssal Plain)

Table 1: NHM station list continued

Station	Date	Longitude	Latitude	Sampling Gear	Min Depth (m)	Max Depth (m)	Start time of trawl	End time of trawl	Description
10376#8	26/05/1981	-33.41	33.18	RMT8M/2	900	1000	2316	16	NE Atlantic (South West of the Azores)
10376#10	27/05/1981	-33.50	33.28	RMT8M/1	500	602	303	128	NE Atlantic (UK/Azores, Madeira abyssal Plain)
10376#25	28/05/1981	-33.29	32.86	RMT8M/1	1095	1205	0818	0948	NE Atlantic (South West of the Azores)
10376#28	28/05/1981	-33.26	33.07	RMT8M/1	795	900	1503	403	NE Atlantic (South West of the Azores)
10376#29	28/05/1981	-33.31	33.11	RMT8M/2	900	1005	1633	1803	NE Atlantic (South West of the Azores)
10376#39	29/05/1981	-33.57	33.37	RMT8M/3	1600	1700	1415	1600	NE Atlantic (South West of the Azores)
10378#13	08/06/1981	-29.89	32.35	RMT8M/3	1000	1100	1052	1222	NE Atlantic (South West of the Azores)
10379#10	12/06/1981	-33.03	34.94	RMT8M/3	1000	1100	28	119	NE Atlantic (South West of the Azores)
10379#19	12/06/1981	-33.25	35.03	RMT8M/2	900	995	1710	1840	NE Atlantic (South West of the Azores)
10379#20	12/06/1981	-33.24	35.09	RMT8M/3	995	1100	1840	2010	NE Atlantic (South West of the Azores)
10379#21	12/06/1981	-33.20	35.15	RMT8M/1	495	600	2227	922	NE Atlantic (South West of the Azores)
10380#14	18/06/1981	-34.08	29.97	RMT8M/3	1000	1100	20	120	NE Atlantic (South West of the Azores)
10382#2	21/06/1981	-31.95	32.53	RMT8M/1	1100	1200	1106	1306	NE Atlantic (South West of the Azores)
10380#37	22/06/1981	-34.34	29.76	RMT8M/4	1120	1200	18	148	NE Atlantic (South West of the Azores)
10382#8	22/06/1981	-31.84	32.58	RMT8M/1	500	605	248	348	NE Atlantic (South West of the Azores)
10382#31	24/06/1981	-32.16	32.70	RMT8	1080	1210	119	249	NE Atlantic (South West of the Azores)
11036#2	01/04/1984	-14.98	39.41	RMT8M/2	900	1005	1100	1200	NE Atlantic (Iberia and Biscay/Abyssal plains)
11038#1	01/04/1984	-14.86	39.58	RMT8M/1	200	300	2213	2313	NE Atlantic (Iberia and Biscay/Abyssal plains)
11038#2	01/04/1984	-14.91	39.57	RMT8M/2	300	405	2213	0015	NE Atlantic (Iberia and Biscay/Abyssal plains)
11038#3	02/04/1984	-14.95	39.55	RMT8M/3	405	500	15	115	NE Atlantic (Iberia and Biscay/Abyssal plains)
11040#3	02/04/1984	-14.75	39.65	RMT8M/3	700	810	1234	1334	NE Atlantic (Iberia and Biscay/Abyssal plains)
11045#2	03/04/1984	-14.98	39.51	RMT8M/2	70	120	249	349	NE Atlantic (Iberia and Biscay/Abyssal plains)
11045#3	03/04/1984	-15.01	39.49	RMT8M/3	120	200	0349	0449	NE Atlantic (Iberia and Biscay/Abyssal plains)
11050#2	07/04/1984	-14.15	45.66	RMT8M/2	600	700	2221	2320	NE Atlantic (Iberia and Biscay/Abyssal plains)
11050#3	07/04/1984	-13.90	45.80	RMT8M/3	700	800	2320	0020	NE Atlantic (Iberia and Biscay/Abyssal plains)
11057#2	10/04/1984	-13.81	45.63	RMT8M/2	300	400	2234	2334	NE Atlantic (Iberia and Biscay/Abyssal plains)
11066#3	13/04/1984	-14.16	43.92	RMT8M/3	700	1000	1223	1313	NE Atlantic (Iberia and Biscay/Abyssal plains)
11069#3	14/04/1984	-14.61	42.46	RMT8M/2	100	600	0409	0505	NE Atlantic (Iberia and Biscay/Abyssal plains)
11071#2	14/04/1984	-14.89	40.95	RMT8M/2	100	600	1858	2002	NE Atlantic (Iberia and Biscay/Abyssal plains)
11074#3	16/04/1984	-14.90	39.57	RMT8M/3	600	1000	0155	0232	NE Atlantic (Iberia and Biscay/Abyssal plains)
11078#2	17/04/1984	-15.09	39.52	RMT8M/2	605	695	2224	2324	NE Atlantic (Iberia and Biscay/Abyssal plains)
11079#2	18/04/1984	-14.90	39.53	RMT8M/2	300	400	0233	0333	NE Atlantic (Iberia and Biscay/Abyssal plains)
11081#1	18/04/1984	-14.98	39.63	RMT8M/1	800	905	0930	1030	NE Atlantic (Iberia and Biscay/Abyssal plains)
11081#3	18/04/1984	-14.98	39.70	RMT8M/3	1000	1100	1130	1230	NE Atlantic (Iberia and Biscay/Abyssal plains)
11083#2	18/04/1984	-15.01	39.70	RMT8M/2	600	700	1602	1702	NE Atlantic (Iberia and Biscay/Abyssal plains)
11095#1	20/04/1984	-15.04	39.77	RMT8M/1	1100	1215	1258	1505	NE Atlantic (Iberia and Biscay/Abyssal plains)
11095#2	20/04/1984	-15.03	39.70	RMT8M/2	1203	1298	1505	1705	NE Atlantic (Iberia and Biscay/Abyssal plains)
11096#1	20/04/1984	-14.95	39.79	RMT8M/1	1400	1500	2342	0342	NE Atlantic (Iberia and Biscay/Abyssal plains)
11096#2	21/04/1984	-14.85	39.81	RMT8M/2	1500	1600	0142	0342	NE Atlantic (Iberia and Biscay/Abyssal plains)
11096#3	21/04/1984	-14.76	39.84	RMT8M/3	1600	1800	0342	0542	NE Atlantic (Iberia and Biscay/Abyssal plains)

Table 1: NHM station list continued

Station	Date	Longitude	Latitude	Sampling Gear	Min Depth (m)	Max Depth (m)	Start time of trawl	End time of trawl	Description
11121#17	03/06/1984	-21.67	41.80	RMT8M/1	900	1000	1820	2024	NE Atlantic (King's Trough flank, passages from UK to madeira)
11121#25	05/06/1984	-21.68	41.30	NBS	4031	4031	323	530	NE Atlantic (King's Trough flank, passages from UK to madeira)
11125#4	06/06/1984	-20.67	39.88	RMT8M/3	600	1000	1313	1401	NE Atlantic (King's Trough flank, passages from UK to madeira)
11132#4	08/06/1984	-19.26	36.28	RMT8M/3	600	1000	1630	1737	NE Atlantic (King's Trough flank, passages from UK to madeira)
11261#19	28/06/1985	-25.24	31.22	RMT8M/1	910	1000	2146	2246	NE Atlantic (King's Trough flank, passages from UK to madeira)
11794#19	22/06/1988	-19.48	47.39	RMT8M/1	1400	1500	1847	1947	NE Atlantic (Great Meteor East, passage to/from UK)
11794#1	23/06/1988	-19.39	47.32	RMT1M/1	800	900	700	800	NE Atlantic(Porcupine Seabight and Abyssal Plain)
11794#2	23/06/1988	-19.34	47.34	RMT8M/2	900	1000	800	900	NE Atlantic(Porcupine Seabight and Abyssal Plain)
11794#35	26/06/1988	-19.56	47.21	RMT8M/1	1100	1200	1710	1810	NE Atlantic(Porcupine Seabight and Abyssal Plain)
11794#67	30/06/1988	-19.27	47.41	RMT8M/3	3255	3500	138	338	NE Atlantic(Porcupine Seabight and Abyssal Plain)
12064#8	22/05/1990	-17.77	48.59	RMT8M/1	710	800	1308	1408	NE Atlantic(Porcupine Seabight and Abyssal Plain)
12069#1	24/05/1990	-17.63	48.37	RMT8M/1	1020	1100	742	843	Atlantic, SW of Ireland
12071#2	25/05/1990	-17.66	48.48	RMT8M/2	65	100	2253	2339	Atlantic, SW of Ireland
12069#3	28/05/1990	-17.67	48.28	RMT8M/7	800	900	943	1043	Atlantic, SW of Ireland
12082#4	29/05/1990	-17.64	48.32	RMT8M/1	695	800	2342	42	Atlantic, SW of Ireland
12181#14	15/09/1990	-19.66	20.49	CCE	615	720	1121	1251	Atlantic, SW of Ireland
12181#15	15/09/1990	-19.65	20.44	CCE	910	1295	1559	1759	Off coast of Western Sahara, NW Africa
12183#5	19/09/1990	-19.94	17.04	RMT8M/1	600	700	942	1042	Off coast of Senegal, NW Africa
12183#9	19/09/1990	-19.93	17.04	RMT8M/2	495	600	1807	1907	Off coast of Senegal, NW Africa
12183#10	20/09/1990	-19.94	17.06	RMT8M/2	800	900	2158	2258	Off coast of Senegal, NW Africa
12183#13	20/09/1990	-19.94	17.06	RMT8M/1	5	100	310	400	Off coast of Senegal, NW Africa
12183#6	20/09/1990	-19.90	17.07	RMT8M/3	700	800	1042	1142	Off coast of Senegal, NW Africa
12183#21	21/09/1990	-20.01	17.04	RMT8M/2	500	600	2333	33	Off coast of Senegal, NW Africa
12183#23	21/09/1990	-20.01	17.11	RMT8M/3	300	400	133	233	Off coast of Senegal, NW Africa
12185#5	25/09/1990	-19.94	17.04	RMT8M/7	600	700	942	1042	Atlantic, NE of Cabo Verde Islands

Appendices

Table 2 Station list of all *Atolla* sp. distribution data available from the Smithsonian National Museum of Natural History, along with associated sample information. Data available was for 5 species: *A. chuni*, *A. parva*, *A. russelli*, *A. gigantea* and *A. wyvillei*. Data available as Excel worksheet on accompanying digital data. Total number of stations = 233 across the world’s oceans.

Atolla chuni

Current Identification	Date Collected	Station Number	Catalog Number	Specimen Count	Preparation	Collector(s)	Collection Method	Ocean	Expedition Name	Vessel	Cruise	Depth (m)	Accession Number
<i>Atolla chuni</i> (Van hoeffen, 1902)	06-Mar-71	WH-354-II-71	USNM 58478	Larson, R.J. 2	Formalin	Gibbs; Roper		South Atlantic Ocean		Walther Hewig R/V		2000	294756
<i>Atolla chuni</i> (Van hoeffen, 1902)	06-Mar-71	WH-427-71	USNM 58479	Larson, R.J. 1	Formalin	Gibbs; Roper		South Atlantic Ocean		Walther Hewig R/V		2000	294756
<i>Atolla chuni</i> (Van hoeffen, 1902)	05-Mar-71	WH-355-II-71	USNM 58480	Larson, R.J. 2	Formalin	Gibbs; Roper		South Atlantic Ocean		Walther Hewig R/V		300 to 1015	294756
<i>Atolla chuni</i> (Van hoeffen, 1902)	05-Mar-71	WH-361-II-71	USNM 58481	Larson, R.J. 1	Formalin	Gibbs; Roper		South Atlantic Ocean		Walther Hewig R/V		2000	294756
<i>Atolla chuni</i> (Van hoeffen, 1902)	05-Mar-71	WH-362-II-71	USNM 58482	Larson, R.J. 1	Formalin	Gibbs; Roper		South Atlantic Ocean		Walther Hewig R/V		2000	294756
<i>Atolla chuni</i> (Van hoeffen, 1902)	18-Mar-71	WH-402-III-71	USNM 58483	Larson, R.J. 2	Formalin	Gibbs; Roper		South Atlantic Ocean		Walther Hewig R/V		800 to 820	294756
<i>Atolla chuni</i> (Van hoeffen, 1902)	11-Mar-71	WH-376-I-71	USNM 58485	Larson, R.J. 2	Formalin	Gibbs; Roper		South Atlantic Ocean		Walther Hewig R/V		2000	294756
<i>Atolla chuni</i> (Van hoeffen, 1902)	18-Apr-66	1646	USNM 58799	Larson, R.J. 6	Formalin	University of Southern California	Trawl - IKMMWT	South Pacific Ocean	USAP	Elanin R/V	23	1783 to 1950	333053
<i>Atolla chuni</i> (Van hoeffen, 1902)	10-Oct-66	327	USNM 58800	Larson, R.J. 1	Formalin	Smithsonian Oceanographic Sorting Center	Trawl - IKMMWT	South Pacific Ocean	USAP	Elanin R/V	25	680	333053
<i>Atolla chuni</i> (Van hoeffen, 1902)	29-Jul-62	125	USNM 58802	Larson, R.J. 20	Formalin	University of Southern California	Trawl - IKMMWT	South Atlantic Ocean	USAP	Elanin R/V	4	1830	333053
<i>Atolla chuni</i> (Van hoeffen, 1902)	21-Nov-64	1392	USNM 58804	Larson, R.J. 4	Formalin	University of Southern California	Trawl - IKMMWT	South Pacific Ocean	USAP	Elanin R/V	15	897	333053
<i>Atolla chuni</i> (Van hoeffen, 1902)	03-Apr-66	1608	USNM 58806	Larson, R.J. 2	Formalin	University of Southern California	Trawl - IKMMWT	South Pacific Ocean	USAP	Elanin R/V	23	1682 to 1784	333053
<i>Atolla chuni</i> (Van hoeffen, 1902)	28-Jun-64	1167	USNM 58807	Larson, R.J. 2	Formalin	University of Southern California	Trawl - IKMMWT	South Pacific Ocean	USAP	Elanin R/V	13	1047	333053
<i>Atolla chuni</i> (Van hoeffen, 1902)	18-Jul-68	2240	USNM 58811	Larson, R.J. 2	Formalin	University of Southern California	Trawl - IKMMWT	Indian Ocean	USAP	Elanin R/V	34	950 to 1100	333053
<i>Atolla chuni</i> (Van hoeffen, 1902)	12-Mar-66	1689	USNM 58812	Larson, R.J. 2	Formalin	University of Southern California	Trawl - IKMMWT	South Pacific Ocean	USAP	Elanin R/V	34	1047	333053
<i>Atolla chuni</i> (Van hoeffen, 1902)	12-Mar-66	1689	USNM 58817	Larson, R.J. 2	Formalin	University of Southern California	Trawl - IKMMWT	South Pacific Ocean	USAP	Elanin R/V	23	750 to 1150	333053
<i>Atolla chuni</i> (Van hoeffen, 1902)	20-Nov-64	1389	USNM 58818	Larson, R.J. 1	Formalin	University of Southern California	Trawl - IKMMWT	South Pacific Ocean	USAP	Elanin R/V	15	1537 to 2086	333053
<i>Atolla chuni</i> (Van hoeffen, 1902)	02-Apr-66	338	USNM 58819	Larson, R.J. 1	Formalin	Smithsonian Oceanographic Sorting Center	Trawl - IKMMWT	South Pacific Ocean	USAP	Elanin R/V	25	530	333053
<i>Atolla chuni</i> (Van hoeffen, 1902)	07-Apr-66	1606	USNM 58820	Larson, R.J. 7	Formalin	University of Southern California	Trawl - IKMMWT	South Pacific Ocean	USAP	Elanin R/V	23	775	333053
<i>Atolla chuni</i> (Van hoeffen, 1902)	05-May-66	1685	USNM 58821	Larson, R.J. 2	Formalin	University of Southern California	Trawl - IKMMWT	South Pacific Ocean	USAP	Elanin R/V	23	1500 to 2250	333053
<i>Atolla chuni</i> (Van hoeffen, 1902)	11-13	1113	USNM 58822	Larson, R.J. 17	Formalin	University of Southern California	Trawl - IKMMWT	South Pacific Ocean	USAP	Elanin R/V	13	512 to 549	333053
<i>Atolla chuni</i> (Van hoeffen, 1902)	06-Jun-68	2205	USNM 58823	Larson, R.J. 2	Formalin	University of Southern California	Trawl - IKMMWT	South Pacific Ocean	USAP	Elanin R/V	34		333053
<i>Atolla chuni</i> (Van hoeffen, 1902)	22-Apr-66	1652	USNM 58824	Larson, R.J. 1	Formalin	University of Southern California	Trawl - IKMMWT	South Pacific Ocean	USAP	Elanin R/V	23	350 to 450	333053
<i>Atolla chuni</i> (Van hoeffen, 1902)	30-Dec-63	883	USNM 58825	Larson, R.J. 6	Formalin	University of Southern California	Trawl - IKMMWT	South Pacific Ocean	USAP	Elanin R/V	11	1832	333053
<i>Atolla chuni</i> (Van hoeffen, 1902)	24-Jan-64	891	USNM 58826	Larson, R.J. 18	Formalin	University of Southern California	Trawl - IKMMWT	South Pacific Ocean	USAP	Elanin R/V	13	714 to 851	333053
<i>Atolla chuni</i> (Van hoeffen, 1902)	04-Jan-64	891	USNM 58831	Larson, R.J. 4	Formalin	University of Southern California	Trawl - IKMMWT	South Pacific Ocean	USAP	Elanin R/V	11	1347 to 1702	333053
<i>Atolla chuni</i> (Van hoeffen, 1902)	12-Nov-64	1352	USNM 58832	Larson, R.J. 15	Formalin	University of Southern California	Trawl - IKMMWT	South Pacific Ocean	USAP	Elanin R/V	14	2086 to 2416	333053
<i>Atolla chuni</i> (Van hoeffen, 1902)	29-Sep-68	2299	USNM 58834	Larson, R.J. 1	Formalin	University of Miami	Trawl - IKMMWT	Indian Ocean	USAP	Elanin R/V	35	735	333053
<i>Atolla chuni</i> (Van hoeffen, 1902)	22-Sep-68	2294	USNM 58835	Larson, R.J. 1	Formalin	University of Miami	Trawl - IKMMWT	Indian Ocean	USAP	Elanin R/V	35	850	333053
<i>Atolla chuni</i> (Van hoeffen, 1902)	13-Sep-63	738	USNM 58838	Larson, R.J. 4	Formalin	University of Southern California	Trawl - IKMMWT	South Atlantic Ocean	USAP	Elanin R/V	9	778	333053
<i>Atolla chuni</i> (Van hoeffen, 1902)	18-Jul-62	109	USNM 73816	Larson, R.J. 4	Formalin	University of Southern California	Trawl - IKMMWT	South Atlantic Ocean	USAP	Elanin R/V	4	915	356847
<i>Atolla chuni</i> (Van hoeffen, 1902)	28-Jul-62	123	USNM 73817	Larson, R.J. 14	Formalin	University of Southern California	Trawl - IKMMWT	South Atlantic Ocean	USAP	Elanin R/V	4	2439	356847
<i>Atolla chuni</i> (Van hoeffen, 1902)	05-Dec-62	354	USNM 73819	Larson, R.J. 3	Formalin	University of Southern California	Trawl - IKMMWT	South Atlantic Ocean	USAP	Elanin R/V	6	1832 to 2145	356847
<i>Atolla chuni</i> (Van hoeffen, 1902)	19-Aug-63	668	USNM 73820	Larson, R.J. 4	Formalin	University of Southern California	Trawl - IKMMWT	South Atlantic Ocean	USAP	Elanin R/V	9	1495	356847
<i>Atolla chuni</i> (Van hoeffen, 1902)	22-Nov-63	866	USNM 73826	Larson, R.J. 1	Formalin	University of Southern California	Trawl - IKMMWT	South Pacific Ocean	USAP	Elanin R/V	10	1239	356847
<i>Atolla chuni</i> (Van hoeffen, 1902)	27-Nov-63	874	USNM 73827	Larson, R.J. 2	Formalin	University of Southern California	Trawl - IKMMWT	South Pacific Ocean	USAP	Elanin R/V	10	1491	356847
<i>Atolla chuni</i> (Van hoeffen, 1902)	04-Dec-63	882	USNM 73828	Larson, R.J. 9	Formalin	University of Southern California	Trawl - IKMMWT	South Pacific Ocean	USAP	Elanin R/V	11	1347 to 1702	356847
<i>Atolla chuni</i> (Van hoeffen, 1902)	04-Dec-63	881	USNM 73829	Larson, R.J. 9	Formalin	University of Southern California	Trawl - IKMMWT	South Pacific Ocean	USAP	Elanin R/V	11	1347 to 1702	356847
<i>Atolla chuni</i> (Van hoeffen, 1902)	24-May-64	1106	USNM 73834	Larson, R.J. 11	Formalin	University of Southern California	Trawl - IKMMWT	South Pacific Ocean	USAP	Elanin R/V	13	714 to 769	356847

Table 2: Smithsonian samples continued

Atolla chuni continued; *Atolla parva*

Current Identification	Date Collected	Station Number	Catalog Number	Latitude	Longitude	Identified By	Specimen Count	Preparation	Collector(s)	Collection Method	Ocean	Expedition Name	Vessel	Cruise	Depth (m)	Accession Number
<i>Atolla chuni</i> (Vanhooffen, 1920)	30-Jun-64	1170	USNM 73836	-55.042	-129.702	Larson, R. J.	3	Formalin	University of Southern California	Trawl - IMAMT	South Pacific Ocean	USAP	Etanin R/V	13	2880 to 3050	356847
<i>Atolla chuni</i> (Vanhooffen, 1920)	13-Aug-64	1214	USNM 73837	-59.458	-132.598	Larson, R. J.	3	Formalin	University of Southern California	Trawl - IMAMT	South Pacific Ocean	USAP	Etanin R/V	14	2200	356847
<i>Atolla chuni</i> (Vanhooffen, 1920)	29-Aug-64	1235	USNM 73838	-60.025	-132.536	Larson, R. J.	1	Formalin	University of Southern California	Trawl - IMAMT	South Pacific Ocean	USAP	Etanin R/V	14	1700 to 1850	356847
<i>Atolla chuni</i> (Vanhooffen, 1920)	29-Aug-64	1236	USNM 73839	-59.742	-132.536	Larson, R. J.	16	Formalin	University of Southern California	Trawl - IMAMT	South Pacific Ocean	USAP	Etanin R/V	22	1100 to 1039	356847
<i>Atolla chuni</i> (Vanhooffen, 1920)	22-Jul-68	2244	USNM 73843	-54.3	-135.07	Larson, R. J.	1	Formalin	University of Southern California	Trawl - IMAMT	Indian Ocean	USAP	Etanin R/V	34	1000 to 1050	356847
<i>Atolla chuni</i> (Vanhooffen, 1920)	24-Jul-68	2245	USNM 73844	-52.1792	-135.006	Larson, R. J.	1	Formalin	University of Southern California	Trawl - IMAMT	Indian Ocean	USAP	Etanin R/V	34	1000 to 1100	356847
<i>Atolla chuni</i> (Vanhooffen, 1920)	23-Oct-62	278	USNM 58798	-67.05	-75.058	Larson, R. J.	3	Formalin	University of Southern California	Net - Plankton	Antarctic Ocean	USAP	Etanin R/V	5	4	333053
<i>Atolla chuni</i> (Vanhooffen, 1920)	03-May-66	1683	USNM 58801	-60.392	-114.433	Larson, R. J.	1	Formalin	University of Southern California	Trawl - IMAMT	Antarctic Ocean	USAP	Etanin R/V	23	1611 to 1783	333053
<i>Atolla chuni</i> (Vanhooffen, 1920)	26-Jan-64	946	USNM 58803	-67.65	-90.45	Larson, R. J.	2	Formalin	University of Southern California	Trawl - IMAMT	Antarctic Ocean	USAP	Etanin R/V	11	1711	333053
<i>Atolla chuni</i> (Vanhooffen, 1920)	29-May-64	1120	USNM 58805	-62.158	-89.925	Larson, R. J.	2	Formalin	University of Southern California	Trawl - IMAMT	Antarctic Ocean	USAP	Etanin R/V	13	824 to 851	333053
<i>Atolla chuni</i> (Vanhooffen, 1920)	24-Aug-64	1245	USNM 58808	-60.125	-141.083	Larson, R. J.	6	Formalin	University of Southern California	Trawl - IMAMT	Antarctic Ocean	USAP	Etanin R/V	14	3455 to 3660	333053
<i>Atolla chuni</i> (Vanhooffen, 1920)	26-Apr-66	1666	USNM 58809	-62.467	-108.642	Larson, R. J.	3	Formalin	University of Southern California	Trawl - IMAMT	Antarctic Ocean	USAP	Etanin R/V	23	1785 to 2117	333053
<i>Atolla chuni</i> (Vanhooffen, 1920)	19-Jan-64	934	USNM 58810	-61.75	-108.642	Larson, R. J.	1	Formalin	University of Southern California	Trawl - IMAMT	Antarctic Ocean	USAP	Etanin R/V	11	165	333053
<i>Atolla chuni</i> (Vanhooffen, 1920)	19-Jan-64	934	USNM 58811	-61.93	-105.933	Larson, R. J.	5	Formalin	University of Southern California	Trawl - IMAMT	Antarctic Ocean	USAP	Etanin R/V	14	1365	333053
<i>Atolla chuni</i> (Vanhooffen, 1920)	14-Apr-66	1634	USNM 58813	-62.417	-101.025	Larson, R. J.	2	Formalin	University of Southern California	Trawl - IMAMT	Antarctic Ocean	USAP	Etanin R/V	23	900 to 1025	333053
<i>Atolla chuni</i> (Vanhooffen, 1920)	10-Aug-62	143	USNM 58815	-60.05	-65.225	Larson, R. J.	1	Formalin	University of Southern California	Trawl - IMAMT	Antarctic Ocean	USAP	Etanin R/V	4	609	333053
<i>Atolla chuni</i> (Vanhooffen, 1920)	25-Oct-63	793	USNM 58816	-64.275	-82.608	Larson, R. J.	2	Formalin	University of Southern California	Trawl - IMAMT	Antarctic Ocean	USAP	Etanin R/V	10	3294	333053
<i>Atolla chuni</i> (Vanhooffen, 1920)	27-Oct-63	796	USNM 58827	-66.2	-82.425	Larson, R. J.	1	Formalin	University of Southern California	Trawl - IMAMT	Antarctic Ocean	USAP	Etanin R/V	10	3294	333053
<i>Atolla chuni</i> (Vanhooffen, 1920)	24-Apr-66	1658	USNM 58828	-60.017	-108.233	Larson, R. J.	2	Formalin	University of Southern California	Trawl - IMAMT	Antarctic Ocean	USAP	Etanin R/V	23	1400 to 1550	333053
<i>Atolla chuni</i> (Vanhooffen, 1920)	19-Aug-64	1234	USNM 58829	-61.533	-135.933	Larson, R. J.	1	Formalin	University of Southern California	Trawl - IMAMT	Antarctic Ocean	USAP	Etanin R/V	14	1950	333053
<i>Atolla chuni</i> (Vanhooffen, 1920)	18-Nov-63	859	USNM 58830	-62.792	-79.05	Larson, R. J.	2	Formalin	University of Southern California	Trawl - IMAMT	Antarctic Ocean	USAP	Etanin R/V	10	824 to 3052	333053
<i>Atolla chuni</i> (Vanhooffen, 1920)	12-Apr-64	1077	USNM 58832	-61.642	-131.58	Larson, R. J.	1	Formalin	University of Southern California	Trawl - IMAMT	Antarctic Ocean	USAP	Etanin R/V	12	254	333053
<i>Atolla chuni</i> (Vanhooffen, 1920)	12-Jan-64	912	USNM 58836	-63.83	-131.58	Larson, R. J.	4	Formalin	University of Southern California	Trawl - IMAMT	Antarctic Ocean	USAP	Etanin R/V	11	600 to 874	333053
<i>Atolla chuni</i> (Vanhooffen, 1920)	26-Mar-66	1663	USNM 58837	-62.417	-108.592	Larson, R. J.	2	Formalin	University of Southern California	Trawl - IMAMT	Antarctic Ocean	USAP	Etanin R/V	23	600 to 100	333053
<i>Atolla chuni</i> (Vanhooffen, 1920)	15-Aug-64	1220	USNM 58840	-60.917	-160.658	Larson, R. J.	5	Formalin	University of Southern California	Trawl - IMAMT	Antarctic Ocean	USAP	Etanin R/V	14	275	333053
<i>Atolla chuni</i> (Vanhooffen, 1920)	22-Oct-62	275	USNM 73818	-66.475	-72.908	Larson, R. J.	1	Formalin	University of Southern California	Trawl - IMAMT	Antarctic Ocean	USAP	Etanin R/V	5	1885	356847
<i>Atolla chuni</i> (Vanhooffen, 1920)	25-Oct-63	793	USNM 73821	-64.275	-82.608	Larson, R. J.	3	Formalin	University of Southern California	Trawl - IMAMT	Antarctic Ocean	USAP	Etanin R/V	10	3294	356847
<i>Atolla chuni</i> (Vanhooffen, 1920)	28-Oct-63	802	USNM 73822	-65.992	-82.583	Larson, R. J.	1	Formalin	University of Southern California	Trawl - IMAMT	Antarctic Ocean	USAP	Etanin R/V	10	1592	356847
<i>Atolla chuni</i> (Vanhooffen, 1920)	30-Oct-63	811	USNM 73823	-64.767	-78.1	Larson, R. J.	1	Formalin	University of Southern California	Trawl - IMAMT	Antarctic Ocean	USAP	Etanin R/V	10	461 to 1263	356847
<i>Atolla chuni</i> (Vanhooffen, 1920)	04-Nov-63	832	USNM 73824	-62.608	-74.675	Larson, R. J.	1	Formalin	University of Southern California	Trawl - IMAMT	Antarctic Ocean	USAP	Etanin R/V	10	1775 to 2723	356847
<i>Atolla chuni</i> (Vanhooffen, 1920)	06-Nov-63	839	USNM 73825	-62.167	-75.208	Larson, R. J.	5	Formalin	University of Southern California	Trawl - IMAMT	Antarctic Ocean	USAP	Etanin R/V	10	824	356847
<i>Atolla chuni</i> (Vanhooffen, 1920)	12-Jan-64	912	USNM 73830	-63.142	-134.58	Larson, R. J.	3	Formalin	University of Southern California	Trawl - IMAMT	Antarctic Ocean	USAP	Etanin R/V	11	312	356847
<i>Atolla chuni</i> (Vanhooffen, 1920)	12-Jan-64	913	USNM 73831	-63.142	-134.58	Larson, R. J.	3	Formalin	University of Southern California	Trawl - IMAMT	Antarctic Ocean	USAP	Etanin R/V	11	312	356847
<i>Atolla chuni</i> (Vanhooffen, 1920)	21-Mar-64	1020	USNM 73832	-63.88	-131.35	Larson, R. J.	1	Formalin	University of Southern California	Trawl - IMAMT	Antarctic Ocean	USAP	Etanin R/V	12	2159 to 2562	356847
<i>Atolla chuni</i> (Vanhooffen, 1920)	29-Mar-64	1038	USNM 73833	-60.442	-34.108	Larson, R. J.	1	Formalin	University of Southern California	Trawl - IMAMT	Antarctic Ocean	USAP	Etanin R/V	12	851 to 1281	356847
<i>Atolla chuni</i> (Vanhooffen, 1920)	07-Jun-64	1132	USNM 73835	-66.175	-92.833	Larson, R. J.	1	Formalin	University of Southern California	Trawl - IMAMT	Antarctic Ocean	USAP	Etanin R/V	13	1318 to 1812	356847
<i>Atolla chuni</i> (Vanhooffen, 1920)	07-Apr-66	1630	USNM 73840	-63.5	-94.05	Larson, R. J.	1	Formalin	University of Southern California	Trawl - IMAMT	Antarctic Ocean	USAP	Etanin R/V	23	1250	356847
<i>Atolla chuni</i> (Vanhooffen, 1920)	15-Apr-66	1637	USNM 73841	-63.742	-101.867	Larson, R. J.	1	Formalin	University of Southern California	Trawl - IMAMT	Antarctic Ocean	USAP	Etanin R/V	23	825 to 1350	356847
<i>Atolla chuni</i> (Vanhooffen, 1920)	01-May-66	1679	USNM 73842	-62.2	-134.842	Larson, R. J.	10 ea.	Formalin	University of Southern California	Trawl - IMAMT	Antarctic Ocean	USAP	Etanin R/V	23	1130 to 1180	356847

Current Identification	Date Collected	Station Number	Catalog Number	Latitude	Longitude	Identified By	Specimen Count	Preparation	Collector(s)	Collection Method	Ocean	Expedition Name	Vessel	Cruise	Depth (m)	Accession Number
<i>Atolla parva</i> (Russell, 1958)	20-Aug-66	1793	USNM 58870	-39.75	-127.008	Larson, R. J.	1	Formalin	University of Southern California	Trawl - IMAMT	South Pacific Ocean	USAP	Etanin R/V	24	1200	333053
<i>Atolla parva</i> (Russell, 1958)	19-Aug-66	1765	USNM 58871	-38.208	-134.608	Larson, R. J.	1	Formalin	University of Southern California	Trawl - IMAMT	South Pacific Ocean	USAP	Etanin R/V	24	2860	333053
<i>Atolla parva</i> (Russell, 1958)	09-Sep-66	1766	USNM 58872	-38.208	-134.608	Larson, R. J.	1	Formalin	University of Southern California	Trawl - IMAMT	South Pacific Ocean	USAP	Etanin R/V	24	2860	333053
<i>Atolla parva</i> (Russell, 1958)	17-Sep-75	A-51	USNM 59326	33.17	-118.5	Larson, R. J.	1	Alcohol (Ethanol)	United States Fish Commission	Trawl - Blake Rea	North Pacific Ocean	USAP	Etanin R/V	700	1554	327005
<i>Atolla parva</i> (Russell, 1958)	04-Jun-70	5471	USNM 58549	32	-64.27	Larson, R. J.	1	Formalin	Gilbes Reper	Trawl - IMAMT, 10 North Atlantic Ocean	North Pacific Ocean	USAP	Etanin R/V	0 to 150	319613	
<i>Atolla parva</i> (Russell, 1958)	19-Jun-69	RH667-39	USNM 58516	13.5825	-123.785	Larson, R. J.	1	Formalin	United States Fish Commission	Trawl - Agassiz Bay North Pacific Ocean	North Pacific Ocean	USAP	Etanin R/V	31	471 to 627	227207
<i>Atolla parva</i> (Russell, 1958)	23-Nov-67	RH667-41	USNM 58617	10.917	-149.3	Larson, R. J.	1	Formalin	Smithsonian Institution	Trawl - IMAMT	North Pacific Ocean	USAP	Etanin R/V	31	627	227207
<i>Atolla parva</i> (Russell, 1958)	25-Nov-67	RH667-41	USNM 58759	4.35	-154.608	Larson, R. J.	1	Formalin	Smithsonian Institution	Trawl - IMAMT	North Pacific Ocean	USAP	Etanin R/V	31	0 to 1000	332050
<i>Atolla parva</i> (Russell, 1958)	27-Apr-78	252	USNM 58760	21.33	-138.3	Larson, R. J.	2	Formalin	Smithsonian Institution	Trawl - IMAMT	South Pacific Ocean	Sargo Exped/Hana Keoki R/V	21	825 to 1000	333053	
<i>Atolla parva</i> (Russell, 1958)	28-Apr-66	1765	USNM 58866	-39.75	-127.008	Larson, R. J.	1	Formalin	Smithsonian Oceanographic Sorting Center	Trawl - IMAMT	South Pacific Ocean	USAP	Etanin R/V	24	150 to 324	333053
<i>Atolla parva</i> (Russell, 1958)	28-May-62	226	USNM 58867	-40.27	-130.15	Larson, R. J.	1	Formalin	University of Southern California	Trawl - IMAMT	South Pacific Ocean	USAP	Etanin R/V	5	1500	333053
<i>Atolla parva</i> (Russell, 1958)	24-Aug-66	1804	USNM 58868	-39.625	-125.867	Larson, R. J.	1	Formalin	University of Southern California	Trawl - IMAMT	South Pacific Ocean	USAP	Etanin R/V	24	1500	333053
<i>Atolla parva</i> (Russell, 1958)	26-Jul-66	1799	USNM 58869	-40.258	-144.733	Larson, R. J.	1	Formalin	University of Southern California	Trawl - IMAMT	South Pacific Ocean	USAP	Etanin R/V	24	1125	333053

Table 2: Smithsonian samples continued

Atolla russelli; *Atolla gigantea*

Current Identification	Date Collected	Station Number	Catalog Number	Latitude	Longitude	Identified By	Specimen Count	Preparation	Collector(s)	Collection Method	Ocean	Expedition Name	Vessel	Cruise	Depth (m)	Accession Number
<i>Atolla russelli</i> (Reptin, 1962)	09-Jun-70	6-B	USNM 59709	32.37	-64.23	Larson, R. J.	1	Formalin	United States Navy	Trawl - IKMMT, 3	North Atlantic Ocean	Ocean Actin Pro Sands R/V		10	230	319313
Current Identification	Date Collected	Station Number	Catalog Number	Latitude	Longitude	Identified By	Specimen Count	Preparation	Collector(s)	Collection Method	Ocean	Expedition Name	Vessel	Cruise	Depth (m)	Accession Number
<i>Atolla gigantea</i> (Mars, 1897)	16-Dec-09	5647	USNM 28690	-5.5667	122.304	Mayer, A. G.	1	Formalin	United States Fish Commission	Trawl - Agassiz	Indian Ocean	Philippines ExAlbatross R/V			949	

Table 2: Smithsonian samples continued

Atolla wyvillei

Current Identification	Date Collected	Station Number	Catalog Number	Latitude	Longitude	Identified By	Specimen Count	Preparation	Collector(s)	Collection Method	Ocean	Expedition Name	Vessel	Cruise	Depth (m)	Accession Number
Atolla wyvillei (Haeckel, 1880)	31 Aug 1885	2569	USNM 13672	38.4333	-68.0583	Fewkes, J. W.	1	Alcohol (Ethanol)	United States Fish Commission	Trawl - Large Bea North Atlantic Ocean	North Atlantic Ocean	Hawaiian Exped	Albatross R/V		3259	53758
Atolla wyvillei (Haeckel, 1880)	31 Sep 1885	2717	USNM 13245	38.4333	-71.2607	Fewkes, J. W.	2 ca.	Alcohol (Ethanol)	United States Fish Commission	Trawl - Large Bea North Atlantic Ocean	North Atlantic Ocean	Hawaiian Exped	Albatross R/V		3259	53758
Atolla wyvillei (Haeckel, 1880)	27 Oct 1885	2718	USNM 13246	38.3333	-71.2607	Fewkes, J. W.	3	Alcohol (Ethanol)	United States Fish Commission	Trawl - Large Bea North Atlantic Ocean	North Atlantic Ocean	Hawaiian Exped	Albatross R/V		3259	53758
Atolla wyvillei (Haeckel, 1880)	26 Oct 1886	2732	USNM 15756	37.45	-73.95	Fewkes, J. W.	3	Alcohol (Ethanol)	United States Fish Commission	Trawl - Large Bea North Atlantic Ocean	North Atlantic Ocean	Hawaiian Exped	Albatross R/V		2107	46886
Atolla wyvillei (Haeckel, 1880)	17-Jun-02	4005	USNM 23201	21.8528	-159.64	Mayer, A. G.	1	Alcohol (Ethanol)	United States Fish Commission	Trawl - Tanner Be North Pacific Ocean	North Pacific Ocean	Philippines Exped	Albatross R/V		878 to 1055	46886
Atolla wyvillei (Haeckel, 1880)	10-Apr-08	5203	USNM 27926	9.9667	125.128	Mayer, A. G.	1	Alcohol (Ethanol)	United States Fish Commission	Trawl - Agassiz be North Pacific Ocean	North Pacific Ocean	Philippines Exped	Albatross R/V		1417	49876
Atolla wyvillei (Haeckel, 1880)	10-Apr-08	5202	USNM 27927	10.2	125.069	Mayer, A. G.	3	Alcohol (Ethanol)	United States Fish Commission	Multiple gears ds South Pacific Ocean	South Pacific Ocean	Philippines Exped	Albatross R/V		918	49876
Atolla wyvillei (Haeckel, 1880)	21-Nov-04	4672	USNM 28034	-13.1917	-78.3	Bigelow, H. B.	1	Alcohol (Ethanol)	United States Fish Commission	Multiple gears us South Pacific Ocean	South Pacific Ocean	Eastern Pacific	Albatross R/V		732	49746
Atolla wyvillei (Haeckel, 1880)	12-Nov-04	4655	USNM 28339	-5.9583	-81.8333	Bigelow, H. B.	1	Alcohol (Ethanol)	United States Fish Commission	Multiple gears us South Pacific Ocean	South Pacific Ocean	Eastern Pacific	Albatross R/V		732	49746
Atolla wyvillei (Haeckel, 1880)	12-Nov-04	4655	USNM 28339	-5.9583	-81.8333	Bigelow, H. B.	1	Alcohol (Ethanol)	United States Fish Commission	Multiple gears us South Pacific Ocean	South Pacific Ocean	Eastern Pacific	Albatross R/V		732	49746
Atolla wyvillei (Haeckel, 1880)	10-Apr-08	5203	USNM 28332	9.9667	125.128	Mayer, A. G.	1	Alcohol (Ethanol)	United States Fish Commission	Trawl - Agassiz be North Pacific Ocean	North Pacific Ocean	Philippines Exped	Albatross R/V		1417	49876
Atolla wyvillei (Haeckel, 1880)	27-Dec-08	5348	USNM 28681	10.9625	118.638	Mayer, A. G.	1	Formalin	United States Fish Commission	Trawl - Tanner Be North Pacific Ocean	North Pacific Ocean	Philippines Exped	Albatross R/V		686	53758
Atolla wyvillei (Haeckel, 1880)	17-Dec-09	5550	USNM 28683	-4.8958	121.483	Mayer, A. G.	1	Formalin	United States Fish Commission	Trawl - Agassiz be South Pacific Ocean	South Pacific Ocean	Philippines Exped	Albatross R/V		988	53758
Atolla wyvillei (Haeckel, 1880)	19-Aug-09	5533	USNM 28684	9.4542	123.53	Mayer, A. G.	1	Formalin	United States Fish Commission	Trawl - Tanner Be North Pacific Ocean	North Pacific Ocean	Philippines Exped	Albatross R/V		790	53758
Atolla wyvillei (Haeckel, 1880)	20-Jul-08	5285	USNM 28685	13.66	120.549	Mayer, A. G.	8 ca.	Formalin	United States Fish Commission	Trawl - Agassiz be North Pacific Ocean	North Pacific Ocean	Philippines Exped	Albatross R/V		497	53758
Atolla wyvillei (Haeckel, 1880)	17-Dec-09	5652	USNM 28687	-4.5833	121.385	Mayer, A. G.	4	Formalin	United States Fish Commission	Trawl - Agassiz be North Pacific Ocean	North Pacific Ocean	Philippines Exped	Albatross R/V		960	53758
Atolla wyvillei (Haeckel, 1880)	19-Dec-09	5657	USNM 28688	-3.3278	120.608	Mayer, A. G.	4	Formalin	United States Fish Commission	Trawl - Agassiz be South Pacific Ocean	South Pacific Ocean	Philippines Exped	Albatross R/V		900	53758
Atolla wyvillei (Haeckel, 1880)	02-Aug-09	5493	USNM 28689	9.0667	125.333	Mayer, A. G.	4	Formalin	United States Fish Commission	Trawl - Tanner Be North Pacific Ocean	North Pacific Ocean	Philippines Exped	Albatross R/V		874	53758
Atolla wyvillei (Haeckel, 1880)	17-Dec-08	5490	USNM 28690	10.7778	118.463	Bigelow, H. B.	1	Formalin	United States Fish Commission	Trawl - Tanner Be North Pacific Ocean	North Pacific Ocean	Philippines Exped	Albatross R/V		1097	53758
Atolla wyvillei (Haeckel, 1880)	06-Apr-09	5430	USNM 28938	9.9667	119.065	Bigelow, H. B.	1 ca.	Formalin	United States Fish Commission	Trawl - Agassiz be North Pacific Ocean	North Pacific Ocean	Philippines Exped	Albatross R/V		010, 849	52960
Atolla wyvillei (Haeckel, 1880)	20 Mar 1889	3009	USNM 29423	9.8278	-111.7	Bigelow, H. B.	1	Formalin	United States Fish Commission	Trawl - Large Bea North Pacific Ocean	North Pacific Ocean	Northwestern	Albatross R/V		1567	53758
Atolla wyvillei (Haeckel, 1880)	21-May-06	4760	USNM 29657	53.8833	-144.883	Bigelow, H. B.	3	Alcohol (Ethanol)	United States Fish Commission	Multiple gears us North Pacific Ocean	North Pacific Ocean	Northwestern	Albatross R/V		549 to 1410	53758
Atolla wyvillei (Haeckel, 1880)	03-Jun-06	4767	USNM 29658	54.2	179.125	Bigelow, H. B.	8	Alcohol (Ethanol)	United States Fish Commission	Multiple gears us North Pacific Ocean	North Pacific Ocean	Northwestern	Albatross R/V		1538	53758
Atolla wyvillei (Haeckel, 1880)	14 Sep 1889	3685	USNM 29678	47.4917	-125.717	Bigelow, H. B.	1	Alcohol (Ethanol)	United States Fish Commission	Trawl - Tanner Be North Pacific Ocean	North Pacific Ocean	Northwestern	Albatross R/V		1163	53758
Atolla wyvillei (Haeckel, 1880)	28 Jun 1889	3070	USNM 29679	30.4	129.1	Bigelow, H. B.	2	Alcohol (Ethanol)	United States Fish Commission	Trawl - Large Bea North Pacific Ocean	North Pacific Ocean	Northwestern	Albatross R/V		660	53758
Atolla wyvillei (Haeckel, 1880)	13-Aug-06	4917	USNM 29680	47.4833	-125.558	Bigelow, H. B.	1	Alcohol (Ethanol)	United States Fish Commission	Trawl - Large Bea North Pacific Ocean	North Pacific Ocean	Northwestern	Albatross R/V		4259	53758
Atolla wyvillei (Haeckel, 1880)	28 Jun 1889	3071	USNM 29681	30.4	129.1	Bigelow, H. B.	2	Alcohol (Ethanol)	United States Fish Commission	Multiple gears us North Pacific Ocean	North Pacific Ocean	Northwestern	Albatross R/V		910, 794	53758
Atolla wyvillei (Haeckel, 1880)	11-Aug-06	4909	USNM 29682	31.6417	-129.458	Bigelow, H. B.	2	Alcohol (Ethanol)	United States Fish Commission	Multiple gears us North Pacific Ocean	North Pacific Ocean	Northwestern	Albatross R/V		2067	53758
Atolla wyvillei (Haeckel, 1880)	29-May-06	4764	USNM 29684	53.3333	-171	Bigelow, H. B.	1	Alcohol (Ethanol)	United States Fish Commission	Trawl - Agassiz be North Pacific Ocean	North Pacific Ocean	Northwestern	Albatross R/V		549 to 2226	53758
Atolla wyvillei (Haeckel, 1880)	29-May-06	4765	USNM 29688	53.2	-171.617	Bigelow, H. B.	1	Alcohol (Ethanol)	United States Fish Commission	Multiple gears us North Pacific Ocean	North Pacific Ocean	Northwestern	Albatross R/V		2469	53758
Atolla wyvillei (Haeckel, 1880)	22-Aug-06	4953	USNM 29732	31.65	132.911	Bigelow, H. B.	1	Alcohol (Ethanol)	United States Fish Commission	Trawl - Agassiz be North Pacific Ocean	North Pacific Ocean	Northwestern	Albatross R/V		549 to 3230	53758
Atolla wyvillei (Haeckel, 1880)	31-May-06	4766	USNM 29733	52.6333	-174.817	Bigelow, H. B.	2	Alcohol (Ethanol)	United States Fish Commission	Multiple gears us North Pacific Ocean	North Pacific Ocean	Northwestern	Albatross R/V		1187	53758
Atolla wyvillei (Haeckel, 1880)	30-Aug-06	4971	USNM 29734	33.3917	135.567	Bigelow, H. B.	1	Alcohol (Ethanol)	United States Fish Commission	Trawl - Tanner Be North Pacific Ocean	North Pacific Ocean	Northwestern	Albatross R/V		1039 to 1068	53758
Atolla wyvillei (Haeckel, 1880)	04-Jun-06	4774	USNM 29735	54.55	178.75	Bigelow, H. B.	1	Alcohol (Ethanol)	United States Fish Commission	Trawl - Tanner Be North Pacific Ocean	North Pacific Ocean	Northwestern	Albatross R/V		1933	53758
Atolla wyvillei (Haeckel, 1880)	07-Jun-06	4917	USNM 29736	52.0167	124.65	Bigelow, H. B.	1	Alcohol (Ethanol)	United States Fish Commission	Trawl - Agassiz be North Pacific Ocean	North Pacific Ocean	Northwestern	Albatross R/V		660	53758
Atolla wyvillei (Haeckel, 1880)	13-Aug-06	4917	USNM 29737	30.4	129.1	Bigelow, H. B.	1	Alcohol (Ethanol)	United States Fish Commission	Trawl - Agassiz be North Pacific Ocean	North Pacific Ocean	Northwestern	Albatross R/V		660	53758

Appendices

Table 2: Smithsonian samples continued

Atolla wyvillei continued

Current Identification	Date Collected	Station Number	Catalog Number	Latitude	Longitude	Identified By	Specimen Count	Preparation	Collector(s)	Collection Method	Ocean	Expedition Name	Vessel	Cruise	Depth (m)	Accession Number
<i>Atolla wyvillei</i> (Haacke), 1880	5 Nov-1883	2104	USNM 6723	38.8	-72.675	Fewkes, J. W.	1	Alcohol (Ethanol)	United States Fish Commission	Trawl - Beam	North Atlantic Ocean	USAP	Albatross R/V		1522	35687
<i>Atolla wyvillei</i> (Haacke), 1880	10-Nov-83	846	USNM 7284	-57.658	-74.708	Larson, R. J.	12	Formalin	University of Southern California	Trawl - IKMWT	South Pacific Ocean	USAP	Etanin R/V	4	1866	35687
<i>Atolla wyvillei</i> (Haacke), 1880	31-Dec-63	852	USNM 7285	-56.65	-74.983	Larson, R. J.	2	Formalin	University of Southern California	Trawl - IKMWT	South Pacific Ocean	USAP	Etanin R/V	10	3111	35687
<i>Atolla wyvillei</i> (Haacke), 1880	13-Dec-63	886	USNM 7287	-57.325	-115.258	Larson, R. J.	4	Formalin	University of Southern California	Trawl - IKMWT	South Pacific Ocean	USAP	Etanin R/V	11	1503 to 3074	35687
<i>Atolla wyvillei</i> (Haacke), 1880	04-Jan-64	891	USNM 7288	-59.783	-114.808	Larson, R. J.	11	Formalin	University of Southern California	Trawl - IKMWT	South Pacific Ocean	USAP	Etanin R/V	11	1347 to 1702	35687
<i>Atolla wyvillei</i> (Haacke), 1880	10-Apr-64	1071	USNM 7289	-59.133	-136.692	Larson, R. J.	3	Formalin	University of Southern California	Trawl - IKMWT	South Atlantic Ocean	USAP	Etanin R/V	12	1967 to 2333	35687
<i>Atolla wyvillei</i> (Haacke), 1880	12-Nov-64	1362	USNM 73803	-57.492	-139.492	Larson, R. J.	6	Formalin	University of Southern California	Trawl - IKMWT	South Pacific Ocean	USAP	Etanin R/V	15	2306 to 2416	35687
<i>Atolla wyvillei</i> (Haacke), 1880	20-Nov-64	1389	USNM 73804	-55.925	-149.833	Larson, R. J.	13	Formalin	University of Southern California	Trawl - IKMWT	South Pacific Ocean	USAP	Etanin R/V	23	1537 to 2086	35687
<i>Atolla wyvillei</i> (Haacke), 1880	09-Apr-66	1609	USNM 73805	-58.042	-77.2	Larson, R. J.	3	Formalin	University of Southern California	Trawl - IKMWT	South Pacific Ocean	USAP	Etanin R/V	23	1882 to 1784	35687
<i>Atolla wyvillei</i> (Haacke), 1880	19-Apr-66	1618	USNM 73811	-58.508	-101.2	Larson, R. J.	25	Formalin	University of Southern California	Trawl - IKMWT	South Pacific Ocean	USAP	Etanin R/V	23	700 to 925	35687
<i>Atolla wyvillei</i> (Haacke), 1880	29-Apr-66	1619	USNM 73812	-58.567	-101.567	Larson, R. J.	8	Formalin	University of Southern California	Trawl - IKMWT	South Pacific Ocean	USAP	Etanin R/V	23	700 to 925	35687
<i>Atolla wyvillei</i> (Haacke), 1880	29-May-68	2189	USNM 73813	-55.627	-121.925	Larson, R. J.	3	Formalin	University of Southern California	Trawl - IKMWT	South Pacific Ocean	USAP	Etanin R/V	33	1829	35687
<i>Atolla wyvillei</i> (Haacke), 1880	29-May-68	2299	USNM 73815	-52.008	-123.967	Larson, R. J.	7	Formalin	University of Miami	Trawl - IKMWT	Indian Ocean	USAP	Etanin R/V	35	735	35687
<i>Atolla wyvillei</i> (Haacke), 1880	18 Jul-1884	2053	USNM 8742	37.1333	-74.55	Fewkes, J. W.	1	Alcohol (Ethanol)	United States Fish Commission	Trawl - Large Beam	North Atlantic Ocean	USAP	Albatross R/V		786	
<i>Atolla wyvillei</i> (Haacke), 1880	18 Jul-1883	2037	USNM 9181	38.8333	-69.397	Fewkes, J. W.	1	Alcohol (Ethanol)	United States Fish Commission	Trawl - Beam	North Atlantic Ocean	USAP	Albatross R/V		3166	
<i>Atolla wyvillei</i> (Haacke), 1880	17 Jul-1883	2034	USNM 9182	39.4528	-69.389	Fewkes, J. W.	1	Alcohol (Ethanol)	United States Fish Commission	Trawl - Beam	North Atlantic Ocean	USAP	Albatross R/V		2462	
<i>Atolla wyvillei</i> (Haacke), 1880	29 Jul-1883	2040	USNM 9183	38.5869	-68.267	Fewkes, J. W.	1	Alcohol (Ethanol)	United States Fish Commission	Trawl - Deep Sea	North Atlantic Ocean	USAP	Albatross R/V		4071	
<i>Atolla wyvillei</i> (Haacke), 1880	31 Jul-1883	2045	USNM 9309	40.0722	-68.736	Fewkes, J. W.	1	Alcohol (Ethanol)	United States Fish Commission	Trawl - Beam	North Atlantic Ocean	USAP	Albatross R/V		682	
<i>Atolla wyvillei</i> (Haacke), 1880	12-Jun-68	2210	USNM 58841	-60.67	160.48	Larson, R. J.	14	Formalin	University of Southern California	Trawl - IKMWT	Antarctic Ocean	USAP	Etanin R/V	34	1280	333053
<i>Atolla wyvillei</i> (Haacke), 1880	13-Feb-72	892	USNM 58842	-76.0233	-160.863	Larson, R. J.	1	Formalin	University of Southern California	Net - WPZ	Antarctic Ocean	USAP	Etanin R/V	51	500	333053
<i>Atolla wyvillei</i> (Haacke), 1880	16-Jul-68	2238A	USNM 58845	-60.02	145.3	Larson, R. J.	11	Formalin	University of Southern California	Trawl - IKMWT	Antarctic Ocean	USAP	Etanin R/V	84	1000	333053
<i>Atolla wyvillei</i> (Haacke), 1880	18-Jul-72	893	USNM 58846	-60.02	145.3	Larson, R. J.	2	Formalin	University of Southern California	Trawl - IKMWT	Antarctic Ocean	USAP	Etanin R/V	84	1000	333053
<i>Atolla wyvillei</i> (Haacke), 1880	11-Apr-66	1627	USNM 58849	-60.983	-160.884	Larson, R. J.	7	Formalin	University of Southern California	Trawl - IKMWT	Antarctic Ocean	USAP	Etanin R/V	23	1125 to 1300	333053
<i>Atolla wyvillei</i> (Haacke), 1880	09-Feb-68	2111	USNM 58854	-74.175	-174.825	Larson, R. J.	2	Formalin	University of Southern California	Trawl - IKMWT	Antarctic Ocean	USAP	Etanin R/V	32	1880	333053
<i>Atolla wyvillei</i> (Haacke), 1880	06-Jan-64	895	USNM 58856	-60.875	-114.867	Larson, R. J.	9	Formalin	University of Southern California	Trawl - IKMWT	Antarctic Ocean	USAP	Etanin R/V	11	2315	333053
<i>Atolla wyvillei</i> (Haacke), 1880	03-Aug-62	132	USNM 73777	-61.542	-82.292	Larson, R. J.	43	Formalin	University of Southern California	Trawl - IKMWT	Antarctic Ocean	USAP	Etanin R/V	4	1219	35687
<i>Atolla wyvillei</i> (Haacke), 1880	23-Oct-63	785	USNM 73779	-62.725	-83.033	Larson, R. J.	3	Formalin	University of Southern California	Trawl - IKMWT	Antarctic Ocean	USAP	Etanin R/V	10	3660 to 4099	35687
<i>Atolla wyvillei</i> (Haacke), 1880	25-Oct-63	793	USNM 73781	-64.275	-82.608	Larson, R. J.	1	Formalin	University of Southern California	Trawl - IKMWT	Antarctic Ocean	USAP	Etanin R/V	10	3294	35687
<i>Atolla wyvillei</i> (Haacke), 1880	30-Oct-63	811	USNM 73782	-64.767	-78.1	Larson, R. J.	14	Formalin	University of Southern California	Trawl - IKMWT	Antarctic Ocean	USAP	Etanin R/V	30	461 to 1263	35687
<i>Atolla wyvillei</i> (Haacke), 1880	05-Nov-63	886	USNM 73783	-61.167	-75.175	Larson, R. J.	3	Formalin	University of Southern California	Trawl - IKMWT	Antarctic Ocean	USAP	Etanin R/V	30	2745	35687
<i>Atolla wyvillei</i> (Haacke), 1880	06-Nov-63	899	USNM 73786	-62.292	-75.208	Larson, R. J.	15	Formalin	University of Southern California	Trawl - IKMWT	Antarctic Ocean	USAP	Etanin R/V	30	824 to 1052	35687
<i>Atolla wyvillei</i> (Haacke), 1880	18-Nov-63	902	USNM 73787	-62.292	-75.208	Larson, R. J.	14	Formalin	University of Southern California	Trawl - IKMWT	Antarctic Ocean	USAP	Etanin R/V	30	824 to 1052	35687
<i>Atolla wyvillei</i> (Haacke), 1880	13-Jan-64	914	USNM 73790	-65.792	-114.733	Larson, R. J.	20	Formalin	University of Southern California	Trawl - IKMWT	Antarctic Ocean	USAP	Etanin R/V	11	1169	35687
<i>Atolla wyvillei</i> (Haacke), 1880	15-Jan-64	917	USNM 73793	-66.65	-115.408	Larson, R. J.	4	Formalin	University of Southern California	Trawl - IKMWT	Antarctic Ocean	USAP	Etanin R/V	11	580	35687
<i>Atolla wyvillei</i> (Haacke), 1880	21-Jan-64	936	USNM 73792	-70.117	-101.258	Larson, R. J.	3	Formalin	University of Southern California	Trawl - IKMWT	Antarctic Ocean	USAP	Etanin R/V	11	2379	35687
<i>Atolla wyvillei</i> (Haacke), 1880	22-Jan-64	940	USNM 73793	-70.117	-98.833	Larson, R. J.	2	Formalin	University of Southern California	Trawl - IKMWT	Antarctic Ocean	USAP	Etanin R/V	11	1049	35687
<i>Atolla wyvillei</i> (Haacke), 1880	24-Jan-64	944	USNM 73794	-68.925	-95.075	Larson, R. J.	1	Formalin	University of Southern California	Trawl - IKMWT	Antarctic Ocean	USAP	Etanin R/V	11	3029	35687
<i>Atolla wyvillei</i> (Haacke), 1880	26-Jan-64	946	USNM 73795	-67.65	-90.45	Larson, R. J.	3	Formalin	University of Southern California	Trawl - IKMWT	Antarctic Ocean	USAP	Etanin R/V	11	1711	35687
<i>Atolla wyvillei</i> (Haacke), 1880	19-Mar-64	1014	USNM 73796	-65.075	-88.008	Larson, R. J.	6	Formalin	University of Southern California	Trawl - IKMWT	Antarctic Ocean	USAP	Etanin R/V	12	1025 to 1153	35687
<i>Atolla wyvillei</i> (Haacke), 1880	21-Mar-64	1020	USNM 73797	-63.883	-84.375	Larson, R. J.	4	Formalin	University of Southern California	Trawl - IKMWT	Antarctic Ocean	USAP	Etanin R/V	12	2359 to 2562	35687
<i>Atolla wyvillei</i> (Haacke), 1880	23-Mar-64	1022	USNM 73798	-62.992	-84.375	Larson, R. J.	2	Formalin	University of Southern California	Trawl - IKMWT	Antarctic Ocean	USAP	Etanin R/V	12	695 to 824	35687
<i>Atolla wyvillei</i> (Haacke), 1880	25-Mar-64	1024	USNM 73799	-62.992	-84.375	Larson, R. J.	6	Formalin	University of Southern California	Trawl - IKMWT	Antarctic Ocean	USAP	Etanin R/V	12	695 to 824	35687
<i>Atolla wyvillei</i> (Haacke), 1880	07-Jun-64	1131	USNM 73800	-65.175	-92.833	Larson, R. J.	8	Formalin	University of Southern California	Trawl - IKMWT	Antarctic Ocean	USAP	Etanin R/V	13	824 to 849	35687
<i>Atolla wyvillei</i> (Haacke), 1880	07-Jun-64	1133	USNM 73802	-66.942	-92.725	Larson, R. J.	1	Formalin	University of Southern California	Trawl - IKMWT	Antarctic Ocean	USAP	Etanin R/V	13	1318 to 1812	35687
<i>Atolla wyvillei</i> (Haacke), 1880	09-Apr-66	1615	USNM 73806	-62.292	-95.767	Larson, R. J.	23	Formalin	University of Southern California	Trawl - IKMWT	Antarctic Ocean	USAP	Etanin R/V	13	560 to 791	35687
<i>Atolla wyvillei</i> (Haacke), 1880	10-Apr-66	1623	USNM 73807	-61.458	-95.867	Larson, R. J.	4	Formalin	University of Southern California	Trawl - IKMWT	Antarctic Ocean	USAP	Etanin R/V	23	800 to 1025	35687
<i>Atolla wyvillei</i> (Haacke), 1880	14-Apr-66	1634	USNM 73808	-62.417	-101.025	Larson, R. J.	11	Formalin	University of Southern California	Trawl - IKMWT	Antarctic Ocean	USAP	Etanin R/V	23	575 to 725	35687
<i>Atolla wyvillei</i> (Haacke), 1880	15-Apr-66	1637	USNM 73809	-63.742	-101.967	Larson, R. J.	10	Formalin	University of Southern California	Trawl - IKMWT	Antarctic Ocean	USAP	Etanin R/V	23	900 to 1025	35687
<i>Atolla wyvillei</i> (Haacke), 1880	16-Apr-66	1641	USNM 73810	-61.358	-101.6	Larson, R. J.	26	Formalin	University of Southern California	Trawl - IKMWT	Antarctic Ocean	USAP	Etanin R/V	23	825 to 1350	35687
<i>Atolla wyvillei</i> (Haacke), 1880	19-Jul-68	2241	USNM 73814	-60.017	135.253	Larson, R. J.	7	Formalin	University of Southern California	Trawl - IKMWT	Antarctic Ocean	USAP	Etanin R/V	34	750 to 850	35687
<i>Atolla wyvillei</i> (Haacke), 1880	14-Aug-07	86	USNM 1110162	27.1108	-91.1646	Ames, Cheryl L	4	Formalin	University of Southern California	Trawl - IKMWT	Antarctic Ocean	USAP	Etanin R/V	34	924 to 952	35687
<i>Atolla wyvillei</i> (Haacke), 1880	15-Aug-07	87	USNM 1110169	27.11	-91.1699	Ames, Cheryl L	2	Formalin	University of Southern California	Trawl - IKMWT	Antarctic Ocean	USAP	Etanin R/V	34	924 to 952	35687
<i>Atolla wyvillei</i> (Haacke), 1880	02-Dec-64	561	USNM 1145042	21.18	-158.3	Ames, Cheryl L	1	Formalin	Ros S. W. Quattrini, A. McJames, C. L.	Trawl - Tucker, 2	North Atlantic Ocean	USGS CEMO I	CH-2007	689 to 972	2004005	
<i>Atolla wyvillei</i> (Haacke), 1880	15-Aug-07	873	USNM 1145043	21.18	-158.3	Ames, Cheryl L	1	Formalin	Ros S. W. Quattrini, A. McJames, C. L.	Trawl - Tucker, 2	North Atlantic Ocean	USGS CEMO I	CH-2007	975 to 1017	2004005	
<i>Atolla wyvillei</i> (Haacke), 1880	02-Dec-09	5631	USNM 26868	-0.95	127.933	Mayer, A. G.	1	Formalin	United States Fish Commission	Trawl - Agassiz	Indian Ocean	Philippines Ex-Albatross R/V		1479		
<i>Atolla wyvillei</i> (Haacke), 1880	19-Jun-09	5471	USNM 26866	13.5825	123.985	Mayer, A. G.	2	Formalin	United States Fish Commission	Trawl - Agassiz	Indian Ocean	Philippines Ex-Albatross R/V		1089		

Table 3 List of species data sourced from the Global Biodiversity Information Facility (GBIF)

Data available at <https://www.gbif.org/occurrence/>.

[illegible]

Table 3: GBIF data sources continued

Data Source	Species	Cruise	Longitude	Latitude	Date	Area
GBIF	<i>A. parva</i>	Naturalis Biodiversity Center (NL) - Onidaria	-35	41.8		Iberian Basin
GBIF	<i>A. parva</i>	Naturalis Biodiversity Center (NL) - Onidaria	-34.3	41.7		Iberian Basin
GBIF	<i>A. parva</i>	Naturalis Biodiversity Center (NL) - Onidaria	-35.5	40.9		Iberian Basin
GBIF	<i>A. parva</i>	Naturalis Biodiversity Center (NL) - Onidaria	-28.8	40.9		Iberian Basin
GBIF	<i>A. parva</i>	Naturalis Biodiversity Center (NL) - Onidaria	-31.5	35.2		Iberian Basin
GBIF	<i>A. parva</i>	Naturalis Biodiversity Center (NL) - Onidaria	-30.7	34.2		Iberian Basin
GBIF	<i>A. parva</i>	Naturalis Biodiversity Center (NL) - Onidaria	-29.8	30.1		Iberian Basin
GBIF	<i>A. parva</i>	Naturalis Biodiversity Center (NL) - Onidaria	-30	30.1		Iberian Basin
GBIF	<i>A. parva</i>	Naturalis Biodiversity Center (NL) - Onidaria	-31.2	25.4		North Atlantic
GBIF	<i>A. parva</i>	Naturalis Biodiversity Center (NL) - Onidaria	-36.4	24.9		North Atlantic
GBIF	<i>A. parva</i>	Naturalis Biodiversity Center (NL) - Onidaria	134.3	-4.5		South Pacific
GBIF	<i>A. tenella</i>	Archives of the Arctic Seas Zooplankton	142.3	84.6	01/09/1971	Arctic
GBIF	<i>A. tenella</i>	Zooplankton Easter Arctic Ocean Polarstern 1995-1998	106.8	81.2	01/08/1995	Arctic
GBIF	<i>A. tenella</i>	Zooplankton Easter Arctic Ocean Polarstern 1995-1998	136.5	81.1	01/08/1995	Arctic
GBIF	<i>A. tenella</i>	Zooplankton Easter Arctic Ocean Polarstern 1995-1998	122.7	80.9	01/09/1995	Arctic
GBIF	<i>A. tenella</i>	Zooplankton Easter Arctic Ocean Polarstern 1995-1998	125.8	86.2	01/08/1996	Arctic
GBIF	<i>A. tenella</i>	Zooplankton Easter Arctic Ocean Polarstern 1995-1998	177.1	85.8	01/07/1998	Arctic
GBIF	<i>A. tenella</i>	Zooplankton Easter Arctic Ocean Polarstern 1995-1998	177.1	85.8	01/07/1998	Arctic
GBIF	<i>A. tenella</i>	Zooplankton Easter Arctic Ocean Polarstern 1995-1998	155.4	85.4	01/07/1998	Arctic
GBIF	<i>A. tenella</i>	Zooplankton Easter Arctic Ocean Polarstern 1995-1998	172.4	85.1	01/07/1998	Arctic
GBIF	<i>A. tenella</i>	Geographically tagged INSDC sequences	-156.6	72.9		Arctic
GBIF	<i>A. tenella</i>	Geographically tagged INSDC sequences	-156.6	72.9		Arctic
GBIF	<i>A. vanhoffen</i>	Naturalis Biodiversity Center (NL) - Onidaria	-29.5	50.4		PAP
GBIF	<i>A. vanhoffen</i>	Naturalis Biodiversity Center (NL) - Onidaria	-35	41.8		Iberian Basin
GBIF	<i>A. vanhoffen</i>	Naturalis Biodiversity Center (NL) - Onidaria	-35.7	41.2		Iberian Basin
GBIF	<i>A. vanhoffen</i>	Naturalis Biodiversity Center (NL) - Onidaria	-35.3	37.8		Iberian Basin
GBIF	<i>A. vanhoffen</i>	Naturalis Biodiversity Center (NL) - Onidaria	-20.3	27		North Atlantic
GBIF	<i>A. vanhoffen</i>	Naturalis Biodiversity Center (NL) - Onidaria	133.2	-4.4		South Pacific
GBIF	<i>A. vanhoffen</i>	Naturalis Biodiversity Center (NL) - Onidaria	131.1	-4.6		South Pacific
GBIF	<i>A. vanhoffen</i>	Naturalis Biodiversity Center (NL) - Onidaria	131.2	-6.5		South Pacific

Table 3: GBIF data sources continued

Data Source	Species	Cruise	Longitude	Latitude	Date	Area
GBIF	<i>A. wyvillei</i>	Fish and Zooplankton from RMT-8 net hauls on the BROKE Voyage	96.1	-62.7	01/01/1996	Southern
GBIF	<i>A. wyvillei</i>	Fish and Zooplankton from RMT-8 net hauls on the BROKE Voyage	96.6	-63.5	01/01/1996	Southern
GBIF	<i>A. wyvillei</i>	Fish and Zooplankton from RMT-8 net hauls on the BROKE Voyage	139.8	-63.6	01/01/1996	Southern
GBIF	<i>A. wyvillei</i>	Fish and Zooplankton from RMT-8 net hauls on the BROKE Voyage	139.8	-63.6	01/01/1996	Southern
GBIF	<i>A. wyvillei</i>	Fish and Zooplankton from RMT-8 net hauls on the BROKE Voyage	128.4	-64	01/01/1996	Southern
GBIF	<i>A. wyvillei</i>	Fish and Zooplankton from RMT-8 net hauls on the BROKE Voyage	125.9	-64	01/01/1996	Southern
GBIF	<i>A. wyvillei</i>	Fish and Zooplankton from RMT-8 net hauls on the BROKE Voyage	112.3	-64.5	01/01/1996	Southern
GBIF	<i>A. wyvillei</i>	Fish and Zooplankton from RMT-8 net hauls on the BROKE Voyage	150	-64.6	01/01/1996	Southern
GBIF	<i>A. wyvillei</i>	Fish and Zooplankton from RMT-8 net hauls on the BROKE Voyage	128.4	-65.1	01/01/1996	Southern
GBIF	<i>A. wyvillei</i>	Fish and Zooplankton from RMT-8 net hauls on the BROKE Voyage	112.3	-65.2	01/01/1996	Southern
GBIF	<i>A. wyvillei</i>	Fish and Zooplankton from RMT-8 net hauls on the BROKE Voyage	120.3	-65.5	01/01/1996	Southern
GBIF	<i>A. wyvillei</i>	Fish and Zooplankton from RMT-8 net hauls on the BROKE Voyage	112.2	-65.5	01/01/1996	Southern
GBIF	<i>A. wyvillei</i>	Fish and Zooplankton from RMT-8 net hauls on the BROKE Voyage	138.8	-65.6	01/01/1996	Southern
GBIF	<i>A. wyvillei</i>	Fish and Zooplankton from RMT-8 net hauls on the BROKE Voyage	85.5	-65.6	01/01/1996	Southern
GBIF	<i>A. wyvillei</i>	Fish and Zooplankton from RMT-8 net hauls on the BROKE Voyage	139.9	-66	01/01/1996	Southern
GBIF	<i>A. wyvillei</i>	Fish and Zooplankton from RMT-8 net hauls on the BROKE Voyage	80	-66	01/01/1996	Southern

Appendix B – List of gear types

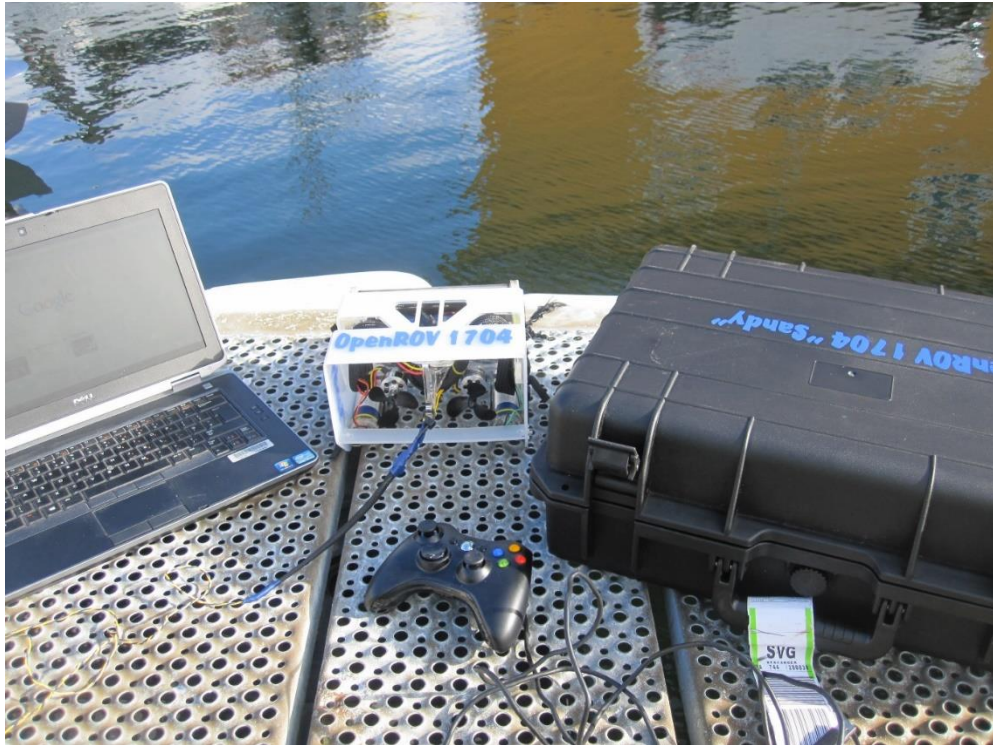
Table 2 List of gear types to sample the Discovery collections material held within the Natural History Museum London collections. Abbreviations listed below.

Abbreviation	Description
EMT	Engel's Midwater Trawl
IKMT	Isaacs-Kidd Midwater Trawl
N113	Net with mouth = 1 m ²
N70	Plankton net used obliquely (N70B) or vertically (N70V)
N50	Phytoplankton net with mouth = 50 cm in diameter
NN	Neuston Net
FRN	Free rise net with mouth = 30 ft. diameter
W/B	Water bottles (used for hydrographic sampling)
Bacterial W/B	Niskin or Zobell samplers
Chlorophyll W/B	7.5 litre water bottles
BT	Bathymograph
CDB(E)	Electrical catch dividing bucket
PES	Precision echo sounder
U/C	Underwater camera
RMT 1 + 8	Rectangular midwater trawl. Mesh size 4.5 mm, nominal mouth area 8 m ² .
RMT 1	Rectangular midwater trawl. Mesh size 0.33 mm, nominal mouth area 1 m ² .
RMT 25	Rectangular midwater trawl with a sampling area of 25 m ² (nominal mouth area).
BN 2.4	Bottom net with a mouth area of 2.4 m.
N113	Ring net with mouth area of 1 m ² , mesh size 0.32 mm.

Appendix C – Lurefjorden fieldwork images

'OpenROV' remotely operated vehicle (ROV) trialled in Lurefjorden, Norway (Aug 2015):





Sample net used for the collection of *P. periphylla* within Lurefjorden during vertical tows:



Large quantities of nematocysts on the sample net shed during collection:



Table 5 List of *P. periphylla* specimens used within Chapter 6 for the extraction of statoliths. All material obtained from Lurefjorden, Norway (Aug 2015).

Specimen number	Coronal diameter (mm)	Method
1	95	Manual extraction
2	95	Manual extraction
3	135	Manual extraction
4	115	Manual extraction
5	25	Manual extraction
6	107	Manual extraction
7	155	Manual extraction
8	170	Manual extraction
9	170	Manual extraction
10	161	Manual extraction
11	67	Manual extraction
12	74	Manual extraction
13	145	Manual extraction
14	165	Manual extraction
15	165	Manual extraction
16	170	Manual extraction
17	180	Manual extraction
18	117	Manual extraction
19	117	Manual extraction
20	122	Manual extraction
21	159	Manual extraction
22	25	Manual extraction
23	25	Manual extraction
24	141	Manual extraction
25	104	Manual extraction
26	103	Manual extraction
27	25	Manual extraction
28	31	Manual extraction
29	31	Manual extraction
30	32	Manual extraction
31	32	Manual extraction
32	29	Manual extraction
33	29	Manual extraction
34	179	Manual extraction
35	179	Manual extraction
36	30	Manual extraction
37	30	Manual extraction
38	35	Manual extraction
39	102	Manual extraction
40	85	Manual extraction
41	85	Manual extraction
42	20	Manual extraction
43	20	Manual extraction
44	92	Manual extraction
45	92	Manual extraction
46	19	Manual extraction
47	34	Manual extraction
48	34	Manual extraction
49	104	Manual extraction
50	104	Manual extraction
51	14	Manual extraction
52	15	Manual extraction
53	99	Manual extraction
54	99	Manual extraction
55	113	Manual extraction
56	113	Manual extraction
57	116	Manual extraction
58	116	Manual extraction
59	33	Manual extraction
60	33	Manual extraction
61	115	Manual extraction
62	115	Manual extraction
63	123	Manual extraction
64	104	Manual extraction
65	33	Manual extraction
66	22	Manual extraction
67	22	Manual extraction
68	103	Manual extraction
69	104	Manual extraction
70	109	Manual extraction
71	109	Manual extraction
72	117	Manual extraction
73	95	Critical point drying (CPD)
74	95	Critical point drying (CPD)
75	135	Weak bleach
76	115	Weak bleach
77	25	Weak bleach
78	107	Weak bleach
79	155	Weak bleach
80	170	Pancreatin
81	25	Pancreatin
82	103	Proteinase K
83	117	Proteinase K

List of References

- Aiken, J. et al. (2000) 'The Atlantic Meridional Transect: Overview and synthesis of data', *Progress in Oceanography*, 45(3–4), pp. 257–312.
- van Aken, H. M. (2000) 'The hydrography of the mid-latitude northeast Atlantic Ocean: The deep water masses', *Deep Sea Research Part I: Oceanographic Research Papers*, 47(5), pp. 757–788.
- Allcock, A. L. and Strugnell, J. M. (2012) 'Southern Ocean diversity : new paradigms from molecular ecology', *Trends in Ecology & Evolution*. Elsevier Ltd, 27(9), pp. 520–528.
- Angel, M. (1974) *RRS Discovery Cruise 61 30 Mar- 16 May 1974*. Wormley.
- Angel, M. (1984) 'A vertical profile of planktonic Ostracods from depths of 1500-3900 m at a Northeast Atlantic station', in Maddock, R. (ed.) *Proceedings of the Eighth International Symposium on Ostracoda July 26-29 1982*. University of Houston, pp. 549–559.
- Angel, M. V. et al. (1978) *R.R.S. Discovery Cruise 92 Cruise Report: Midwater and benthic sampling in the Porcupine Sea Bight and midwater studies along the 13 degrees west and 17 degrees west and around 42 degrees north 17 degrees west*. Wormley.
- Angel, M. V. (1984) 'The diel migrations and distributions within a mesopelagic community in the North East Atlantic. 3. Planktonic ostracods, a stable component in the community', *Progress in Oceanography*, 13(3–4), pp. 319–351.
- Angel, M. V and Baker, A. D. C. (1982) 'Vertical distribution of the standing crop of plankton and micronekton at three stations in the northeast Atlantic', *Deep Sea Research Part B. Oceanographic Literature Review*, 30(6), p. 463.
- Angel, M. V and Baker, A. D. C. (1983) 'Vertical distribution of the standing crop of plankton and micronekton at three stations in the northeast Atlantic', *Deep Sea Research Part B. Oceanographic Literature Review*, 30(January 1983), p. 463.
- Anger, K. and Moreira, G. (1998) 'Morphometric and reproductive traits of tropical caridean shrimps', *Journal of Crustacea Biology*, 18(4), pp. 823–838.
- Arai, M. N. (1997) *A functional biology of scyphozoa*. First. Chapman and Hall.
- Arai, M. N. (2001) 'Pelagic coelenterates and eutrophication: A review', *Hydrobiologia*, 451, pp. 69–87.
- Arai, M. N. (2005) 'Predation on pelagic coelenterates : a review', *Journal Marine Biological Association*, 85, pp. 523–536.
- Arai, M. N., Ford, J. A. and Whyte, J. N. C. (1989) 'Biochemical composition of fed and starved *Aequorea victoria* (Murbach et Shearer, 1902) (Hydromedusa)', *Journal of Experimental Marine Biology and Ecology*, 127, pp. 289–299.
- Arnett, A. E. and Gotelli, N. J. (2003) 'Bergmann's rule in larval ant lions: Testing the starvation resistance hypothesis', *Ecological Entomology*, 28(6), pp. 645–650.
- Ashton, K. G. and Feldman, C. R. (2003) 'Bergmann's rule in nonavian reptiles: turtles follow it, lizards and snakes reverse it.', *Evolution*, 57(5), pp. 1151–1163.
- Attrill, M. J. and Edwards, M. (2008) 'Reply to Haddock SHD: reconsidering evidence for potential climate-related increases in jellyfish', *Limnological Oceanography*, 53, pp. 2763–2766.

List of References

- Attrill, M., Wright, J. and Edwards, M. (2007) 'Climate-related increases in jellyfish frequency suggest a more gelatinous future for the North Sea', *Limnology and Oceanography*, 52(1), pp. 480–485.
- Bailey, D. M. et al. (2009) 'Long-term changes in deep-water fish populations in the northeast Atlantic: A deeper reaching effect of fisheries?', *Proceedings of the Royal Society B: Biological Sciences*, 276(1664), pp. 1965–1969.
- Bailey, P. M. et al. (2003) 'Jellyfish envenoming syndromes: Unknown toxic mechanisms and unproven therapies', *Medical Journal of Australia*, 178(1), pp. 34–37.
- Baker, A. R. and Jickells, T. D. (2017) 'Progress in Oceanography Atmospheric deposition of soluble trace elements along the Atlantic Meridional Transect (AMT)', *Progress in Oceanography*. The Authors, 158, pp. 41–51.
- Båmstedt, U. (2003) 'An evaluation of acoustic and video methods to estimate the abundance and vertical distribution of jellyfish', *Journal of Plankton Research*, 25(11), pp. 1307–1318.
- Barbier, E. B. (2001) 'A note on the economics of biological invasions', *Ecological Economics*, 39(2), pp. 197–202.
- Barham, E. G. and Pickwell, G. V (1969) 'The giant isopod , *Anuropus* : A scyphozoan symbiont', *Deep-Sea Research*, 16(16), pp. 525–529.
- Basson, M. et al. (2002) *The Effects of Fishing on Deep-water Fish Species to the West of Britain*, Joint Nature Conservation Committee.
- Battle, E. (2004) *Deep-sea bioluminescence of the Porcupine Seabight and Porcupine Abyssal Plain, NE Atlantic Ocean*. PhD thesis, University of Aberdeen.
- Bayha, K. M. et al. (2010) 'Evolutionary relationships among scyphozoan jellyfish families based on complete taxon sampling and phylogenetic analyses of 18S and 28S ribosomal DNA.', *Integrative and comparative biology*, 50(3), pp. 436–55.
- Bayha, K. M. and Dawson, M. N. (2010) 'New family of allomorphic jellyfishes, Drymonematidae (scyphozoa, Discomedusae), emphasizes evolution in the functional morphology and trophic ecology of gelatinous zooplankton', *Biological Bulletin*, 219(3), pp. 249–267.
- Bayha, K. M. and Graham, W. M. (2014) 'Nonindigenous marine jellyfish: Invasiveness, invasibility and impacts', in Pitt, K. A. and Lucas, C. H. (eds) *Jellyfish Blooms*. Dordrecht: Springer, pp. 45–77.
- Beaugrand, G. and Reid, P. (2003) 'Long-term changes in phytoplankton, zooplankton and salmon related to climate', *Global Change Biology*, 9(6).
- Beck, J. et al. (2012) 'What's on the horizon for macroecology?', *Ecography*, 35(8), pp. 673–683.
- Becker, A. et al. (2005) 'Calcium sulfate hemihydrate is the inorganic mineral in statoliths of scyphozoan medusae (Cnidaria).', *Dalton transactions (Cambridge, England : 2003)*, (8), pp. 1545–50.
- Belk, M. C. et al. (2002) 'Bergmann's Rule in Ectotherms : A Test Using Freshwater Fishes Bergmann's Rule in Ectotherms : A Test Using Freshwater Fishes', 6(Dec 22), pp. 83–88.
- Bergmann, C. (1848) 'Über die Verhältnisse der Wärmeökonomie der Thiere zu ihrer Grösse', *Göttinger Studien*, 3, pp. 595–708.
- Berrill, B. Y. N. J. (1949) 'Developmental analysis of scyphomedusae', *Biological Reviews*, 24(4), pp. 393–409.

List of References

- Bett, B. J. et al. (2001) 'Temporal variability in phytodetritus and megabenthic activity at the seabed in the deep northeast Atlantic', *Progress in Oceanography*, 50(1–4), pp. 349–368.
- Bez-Ezra, J. et al. (2010) 'Effect of fixation on the amplification of nucleic acids from paraffin-embedded material by the polymerase chain reaction', *Journal of Histochemistry and Cytochemistry*, 39, pp. 351–354.
- Bieri, R. (1966) 'Feeding preferences and rates of the snail, *Ianthina prolongata*, the barnacle, *Lepas anserifera*, the nudibranchs *Glaucus atlanticum* and *Fiona pinnata*, and the food web in the marine neuston', *Publications of the Seto Marine Biological Laboratory*, 14, pp. 161–170.
- Bigelow, H. B. (1938) 'Plankton of the Bermuda Oceanographic Expeditions, VIII: Medusae taken during the years 1929 and 1930', *Zoologica*, 23(2), pp. 99–189.
- Billett, D. S. M. et al. (2001) 'Long-term change in the megabenthos of the Porcupine Abyssal Plain (NE Atlantic)', *Progress in Oceanography*, 50(1–4), pp. 325–348.
- Blackburn, T. M. and Hawkins, B. A. (2004) 'Bergmann's rule and the mammal fauna of northern North America', *Ecography*, 27(6), pp. 715–724.
- Boakes, E. H. et al. (2010) 'Distorted views of biodiversity: spatial and temporal bias in species occurrence data.', *PLoS biology*, 8(6), p. e1000385.
- Bosch-Belmar, M. et al. (2017) 'Jellyfish blooms perception in Mediterranean finfish aquaculture', *Marine Policy*, 76(November 2016), pp. 1–7.
- Bowling, A. J. and Vaughn, K. C. (2008) 'A simple technique to minimize heat damage to specimens during thermal polymerization of LR White in plastic and gelatin capsules', *Journal of Microscopy*, 231(1), pp. 186–189.
- Bozman, A. (2015) 'Discussion with Andrea Bozman to obtain specimens of a known age of *P. periphylla* for sclerochronology study'. Barcelona.
- Bozman, A. et al. (2017) 'Jellyfish distribute vertically according to irradiance', *Journal of Plankton Research*, 39(2), pp. 280–289.
- Bradshaw, C. and McMahon, C. (2008) 'Fecundity', in Jorgensen, S. and Fath, B. (eds) *Encyclopedia of Ecology*. Amsterdam: Elsevier B.V., pp. 1535–1543.
- Bramwell, N. and Burns, B. (1988) 'The effect of fixative type and fixation time on the quantity and quality of extractable DNA from hybridisation studies on lymphoid tissue', *Experimental Hematology*, 16, pp. 730–732.
- Brandt, A., Linse, K. and Muhlenhardt-Siegel, U. (1997) 'Biogeography of Crustacea and Mollusca of the Magellan and Antarctic Region', *Biogeography of Crustacea and Mollusca in the Beagle Channel*, 63, pp. 383–389.
- Brierley, A. et al. (2001) 'Acoustic observations of jellyfish in the Namibian Benguela', *Marine Ecology Progress Series*, 210, pp. 55–66.
- Brierley, L. (2009) 'Art Forms in Nature: Examination and conservation of a Blaschka glass model of the protozoan *Aulosphaera elegantissima*', *Studies in Conservation*, 54, pp. 255–267.
- Brinkman, D. L. et al. (2012) 'Venom Proteome of the Box Jellyfish *Chironex fleckeri*', *PLoS ONE*, 7(12).
- Broch, H. (1913) 'Scyphomedusae from the "Michael Sars" North Atlantic deep-sea expedition 1910', *Report on the Scientific Results of the 'Michael Sars' North Atlantic Deep-Sea Expedition 1910*, 3(1), pp. 1–20.

List of References

- Brodeur, R., Sugisaki, H. and Jr, G. H. (2002) 'Increases in jellyfish biomass in the Bering Sea: implications for the ecosystem', 233, pp. 89–103.
- Brotz, L. et al. (2012) 'Increasing jellyfish populations: trends in Large Marine Ecosystems', *Hydrobiologia*, 690(1), pp. 3–20.
- Browne, E. T. (1915) *Medusae from the Indian Ocean (Collected by Prof Stanley Gardiner, in HMS 'Sealark' in 1905)*.
- Bucklin, A., Steinke, D. and Blanco-Bercial, L. (2011) 'DNA barcoding of marine metazoa.', *Annual review of marine science*, 3, pp. 471–508.
- Buddemeier, R. W. and Taylor, F. W. (1978) 'Sclerochronology', *Quaternary Geochronology: Methods and Applications*, pp. 25–40.
- Burnett, J. W. (2001) 'Medical aspects of jellyfish envenomation: Pathogenesis, case reporting and therapy', *Hydrobiologia*, 451, pp. 1–9..
- Caddy, J. and Gulland, J. (1983) 'Historical patterns of fish stocks', *Marine Policy*, 7(4), pp. 267–278.
- Cailliet, G. M. et al. (2001) 'Age determination and validation studies of marine fishes : do deep-dwellers live longer ?', *Experimental Gerontology*, 36, pp. 739–764.
- Calder, W. (1984) *Size, function and life history*. Cambridge, MA: Harvard University Press.
- Campana, S. E. and Neilson, J. D. (1985) 'Microstructure of fish otoliths', *Canadian Journal of Fisheries and Aquatic Science*, 42, pp. 1014–1032.
- Campos, P. F. and Gilbert, T. M. P. (2012) 'DNA extraction from formalin-fixed material', *Methods in Molecular Biology*, 840(840).
- Cantero, A. and Horton, T. (2017) 'Benthic hydroids (Cnidaria, Hydrozoa) from bathyal and abyssal depths of the Northeast Atlantic held in the modern Discovery collections', *Zootaxa*, 4347(1), pp. 1–30.
- Cardoso, R. S. and Defeo, O. (2003) 'Geographical patterns in reproductive biology of the Pan-American sandy beach isopod *Excirrolana braziliensis*', *Marine Biology*, 143(3), pp. 573–581.
- Cary, L. (1915) 'The influence of the marginal sense organs on the functional activity in *Cassiopea xamanchana*', *Zoology*, pp. 611–616.
- Ceccaldi, H. J. (1972) 'Observations biologiques de *Cestus veneris*', *Tethys*, 4, pp. 707–710.
- Cegolon, L. et al. (2013) 'Jellyfish Stings and Their Management : A Review', *Marine Drugs*, 11, pp. 523–550. doi: 10.3390/md11020523.
- Ceh, J. et al. (2015) 'The elusive life cycle of scyphozoan jellyfish - Metagenesis revisited', *Scientific Reports*. Nature Publishing Group, 5, pp. 1–13. doi: 10.1038/srep12037.
- Chalfie, M. (1995) 'Green Fluorescent Protein', *Photochemistry and Photobiology*, 62(4), pp. 5–10.
- Chapman, D. M. (1985) 'X-ray microanalysis of selected coelenterate statoliths', *Journal of the Marine Biological Association of the United Kingdom*, 65(03), pp. 617–627.
- Child, C. A. and Harbison, G. R. (1986) 'A parasitic association between a Pycnogonic and a Schyphomedusa in midwater', *Journal of the Marine Biological Association of the United Kingdom*. University of Southampton Library, 66(1986), pp. 113–117.
- Childress, J. J. (1995) 'Are there physiological and biochemical adaptations of metabolism in deep-

List of References

sea animals?', *Trends in ecology & evolution*, 10(1), pp. 30–6.

Choy, A., Haddock, S.D.H. and Robison, B.H. (2017). Deep pelagic food web structure as revealed by *in situ* feeding observations. *Proceedings of the Royal Society B: Biological Sciences*, 284(1868), 20172116.

Christiansen, B. et al. (2010) 'The near-bottom plankton community at the Porcupine Abyssal Plain, NE-Atlantic: Structure and vertical distribution', *Marine Biology Research*, 6(2), pp. 113–124.

Clarke, A., Holmes, L. J. and Gore, D. J. (1992) 'Proximate and elemental composition of gelatinous zooplankton from the Southern Ocean', *Journal of Experimental Marine Biology and Ecology*, 155, pp. 55–68.

Collins, A. (2002) 'Phylogeny of Medusozoa and the evolution of cnidarian life cycles', *Journal of Evolutionary Biology*, 15(3), pp. 418–432..

Collins, A. G. (2002) 'Phylogeny of Medusozoa and the evolution of cnidarian life cycles', *Journal of Evolutionary Biology*, 15(3), pp. 418–432.

Condon, R. H. et al. (2012) 'Questioning the Rise of Gelatinous Zooplankton in the World's Oceans', *BioScience*, 62(2), pp. 160–169.

Condon, R. H., Duarte, C. M., Pitt, K. A., et al. (2013) 'Recurrent jellyfish blooms are a consequence of global oscillations.', *Proceedings of the National Academy of Sciences of the United States of America*, 110(3), pp. 1000–5.

Costello, J. (1998) 'Physiological response of the hydromedusa *Cladonema californicum* Hyman (Anthomedusa: Cladonemidae) to starvation and renewed feeding', *Journal of Experimental Marine Biology and Ecology*, 225, pp. 13–28.

Costello, J. and Colin, S. (1995) 'Flow and feeding by swimming scyphomedusae', *Marine Biology*, 124, pp. 399–406.

Cushing, D. (1982) *Climate and Fisheries*. New York: Academic Press Inc.

Cushman, J., Lawton, J. and Manly, B. (1993) 'Latitudinal patterns in Europe ant assemblages: variation in species richness and body size', *Oecologia*, 95, pp. 30–37.

Dalpadado, P. et al. (1998) 'Summer distribution patterns and biomass estimates of macrozooplankton and micronekton in the Nordic Seas', *Sarsia*, 83, pp. 103–116.

Danovaro, R. et al. (2017) 'The deep-sea under current change', *Current Biology*, 27(11), pp. R461–R465.

Danovaro, R., Snelgrove, P. V. R. and Tyler, P. (2014) 'Challenging the paradigms of deep-sea ecology.', *Trends in ecology & evolution*. Elsevier Ltd, pp. 1–11.

Daufresne, M., Lengfellner, K. and Sommer, U. (2009) 'Global warming benefits the small in aquatic ecosystems', *Proceedings of the National Academy of Sciences of the United States of America*, 106(31), pp. 12788–12793.

Davis, M. P. et al. (2014) 'Species-specific bioluminescence facilitates speciation in the deep sea', *Marine Biology*, 161(5), pp. 1139–1148.

Dawson, M. (2004) 'Some implications of molecular phylogenetics for understanding biodiversity in jellyfishes, with emphasis on Scyphozoa', *Hydrobiologia*, 530–531(1–3), pp. 249–260.

Dawson, M. N. (2004) 'Some implications of molecular phylogenetics for understanding biodiversity

List of References

in jellyfishes , with emphasis on Scyphozoa', *Hydrobiologia*, 530, pp. 249–260.

Dawson, M. N. (2005) 'Incipient speciation of *Catostylus mosaicus* (Scyphozoa, Rhizostomeae, Catostylidae), comparative phylogeography and biogeography in south-east Australia', *Journal of Biogeography*, 32(3), pp. 515–533.

Dawson, M. N. (2016) 'Discussion with Mike Dawson on extracting quality DNA from jellyfish, particularly formalin-fixed historic samples. Discussion included optimal sampling locations on the jellyfish body for sampling DNA (muscle, gonad, tentacle).' Barcelona.

Dawson, M. N. and Jacobs, D. K. (2001) 'Molecular evidence for cryptic species of *Aurelia aurita* (Cnidaria, Scyphozoa)', *Biological Bulletin*, 200, pp. 92–96.

Dawson, M. N., Raskoff, K. a and Jacobs, D. K. (1998) 'Field preservation of marine invertebrate tissue for DNA analyses.', *Molecular marine biology and biotechnology*, 7(2), pp. 145–52.

Decker, M. B. et al. (2007) 'Predicting the distribution of the scyphomedusa *Chrysaora quinquecirrha* in Chesapeake Bay', *Marine Ecology Progress Series*, 329, pp. 99–113.

Defeo, O. and Cardoso, R. S. (2002) 'Macroecology of population dynamics and life history traits of the mole crab *Emerita brasiliensis* in Atlantic sandy beaches of South America', *Marine Ecology Progress Series*, 239, pp. 169–179.

Deibel, D. and Lowen, B. (2012) 'A review of the life cycles and life-history adaptations of pelagic tunicates to environmental conditions', *ICES Journal of Marine Science*, 69(3), pp. 358–369.

Devaney, D. and Eldredge, L. (1977) 'Reef and shore fauna of Hawaii. Section 1: protozoa though Ctenophora', *Bernice P Bishop Museum Special Publication*, 64.

Dickson, R. et al. (1988) 'North winds and production in the eastern North Atlantic', *Journal of Plankton Research*, 10(1), pp. 151–169.

Diniz-Filho, J. A. F. and Bini, L. M. (2008) 'Macroecology, global change and the shadow of forgotten ancestors', *Global Ecology and Biogeography*, 17, pp. 11–17.

Dittrich, B. (1988) 'Studies on the life cycle and reproduction of the parasitic amphipod *Hyperia galba* in the North Sea', *Helgolander Meeresunters*, 42, pp. 79–98.

Domanski, P. (1984) 'The diel migrations and distributions within a mesopelagic community in the North East Atlantic. 8. A multivariate analysis of community structure', *Progress in Oceanography*, 13(3–4), pp. 389–424.

Dong, Z., Liu, D. and Keesing, J. K. (2010) 'Jellyfish blooms in China: Dominant species, causes and consequences.', *Marine pollution bulletin*. Elsevier Ltd, 60(7), pp. 954–63.

Dorschel, B. et al. (2010) 'Atlas of the deep-water seabed: Ireland', in *Atlas of the Deep-Water Seabed: Ireland*. Dordrecht: Springer-Verlag, pp. 1–164.

Doty, M. (1961) '*Acanthophora*, a possible invader of the marine flora of Hawaii', *Pacific Science*, 15, pp. 547–552.

Doyle, T. K. et al. (2007) 'The broad-scale distribution of five jellyfish species across a temperate coastal environment', *Hydrobiologia*, 579(1), pp. 29–39.

Doyle, T. K. et al. (2014) 'Ecological and societal benefits of jellyfish', in Pitt, K. A. and Lucas, C. H. (eds) *Jellyfish Blooms*. Dordrecht: Springer, pp. 105–127.

Drazen, J. C. and Haedrich, R. L. (2012) 'Deep-Sea Research I A continuum of life histories in deep-

List of References

sea demersal fishes', *Deep-Sea Research Part I*. Elsevier, 61, pp. 34–42.

Duarte, C. M., Pitt, K. A. and Lucas, C. H. (2014) 'Introduction: Understanding jellyfish blooms', in Pitt, K. A. and Lucas, C. H. (eds) *Jellyfish Blooms*. Dordrecht: Springer, pp. 1–5.

Eckelbarger, K. J. and Larson, R. (1992) 'Ultrastructure of the ovary and oogenesis in the jellyfish *Linuche unguiculata* and *Stomolophus meleagris*, with a review of ovarian structure in the Scyphozoa', *Marine Biology*, 643, pp. 633–643.

Eckelbarger, K. and Larson, R. (1988) 'Ovarian morphology and oogenesis in *Aurelia surita* (Scyphozoa: Semaestomae): Ultrastructural evidence of heterosynthetic yolk formation in a primitive metazoan', *Marine Biology*, 100, pp. 103–115.

Edgar, G. J. et al. (2016) 'New Approaches to Marine Conservation Through Scaling Up of Ecological Data', *Annual Review of Marine Science*, 8(1), p. 150807173619006.

Edwards, M., Reid, P. and Planque, B. (2001) 'Long-term and regional variability of phytoplankton biomass in the Northeast Atlantic (1960–1995)', *ICES Journal of Marine Science*, 58(1), pp. 39–49.

Eggers, N. and Jarms, G. (2007) 'The morphogenesis of ephyra in Coronatae (Cnidaria, Scyphozoa)', *Marine Biology*, 152(3), pp. 495–502.

Etter, R. J. et al. (2005) 'Population differentiation decreases with depth in deep-sea bivalves', *Evolution*, 59(7), pp. 1479–1491.

Fang, S., Wan, Q. and Fujihara, N. (2002) 'Formalin-removal from archival tissue by critical point drying', *Biotechniques*, 33, pp. 604–611.

Fasham, M. J. R. and Pugh, P. (1976) 'Observations on the horizontal coherence of chlorophyll a and temperature', *Deep-Sea Research*, 23(1975), pp. 527–538.

Fischer, A. H. et al. (2008) 'Hematoxylin and eosin staining of tissue and cell sections', *Cold Spring Harbor Protocols*, 4986.

Flynn, B. and Gibbons, M. (2007) 'A note on the diet and feeding of *Chrysaora hysoscella* in Walvis Bay Lagoon, Namibia, during September 2003', *African Journal of Marine Science*, 29(2), pp. 303–307.

Fosså, J. H. (1992) 'Mass occurrence of *Periphylla periphylla* (Scyphozoa, Coronatae) in a Norwegian fjord', *Sarsia*, 77(3), pp. 237–251.

Foxton, P. et al. (1971) *RRS Discovery Cruise 39 Report, April - June 1971: Plankton Investigations at 60 degrees North, 20 degrees West and 53 degrees North, 20 degrees West*. Wormley.

France, S. C. and Kocher, T. D. (1996) 'Geographic and bathymetric patterns of mitochondrial 16S rRNA sequence divergence among deep-sea amphipods, *Eurythenes gryllus*', *Marine Biology*, 126(4), pp. 633–643.

Fransway, A. F. (1991) 'The problem of preservation in the 1990s: I. Statement of the problem, solution(s) of the industry, and the current use of formaldehyde and formaldehyde-releasing biocides', *American Journal of Contact Dermatitis*, 2(1).

Frigstad, H. et al. (2015) 'Links between surface productivity and deep ocean particle flux at the Porcupine Abyssal Plain sustained observatory', *Biogeosciences*, 12(19), pp. 5885–5897..

Fromentin, J. M. and Planque, B. (1996) '*Calanus* and environment in the eastern North Atlantic. II. Influence of the North Atlantic Oscillation on *C. finmarchicus* and *C. helgolandicus*', *Marine Ecology Progress Series*, 134, pp. 111–118.

List of References

- Fuentes, V. L. et al. (2010) 'Blooms of the invasive ctenophore, *Mnemiopsis leidyi*, span the Mediterranean Sea in 2009', *Hydrobiologia*, 645(1), pp. 23–37.
- Gage, J. (2003) 'Food inputs, utilization, carbon flow and energetics', in Tyler, P. (ed.) *Ecosystems of the Deep Oceans*. Amsterdam: Elsevier, pp. 313–381.
- Gage, J. D. and Tyler, P. A. (1991) *Deep-sea biology*. Cambridge: Cambridge University Press.
- Galley, E. A. et al. (2005) 'Reproductive biology and biochemical composition of the brooding echinoid *Amphipneustes lorioli* on the Antarctic continental shelf', *Marine Biology*, 148(1), pp. 59–71.
- Gambi, C. et al. (2017) 'Functional response to food limitation can reduce the impact of global change in the deep-sea benthos', *Global Ecology and Biogeography*, 26(9), pp. 1008–1021.
- Geist, V. (1987) 'Bergmann's rule is invalid', *Canadian Journal of Zoology*, 65, pp. 1035–1038.
- Geist, V. (1990) 'Bergmann's rule is invalid: a reply to J.D. Paterson', *Canadian Journal of Zoology*, 68, pp. 1613–1615.
- Gershwin, L.-A. et al. (2013) *Biology and ecology of irukandji jellyfish (cnidaria: cubozoa)*. 1st edn, *Advances in marine biology*. 1st edn. Edited by M. Lesser. Elsevier Ltd.
- Gershwin, L. A. (2005) *Taxonomy and Phylogeny of Australian Cubozoa*. James Cook University Australia.
- Gibbons, M. J. and Richardson, A. J. (2009) 'Patterns of jellyfish abundance in the North Atlantic', *Hydrobiologia*, 616, pp. 51–65.
- Glover, A. G. et al. (2010) 'Temporal Change in Deep-Sea Benthic Ecosystems : A Review of the Evidence From Recent Time-Series Studies', *Advances in Marine Biology*, 58, pp. 0–73.
- Goldstein, J. and Riisgard, H. U. (2016) 'Population dynamics and factors controlling somatic degrowth of the common jellyfish, *Aurelia aurita*, in a temperate semi-enclosed cove (Kertinge Nor, Denmark)', *Marine Biology*, 163(33).
- Gonçalves, G. R. L. et al. (2016) 'Decapod crustacean associations with scyphozoan jellyfish (Rhizostomeae : Pelagiidae) in the Southeastern Brazilian coast', *Symbiosis*. Symbiosis, 69, pp. 193–198..
- González-Dávila, M. et al. (2010) 'The water column distribution of carbonate system variables at the ESTOC site from 1995 to 2004', *Biogeosciences*, 7(10), pp. 3067–3081.
- Gooday, A. J. et al. (2010) 'Decadal-scale changes in shallow-infaunal foraminiferal assemblages at the Porcupine Abyssal Plain, NE Atlantic', *Deep-Sea Research Part II: Topical Studies in Oceanography*. Elsevier, 57(15), pp. 1362–1382.
- Gordon, M. and Seymour, J. (2012) 'Growth, development and temporal variation in the onset of six *Chironex fleckeri* medusae seasons: a contribution to understanding jellyfish ecology.', *PloS one*, 7(2), p. e31277.
- Gorsky, G. et al. (2000) 'Zooplankton Distribution in Four Western Norwegian Fjords', *Estuarine, Coastal and Shelf Science*, 50(1), pp. 129–135.
- Gotelli, N. J. et al. (2017) 'Community-level regulation of temporal trends in biodiversity', *Science Advances*, 3(7).
- Graham, L. J. et al. (2014) 'Where next for macroecology : citizen macroecology?', *Frontiers of*

List of References

Biogeography, 6(1), pp. 16–19.

Graham, W. M. et al. (2003) 'Ecological and economic implications of a tropical jellyfish invader in the Gulf of Mexico', pp. 53–69.

Graham, W. M. and Bayha, K. M. (2007) 'Biological invasions by marine jellyfish', *Ecological Studies*, 193, pp. 239–235.

Haddock, S. H. D. (2004) 'A golden age of gelata: past and future research on planktonic ctenophores and cnidarians', *Hydrobiologia*, 530–531(1–3), pp. 549–556.

Haddock, S. H. D. and Case, J. F. (1999) 'Bioluminescence spectra of shallow and deep-sea gelatinous zooplankton: ctenophores, medusae and siphonophores', *Marine Biology*, 133(3), pp. 571–582.

Haeckel, E. (1881) 'Report on the deep-sea medusae dredged by HMS Challenger, during the years 1873–1876', *Zoology*, 4(2), pp. 1–154.

Hale, G. (1999) *The Classification and Distribution of the Class Scyphozoa*. University of Oregon.

Hall, S. and Thatje, S. (2011) 'Temperature-driven biogeography of the deep-sea family Lithodidae (Crustacea: Decapoda: Anomura) in the Southern Ocean', *Polar Biology*, 34(3), pp. 363–370.

Hamner, W. M. et al. (1975) 'Underwater observations of gelatinous zooplankton: Sampling problems, feeding biology, and behaviour', *Limnology and Oceanography*, 20(6), pp. 907–917.

Hamner, W. M. and Dawson, M. N. (2009) 'Review and synthesis on the systematics and evolution of jellyfish blooms: Advantageous aggregations and adaptive assemblages', in Pitt, K. A. and Purcell, J. E. (eds) *Jellyfish Blooms: Causes, Consequences and Recent Advances. Developments in Hydrobiology*. Dordrecht: Springer, pp. 161–191.

Hamner, W. M. and Jenssen, R. M. (1974) 'Growth, Degrowth, and Irreversible Cell Differentiation in *Aurelia aurita*', *American Zoology*, 849, pp. 833–849.

Han, J. et al. (2016) 'The earliest pelagic jellyfish with rhopalia from Cambrian Chengjiang Lagerstätte', *Palaeogeography, Palaeoclimatology, Palaeoecology*. Elsevier B.V., 449(April), pp. 166–173.

Hanken, J. (2003) 'Direct development', in Hall, B. K. and Olson, W. M. (eds) *Keywords and Concepts in Evolutionary Developmental Biology*. Cambridge, MA: Harvard University Press, pp. 97–102.

Hardy, A. (1926) 'A new method of plankton research', *Nature*, 118, p. 630.

Hargreaves, P. M. (1985) 'The vertical distribution of Decapoda, Euphausiacea, and Mysidacea at 42°N, 17°W', *Biological Oceanography*, 3(4), pp. 431–464.

Hartman, S. et al. (2012) 'The Porcupine Abyssal Plain fixed-point sustained observatory (PAP-SO): variations and trends from the Northeast Atlantic fixed-point time series', *ICES Journal of Marine Science*, 69(5), pp. 1319–1329.

Hartwick, R. (1991) 'Observations on the anatomy, behaviour, reproduction and life-cycle of the cubozoan *Carybdea sivickisi*', *Hydrobiologia*, 216, pp. 171–179.

Heins, A., Sötje, I. and Holst, S. (2017) 'Assessment of investigation techniques for scyphozoan statoliths, with focus on early development of the jellyfish *Sanderia malayensis*', *Marine Ecology Progress Series*

Hélaouët, P., Beaugrand, G. and Reygondeau, G. (2016) 'Reliability of spatial and temporal patterns of *C. fi nmarchicus* inferred from the CPR survey', *Journal of Marine Systems*. Elsevier B.V., 153, pp.

List of References

18–24.

Herring, P. J. and Widder, E. (2004) 'Bioluminescence of deep-sea coronate medusae (Cnidaria: Scyphozoa)', *Marine Biology*, 146(1), pp. 39–51.

Himes, J. (2007) *Sperm longevity in the midwater gelata, Atolla sp., Aurelia labiata, sp., Nanomia bijuga, and Poralia sp.* University of California.

Hobson, K. A. and Sease, J. L. (1998) 'Stable Isotope Analyses of Tooth Annuli Reveal Temporal Dietary Records : an Example Using Steller Sea Lions', *Marine Ecology Progress Series*, 14(1), pp. 116–129.

Holland, B. et al. (2004) 'Global phylogeography of *Cassiopea* of the Hawaiian Islands', *Marine Biology*, 145, pp. 1119–1128.

Holland, B. S. et al. (2004) 'Global phylogeography of *Cassiopea* (Scyphozoa: Rhizostomeae): Molecular evidence for cryptic species and multiple invasions of the Hawaiian Islands', *Marine Biology*, 145, pp. 1119–1128.

Holst, S. et al. (2007) 'Life cycle of the rhizostome jellyfish *Rhizostoma octopus* (L.)(Scyphozoa, Rhizostomeae), with studies on cnidocysts and statoliths', *Marine Biology*, 151(5), pp. 1695–1710.

Holst, S. et al. (2016) 'Potential of X-ray micro-computed tomography for soft-bodied and gelatinous cnidarians with special emphasis on scyphozoan and cubozoan statoliths', *Journal of Plankton Research*, 0(0), pp. 1–18.

Hopf, J. and Kingsford, M. (2013) 'The utility of statoliths and bell size to elucidate age and condition of a scyphomedusa (*Cassiopea* sp.)', *Marine Biology*, 160(4), pp. 951–960.

Hopkins, T. L. and Torres, J. J. (1988) 'The Zooplankton Community in the Vicinity of the Ice Edge, Western Weddell Sea, March 1986', *Polar Biology*, (9), pp. 79–87.

Hughes, S. J. M. et al. (2011) 'Deep-sea echinoderm oxygen consumption rates and an interclass comparison of metabolic rates in Asteroidea, Crinoidea, Echinoidea, Holothuroidea and Ophiuroidea.', *The Journal of experimental biology*, 214(Pt 15), pp. 2512–21.

Hunt, G. and Roy, K. (2006) 'Climate change, body size evolution, and Cope's Rule in deep-sea ostracodes', *Proceedings of the National Academy of Sciences*, 103(5), pp. 1347–1352.

Hunt, J. C. and Lindsay, D. J. (1998) 'Observations on the behavior of *Atolla* (Scyphozoa : Coronatae) and *Nanomia* (Hydrozoa : Physonectae): use of the hypertrophied tentacle in prey capture', *Plankton Biology and Ecology*, 45(2), pp. 239–242.

Hunter, E., Laptikhovsky, V. V. and Hollyman, P. R. (2018) 'Innovative use of sclerochronology in marine resource management', *Marine Ecology Progress Series*, 598, pp. 155–158..

Hurrell, J. W. (1995) 'Decadal Trends in the North Atlantic Oscillation : Regional Temperatures and Precipitation', *Science*, 269(August).

Hwang, D. S. et al. (2014) 'Complete mitochondrial genome of the moon jellyfish, *Aurelia* sp. nov. (Cnidaria, Scyphozoa)', *Mitochondrial DNA*, 25(1), pp. 27–28.

Iken, K. et al. (2001) 'Food web structure of the benthic community at the Porcupine Abyssal Plain (NE Atlantic): A stable isotope analysis', *Progress in Oceanography*, 50(1–4), pp. 383–405.

Irigoin, X. et al. (2000) 'North Atlantic Oscillation and spring bloom phytoplankton composition in the English Channel', *Journal of Plankton Research*, 22(12), pp. 2367–2371..

Ishii, H. et al. (1995) 'Population dynamics of the jellyfish *Aurelia aurita*, in Tokyo Bay in 1993 with

List of References

- determination of ATP-related compounds', *Bulletin of the Plankton Society of Japan*, 42, pp. 171–176.
- Ishii, H. and Båmstedt, U. (1998) 'Food regulation of growth and maturation in a natural population of *Aurelia aurita* (L.)', 20, pp. 805–816.
- Iyake, H. M., Wao, K. I. and Akinuma, Y. K. (1997) 'Life History and Environment of *Aurelia aurita*', *South Pacific Study*, 17, pp. 273–285.
- Jarms, G. et al. (1999) 'The holopelagic life cycle of the deep-sea medusa', *Sarsia*, 84, pp. 55–65.
- Jarms, G., Morandini, A. and Silveira, F. (2002) 'Polyps of the families Atorellidae and Nausithoidae (Scyphozoa: Coronatae) new to the Brazilian fauna', *Biota Neotropica*, 2(1), pp. 1–11.
- Jarms, G., Morandini, A. and da Silveira, F. (2002) 'Cultivation of polyps and medusae of Coronatae (Cnidaria, Scyphozoa) with a brief review of important characters', *Helgoland Marine Research*, 56(3), pp. 203–210.
- Jarms, G., Tiemann, H. and Båmstedt, U. (2002) 'Development and biology of *Periphylla periphylla* (Scyphozoa: Coronatae) in a Norwegian fjord', *Marine Biology*, 141(4), pp. 647–657.
- Jones, D. (1976) 'Chemistry of fixation and preservation with aldehydes', in Steedman, H. (ed.) *Zooplankton fixation and preservation*. Paris: The Unesco Press.
- K., R. (2002) 'Foraging, prey capture, and gut contents of the mesopelagic narcomedusa *Solmissus* spp. (Cnidaria: Hydrozoa)', *Marine Biology*, 141(6), pp. 1099–1107.
- Kaartvedt, S. et al. (2007) 'Diel vertical migration of individual jellyfish (*Periphylla periphylla*)', 52(November 2004), pp. 975–983.
- Kalogeropoulou, V. et al. (2010) 'Temporal changes (1989-1999) in deep-sea metazoan meiofaunal assemblages on the Porcupine Abyssal Plain, NE Atlantic', *Deep-Sea Research Part II*, 57, pp. 1383–1395.
- Kawamura, M. et al. (2003) 'The relationship between fine rings in the statolith and growth of the cubomedusa *Chiropsalmus quadrigatus* (Cnidaria: Cubozoa) from Okinawa Island, Japan', 50(2), pp. 37–42.
- Kayal, E. et al. (2013) 'Cnidarian phylogenetic relationships as revealed by mitogenomics', *Evolutionary Biology*, 13(5), pp. 1–18.
- Kelly, N. E. et al. (2010) 'Biodiversity of the deep-sea continental margin bordering the Gulf of Maine (NW Atlantic): relationships among sub-regions and to shelf systems.', *PloS one*, 5(11), p. e13832..
- Kemp, K. M. et al. (2006) 'Consumption of large bathyal food fall, a six month study in the NE Atlantic', *Marine Ecology Progress Series*, 310, pp. 64–76.
- Kideys, A. E. (1994) 'Recent dramatic changes in the Black Sea ecosystem: The reason for the sharp decline in Turkish anchovy fisheries', *Journal of Marine Systems*, 5, pp. 171–181.
- Kingsford, M. J. and Mooney, C. J. (2014) 'The Ecology of Box Jellyfishes (Cubozoa) The Ecology of Box Jellyfishes (Cubozoa)', in Pitt, K. A. and Lucas, C. H. (eds) *Jellyfish Blooms*. Dordrecht: Springer, pp. 267–302.
- Klevjer, T., Kaartvedt, S. and Båmstedt, U. (2009) 'In situ behaviour and acoustic properties of the deep living jellyfish *Periphylla periphylla*', *Journal of Plankton Research*, 31(8), pp. 793–803.
- Kogovšek, T., Bogunovic, B. and Malej, A. (2010) 'Reccurrence of bloom-forming scyphomedusae:

List of References

- Wavelet analysis of a 200-year time series', *Hydrobiologia*, 645, pp. 81–96.
- Kramp, P. (1959) 'Stephanoscyphus', *Galathea Report*.
- Kramp, P. (1961) 'Order Coronatae', in *Synopsis of the medusae of the world*. Cambridge: Cambridge University Press, pp. 311–322.
- Kramp, P. L. (1961) 'Synopsis of the medusae of the world', *Journal of the Marine Biological Association of the UK*, 40, pp. 1–469.
- Kramp, P. L. (1965) 'Some medusae (mainly scyphomedusae) from Australia coastal waters', *Transactions of the Royal Society of South Australia*, 89, pp. 257–278.
- Kremer, P. et al. (1990) 'Significance of photosynthetic endosymbionts to the carbon budget of the scyphomedusa *Linuche unguiculata*', *Limnology and Oceanography*, 35(3), pp. 609–624.
- de Lafontaine, Y. and Leggett, W. C. (1989) 'Changes in size and weight of hydromedusae during formalin preservation', *Bulletin of Marine Science*, 44(3), pp. 1129–1137.
- Lampitt, R. (2014) 'RRS Discovery Cruise DY032, 20 Jun - 07 Jul 2014. Cruise to the Porcupine Abyssal Plain sustained observatory', *National Oceanography Centre Southampton Cruise Report*, 43, p. 143.
- Lampitt, R. S., Billett, D. S. M. and Martin, A. P. (2010) 'The sustained observatory over the Porcupine Abyssal Plain (PAP): Insights from time series observations and process studies', *Deep Sea Research Part II: Topical Studies in Oceanography*. Elsevier, 57(15), pp. 1267–1271.
- Larkin, K. E., Ruhl, H. and Bagley, P. (2010) 'Benthic biology time-series in the deep sea: Indicators of change', in Harrison, D. and Stammer, D. (eds) *Proceedings of Ocean Obs '09: Sustained Ocean Observations and Information for Society*. Venice: ESA Publication WPP, pp. 1–17.
- Larson, R. (1979) 'Feeding in coronate medusae (Class Scyphozoa, Order Coronatae)', *Marine Behaviour and Physiology*, 6, pp. 123–129.
- Larson, R. J. (1986) 'Pelagic scyphomedusae (Scyphozoa: Coronatae and Semaestomeae) of the Southern Ocean', *Biology of the Antarctic Seas XVI*, 41, pp. 59–165.
- Larson, R. J. and Harbison, G. R. (1990) 'Medusae from McMurdo Sound, Ross Sea including the descriptions of two new species, *Leuckartiara brownei* and *Benthocodon hyalinus*', *Polar Biology*, 11, pp. 19–25.
- Larson, R. J., Mills, C. E. and Harbison, G. R. (1991) 'Western Atlantic midwater hydrozoan and scyphozoan medusae: in situ studies using manned submersibles', *Hydrobiologia*, 216–217(1), pp. 311–317.
- Laval, P. (1980) 'Hyperiid amphipods as crustacean parasitoids associated with gelatinous zooplankton', *Oceanography and Marine Biology: An Annual Review*, 18, pp. 11–56.
- Lebrato, M. et al. (2011) 'Depth attenuation of organic matter export associated with jelly falls', *Limnology and Oceanography*, 56(5), pp. 1917–1928.
- Lebrato, M. et al. (2012) 'Jelly-falls historic and recent observations: A review to drive future research directions', *Hydrobiologia*, 690(1), pp. 227–245.
- Leeney, R. et al. (2008) 'Spatio-temporal analysis of cetacean strandings and bycatch in a UK fisheries hotspot', *Biodiversity and Conservation*, 17, pp. 2323–2338.
- Lehtiniemi, M. et al. (2011) 'Spreading and physico-biological reproduction limitations of the invasive American comb jelly *Mnemiopsis leidyi* in the Baltic Sea', *Biological Invasions*, 14(2), pp. 341–354.

List of References

- Levin, L. A. and Le Bris, N. (2015) 'The deep ocean under climate change', *Science*, 350(6262).
- Lewis, C. and Long, T. A. F. (2005) 'Courtship and reproduction in *Carybdea sivickisi* (Cnidaria: Cubozoa)', *Marine Biology*, 147(2), pp. 477–483.
- Licandro, P. et al. (2010) 'A blooming jellyfish in the northeast Atlantic and Mediterranean.', *Biology letters*, 6(5), pp. 688–91.
- Lilley, M. K. S. et al. (2011) 'Global patterns of epipelagic gelatinous zooplankton biomass', *Marine Biology*, 158(11), pp. 2429–2436.
- Lilley, M. K. S. et al. (2014) 'Individual shrinking to enhance population survival: Quantifying the reproductive and metabolic expenditures of a starving jellyfish, *Pelagia noctiluca*', *Journal of Plankton Research*, 36(6), pp. 1585–1597.
- Lindsay, D. J. et al. (2004) 'The scyphomedusan fauna of the Japan Trench: Preliminary results from a remotely-operated vehicle', *Hydrobiologia*, 530/531, pp. 537–547. doi: 10.1007/978-1-4020-2762-8.
- Lindsay, D. J. (2018) 'Discussion regarding the various species of *Atolla*, including a potential new species nova, SuperAtolla, as being described by D. Lindsay and G. Matsumoto.'
- Lindstedt, S. and Boyce, M. (1985) 'Seasonality, fasting endurance, and body size in mammals', *American Naturalist*, 125, pp. 873–878.
- Link, J. and Ford, M. (2006) 'Widespread and persistent increase of Ctenophora in the continental shelf ecosystem off NE USA', *Marine Ecology Progress Series*, 320, pp. 153–159.
- Linse, K., Barnes, D. and Enderlein, P. (2006) 'Body size and growth of benthic invertebrates along an Antarctic latitudinal gradient', *Deep Sea Research Part II: Topical Studies in Oceanography*, 53, pp. 921–931.
- Lister, A. et al. (2011) 'Natural history collections as sources of long-term datasets', *Trends in Ecology and Evolution*, 26(4), pp. 153–154..
- Lo, W. et al. (2008) 'Enhancement of jellyfish (*Aurelia aurita*) populations by extensive aquaculture rafts in a coastal lagoon in Taiwan', *ICES Journal of Marine Science*, 65(3), pp. 453–461.
- Lonsdale, D. and Levinton, J. (1985) 'Latitudinal Differentiation in Copepod Growth : An Adaptation to Temperature', *Ecology*, 66(5), pp. 1397–1407.
- Lucas, C. H. (2001) 'Reproduction and life history strategies of the common jellyfish, *Aurelia aurita*, in relation to its ambient environment', *Hydrobiologia*, (Table 1), pp. 229–246.
- Lucas, C. H. (2009) 'Biochemical composition of the mesopelagic coronate jellyfish *Periphylla periphylla* from the Gulf of Mexico', *Journal of the Marine Biological Association of the United Kingdom*, 89(01), pp. 77–81.
- Lucas, C. H., Jones, D. O. B., et al. (2014) 'Gelatinous zooplankton biomass in the global oceans: Geographic variation and environmental drivers', *Global Ecology and Biogeography*, 23, pp. 701–714.
- Lucas, C. H. and Dawson, M. N. (2014) 'What are jellyfishes and thaliaceans and why do they bloom?', in Pitt, K. A. and Lucas, C. H. (eds) *Jellyfish Blooms*. Dordrecht: Springer, pp. 9–44.
- Lucas, C. H., Gelcich, S. and Uye, S. (2014) 'Living with Jellyfish : Management and Adaptation Strategies Living with Jellyfish : Management', in Pitt, K. A. and Lucas, C H (eds) *Jellyfish Blooms*. Dordrecht: Springer, pp. 129–150.

List of References

- Lucas, C. H. and Lawes, S. (1998) 'Sexual reproduction of the scyphomedusa *Aurelia aurita* in relation to temperature and variable food supply', *Marine Biology*, 131(4), pp. 629–638.
- Lucas, C. H. and Reed, A. J. (2009) 'Observations on the life histories of the narcomedusae *Aeginura grimaldii*, *Cunina peregrina* and *Solmissus incisa* from the western North Atlantic', *Marine Biology*, 156(3), pp. 373–379.
- Lucas, C. H. and Reed, A. J. (2010) 'Gonad morphology and gametogenesis in the deep-sea jellyfish *Atolla wyvillei* and *Periphylla periphylla* (Scyphozoa: Coronatae) collected from Cape Hatteras and the Gulf of Mexico', *Journal of the Marine Biological Association of the United Kingdom*, 90(06), pp. 1095–1104.
- Lynam, C. et al. (2005) 'Evidence for impacts by jellyfish on herring recruitment in the North Sea Fishing down the food web', *Marine Ecology Progress Series*, 298, pp. 157–167.
- Lynam, C. P. et al. (2006) 'Jellyfish overtake fish in a heavily fished ecosystem.', *Current biology : CB*, 16(13), pp. R492-3.
- Lynam, C. P., Attrill, M. J. and Skogen, M. D. (2010) 'Climatic and oceanic influences on the abundance of gelatinous zooplankton in the North Sea', *Journal of the Marine Biological Association of the United Kingdom*, 90(6), pp. 1153–1159.
- Lynam, C. P., Hay, S. J. and Brierley, A. S. (2004) 'Interannual variability in abundance of North Sea jellyfish and links to the North Atlantic Oscillation', *Limnology and Oceanography*, 49(3), pp. 637–643.
- Maas, O. (1884) 'Report on the Medusae coll. by US fish comm. steamer "Albatross" in the region of the Gulf Stream', *US Comm. of Fish and Fisheries: Report of the Commissioner*, p. 984.
- Macpherson, E. (2002) 'Large-scale species-richness gradients in the Atlantic Ocean.', *Proceedings. Biological sciences / The Royal Society*, 269(1501), pp. 1715–20.
- Macpherson, E. (2003) 'Species range size distributions for some marine taxa in the Atlantic Ocean. Effect of latitude and depth', *Biological Journal of the Linnean Society*, 80(3), pp. 437–455.
- Madin, L. (1988) 'Feeding behaviour of tentaculate predators: In situ observations and a conceptual model', *Bulletin of Marine Science*, 43(3), pp. 413–429.
- Malej, A. et al. (2012) 'Blooms and population dynamics of moon jellyfish in the northern Adriatic', *Cahiers de Biologie Marine*, 53(September 2011), pp. 337–342.
- Martorelli, S. and Cremonese, F. (1998) 'A proposed three-host life history of *Meniscus filiformis* in the SouthWest Atlantic Ocean', *Canadian Journal of Zoology*, 76, pp. 1199–1203.
- Martorelli, S. R. (2001) 'Digenea parasites of jellyfish and ctenophores of the southern Atlantic', *Hydrobiologia*, 451, pp. 305–310.
- Mauchline, J. and Harvey, P. F. (1983) 'The Scyphomedusae of the Rockall Trough, northeastern Atlantic Ocean', *Journal of Plankton Research*, 5(6), pp. 881–890.
- Mayer, A. G. (1910) *Medusae of the world, III: the Scyphomedusae*. Washington: Carnegie Institute.
- McClain, C. R. (2004) 'Connecting species richness , abundance and body size in deep-sea gastropods', *Global*, 13, pp. 327–334.
- McClain, C. R. et al. (2009) 'Patterns in deep-sea macroecology', in Witman, J. D. and Roy, K. (eds) *Marine Macroecology*. Chicago: The University of Chicago Press, pp. 1–34.

List of References

- McClain, C. R., Boyer, A. G. and Rosenberg, G. (2006) 'The island rule and the evolution of body size in the deep sea', *Journal of Biogeography*, 33(9), pp. 1578–1584.
- McDermott, J., Zubkoff, P. and Lin, A. (1982) 'The Occurrence of the Anemone *Peachia parasitica* as a Symbiont in the Scyphozoan *Cyanea capillata* in the Lower Chesapeake Bay', *Estuaries*, 5, pp. 319–321.
- Medina, M. et al. (2001) 'Evaluating hypotheses of basal animal phylogeny using complete sequences of large and small subunit rRNA.', *Proceedings of the National Academy of Sciences of the United States of America*, 98(17), pp. 9707–9712.
- Meiri, S. (2011) 'Bergmann's rule-what's in a name?', *Global Ecology and Biogeography*, 20(1), pp. 203–207.
- Mejía-sánchez, N. et al. (2013) 'Getting information from ethanol preserved nematocysts of the venomous cubomedusa *Chiropsalmus quadrumanus*: a simple technique to facilitate the study of nematocysts Obteniendo información de nematocistos de la cubomedusa venenosa *Chiropsalmus quadrumanu*', 41(1), pp. 166–169.
- Mendoza, R. P. R. (2006) 'Otoliths and their applications in fishery science', *Ribarstvo*, 64(3), pp. 89–102.
- Mianzan, H. and Cornelius, P. (1999) 'Cubomedusae and Scyphomedusae', in Boltovsky, D. (ed.) *South Atlantic Zooplankton*. Leiden: Backhuys Publishers, pp. 513–559.
- Mianzan, H., Dawson, E. W. and Mills, C. E. (2008) 'Phylum Ctenophora: Comb jellies', in *New Zealand inventory of biodiversity*. Christchurch, NZ: Canterbury University Press, pp. 49–58.
- Mills, C. (1995) 'Medusae, siphonophores, and ctenophores as planktivorous predators in changing global ecosystems', *ICES Journal of Marine Science*, 52(3–4), pp. 575–581.
- Mills, C. E. (2001) 'Jellyfish blooms: are populations increasing globally in response to changing ocean conditions?', *Hydrobiologia*, 451, pp. 55–68.
- Mills, C. E. and Goy, J. (1988) 'In situ observations of the behaviour of mesopelagic *Solmissus narcomedusae* (Cnidaria, Hydrozoa)', *Bulletin of Marine Science*, 43(3), pp. 739–751.
- Mills, C. E. and Sommer, F. (1995) 'Invertebrate introductions in marine habitats: two species of hydromedusae (Cnidaria) native to the Black Sea, *Maeotias inexpectata* and *Blackfordia virginica*, invade San Francisco Bay', *Marine Biology*, 122, pp. 279–288.
- Mills, C., Larson, R. and Youngbluth, M. (1987) 'A new species of coronate scyphomedusa from the Bahamas, *Aurelia octogonos*', *Bulletin of Marine Science*, 40(3), pp. 423–427.
- Miyake, H., Iwao, K. and Kakinuma, Y. (1997) 'Life History and Environment of *Aurelia aurita*', *South Pacific Study*, 17(2), pp. 273–285.
- Monger, B. C. et al. (1998) 'Sound scattering by the gelatinous zooplankters *Aequorea victoria* and *Pleurobrachia bachei*', *Deep-Sea Research Part II: Topical Studies in Oceanography*, 45(7), pp. 1255–1271.
- Moore, P. G., Rainbow, P. S. and Larson, R. J. (1993) 'The mesopelagic shrimp *Notostomus robustus* Smith (Decapoda: Oplophoridae) observed in situ feeding on the medusan *Atolla wyvillei* Haeckel in the Northwest Atlantic, with notes on gut contents and mouthpart morphology', *Journal of Crustacean Biology*, 13(4), pp. 690–696.
- de Moraes, I. et al. (2017) 'Fecundity and reproductive output of the caridean shrimp *Periclimenes paivai* associated with scyphozoan jellyfish', *Invertebrate Reproduction & Development*. Taylor &

List of References

Francis, 61(2), pp. 71–77.

Morandini, A. C. (2003) 'Deep-Sea medusae (Cnidaria : Cubozoa , Hydrozoa and Scyphozoa) from the coast of Bahia (western South Atlantic , Brazil)', *Mitt. hamb. zool. Mus. Inst.*, (November), pp. 13–25.

Morandini, A. C. and Jarms, G. (2005) 'New combinations for two coronate polyp species (Atorellidae and Nausithoidae, Coronatae, Scyphozoa, Cnidaria)', *Contributions to Zoology*, 74(1/2), pp. 117–123.

Morandini, A. and da Silveira, F. (2001) 'Sexual reproduction of *Nausithoe aurea* (Scyphozoa, Coronatae). Gametogenesis, egg release, embryonic development, and gastrulation', *Scientia Marina*, 65(2), pp. 139–149.

Morin, J. G. (1983) 'Coastal bioluminescence: Patterns and functions', *Bulletin of Marine Science*, 33(4), pp. 787–817.

Mutlu, E. (1996) 'Target strength of the common jellyfish (*Aurelia aurita*): A preliminary experimental study with a dual-beam acoustic system', *ICES Journal of Marine Science*, 53(2), pp. 309–311.

Natsukari, Y. and Komine, N. (1992) 'Age and growth estimation of the European squid, *Loligo vulgaris*, based on statolith microstructure', *Journal of the Marine Biological Association of the United Kingdom*. University of Southampton Library, 72(2), pp. 271–280.

Nawroth, J. C. et al. (2010) 'Phenotypic plasticity in juvenile jellyfish medusae facilitates effective animal-fluid interaction', *Biology Letters*, 6(3), pp. 389–393.

Olabarria, C. (2005) 'Patterns of bathymetric zonation of bivalves in the Porcupine Seabight and adjacent Abyssal plain, NE Atlantic', *Deep-Sea Research Part I: Oceanographic Research Papers*, 52(1), pp. 15–31.

Olabarria, C. and Thurston, M. H. (2003) 'Latitudinal and bathymetric trends in body size of the deep-sea gastropod *Troschelia berniciensis* (King)', *Marine Biology*, 143(4), pp. 723–730.

Olalla-Tárraga, M. Á. and Rodríguez, M. Á. (2007) 'Energy and interspecific body size patterns of amphibian faunas in Europe and North America: Anurans follow Bergmann's rule, urodeles its converse', *Global Ecology and Biogeography*, 16(5), pp. 606–617.

Olesen, N. J., Frandsen, K. and Riisgard, H. U. (1994) 'Population dynamics , growth and energetics of jellyfish *Aurelia aurita* in a shallow fjord', *Marine Ecology Progress Series*, 105, pp. 9–18.

Ortman, B. D. et al. (2010) 'DNA Barcoding the Medusozoa using mtCOI', *Deep-Sea Research Part II: Topical Studies in Oceanography*, 57(24–26), pp. 2148–2156.

Osborn, D. A. (2000) 'Cnidarian "Parasites" on *Solmissus incisa* , a Narcomedusa *', *Scientia Marina*, 64, pp. 157–163.

Osborn, D. A. et al. (2007) 'The habitat of mesopelagic scyphomedusae in Monterey Bay, California', *Deep Sea Research Part I: Oceanographic Research Papers*, 54(8), pp. 1241–1255.

Ottersen, G. et al. (2001) 'Ecological effects of the North Atlantic Oscillation', *Oecologia*, 128(1), pp. 1–14.

Padilla, D. K. and Savedo, M. M. (2013) 'Chapter two - A systematic review of phenotypic plasticity in marine invertebrates and plant systems', *Advances in Marine Biology*, 65, pp. 67–94.

Pagès, F. (2000) 'Biological associations between barnacles and jellyfish with emphasis on the ectoparasitism of *Alepa pacifica* (Lepadomorpha) on *Diplulmaris malayensis* (Scyphozoa)', *Journal of Natural History*, 34, pp. 2045–2056.

List of References

- Pages, F., White, M. and Rodhouse, P. (1996) 'Abundance of gelatinous carnivores in the nekton community of the Antarctic Polar Frontal Zone in summer 1994', *Marine Ecology Progress Series*, 141, pp. 139–147.
- Palero, F. et al. (2010) 'DNA extraction from formalin-fixed tissue: new light from the deep sea', *Scientia Marina*, 74(3), pp. 465–470.
- Parsons, T. and Lalli, C. (2002) 'Jellyfish population explosions: Revisiting a hypothesis of possible causes', *La mer*, 40, pp. 111–121.
- Partridge, L. and Coyne, J. (1997) 'Bergmann's Rule in Ectotherms : Is It Adaptive ?', *Evolution*, 51(2), pp. 632–635.
- Paterson, J. (1990) 'Comment - Bergmann's rule is invalid: a reply to V. Geist', *Canadian Journal of Zoology*, 68, pp. 1610–1612.
- Pauly, D. et al. (2009) 'Jellyfish in ecosystems, online databases, and ecosystem models', *Hydrobiologia*, 616(1), pp. 67–85.
- Pauly, D. and Deng Palomares, M. L. (2001) 'Fishing down marine food webs: An update', *Waters in Peril*, pp. 47–56.
- Petersen, K. (1976) 'Fixation and preservation of planktonic coelenterates', in Steedman, H. F. (ed.) *Zooplankton fixation and preservation*. Paris: The Unesco Press.
- Pikesley, S. et al. (2012) 'Cetacean sightings and strandings: Evidence for spatial and temporal trends?', *Journal of the Marine Biological Association of the UK*, 92, pp. 1809–1820.
- Pikesley, S. K. et al. (2014) 'Cnidaria in UK coastal waters: description of spatio-temporal patterns and inter-annual variability', *Journal of the Marine Biological Association of the United Kingdom*, pp. 1–8.
- Pitt, K A et al. (2014) 'Bloom and bust: Why do jellyfish blooms collapse?', in Pitt, K. A. and Lucas, C. H. (eds) *Jellyfish Blooms*. Dordrecht: Springer, pp. 79–104.
- Powell, T. and Steele, J. (1995) *Ecological time series*. London: Chapman and Hall.
- Prymak, O. et al. (2005) 'Application of synchrotron-radiation-based computer microtomography (SRCT) to selected biominerals: Embryonic snails, statoliths of medusae, and human teeth', *Journal of Biological Inorganic Chemistry*, 10(6), pp. 688–695.
- Pugh, P. R. (1984) 'The Diel Migrations and Distributions within a Mesopelagic Community in the Northeast Atlantic. 7. Siphonophores', *Progress in Oceanography*, 13(3–4), pp. 491–511.
- Pugh, P. R. (2014) 'Zooplankton displacement volume data provided via email from Cruise 92 and general discussion'.
- Purcell, J. (1988) 'Quantification of *Mnemiopsis leidyi* (Ctenophora, Lobata) from formalin-preserved plankton samples', *Marine Ecology Progress Series*, 45, pp. 197–200.
- Purcell, J. E. et al. (2001) 'Pelagic Cnidarians and Ctenophores in Low Dissolved Oxygen Environments ' A Review', pp. 77–100.
- Purcell, J. E. (2003) 'Predation on zooplankton by large jellyfish (*Aurelia labiata*, *Cyanea capillata*, *Aequorea aequorea*) in Prince William Sound , Alaska', *Marine Ecology Progress Series*, 246, pp. 137–152.
- Purcell, J. E. (2012) 'Jellyfish and Ctenophore Blooms Coincide with Human Proliferations and

List of References

- Environmental Perturbations', *Annual Review of Marine Science*, 4(1), pp. 209–235.
- Purcell, J., Uye, S. and Lo, W. (2007) 'Anthropogenic causes of jellyfish blooms and their direct consequences for humans: a review', *Marine Ecology Progress Series*, 350, pp. 153–174.
- Quicke, D. L. J., Belshaw, R. and Lopez-Vaamonde, C. (1999) 'Preservation of hymenopteran specimens for subsequent molecular and morphological study', *The Norwegian Academy of Science and Letters*, 28(1–2), pp. 261–267.
- Ramšak, B. A. and Stopar, K. (2007) 'Dispersal ecology and phylogeography of Scyphomedusae in the Mediterranean Sea Jellyfish research', *MarBEF Newsletter*, pp. 20–21.
- Raskoff, K. (2001) 'The impact of El Niño events on populations of mesopelagic hydromedusae', *Hydrobiologia*, (1994), pp. 121–129.
- Raskoff, K. a., Purcell, J. E. and Hopcroft, R. R. (2004) 'Gelatinous zooplankton of the Arctic Ocean: in situ observations under the ice', *Polar Biology*, 28(3), pp. 207–217.
- Reed, A. J. et al. (2013) 'Plasticity in shell morphology and growth among deep-sea protobranch bivalves of the genus *Yoldiella* (Yoldiidae) from contrasting Southern Ocean regions', *Deep Sea Research Part I: Oceanographic Research Papers*. Elsevier, 81, pp. 14–24.
- Relvas, P. et al. (2007) 'Physical oceanography of the western Iberia ecosystem: Latest views and challenges', *Progress in Oceanography*, 74(2–3), pp. 149–173.
- Renner, S. S. (2016) 'A Return to Linnaeus' s Focus on Diagnosis , Not Description : The Use of DNA Characters in the Formal Naming of Species', *Systematic biology*, 65(6), pp. 1085–1095.
- Repelin, R. (1966) 'Scyphomeduses Atollidae du bassin de Guinée', *Cah. O.R.S.T.O.M., sér. Océanogr.*, 4(4), pp. 21–31.
- Richardson, A. J. et al. (2009) 'The jellyfish joyride: causes, consequences and management responses to a more gelatinous future.', *Trends in ecology & evolution*. Elsevier Ltd, 24(6), pp. 312–22.
- Riemann, L., Titelman, J. and Båmstedt, U. (2006) 'Links between jellyfish and microbes in a jellyfish dominated fjord', *Marine Ecology Progress Series*, 325(August 2014), pp. 29–42.
- Roe, H. S. J. (1974) 'Observations on the diurnal vertical migrations of an oceanic animal community', *Marine Biology*, 28(2), pp. 99–113.
- Roe, H. S. J. et al. (1984) 'The diel migrations and distributions within a Mesopelagic community in the North East Atlantic. 1. Introduction and sampling procedures', *Progress in Oceanography*, 13(3–4), pp. 245–268.
- Roe, H. S. J. (1984) 'The diel migrations and distributions within a mesopelagic community within the North East Atlantic. 2. Vertical migrations and feeding of Mysids and decapods crustacea.', *Progress and Oceanography*, 13(3–4), pp. 269–318.
- Roe, H.S.J. and Badcock, J. (1984) 'The diel migrations and distributions within a mesopelagic community in the North East Atlantic. 2. Feeding of Mysids and Decapod Crustacea', *Progress in Oceanography*, 13(3–4), pp. 389–424.
- Roe, H S J and Badcock, J. (1984) 'The Diel Migrations and Distributions within a Mesopelagic Community in the North East Atlantic . 5 . Vertical Migrations and Feeding of Fish', *Progress and Oceanography*, 13(1977), pp. 389–424.
- Rombouts, I., Chiba, S. and Legendre, L. (2009) 'Global latitudinal variations in marine copepod

List of References

- diversity and environmental factors', *Proceedings of the Royal Society B: Biological Sciences*, 276, pp. 3053–3062.
- Rosenmai, P. (2014) *Calculating a distance matrix for geographic points using R*, *Eureka Statistics*.
- Rottini Sandrini, L. and Avian, M. (1991) 'Reproduction of *Pelagia noctiluca* in the central and northern Adriatic Sea', *Hydrobiologia*, 216, pp. 197–202.
- Roy, K. and Martien, K. (2001) 'Latitudinal distribution of body size in north-eastern Pacific marine bivalves', *Journal of Biogeography*, 28, pp. 485–493.
- Ruhl, H. A., Ellena, J. A. and Smith, K. L. (2008) 'Connections between climate, food limitation, and carbon cycling in abyssal sediment communities', *Proceedings of the National Academy of Sciences*, 105(44), pp. 17006–17011.
- Russell, F. (1953) *The medusae of the British Isles Volume I: Anthomedusae, Leptomedusae, Limnomedusae, Trachymedusae and Narcomedusae*. London: Cambridge University Press.
- Russell, F. (1957) 'On a new species of Scyphomedusae, *Atolla vanhoffeni* N.Sp.', *Journal of the Marine Biological Association of the UK*, 36, pp. 275–279.
- Russell, F. (1970) 'Periphyllidae', in Russell, F. (ed.) *The Medusae of the British Isles, Vol. II*.
- Russell, F. (1976) 'Scyphomedusae of the North Atlantic', *Fiches d'Identification du Zooplancton*. Edited by H. Fraser, 152, pp. 1–4.
- Russell, F. S. (1958) 'A new species of *Atolla*', *Nature*, 4626, pp. 1811–1812.
- Russell, F. S. (1959) 'Some observations on the scyphomedusa *Atolla*', *Journal of the Marine Biological Association of the UK*, 3, pp. 33–40.
- Russell, F. S. (1970a) 'Atollidae', in Russell, F. S. (ed.) *The Medusae of the British Isles, Vol. II*. Cambridge: Cambridge University Press.
- Russell, F. S. (1970b) 'Structure and characters of pelagic scyphomedusae', in Russell, F. S. (ed.) *The Medusae of the British Isles, Vol. II*. Cambridge: Cambridge University Press.
- Russell, F. S. (1970c) *The Medusae of the British Isles Vol. II: Pelagic Scyphozoa*. Cambridge: Cambridge University Press.
- Schmera, D. et al. (2017) 'Functional diversity: a review of methodology and current knowledge in freshwater macroinvertebrate research', *Hydrobiologia*, 787(1), pp. 27–44.
- Scholander, P. (1955) 'Evolution of climatic adaptation in homeotherms', *Evolution*, 9, pp. 15–26.
- Schroth, W. et al. (2002) 'Speciation and phylogeography in the cosmopolitan marine moon jelly, *Aurelia* sp.', *BMC evolutionary biology*, 2, p. 1.
- Shibata, D. (1994) 'Extraction of DNA from paraffin-embedded tissue for analysis by polymerase chain-reaction - new tricks from an old friend', *Human Pathology*, 25, pp. 561–563.
- Shiganova, T. (1998) 'Invasion of the Black Sea by the ctenophore *Mnemiopsis leidyi* and recent changes in pelagic community structure', *Fisheries Oceanography*, (July), pp. 305–310.
- Shimomura, O., Johnson, F. H. and Saiga, Y. (1962) 'Extraction, purification, and properties of aequorin, a bioluminescent protein from the luminous hydromedusan, *Aequorea*.' *Journal of Cell Comparative Physiology*, 59, pp. 223–239.
- Siegel, V. (1996) 'Zooplankton communities of the southern Bellingshausen Sea (Antarctic) with

List of References

special reference to krill and salps The composition , abundance , biomass and diversity of the epipelagic zooplankton communities of the southern Bellingshausen Sea (Antarctic) w', *Archive of Fish and Marine Research*, 44, pp. 115–139.

Silvertown, J. (2009) 'A new dawn for citizen science', *Trends in Ecology and Evolution*, 24, pp. 467–471.

Smith, K. L. and Druffel, E. R. M. (1998) 'Long time-series monitoring of an abyssal site in the NE Pacific: An introduction', *Deep-Sea Research Part II: Topical Studies in Oceanography*, 45(4–5), pp. 573–586.

Sokal, R. (1979) 'Testing Statistical Significance of Geographic Variation Patterns', *Systematic Zoology*, 28(2), pp. 227–232.

Solheim, H. (2012) *Population trend of Periphylla periphylla in inner Trondheimsfjord*. Norwegian University of Science and Technology.

Soltwedel, T. et al. (2016) 'Natural variability or anthropogenically-induced variation ? Insights from 15 years of multidisciplinary observations at the arctic marine LTER site HAUSGARTEN', *Ecological Indicators*. Elsevier Ltd, 65, pp. 89–102.

Sommer, U. et al. (2017) 'Do marine phytoplankton follow Bergmann's rule sensu lato?', *Biological Reviews*, 92, pp. 1011–1026.

Sørnes, T. et al. (2007) 'Causes for mass occurrences of the jellyfish *Periphylla periphylla*: a hypothesis that involves optically conditioned retention', *Journal of Plankton Research*, 29(2), pp. 157–167.

Sørnes, T. A. et al. (2008) 'Swimming and feeding in *Periphylla periphylla* (Scyphozoa, Coronatae)', *Marine Biology*, 153(4), pp. 653–659.

Sotje, I. (2003) *Derivation of the reduced life cycle of Theoscyphus zibrowii Werner, 1984 (Cnidaria, Scyphozoa)*. University of Hamburg.

Sötje, I. et al. (2011) 'Comparison of the statolith structures of *Chironex fleckeri* (Cnidaria, Cubozoa) and *Periphylla periphylla* (Cnidaria, Scyphozoa): a phylogenetic approach', *Marine biology*, 158(5), pp. 1149–1161.

Sötje, I., Tiemann, H. and Båmstedt, U. (2007) 'Trophic ecology and the related functional morphology of the deepwater medusa *Periphylla periphylla* (Scyphozoa, Coronata)', *Marine Biology*, 150(3), pp. 329–343.

Soto, E. H. et al. (2010) 'Temporal variability in polychaete assemblages of the abyssal NE Atlantic Ocean', *Deep-Sea Research Part II: Topical Studies in Oceanography*, 57(15), pp. 1396–1405.

Spangenberg, D. (1968) 'Statolith differentiation in *Aurelia aurita*', *Jez-A Ecological and Integrative Physiology*, 169(4), pp. 487–499.

Spangenberg, D. and Jernigan, T. (1994) 'Graviceptor development in jellyfish ephyrae in space and on Earth', *Advances in Space Research*, 14(8), pp. 317–325.

Steedman, H. F. (1976) *Zooplankton fixation and preservation*. Edited by H. F. Steedman. Paris: The Unesco Press.

Steele, J. (1995) 'Can ecological concepts span the land and ocean domains?', in Powell, T. and Steele, J. (eds) *Ecological Time Series*. London: Chapman and Hall, pp. 5–19.

Stiasny, G. (1934) 'Scyphomedusae', *Discovery Reports*, 8, pp. 329–396.

List of References

- Summerhayes, C. P. and Thorpe, S. A. (1996) *Oceanography: An illustrated guide*. New Jersey: Taylor & Francis.
- Svendsen, Y. (1990) 'Hosts of third stage larvae of *Hysterothylacium* sp. (Nematoda, Anisakidae) in zooplankton from outer Oslofjord, Norway.', *Sarsia*, 75, pp. 161–167.
- Sweetman, A. K. et al. (2014) 'Rapid scavenging of jellyfish carcasses reveals the importance of gelatinous material to deep-sea food webs', *Proceedings of the Royal Society B: Biological Sciences*, 281(1796), pp. 20142210–20142210.
- Sweetman, A. K. and Chapman, A. (2011) 'First observations of jelly-falls at the seafloor in a deep-sea fjord', *Deep-Sea Research Part I: Oceanographic Research Papers*. Elsevier, 58(12), pp. 1206–1211.
- Taleb-Hossenkhan, N., Bhagwant, S. and Gourrage, N. (2013) 'Extraction of nucleic acids from ancient formalin- and ethanol-preserved specimens of the tapeworm *Bertiella studeri*: which method works best?', *The Journal of parasitology*, 99(3), pp. 410–6.
- Thurston, M. (1977) 'Depth distributions of *Hyperia spinigera* Bovallus 1889 (Crustacea: Amphipoda) and medusae in the North Atlantic Ocean, with notes on the associations between *Hyperia* and coelenterates', in Angel, M. V. (ed.) *A Voyage of Discovery: George Deacon 70th Anniversary Volume*. Oxford: Pergamon Press, pp. 499–536.
- Thurston, M. (2014) 'Discussion on North Atlantic Discovery cruises and associated cruise report information, including sampling methods and locations, as well as data sources.'
- Tiemann, H. et al. (2006a) 'Calcium sulfate hemihydrate (bassanite) statoliths in the cubozoan *Carybdea* sp.', *Zoologischer Anzeiger - A Journal of Comparative Zoology*, 245(1), pp. 13–17.
- Tiemann, H. et al. (2006b) 'Calcium sulfate hemihydrate (bassanite) statoliths in the cubozoan *Carybdea* sp.', *Zoologischer Anzeiger - A Journal of Comparative Zoology*, 245(1), pp. 13–17.
- Tiemann, H. et al. (2009) 'Documentation of potential courtship-behaviour in *Periphylla periphylla* (Cnidaria: Scyphozoa)', *Journal of the Marine Biological Association of the United Kingdom*, 89(01), p. 63.
- Tiemann, H. and Jarms, G. (2010) 'Organ-like gonads, complex oocyte formation, and long-term spawning in *Periphylla periphylla* (Cnidaria, Scyphozoa, Coronatae)', *Marine Biology*, 157(3), pp. 527–535..
- Tiemann, H., Sötje, I. and Jarms, G. (2002) 'Calcium sulfate hemihydrate in statoliths of deep-sea medusae', *Journal of the Chemical Society; Dalton Transactions*, (7), pp. 1266–1268.
- Tiller, R. G. et al. (2014) 'Something fishy: Assessing stakeholder resilience to increasing jellyfish (*Periphylla periphylla*) in Trondheimsfjord, Norway', *Marine Policy*. Elsevier, 46, pp. 72–83.
- Tiller, R. G. et al. (2017) 'Coming Soon to a Fjord Near You: Future Jellyfish Scenarios in a Changing Climate', *Coastal Management*. Taylor & Francis, 45(1), pp. 1–23.
- Towanda, T. and Thuesen, E. V (2006) 'Ectosymbiotic behavior of *Cancer gracilis* and its trophic relationships with its host *Phacellophora camtschatica* and the parasitoid *Hyperia medusarum*', *Marine Ecology Progress Series*, 315, pp. 221–236.
- Tucker, J. W. and Chester, A. J. (1984) 'Effects of Salinity , Formalin Concentration and Buffer on Quality of Preservation of Effects of Salinity , Formalin Concentration and Buffer on Quality of Preservation of Southern Flounder (*Paralichthys lethostigma*) Larvae', *Copeia*, 1984(4), pp. 981–988.

List of References

- Ueno, S., Imai, C. and Mitsutani, A. (1995) 'Fine growth rings found in statolith of a cubomedusa *Carybdea rastoni*', *Journal of Plankton Research*, 17(6), pp. 1381–1384..
- Uye, S. (2008) 'Blooms of the giant jellyfish *Nemopilema nomurai*: A threat to the fisheries sustainability of the East Asian Marginal Seas', *Plankton Bethos Research*, 3, pp. 125–131.
- Uye, S. (2011) 'Human forcing of the copepod-fish-jellyfish triangular trophic relationship', *Hydrobiologia*, 666(1), pp. 71–83.
- Uye, S. and Shimauchi, H. (2005) 'Population biomass, feeding, respiration and growth rates, and carbon budget of the scyphomedusa *Aurelia aurita* in the Inland Sea of Japan', *Journal of Plankton Research*, 27(3), pp. 237–248.
- Vanhoffen, E. (1902) 'Die acraspeden Medusen der deutschen Tiefsee-Expedition 1898-1899', *Wiss. Ergebn. dt. Tiefsee-Exped. 'Valdinia'*, 3, pp. 3–86.
- Vanhoffeni, E. (1880) 'System der Medusen', *Jena*, p. 489.
- Vannuci-Mendes, M. (1944) 'Sobre a larva de *Dibothriorhynchus dinoi*, sp. n. parasita dos Rhizostomata', *Arquivos do Museu Paranaense*, 4, pp. 47–81.
- Vinogradov, M. et al. (1989) 'Ctenophore *Mnemiopsis leidyi* (A. Agassiz) (Ctenophora: Lobata) - new settlers in the Black Sea', *Oceanology*, 29, pp. 293–298.
- Warner, A. and Hays, G. (1994) 'Sampling by the Continuous Plankton Recorder survey', *Progress in Oceanography*, 34, pp. 237–256.
- Werner, B. (1970) 'Contribution to the evolution in the genus *Stephanoscyphus* (Scyphozoa, Coronatae) and ecology and regeneration qualitties of *Stephanoscyphus racemosus* Komai', *Publications of the Seto Marine Biological Laboratory*, 18, pp. 1–20.
- Werner, B. (1973) 'New investigations on systematics and the evolution of the class Scyphozoa and the phylum Cnidaria', *Publications of the Seto Marine Biological Laboratory*, 20, pp. 35–61.
- Werner, B. (1980) 'Life cycles of the Cnidaria', in Tardent, P. and Tardent, R. (eds) *Development and cellular biology of coelenterates*. Amsterdam: Elsevier, pp. 3–10.
- White, O. (Natural H. M. L., Pugh, P. (National O. C. S. and Thurston, M. (National O. C. S. (2013) 'Discussion regarding the preservation of gelatinous zooplankton specimens during the Discovery Expeditions'.
- Wigham, B. D. et al. (2003) 'Is long-term change in the abyssal Northeast Atlantic driven by qualitative changes in export flux? Evidence from selective feeding in deep-sea holothurians', *Progress in Oceanography*, 59(4), pp. 409–441.
- Williams, G. C. and Syoc, R. J. Van (2007) 'Methods of preservation and anesthetization of marine invertebrates', in Calton, J. (ed.) *The Light and Smith Manual: Intertidal Invertebrates from Central California to Oregon*. California: University of California Press, pp. 37–41.
- Williamson, J. et al. (1996) *Venomous and poisonous marine animals: A medical and biological handbook*. New South Wales: UNSW.
- Winans, A. and Purcell, J. (2010) 'Effects of pH on asexual reproduction and statolith formation of the scyphozoan, *Aurelia labiata*', *Hydrobiologia*, 645(1), pp. 39–52.
- Witt, M. et al. (2007) 'Prey landscapes help identify potential foraging habitats for leatherback turtles in the NE Atlantic', *Marine Ecology Progress Series*, 337, pp. 231–243.

List of References

- Witt, M. et al. (2012) 'Basking sharks in the northeast Atlantic: Spatio-temporal trends from sightings in UK waters', *Marine Ecology Progress Series*, 459, pp. 121–134.
- Yamaguchi, M. and Hartwick, R. (1980) 'Early life history of the sea wasp, *Chironex fleckeri* (Class Cubozoa)', in Tardent, P. and Tardent, R. (eds) *Development and cellular biology of coelenterates*. Amsterdam: Elsevier, pp. 11–16.
- Youngbluth, M. et al. (2008) 'Vertical distribution and relative abundance of gelatinous zooplankton, in situ observations near the Mid-Atlantic Ridge', *Deep Sea Research Part II: Topical Studies in Oceanography*, 55(1–2), pp. 119–125.
- Youngbluth, M. and Båmstedt, U. (2001) 'Distribution, abundance, behavior and metabolism of *Periphylla periphylla*, a mesopelagic coronate medusa in a Norwegian fjord', *Hydrobiologia*, 451, pp. 321–333.
- Zaitsev, Y. P. (1992) 'Recent changes in the trophic structure of the Black Sea', *Fisheries Oceanography*, 1(2), pp. 180–190.
- Zeleney, C. (1907) 'The effect of degree of injury, successive injury and functional activity upon regeneration in the scyphomedusan, *Cassiopea xamanchana*', *Journal of Experimental Zoology*, 5, pp. 265–274.
- Zeng, C. et al. (2017) 'Fluorescence-based approach to estimate the chlorophyll-a concentration of a phytoplankton bloom in Ardley Cove (Antarctica)', *Remote Sensing*, 9(3), pp. 1–15.

